

CHEMICAL CONSTITUENTS AND NITRIC OXIDE INHIBITORY ACTIVITY OF *CAPPARIS*
MICRACANTHA AND *MAERUA SIAMENSIS*



A Dissertation Submitted in Partial Fulfillment of the Requirements
for the Degree of Doctor of Philosophy in Pharmacognosy
Department of Pharmacognosy and Pharmaceutical Botany
FACULTY OF PHARMACEUTICAL SCIENCES
Chulalongkorn University
Academic Year 2022
Copyright of Chulalongkorn University

องค์ประกอบทางเคมีและฤทธิ์ยับยั้งไนตริกออกไซด์ของชิงซี่และแจง



วิทยานิพนธ์นี้เป็นส่วนหนึ่งของการศึกษาตามหลักสูตรปริญญาวิทยาศาสตรดุษฎีบัณฑิต

สาขาวิชาเภสัชเวช ภาควิชาเภสัชเวชและเภสัชพฤกษศาสตร์

คณะเภสัชศาสตร์ จุฬาลงกรณ์มหาวิทยาลัย

ปีการศึกษา 2565

ลิขสิทธิ์ของจุฬาลงกรณ์มหาวิทยาลัย

ศศิวิมล นุกุลกิจ : องค์ประกอบทางเคมีและฤทธิ์ยับยั้งไนตริกออกไซด์ของชิงชี่และแจง. (CHEMICAL CONSTITUENTS AND NITRIC OXIDE INHIBITORY ACTIVITY OF *CAPPARIS MICRACANTHA* AND *MAERUA SIAMENSIS*) อ.ที่ปรึกษาหลัก : ผศ. ภก. ดร.ชัยศักดิ์ จันตรีนิยม, อ.ที่ปรึกษาร่วม : รศ. ภก. ดร.รุทธ์ สุทธิศรี, ดร.มัตถกา คงขาว

การศึกษาองค์ประกอบทางเคมีของพืช 2 ชนิดในวงศ์ Capparaceae คือชิงชี่และแจง สามารถสกัดแยกสารบริสุทธิ์ได้ทั้งหมด 13 ชนิด จากการพิสูจน์โครงสร้างด้วยเทคนิคทางสเปกโทสโคปี ร่วมกับการเปรียบเทียบกับสารที่เคยมีการรายงานมาก่อน พบสารที่มีรายงานแล้วทั้งหมด 5 ชนิด จากส่วนลำต้นของชิงชี่ (*Capparis micracantha*) ประกอบด้วยสารในกลุ่มอินโดลอัลคาลอยด์ 1 ชนิด คือ methyl 6-methoxy-3-indolecarbonate, สารในกลุ่มอนุพันธ์ของกรดเบนโซอิก 1 ชนิด คือ vanillic acid, สารในกลุ่มลิกแนน 1 ชนิด คือ (-)-syringaresinol และสารในกลุ่มสติลปินไดเมอร์ 2 ชนิด คือ (+)-ampelopsin A และ (-)-pauciflorol E สำหรับรากของแจง (*Maerua siamensis*) พบสารใหม่ทั้งหมด 8 ชนิด ซึ่งเป็นสารในกลุ่มอินโดลอัลคาลอยด์ ได้แก่ (+)-maeruanitrile A, maeruanitrile B, maeroximes A - C และ maeruabisindoles A - C สารที่แยกได้ทั้งหมดถูกนำมาทดสอบฤทธิ์ยับยั้งการสร้างไนตริกออกไซด์ ในเซลล์แมโครฟาจ RAW 264.7 ที่ถูกเหนี่ยวนำด้วยลิโปโพลีแซ็กคาไรด์เปรียบเทียบกับสารควบคุมผลบวก indomethacin พบว่าสาร (-)-pauciflorol E และ methyl 6-methoxy-3-indolecarbonate จากลำต้นชิงชี่ มีค่าความเข้มข้นที่ยับยั้งการสร้างไนตริกออกไซด์ได้ 50 เปอร์เซ็นต์ IC_{50} เท่ากับ 123.40 ± 4.51 และ 198.00 ± 5.57 ไมโครโมลาร์ ตามลำดับ สำหรับสาร maeruabisindoles B-C, maeroxime C, (+)-maeruanitrile A และ maeruanitrile B จากรากแจง มีค่า IC_{50} เท่ากับ 31.1 ± 1.04 , 56.7 ± 2.2 , 92.2 ± 5.1 , 186.4 ± 13.0 และ 186.8 ± 13.3 ไมโครโมลาร์ ตามลำดับ ในขณะที่สาร indomethacin มีค่า IC_{50} อยู่ในช่วง 150.0 - 166.3 ไมโครโมลาร์ การศึกษานี้สนับสนุนการใช้ลำต้นชิงชี่และรากของแจงเพื่อต้านอักเสบตามภูมิปัญญาการแพทย์แผนไทย

สาขาวิชา เกษศาสตร์
ปีการศึกษา 2565

ลายมือชื่อนิสิต
ลายมือชื่อ อ.ที่ปรึกษาหลัก
ลายมือชื่อ อ.ที่ปรึกษาร่วม
ลายมือชื่อ อ.ที่ปรึกษาร่วม

6076462533 : MAJOR PHARMACOGNOSY

KEYWORD: Capparis micracantha Maerua siamensis nitric oxide production

Sasiwimon Nukulkit : CHEMICAL CONSTITUENTS AND NITRIC OXIDE
INHIBITORY ACTIVITY OF *CAPPARIS MICRACANTHA* AND *MAERUA SIAMENSIS*.

Advisor: Asst. Prof. CHAISAK CHANSRINIYOM, Ph.D. Co-advisor: Assoc. Prof.
RUTT SUTTISRI, Ph.D., Mattaka Khongkow, Ph.D.

The chemical investigation of two plants in Capparaceae family, which are *Capparis micracantha* and *Maerua siamensis*, leads to the isolation of 13 compounds. The structures of the isolates were elucidated using spectroscopy techniques and comparison of the previous reports. Of five known compounds from the stems of *C. micracantha* were an indole alkaloid (methyl 6-methoxy-3-indolecarbonate), a benzoic acid derivative (vanillic acid), a lignan [(-)-syringaresinol], and two stilbene dimers [(+)-ampelopsin A and (-)-pauciflorol E]. In addition, eight new indole alkaloids named (+)-maeruanitrile A, maeruanitrile B, maeroximes A-C and maeruabisindoles A-C were isolated from the roots of *M. siamensis*. All isolates were tested for inhibition of nitric oxide production in lipopolysaccharide-induced RAW 264.7 macrophage cells compared with a positive control (indomethacin). (-)-Pauciflorol E and methyl 6-methoxy-3-indolecarbonate from *C. micracantha* stems exhibited half maximum inhibitory concentration (IC_{50}) values of 123.40 ± 4.51 and $198.00 \pm 5.57 \mu\text{M}$, respectively. Moreover, maeruabisindoles B - C, maeroxime C, (+)-maeruanitrile A and maeruanitrile B from *M. siamensis* roots showed IC_{50} values of 31.1 ± 1.04 , 56.7 ± 2.2 , 92.2 ± 5.1 , 186.4 ± 13.0 and $186.8 \pm 13.3 \mu\text{M}$, respectively, while the IC_{50} of indomethacin was in the range of 150.0 - 166.3 μM . This study supports the use of *C. micracantha* stems and *M. siamensis* roots for anti-inflammation according to Thai traditional medicine knowledge.

Field of Study: Pharmacognosy

Student's Signature

Academic Year: 2022

Advisor's Signature

Co-advisor's Signature

Co-advisor's Signature

ACKNOWLEDGEMENTS

I would like to express my deepest gratitude to my thesis advisor Assistant professor Chaisak Chansriniyom and my thesis co-advisors Associate professor Rutt Suttisri of the Department of Pharmacognosy and Pharmaceutical Botany, Chulalongkorn University, and Dr. Mattaka Khongkow of National Nanotechnology Center (NANOTEC), National Science and Technology Development Agency, for their helpful advice and support.

I would like to thank Miss Angkana Jantimaporn of NANOTEC for her support on inhibition of nitric oxide production assay and Miss Ponsawan Netcharoensirisuk for her support on statistical analysis. In addition, I appreciate Associate Professor Thanyada Rungrotmongkol, Ph. D. and Preeyaporn Poldorn, Ph. D. with their help in computational studies. Moreover, I thank Nonthalert Lertnitikul, Ph.D., Pramote Triboon, Ph. D. and Mr. Jakkrit Seesang for the photos of plants.

I am very thankful to my dissertation committee, including Associate Professor Dr. Hsun-Shuo Chang of School of Pharmacy, College of Pharmacy, Kaohsiung Medical University, Taiwan, who also acts as an external committee member for his guidance and support during my research work aboard.

In addition, I acknowledge a scholarship from the 100th Anniversary Chulalongkorn University Fund for Doctoral Scholarship and CU Graduate School Thesis Grant. Moreover, I thank Natural Products and Nanoparticles Research Unit, and Pharmaceutical Research Instrument Center, Faculty of Pharmaceutical Sciences, Chulalongkorn University. Finally, I would like to express infinite gratitude to my family for their love, understanding, support and encouragement.

Sasiwimon Nukulkit

TABLE OF CONTENTS

	Page
.....	iii
ABSTRACT (THAI).....	iii
.....	iv
ABSTRACT (ENGLISH).....	iv
ACKNOWLEDGEMENTS.....	v
TABLE OF CONTENTS.....	vi
LIST OF TABLES.....	xi
LIST OF FIGURES.....	xiii
LIST OF SCHEMES.....	1
LIST OF ABBREVIATIONS.....	2
CHAPTER I INTRODUCTION.....	4
CHAPTER II LITERATURE REVIEWS.....	7
2.1 Order Brassicales.....	7
2.2 Family Capparaceae.....	8
2.3 Genus <i>Capparis</i>	8
2.4 <i>Capparis micracantha</i> DC.....	9
2.5 Genus <i>Maerua</i>	11
2.6 <i>Maerua siamensis</i> (Kurz) Pax.....	11
2.7 Chemical constituents of plants in the families Brassicaceae and Capparaceae and their biological activities.....	12
CHAPTER III EXPERIMENTAL.....	64

3.1 Source of plant materials	64
3.2 General techniques.....	64
3.2.1 Solvents	64
3.2.2 Analytical normal-phase thin-layer chromatography (TLC)	64
3.2.3 Analytical reversed-phase thin-layer chromatography (RP-18)	64
3.2.4 Column chromatography	65
3.2.4.1 Flash Column Chromatography.....	65
3.2.4.2 Medium Performance Liquid Column Chromatography (MPLC) ...	65
3.2.4.3 Conventional column chromatography.....	65
3.2.4.4 Gel filtration chromatography.....	66
3.3 Spectroscopy.....	66
3.3.1 Ultraviolet absorption spectra	66
3.3.2 Infrared spectra	66
3.3.3 Mass spectrometer	66
3.3.4 Proton and carbon-13 nuclear magnetic resonance (¹ H- and ¹³ C-NMR) spectroscopy	67
3.3.5 Circular dichroism	67
3.3.6 Polarimetry	67
3.3.6.1 Optical rotation.....	67
3.4. Extraction and isolation	67
3.4.1 Extraction of <i>Capparis micracantha</i> stems.....	67
3.4.2 Isolation of compounds from the EtOAc extract of <i>Capparis micracantha</i> stems (CMSE).....	68
3.4.2.1 Isolation of compound 1 (methyl 6-methoxy-3-indolecarbonate).....	69

3.4.2.2 Isolation of compound 2 (vanillic acid)	69
3.4.2.3 Isolation of compound 3 [(-)-syringaresinol]	69
3.4.2.4 Isolation of compound 4 [(+)-ampelopsin A]	70
3.4.2.5 Isolation of compound 5 [(-)-pauciflorol E]	70
3.4.3 Extraction of <i>Maerua siamensis</i> roots	73
3.4.4 Isolation of compounds from EtOAc extract of <i>Maerua siamensis</i> roots	74
3.4.4.1 Isolation of compound 6 [(+)-maeruanitrile A] and compound 7 (maeruanitrile B)	74
3.4.4.2 Isolation of compound 8 (maeroxime A)	74
3.4.4.3 Isolation of compound 9 (maeroxime B)	75
3.4.4.4 Isolation of compound 10 (maeroxime C)	75
3.4.5 Isolation of compounds from <i>n</i> -butanol extract of <i>M. siamensis</i> roots ...	80
3.4.5.1 Isolation of compounds 11 (maeruabisindole A)	80
3.4.5.2 Isolation of compounds 12 (maeruabisindole B)	80
3.4.5.3 Isolation of compounds 13 (maeruabisindole C)	80
3.5 Physical and spectral data of isolated compounds	84
3.5.1 Compound 1 (methyl 6-methoxy-3-indolecarbonate)	84
3.5.2 Compound 2 (vanillic acid)	84
3.5.3 Compound 3 [(-)-syringaresinol]	84
3.5.4 Compound 4 [(+)-ampelopsin A]	85
3.5.5 Compound 5 [(-)-pauciflorol E]	85
3.5.6 Compound 6 [(+)-maeruanitrile A]	85
3.5.7 Compound 7 (maeruanitrile B)	86
3.5.8 Compound 8 (maeroxime A)	86

3.5.9 Compound 9 (maeroxime B).....	87
3.5.10 Compound 10 (maeroxime C).....	87
3.5.11 Compound 11 (maeruabisindole A).....	88
3.5.12 Compound 12 (maeruabisindole B).....	88
3.5.13 Compound 13 (maeruabisindole C).....	89
3.6 Evaluation of inhibitory activity on nitric oxide (NO) production and cytotoxicity	89
3.7 Statistical analysis.....	90
CHAPTER IV RESULTS AND DISCUSSION.....	91
4.1 Identification of compounds isolated from <i>Capparis micracantha</i> stems.....	91
4.1.1 identification of compound 1 (methyl 6-methoxy-3-indolecarbonate)....	91
4.1.2 Identification of compound 2 (vanillic acid)	98
4.1.3 Identification of compound 3 [(-)-syringaresinol]	104
4.1.4 Identification of compound 4 [(+)-ampelopsin A]	112
4.2 Structure elucidation of compounds isolated from <i>Maerua siamensis</i> roots .	131
4.2.1 Structure elucidation of compound 6 [(+)-(maeruanitrile A).....	131
4.2.2 Structure elucidation of compound 7 (maeruanitrile B)	139
4.2.3 Structure elucidation of compound 8 (maeroxime A).....	148
4.2.4 Structure elucidation of compound 9 (maeroxime B).....	158
4.2.5 Structure elucidation of compound 10 (maeroxime C).....	165
4.2.6 Structure elucidation of compound 11 (maeruabisindole A).....	172
4.2.8 Structure elucidation of compound 13 (maeruabisindole C).....	192
4.3 Inhibition of nitric oxide production in LPS-induced macrophages RAW 264.7 by isolated compounds	202

CHAPTER V CONCLUSION 205

REFERENCES 206

VITA..... 222



LIST OF TABLES

	Page
Table 1. Distribution of Indole alkaloids family Brassicaceae	16
Table 2. Chemical constituents of plants in the genus Capparis.....	41
Table 3. Chemical constituents of plants in the genus Maerua.....	59
Table 4. ¹ H- and ¹³ C-NMR data of compound 1 (400 MHz, in acetone-d ₆) and methyl 6-methoxy-3-indolecarbonate (300 MHz, in CDCl ₃).....	93
Table 5. ¹ H- and ¹³ C-NMR data of compound 2 (400 MHz, in acetone-d ₆) and vanillic acid (500 MHz, in CD ₃ OD).....	100
Table 6. ¹ H- and ¹³ C-NMR data of compound 3 (400 MHz, in CDCl ₃) and (-)-syringaresinol (400 MHz, in CDCl ₃).....	106
Table 7. ¹ H- and ¹³ C-NMR data of compound 4 (400 MHz, in CD ₃ OD) and (+)-ampelopsin A (500 MHz, in acetone-d ₆).....	115
Table 8. ¹ H- and ¹³ C-NMR data of compound 5 (400 MHz, in acetone-d ₆) and (-)-pauciflorol E (300 MHz, in acetone-d ₆).....	124
Table 9. ¹ H-, ¹³ C-NMR and HMBC data of compound 6 (400 MHz, acetone-d ₆).....	133
Table 10. ¹ H-, ¹³ C NMR and HBMC data of compound 7 (400 MHz, CD ₃ OD).....	141
Table 11. ¹ H-, ¹³ C-NMR and HMBC data of compound 8 (400 MHz, DMSO-d ₆).....	150
Table 16. ¹ H-, ¹³ C-NMR and HMBC data of compound 9 (400 MHz, DMSO-d ₆).....	159
Table 17. ¹ H-, ¹³ C-NMR and HMBC data of compound 10 (400 MHz, DMSO-d ₆).....	167
Table 18. ¹ H-, ¹³ C-NMR and HBMC data of compound 11 (400 MHz, in DMSO-d ₆).....	175
Table 19. ¹ H-, ¹³ C NMR and HBMC data of compound 12 (400 MHz, in CD ₃ OD).....	185
Table 20. ¹ H-, ¹³ C NMR and HBMC data of compound 13 (400 MHz, in acetone-d ₆).....	194

Table 21. Inhibitory concentrations of isolated compounds from <i>C. micracantha</i> stems on nitric oxide (NO) production and cell viability in LPS-induced RAW 264.7 cells	202
Table 22. Inhibition concentrations of isolated compounds from <i>M. siamensis</i> roots on nitric oxide (NO) production and cell viability in LPS-induced RAW 264.7 cells...	204



LIST OF FIGURES

	Page
Figure 1. <i>Capparis micracantha</i> DC.....	10
Figure 2. <i>Maerua siamensis</i> (Kurz) Pax.....	12
Figure 3. Three types of glucosinolate based on their amino acid precursors (Mithen et al., 2010).....	13
Figure 4. Different products from the hydrolysis of glucosinolates (adapted from (Al-Gendy et al., 2010).....	14
Figure 5. HR-ESI mass spectrum of compound 1.....	93
Figure 6. IR spectrum of compound 1.....	94
Figure 7. ¹ H-NMR spectrum of compound 1 (400 MHz, acetone-d ₆).....	94
Figure 8. ¹ H-NMR spectrum of compound 1 (expansion between δ_{H} 6.5-8.5 ppm)	95
Figure 9. ¹³ C-NMR spectrum of compound 1 (100 MHz, acetone-d ₆).....	95
Figure 10. ¹ H- ¹³ C HSQC spectrum of compound 1.....	96
Figure 11. ¹ H- ¹³ C HMBC spectrum of compound 1.....	96
Figure 12. ¹ H- ¹³ C HMBC spectrum of compound 1.....	97
Figure 13. ¹ H- ¹ H COSY spectrum of compound 1.....	97
Figure 14. ¹ H- ¹ H NOESY spectrum of compound 1.....	98
Figure 15. HR-ESI mass spectrum of compound 2.....	100
Figure 16. IR spectrum of compound 2.....	101
Figure 17. ¹ H-NMR spectrum of compound 2 (400 MHz, acetone-d ₆).....	101
Figure 18. ¹³ C-NMR spectrum of compound 2 (100 MHz, acetone d ₆).....	102
Figure 19. ¹ H- ¹³ C HSQC spectrum of compound 2.....	102
Figure 20. ¹ H- ¹³ C HMBC spectrum of compound 2.....	103

Figure 21. ^1H - ^1H COSY spectrum of compound 2.....	103
Figure 22. ^1H - ^1H NOESY spectrum of compound 2.....	104
Figure 23. HR-ESI mass spectrum of compound 3.....	107
Figure 24. IR spectrum of compound 3.....	107
Figure 25. ^1H -NMR spectrum of compound 3 (400 MHz, CDCl_3).....	108
Figure 26. ^1H -NMR spectrum of compound 3 (expansion between δ_{H} 4.2-6.9 ppm).....	108
Figure 27. ^{13}C -NMR spectrum of compound 3 (100 MHz, CDCl_3).....	109
Figure 28. ^1H - ^{13}C HSQC spectrum of compound 3.....	109
Figure 29. ^1H - ^{13}C HMBC spectrum of compound 3.....	110
Figure 30. ^1H - ^{13}C HMBC spectrum of compound 3.....	110
Figure 31. ^1H - ^1H COSY spectrum of compound 3.....	111
Figure 32. ^1H - ^1H NOESY spectrum of compound 3.....	111
Figure 33. HR-ESI mass spectrum of compound 4.....	116
Figure 34. IR spectrum of compound 4.....	116
Figure 35. ^1H -NMR spectrum of compound 4 (400 MHz, CD_3OD).....	117
Figure 36. ^1H -NMR spectrum of compound 4 (expansion between δ_{H} 5.2-7.2 ppm).....	117
Figure 37. ^{13}C -NMR spectrum of compound 4 (100 MHz, CD_3OD).....	118
Figure 38. ^{13}C -NMR spectrum of compound 4 (expansion between δ_{C} 0-165 ppm).....	118
Figure 39. ^1H - ^{13}C HSQC spectrum of compound 4.....	119
Figure 40. ^1H - ^{13}C HMBC spectrum of compound 4.....	119
Figure 41. ^1H - ^{13}C HMBC spectrum of compound 4.....	120
Figure 42. ^1H - ^{13}C HMBC spectrum of compound 4.....	120
Figure 43. ^1H - ^1H COSY spectrum of compound 4.....	121
Figure 44. ^1H - ^1H NOESY spectrum of compound 4.....	121

Figure 45. HR-ESI mass spectrum of compound 5.....	125
Figure 46. IR spectrum of compound 5	126
Figure 47. ^1H -NMR spectrum of compound 5 (400 MHz, acetone- d_6).....	126
Figure 48. ^1H -NMR spectrum of compound 5 (expansion between δ_{H} 4.4-7.5 ppm) 127	
Figure 49. ^1H -NMR spectrum of compound 5 (expansion between δ_{H} 4.4-7.4 ppm) 127	
Figure 50. ^{13}C -NMR spectrum of compound 5 (100 MHz, acetone- d_6).....	128
Figure 51. ^{13}C -NMR spectrum of compound 5 (expansion between δ_{C} 40-160 ppm)	128
Figure 52. ^1H - ^{13}C HSQC spectrum of compound 5	129
Figure 53. ^1H - ^{13}C HMBC spectrum of compound 5.....	129
Figure 54. ^1H - ^{13}C HMBC spectrum of compound 5.....	130
Figure 55. ^1H - ^1H COSY spectrum of compound 5.....	130
Figure 56. ^1H - ^1H NOESY spectrum of compound 5.....	131
Figure 57. UV spectrum of compound 6	134
Figure 58. HR-ESI mass spectrum of compound 6.....	134
Figure 59. IR spectrum of compound 6	135
Figure 60. The CD spectrum in MeOH of compound 1 (upper left)	135
Figure 61. ^1H -NMR spectrum of compound 6 (600 MHz, acetone- d_6).....	136
Figure 62. ^{13}C -NMR spectrum of compound 6 (150 MHz, acetone- d_6).....	136
Figure 63. ^{13}C -NMR, DEPT135 and DEPT90 spectrum of compound 6	137
Figure 64. ^1H - ^{13}C HSQC spectrum of compound 6	137
Figure 65. ^1H - ^{13}C HMBC spectrum of compound 6.....	138
Figure 66. ^1H - ^1H COSY spectrum of compound 6.....	138
Figure 67. ^1H - ^1H NOESY spectrum of compound 6.....	139

Figure 68. UV spectrum of compound 7	142
Figure 69. HR-ESI mass spectrum of compound 7.....	142
Figure 70. IR spectrum of compound 7	143
Figure 71. ¹ H-NMR spectrum of compound 7 (400 MHz, CD ₃ OD).....	143
Figure 72. ¹³ C-NMR spectrum of compound 7 (100 MHz, CD ₃ OD).....	144
Figure 73. ¹³ C-NMR spectrum of compound 7 (expansion between δ_C 111-141 ppm)	144
Figure 74. ¹³ C-NMR, DEPT 135 and DEPT 90 (150 MHz, CD ₃ OD) spectra of compound 7	145
Figure 75. ¹ H- ¹³ C HSQC spectrum of compound 7	145
Figure 76. ¹ H- ¹³ C HMBC spectrum of compound 7.....	146
Figure 77. ¹ H- ¹³ C HMBC spectrum of compound 7 (expansion between δ_H 3.4-7.5 ppm, δ_C 111-141 ppm)	146
Figure 78. ¹ H- ¹ H COSY spectrum of compound 7.....	147
Figure 79. ¹ H- ¹ H NOESY spectrum of compound 7.....	147
Figure 80. UV spectrum of compound 8	151
Figure 81. HR-ESI mass spectrum of compound 8	151
Figure 82. IR spectrum of compound 8.....	152
Figure 83. ¹ H-NMR spectrum of compound 8 (400 MHz, DMSO-d ₆).....	152
Figure 84. ¹ H-NMR spectrum of compound 8 (expansion between δ_H 6.4-7.5 ppm)	153
Figure 85. ¹³ C-NMR spectrum of compound 8 (400 MHz, DMSO-d ₆).....	153
Figure 86. ¹³ C-NMR, DEPT 135 and DEPT 90 spectrum of compound 8	154
Figure 87. ¹ H- ¹³ C HSQC spectrum of compound 8	154
Figure 88. ¹ H- ¹³ C HMBC spectrum of compound 8.....	155

Figure 89. ^1H - ^{13}C HMBC spectrum of compound 8	155
Figure 90. ^1H - ^1H COSY spectrum of compound 8.....	156
Figure 91. ^1H - ^1H NOESY spectrum of compound 8.....	156
Figure 92. ^1H - ^1H NOESY spectrum of compound 8.....	157
Figure 93. Possible conformations of compound 8, based on the DFT calculation at B3LYP/6-31g (d, p) level.....	157
Figure 94. UV spectrum of compound 9	160
Figure 95. IR spectrum of compound 9.....	160
Figure 96. HR-ESI mass spectrum of compound 9.....	161
Figure 97. ^1H -NMR spectrum of compound 9 (100 MHz, DMSO-d_6).....	161
Figure 98. ^{13}C -NMR spectrum of compound 9 (100 MHz, DMSO-d_6).....	162
Figure 99. ^1H - ^{13}C HSQC spectrum of compound 9	162
Figure 100. ^1H - ^{13}C HMBC spectrum of compound 9	163
Figure 101. ^1H - ^{13}C HMBC spectrum of compound 9	163
Figure 102. ^1H - ^1H COSY spectrum of compound 9.....	164
Figure 103. ^1H - ^1H NOESY spectrum of compound 9	164
Figure 104. Possible conformations of compound 9, based on the DFT calculation at B3LYP/6-31g (d, p) level.....	165
Figure 105. UV spectrum of compound 10.....	167
Figure 106. HR-ESI mass spectrum of compound 10.....	168
Figure 107. IR spectrum of compound 10.....	168
Figure 108. ^1H -NMR spectrum of compound 10 (400 MHz, DMSO-d_6)	169
Figure 109. ^{13}C -NMR spectrum of compound 10 (100 MHz, DMSO-d_6).....	169
Figure 110. ^1H - ^{13}C HSQC spectrum of compound 10.....	170

Figure 111. ^1H - ^{13}C HMBC spectrum of compound 10	170
Figure 112. ^1H - ^1H COSY spectrum of compound 10	171
Figure 113. ^1H - ^1H NOESY spectrum of compound 10	171
Figure 114. Possible conformations of compound 10, based on the DFT calculation at B3LYP/6-31g (d, p) level	172
Figure 115. UV spectrum of compound 11	176
Figure 116. HR-ESI mass spectrum of compound 11	176
Figure 117. IR spectrum of compound 11	177
Figure 118. ^1H -NMR spectrum of compound 11 (400 MHz, DMSO-d_6)	177
Figure 119. ^1H -NMR spectrum of compound 11 (expansion between δ_{H} 6.3-8.3 ppm)	178
Figure 120. ^{13}C -NMR spectrum of compound 11 (100 MHz, DMSO-d_6)	178
Figure 121. ^{13}C -NMR spectrum of compound 11 (100 MHz, DMSO-d_6) (expansion between δ_{C} 90-170 ppm)	179
Figure 122. ^1H - ^{13}C HSQC spectrum of compound 11	179
Figure 123. ^1H - ^{13}C HMBC spectrum of compound 11	180
Figure 124. ^1H - ^{13}C HMBC spectrum of compound 11	180
Figure 125. ^1H - ^{13}C HMBC spectrum of compound 11	181
Figure 126. ^1H - ^{13}C HMBC spectrum of compound 11	181
Figure 127. ^1H - ^1H COSY spectrum of compound 11	182
Figure 128. ^1H - ^1H NOESY spectrum of compound 11	182
Figure 129. UV spectrum of compound 12	186
Figure 130. HR-ESI mass of compound 12	186
Figure 131. IR spectrum of compound 12	187

Figure 132. ^1H -NMR spectrum of compound 12 (400 MHz, CD_3OD).....	187
Figure 133. ^1H -NMR spectrum of compound 12 (expansion between δ_{H} 6.3-8.7 ppm)	188
Figure 134. ^{13}C -NMR spectrum of compound 12 (100 MHz, CD_3OD)	188
Figure 135. ^1H - ^{13}C HSQC spectrum of compound 12.....	189
Figure 136. ^1H - ^{13}C HSQC spectrum of compound 12.....	189
Figure 137. ^1H - ^{13}C HMBC spectrum of compound 12.....	190
Figure 138. ^1H - ^{13}C HMBC spectrum of compound 12.....	190
Figure 139. ^1H - ^1H COSY spectrum of compound 12.....	191
Figure 140. ^1H - ^1H NOESY spectrum of compound 12.....	191
Figure 141. HR-ESI mass spectrum of compound 13	195
Figure 142. UV spectrum of compound 13.....	195
Figure 143. IR spectrum of compound 13.....	196
Figure 144. ^1H -NMR spectrum of compound 13 (400 MHz, acetone- d_6)	196
Figure 145. ^1H -NMR spectrum of compound 13.....	197
Figure 146. ^{13}C -NMR spectrum of compound 13 (100 MHz, acetone- d_6).....	197
Figure 147. ^{13}C -NMR spectrum of compound 13.....	198
Figure 148. ^1H - ^{13}C HSQC spectrum of compound 13.....	198
Figure 149. ^1H - ^{13}C HMBC spectrum of compound 13	199
Figure 150. ^1H - ^{13}C HMBC spectrum of compound 13	199
Figure 151. ^1H - ^{13}C HMBC spectrum of compound 13	200
Figure 152. ^1H - ^1H COSY spectrum of compound 13	200
Figure 153. ^1H - ^1H NOESY spectrum of compound 13	201
Figure 154. ^1H - ^1H NOESY spectrum of compound 13.....	201



จุฬาลงกรณ์มหาวิทยาลัย
CHULALONGKORN UNIVERSITY

LIST OF SCHEMES

Scheme 1. Extraction of <i>Capparis micracantha</i> stems	68
Scheme 2. Isolation of compounds 1 – 3 from the EtOAc extract of <i>C. micracantha</i>	71
Scheme 3. Isolation of compounds 4 – 5 from the EtOAc extract of <i>C. micracantha</i>	72
Scheme 4. Extraction of <i>Maerua siamensis</i> roots	73
Scheme 5. Isolation of compounds 6 – 7 from the EtOAc extract of <i>M. siamensis</i> ..	76
Scheme 6. Isolation of compounds 8 from the EtOAc extract of <i>M. siamensis</i>	77
Scheme 7. Isolation of compounds 9 from the EtOAc extract of <i>M. siamensis</i>	78
Scheme 8. Isolation of compounds 10 from the EtOAc extract of <i>M. siamensis</i>	79
Scheme 9. Isolation of compounds 11 from the butanol extract of <i>M. siamensis</i>	81
Scheme 10. Isolation of compounds 12 from the butanol extract of <i>M. siamensis</i> ..	82
Scheme 11. Isolation of compounds 13 from the butanol extract of <i>M. siamensis</i>	

LIST OF ABBREVIATIONS

acetone- d_6	=	Deuterated acetone
<i>br s</i>	=	Broad singlet (for NMR spectra)
°C	=	Degree Celsius
CC	=	Column Chromatography
CDCl ₃	=	Deuterated chloroform
CH ₂ Cl ₂	=	Dichloromethane
cm	=	Centimeter
cm ⁻¹	=	reciprocal centimeter (unit of wave number)
¹³ C-NMR	=	Carbon-13 Nuclear Magnetic Resonance
1D NMR	=	One-dimensional Nuclear Magnetic Resonance
2D NMR	=	Two-dimensional Nuclear Magnetic Resonance
<i>d</i>	=	Doublet (for NMR spectra)
<i>dd</i>	=	Doublet of doublets (for NMR spectra)
DMSO	=	Dimethylsulfoxide
δ	=	Chemical shift (in part per million unit)
DEPT	=	Distortionless Enhancement by Polarization Transfer
ϵ	=	Molar absorptivity
ESI-MS	=	Electrospray Ionization Mass Spectrometry
EtOAc	=	Ethyl acetate
<i>et al.</i>	=	et alibi (and other)
FCC	=	Flash Column Chromatography
g	=	Gram
HMBC	=	Heteronuclear Multiple Bond Correlation
HR	=	High Resolution
¹ H-NMR	=	Proton Nuclear Magnetic Resonance
HSQC	=	Heteronuclear Single Quantum Coherence
Hz	=	Hertz
IC ₅₀	=	Half maximal inhibitory concentration
IR	=	Infrared spectrum

J	=	Coupling constant
Kg	=	Kilogram
L	=	Liter
λ_{\max}	=	Wavelength at maximal absorption
m	=	Multiplet (for NMR spectra)
MeOH	=	Methanol
mg	=	Milligram
μg	=	Microgram
min	=	Minute
mL	=	Milliliter
μL	=	Microliter
μM	=	Micromolar
mM	=	Millimolar
MS	=	Mass spectrum
MPLC	=	Medium Pressure Column Chromatography
MW	=	Molecular weight
m/z	=	Mass to charge ratio
N/A	=	not available
NI.	=	not indicated
nm	=	Nanometer
NMR	=	Nuclear Magnetic Resonances
NO	=	Nitric oxide
NOESY	=	Nuclear Overhauser Effect Spectroscopy
ν_{\max}	=	Wave number at maximal absorption
ppm	=	Part per million
s	=	Singlet (for NMR spectra)
Si-CC	=	Silica gel Column Chromatography
t	=	Triplet (for NMR spectra)
TLC	=	Thin Layer Chromatography
UV-VIS	=	Ultraviolet and Visible spectrophotometry

CHAPTER I

INTRODUCTION

Inflammation is a general mechanism of body tissues for the prevention of invasion by infectious agents e.g., microbes into hosts. It is part of the biological response to damages from trauma or burns and involves antigen-antibody reactions and several inflammatory mediators such as nitric oxide, prostaglandins and other cytokines. Pain, swelling, warmth, redness and loss of function are significant symptoms of inflammation (Turner *et al.*, 2014). Inflammation can be classified into 3 stages which are acute, subacute or chronic inflammation. Acute inflammation rapidly happens after infection. Blood vessels are dilated and capillary permeability is increased in order to facilitate the movement of plasma and white blood cells to the injured area. Subacute inflammation after happens after acute stage. Leukocyte and chemical mediators are released. These states can be activated by the temperature in the body (fever). The last stage of inflammation, called chronic inflammation, can occur several months after the initial injury. Fibrosis can be found after long-term injury. Chronic inflammation is the cause of various diseases including rheumatoid arthritis and osteoarthritis (Robert and Morrow, 2006). The World Health Organization (WHO) has pointed out that chronic inflammation can lead to a variety of diseases e.g. stroke, respiratory diseases, cardiovascular diseases and cancer (Tsai *et al.*, 2019). Although Inflammation is an important process for the defense mechanism of the body, large scale inflammation or long-term inflammation may contribute to degeneration of the body. Therefore, in order to prevent inflammatory diseases, controlling of chemical mediators is necessary.

Nitric oxide is an important chemical mediator that plays a role in the inflammation process. It can be synthesized by neutrophils, monocytes and macrophages using the enzyme inducible nitric oxide synthase (iNOS) with oxygen and NADPH as co-factors and released into endothelial cells causing vasodilation. But large amount of nitric oxide can cause tissue to degenerate (Sharma *et al.*, 2007). Inhibition of nitric oxide is a needful method to control inflammation (Vane and Botting, 1998). Anti-inflammatory drugs, either steroids or non-steroids (NSAIDS), have been used for

this purpose. However, long-term treatment can lead to various side effects (e.g., peptic ulcer, cataract and osteoporosis).

Many medicinal plants in traditional medicine have been used to treat inflammatory diseases, although there is little scientific evidence to support. Research study on the ability of extracts and chemical constituents of these plants to inhibit production of nitric oxide by macrophages is an alternative in the discovery and development of novel anti-inflammatory drugs for future use with minimal side effects and greater safety.

Family Capparaceae (or Capparidaceae) is a family of flowering plants consisting of 40-45 genera (700-900 species) distributed in tropical and subtropical regions. It is closely related to family Brassicaceae (Cruciferae) (Cronquist, 1981; Heywood, 1993; Mabberley, 1997). Several members of this plant family have been used as herbal drugs, food or cosmetics. Some species have displayed various biological activities such as anti-diabetic, antimicrobial, anticancer and anti-inflammatory (Bektas *et al.*, 2012; Nabavi *et al.*, 2016; Verma *et al.*, 2013). *Capparis* is the largest genus in this family (consisting about 250 species). Major chemical constituents of plants in this genus are alkaloids, glucosinolates and isothiocyanates. Some *Capparis* species are used in traditional medicine to cure inflammatory diseases e.g., rheumatism and cystitis). In Thailand, the roots of *Capparis micracantha* have been used as a component of Ya-Ha-Rak, a traditional Thai drug formula to treat fever symptoms (Palo *et al.*, 2017). Extracts from several parts of *C. spinosa*, or caper bush, have been reported to possess several biological activities. Its fruit and leaf extracts showed antidiabetic activity in rats (Chen *et al.*, 2017). The fruit extract also showed hypotensive effect, whereas both root and fruit extracts showed antimicrobial activity (Zhang and Ma, 2018). Extracts from a number of *Capparis* species including *C. spinosa* (Nabavi *et al.*, 2016; Chen *et al.*, 2017; Nabavi *et al.*, 2016; Zhang and Ma, 2018), *C. ovata* (Bektas *et al.*, 2012), *C. decidua* (Verma *et al.*, 2013), *C. tomentosa* (Akoto *et al.*, 2008) and *C. acutifolia* (Chen *et al.*, 2017) were demonstrated to have anti-inflammatory activity.

Maerua is another genus of family Capparaceae. It consists of approximately 90 species (Chayamarit, 1991). Major chemical constituents of *Maerua* were reported

to be alkaloids, flavonoids, glucosinolates and isothiocyanates (Nobsathian *et al.*, 2018). Members of this genus have been employed to treat several ailments such as fever, stomach ache, skin infection, diabetes, and urinary calculi. Biological activities of extracts from *Maerua* species have also been reported. Methanol extracts of *Maerua angolensis* and *M. pseudopetalosa* showed antimicrobial activity. Extracts from *M. crassifolia*, *M. angolensis* and *M. apetala* were reported as exhibiting anti-inflammatory activity (Lincy *et al.*, 2014). Extracts from *M. siamensis* showed anti-inflammatory property by inhibition of albumin denaturation (Theanphong and Somwong, 2022).

Therefore, this study focused on *Capparis micracantha* and *Maerua siamensis*, two members of family Capparaceae used in traditional Thai medicine for treatment of diseases and symptoms associated with inflammation. Preliminary study of the extracts from the stems of *C. micracantha* and the roots *M. siamensis* showed their ability to inhibit nitric oxide production. Attempt to isolate their chemical constituents and evaluate their inhibitory activity on nitric oxide production might support the uses of these plants in traditional medicine and yield new anti-inflammatory drugs for the future, as well as providing chemotaxonomic information in the study of family Capparaceae.

The major objectives of this study were as follows.

1. To isolate and purify the chemical constituents from *Capparis micracantha* and *Maerua siamensis*.
2. To elucidate the chemical structures of the isolated compounds.
3. To examine inhibitory activity of these compounds on nitric oxide production in macrophages.

CHAPTER II

LITERATURE REVIEWS

2.1 Order Brassicales

Order Brassicales (or Capparales) is a group of dicotyledons in the APG III system, which consists of 17 families including Akaniaceae, Bataceae, Brassicaceae, Capparaceae, Caricaceae, Cleomaceae, Emblingiaceae, Gyrostemonaceae, Koeberliniaceae, Limnanthaceae, Moringaceae, Pentadiplandraceae, Resedaceae, Salvadoraceae, Setchellanthaceae, Tovariaceae and Tropaeolaceae (Hall *et al.*, 2002). A characteristic of these families within the order is the production of indole glucosinolates, which can protect the plant itself from herbivore and parasitism and can sometimes be used as flavoring agent eliciting pungent taste (Simpson, 2019).

Within this order, family Brassicaceae is the largest with approximately 340 genera and 3,350 species that are economically important as food, such as many vegetables including broccoli, brussels sprouts, cauliflowers and cabbages, industrial crops, and ornamental plants. These families are distributed worldwide, but most of them are found in northern regions, around Mediterranean basin, south-western and central Asia. Although Capparaceae is related to the herbaceous Brassicaceae, some species can sometimes be big woody trees. These Capparaceae plants usually have elongate gynophore or androgynophore, many stamens and unilocular ovary in a parietal placentation (Al-Shehbaz *et al.*, 2006; Bailey *et al.*, 2006; Beilstein *et al.*, 2008). In the past, Cleomaceae used to be a genus (*Cleome*) within family Capparaceae. But in 2016, APG IV classification system has separated this genus into a new monophyletic family (Simpson, 2019). *Cleome* species have different characteristics from other plants in the family Capparaceae including being herbaceous, having dehiscent fruit with a replum and unilocular ovary. Recently, chemical constituents and DNA phylogeny of Brassicaceae and Capparaceae have been studied to provide their chemotaxonomic data.

2.2 Family Capparaceae

Capparaceae (or Capparidaceae) is a medium-size family in order Brassicales that is closely related to family Brassicaceae (Cruciferae). It consists of approximately 29 genera and 381 species. This family used to be divided into 2 subfamilies: Capparoidae and Cleomoidae. There are about 25 genera and 440 species within subfamily Capparoidae which are shrub or small tree bearing fleshy fruit (dehiscent or indehiscent). Subfamily Cleomoidae consisted of about 8 genera and 275 species which were herbaceous and had dehiscent fruits. Plants in this family are widely distributed in the tropical and subtropical regions (Kamel *et al.*, 2009). In Thailand, three genera of this family have been recorded, including *Capparis*, *Crateva* and *Maerua*.

Plants in Capparaceae can be herb, shrub or, sometimes, woody tree. Their leaves are simple or palmately compound. The leaf arrangement is alternate or, rarely, opposite. The texture of leaves is glabrous or furnished with glands or glandular hairs. These leaves are either stipulate or exstipulate. The flower is solitary or in axillary or terminal inflorescence, of racemes or corymbs. Flowers are bisexual or rarely unisexual, actinomorphic or zygomorphic. There are 4-8 sepals and 4-16 petals. The stamens are free, few to many. The ovary is superior, mostly borne on gynophore, or sessile. Ovules are few to many. Fruit is berry, drupe, nutlet or siliquiform. Seeds are often many (Kamel *et al.*, 2009).

2.3 Genus *Capparis*

Capparis is a big genus in the family Capparaceae consisting of 250 species which are distributed worldwide in the tropical and subtropical regions. Their flowers have numerous stamens and a short or elongated androgynophore. Plants in this genus can strongly grow in adverse conditions (water stresses, photo-inhibition and high irradiance) (Cristina *et al.*, 2006). Historically, several *Capparis* species have been used since ancient times as drug and food. For example, the roots of *Capparis spinosa* were consumed by Egyptians and Arabs to treat kidney disease, liver disease and stomach problem. The leaves of this plants were used to cure skin diseases and earache,

whereas the buds were used to treat disease of the spleen. Pickled flower buds, unripe fruits and shoots of some *Capparis* plants are usually stored in salt, vinegar and brine for used as appetizer (Tlili *et al.*, 2011). In Thailand, there are 17 species of the genus *Capparis* as listed below.

No.	Name of species	Thai names
1	<i>Capparis acuminata</i> Willd.	แมงซอ
2	<i>C. acutifolia</i> Sw. subsp. <i>sabiaefolia</i> Jacobs	ตาฉู่แม
3	<i>C. diffusa</i> Ridl.	หนามเกี่ยวไก่
4	<i>C. echinocarpa</i> Pierre ex Gagnep.	เกี่ยวไก่
5	<i>C. flavicans</i> Kurz.	จ้าวเลีย
6	<i>C. floribunda</i> Wight.	เปตาดเขา
7	<i>C. glauca</i> Wall.	หางนกกะลิง
8	<i>C. grandis</i> Linn. f.	ค้อนกลอง
9	<i>C. micracantha</i> DC.	ชิงซี่
10	<i>C. pranensis</i> Jacobs.	เพ็ดตึงตัง
11	<i>C. pyrifolia</i> Lamk.	หนามหางนกกะลิง
12	<i>C. radula</i> Gagnep.	หนามดำ
13	<i>C. sepiaria</i> Linn.	หนามวัวซัง
14	<i>C. siamensis</i> Kurz.	พุงแก
15	<i>C. tenera</i> Dalz.	หนามเล็บแมว
16	<i>C. thorelii</i> Gagnep.	จ้าวซัง
17	<i>C. zeylanica</i> Linn.	สะแอะ

2.4 *Capparis micracantha* DC.

Capparis micracantha DC. is a shrub or small tree that can grows up to 2-6 meters. The plant can sometimes have spines on its stem, the length of spines is about 2-4 mm. The leaves are simple, 3-5 cm long and 9.4-24 cm wide. The shape of these leaves is ovate-lanceolate or oblong-lanceolate or oblong to elliptic. The leaves are glabrous and light green in color. Their petioles are 0.1-1 cm long. The flowers are

solitary, or in clusters of 1-7 flowers, with peduncles which are 1-2 cm in length. The shape of sepals is ovate to oblong, the petals are free, nearly boat-shaped or oblong to oblanceolate, 3-7 mm wide and 10-22 long. The petals are white, with dark red, dark violet or brownish spots. The number of stamens is 20-35. The filaments are 18-30 mm long. The ovary is borne on a gynophore of 2-3.5 cm in length. Its fruit is simple, ovoid or rounded. The color of fruits is yellow, red, or black. (Chayamarit, 1991).



Figure 1. *Capparis micracantha* DC.

A) Flowers **B)** Habit **C)** Leaves

(Photos by L. Nonthalert.)

2.5 Genus *Maerua*

Genus *Maerua* comprises 90 species in family Capparaceae. Most of these plants are distributed in tropical Asia and Africa. There is only one *Maerua* species in Thailand (*M. siamensis*). Plants of this genus are either shrub or tree. Their leaves are compound, 3-folioate. The flowers are in clusters or sometimes solitary. The inflorescences are corymbose or racemose. The flower has 4 sepals separated at base but has no petal. The number of stamens is few to numerous (20-40). The gynophore is long, bearing an ovary with one locule and numerous ovules. The stigma is disc-shaped. The fruits are round and glabrous and the seeds are large, 1-3 in number (Chayamarit, 1991).

2.6 *Maerua siamensis* (Kurz) Pax

Maerua siamensis (Kurz) Pax, which is the only *Maerua* species found in Thailand, is a shrub or small tree, up to 5-10 meters in height. Its twig is glabrous, with palmately compound leaves of 3 leaflets (or, rarely, 4-5 leaflets). The leaf shape is ovate or oblong (1-3 cm wide and 5-7 cm long) The leaf base is obtuse or hastate, and the leaf apex is cuspidate. The flower has no petal but has 4 distinct greenish-white sepals. The flowers are in terminal or axillary inflorescence. Some flowers can singly bloom from leaf axil. Its roots have been used as herbal drug to treat cystitis, to relieve pain and inflammation (Chayamarit, 1991).

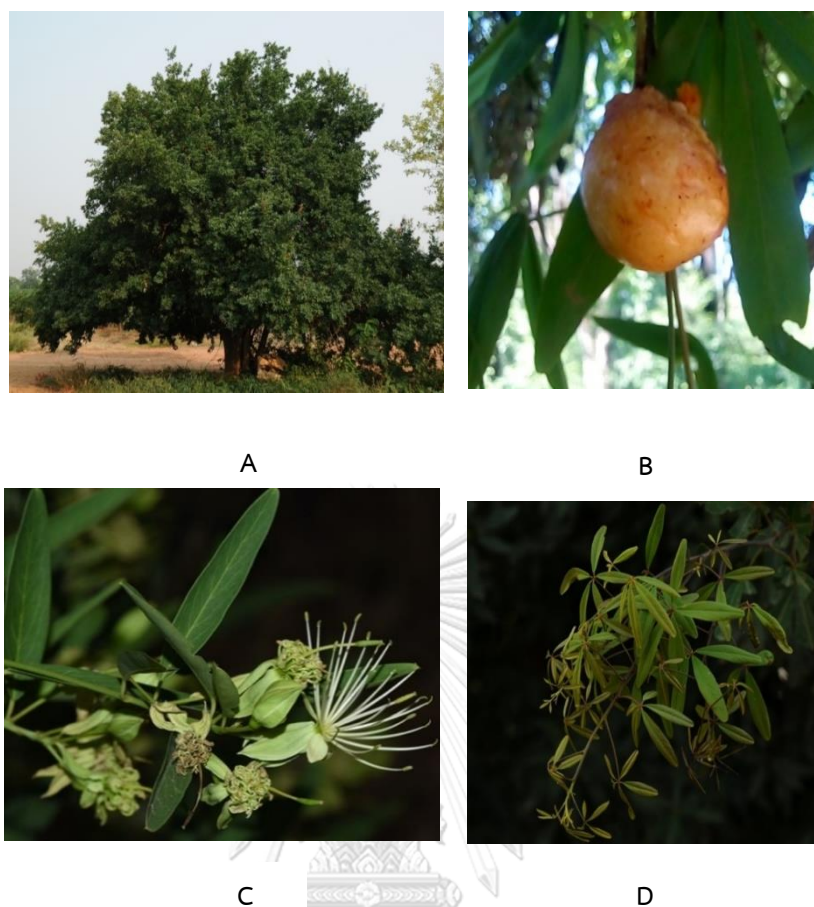


Figure 2. *Maerua siamensis* (Kurz) Pax

A) Habit B) Fruits C) Flowers D) Leaves

(Photos by S. Nukulkit., P. Triboun and J. Seesang.)

2.7 Chemical constituents of plants in the families Brassicaceae and Capparaceae and their biological activities

Many vegetable plants belong to family Brassicaceae. Examples are broccoli (*Brassica oleracea* var. *italica*), cabbage (*B. oleracea* var. *capitata*), cauliflower (*B. oleracea* var. *botrytis*), kohlrabi (*B. oleracea* var. *gongylodes*) and brussels sprouts (*B. oleracea* var. *gemmifera*). Major constituents in this family are glucosinolates and their derivatives, which are beneficial to these plants by protecting them from pathogens and insects. During cutting, chopping or chewing the plant, plant enzymes (e.g., β -thioglucosidase or myrosinase) are released and can cause hydrolysis of the glucosinolates. The aglycones of these glucosinolates can be divided into three groups:

aliphatic, indole and aromatic (Mithen *et al.*, 2010) (**Figure 3**). In addition to isothiocyanate, break-down products from glucosinolate can also be epithionitrile, thiocyanate, nitrile and oxazolidine-thione (Al-Gendy *et al.*, 2010) (**Figure 4**).

Several indole phytoalexins in Brassicaceae displayed interesting biological activities (Vig *et al.*, 2009). For example, brassinin (**10**) has been reported to be cytotoxic toward leukemic cancer cell line, to exhibit cancer chemopreventive activity (Mehta *et al.*, 1995), to enhance apoptosis and inhibit the metastasis of human prostate cancer (PC-3) cells (Kim *et al.*, 2015). 1-Methoxybrassinin (**115**), firstly isolated from chinese cabbage, was reported to be anti-proliferative against human colon cancer (Caco-2) cells (Chripkova *et al.*, 2014) and anticancer against T-Jurkat leukemic cells (Pilatova *et al.*, 2005).

Tryptanthrin (**143**), isolated from the leaves of *Strobilanthes cusia* (family Acanthaceae), showed antiviral activity against human coronavirus NL63 (Tsai *et al.*, 2020). This compound, which was also found in *Isatis* plants in Brassicaceae, showed anti-inflammatory activity through inhibition of cyclooxygenase-2 (Danz *et al.*, 2001), and inhibitory effect on prostaglandin and leukotriene synthesis (Danz *et al.*, 2002).

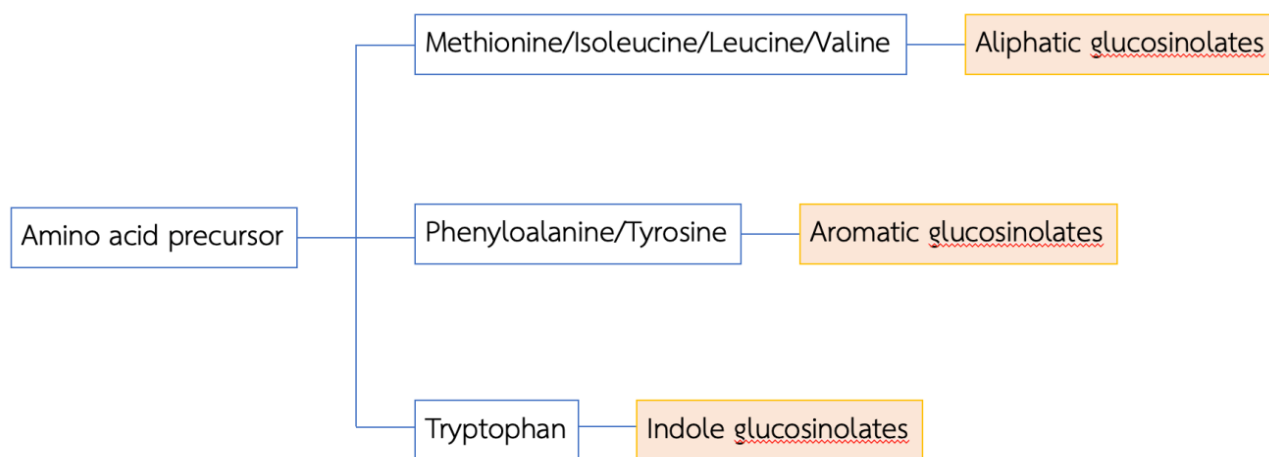


Figure 3. Three types of glucosinolate based on their amino acid precursors (Mithen *et al.*, 2010)

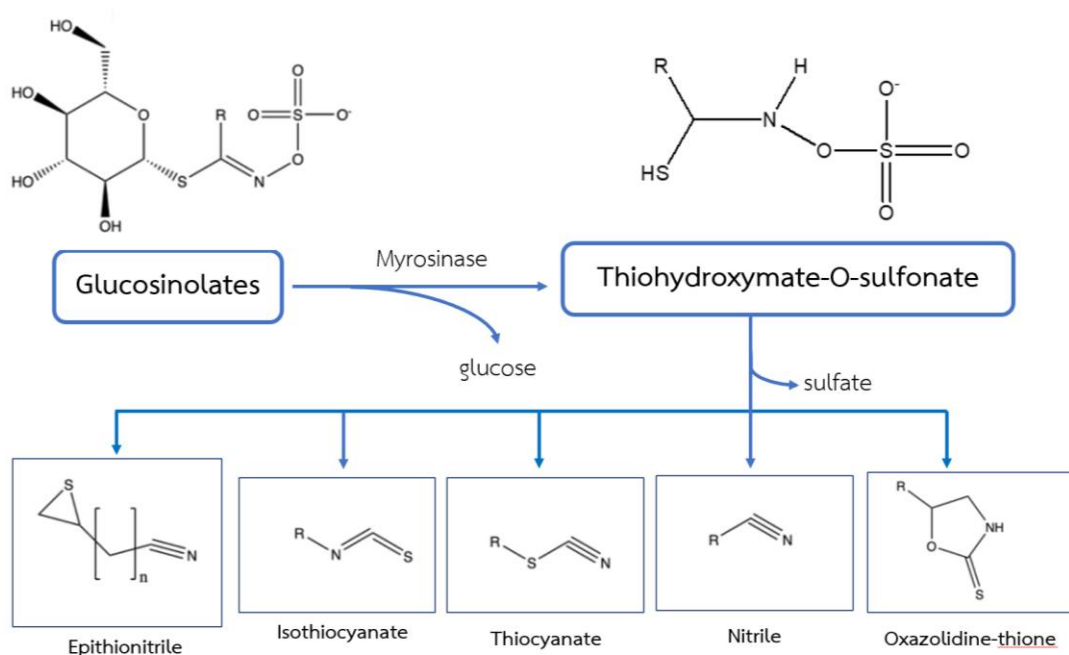


Figure 4. Different products from the hydrolysis of glucosinolates (adapted from (Al-Gendy *et al.*, 2010))

Many secondary metabolites isolated and identified from Brassicaceae plants are indole alkaloids, as shown in **Table 1**. For example, several plants in the genus *Isatis* have been used for treatment of influenza, common cold and infection in traditional Chinese medicine. Extracts from these plants were reported to demonstrate anti-inflammatory activity through inhibition of nitric oxide production (Yang *et al.*, 2014), and antiviral effect against coxsackievirus B3 and influenza virus type A. Indole alkaloids from the roots of *Isatis indigodica* such as isatigotindoliosides C (**73**) and E (**75**) (Meng *et al.*, 2017) showed antiviral activity against coxsackievirus B3, whereas (-)-*R*-2-(3-cyanomethyl-4-methoxy-1*H*-indol-7-yl)-2-(1*H*-indol-3-yl) acetonitrile (**19**), (-)-*R*-2-(3-cyanomethyl-4-methoxy-1*H*-indol-7-yl)-2-(4-methoxy-1*H*-indol-3-yl) acetonitrile (**20**) and arvelexin (**1**) were active against influenza virus type A (Chen *et al.*, 2012). Isatindigobisindolosides B (**79**), D (**81**) and F (**83**), isatibisindosulfonic acid B (**67**) and isatindosulfonic acid B (**97**) from the same plant displayed antiviral activity against both viruses (Meng *et al.*, 2017).

Investigation of the roots of another *Isatis* species, *Isatis tinctoria*, revealed the presence of ten indole alkaloids, mostly belonging to the isatindigoside and isatisindigoticanine subtypes (Zhang *et al.*, 2020). These alkaloids exhibited inhibitory effect on nitric oxide production (Zhang *et al.*, 2019)

Families Capparaceae and Brassicaceae are closely associated according to their DNA phylogeny and chemical constituents. Many studies have reported that the major secondary metabolites in Capparaceae are flavonoids, phenolic acids, steroids, triterpenoids, alkaloids, fatty acids and glucosinolates. Break-down products of glucosinolates are similar to those found in Brassicaceae plants, especially indole alkaloids, for examples, (+)-*R*-2-(4-hydroxy-2-oxo-2,3-dihydrobenzofuran-3-yl) acetonitrile (**216**) and (+)-*S*-2-(4-hydroxy-2-oxo-2,3-dihydrobenzofuran-3-yl) acetonitrile (**217**), isolated from *Capparis spinosa* (Capparaceae), are similar to indole-3-acetonitrile (**54**), 1-methoxy-indole-3-acetonitrile (Caulilexin C) (**16**) and indole-3-acetonitrile-6-*O*- β -D-glucopyranoside (**56**), found in Brassicaceae family.

The chemical constituents in genus *Capparis* possess various biological activities, for example, the triterpenoids simiarenol (**210**) and lupeol (**207**) and the plant sterol β -sitosterol (**200**), isolated from *C. dongvanensis*, showed α -glucosidase inhibitory activity (Khang *et al.*, 2021). Ginkgetin (**173**), a biflavonoid found in *C. spinosa*, showed inhibitory effect on NF- κ B activation (H.-F. Zhou *et al.*, 2011). Several flavonoids and their glycosides from this genus exhibited antioxidant activity (Yahia *et al.*, 2020). A triterpenoid, olean-12-en-3 β ,28-diol 3 β -pentacosanoate (**208**), from *C. ovata* showed moderate anti-inflammatory activity (Gazioglu *et al.*, 2020). Additionally, cappariloside A (**152**), firstly purified from *C. spinosa*, showed antiviral activity by inhibiting the replication of H1N1, H3N2, PIV3 and ADV viruses (Li *et al.*, 2018).

The majority of chemical constituents reported from plants in the genus *Maerua* are phenolic compound, fatty acids, triterpenoids and steroids. A small number of alkaloids and flavonoids have also been found. Some of these compounds, e.g., capparilosides A (**152**) and B (**153**) from the leaves and twigs of *M. siamensis*,

exhibited larvicidal activity against the larvae of *Aedes aegypti* mosquito (Nobsathian *et al.*, 2018).

The distribution of chemical constituents in the family Brassicaceae and genera *Capparis* and *Maerua* of family Capparaceae is presented in Tables 1, 2 and 3.

Table 1. Distribution of Indole alkaloids family Brassicaceae

Compound	Source	Plant part	Reference
Arvelexin (1)	<i>Isatis indigotica</i>	Roots	Yang <i>et al.</i> (2014)
	<i>Thlaspi arvense</i>	Leaves	Pedras <i>et al.</i> (2003)
Benzocamalexin (2)	<i>Thellungiella halophila</i>	Aerial parts	Pedras <i>et al.</i> (2009)
Biswasalexin A1 (3)			
Biswasalexin A2 (4)			
Brassicinal A (5)	<i>Brassica napus</i>	Tubers	Pedras <i>et al.</i> (2004)
Brassicinal B (6)	<i>B. campestris</i>	NI.	(Monde <i>et al.</i> , 1991a)
Brassicinal C (7)	<i>B. oleracea</i> <i>B. rapa</i>		
Brassicinate A (8)	<i>B. napus</i>	Tubers	Pedras <i>et al.</i> (2004)
	<i>I. tinctoria</i>	Roots	Zhang <i>et al.</i> (2022)
Brasilexin (9)	<i>B. juncea</i>	Leaves	Devys <i>et al.</i> , 1998
Brassinin (10)	<i>B. campestris</i>	NI.	Takasugi <i>et al.</i> (1987)
Brassitin (11)	<i>Raphanus sativus</i>	Roots	Monde <i>et al.</i> (1995)
Brussalexin A (12)	<i>B. oleracea</i>	NI.	Pedras <i>et al.</i> (2004)
Camalexin (13)	<i>Camelina sativa</i>	Leaves	Browne <i>et al.</i> (1991)

Compound	Source	Plant part	Reference
Caulilexin A (14)	<i>B. oleracea</i>	NI.	Pedras <i>et al.</i> (2006)
Caulilexin B (15)			
Caulilexin C (16)	<i>B. campestris</i> ssp. <i>chinensis</i>	NI.	Kim <i>et al.</i> (2004)
	<i>I. indigotica</i>	Roots	Yang <i>et al.</i> (2014)
Cephalandole B (17)	<i>I. indigotica</i>	Leaves	Yang <i>et al.</i> (2014) Yang and Bao (2020)
2-[Cyano(3-indolyl)methylene]-3-indolone (18)	<i>I. tinctoria</i>	Whole plants	Ahmad <i>et al.</i> (2008)
(-)- <i>R</i> -2-(3-Cyanomethyl-4-methoxy-1 <i>H</i> -indol-7-yl)-2-(1 <i>H</i> -indol-3-yl) acetonitrile (19)	<i>I. indigotica</i>	Roots	Chen <i>et al.</i> (2012)
(-)- <i>R</i> -2-(3-Cyanomethyl-4-methoxy-1 <i>H</i> -indol-7-yl)-2-(4-methoxy-1 <i>H</i> -indol-3-yl) acetonitrile (20)	<i>I. indigotica</i>	Roots	Chen <i>et al.</i> (2012)
Cyclobrassinin (21)	<i>B. campestris</i>	NI.	Takasugi <i>et al.</i> (1987)
Cyclobrassinin sulfoxide (22)	<i>B. juncea</i>	NI.	Devys <i>et al.</i> (1990)
Cyclobrassinone (23)	<i>B. oleracea</i> var <i>gongylodes</i>	Stems	Gross <i>et al.</i> (1994)
Dehydrocyclobrassinin (24)	<i>B. napus</i>	Roots	Pedras <i>et al.</i> (2008a)
9 α ,13 α -Dihydroxylisopropylidenyl-isatisine A (25)	<i>I. tinctoria</i>	Roots	Hong <i>et al.</i> (2019)
(+)-(<i>S</i>)-2-(3,4-Dihydroxy-2-oxoindolin-3-yl) acetonitrile (26)	<i>I. indigotica</i>	Roots	Chen <i>et al.</i> (2012)
Dioxibrassinin (27)	<i>B. oleracea</i>	NI.	Monde <i>et al.</i> (1991a)

Compound	Source	Plant part	Reference
2,2-Di-(3-indolyl)-3-indolone (28)	<i>I. indigotica</i>	Leaves	Yang and Bao (2020)
	<i>I. tinctoria</i>	Roots	Zhang <i>et al.</i> (2022)
Epi glucoisatisin (29)	<i>I. tinctoria</i>	Roots	Frechard <i>et al.</i> (2001)
	<i>I. tinctoria</i>	Whole plants	Ahmad <i>et al.</i> (2008)
Epiisatidifoliumoside A (30)	<i>I. indigotica</i>	Leaves	Guo <i>et al.</i> (2020)
Epiisatidifoliumoside B (31)			
Epiphaitanthrin A (32)	<i>I. indigotica</i>	Roots	Liu <i>et al.</i> (2016)
Erucalexin (33)	<i>Erucastrum gallicum</i>	Leaves	(Pedras <i>et al.</i> , 2006)
Glucobrassicin (34)	<i>B. oleracea</i>	NI.	Gmelin <i>et al.</i> (1960)
Glucoisatisin (35)	<i>I. tinctoria</i>	Seeds	Antoine <i>et al.</i> (2001)
2-[(4- β -D-Glucopyranosyloxy)-1H-indol-3-yl] acetonitrile (36)	<i>I. tinctoria</i>	Roots	Zhang <i>et al.</i> (2022)
β -D-Glucopyranosyl Indole-3-carboxylic acid (37)	<i>I. tinctoria</i>	Roots	Zhang <i>et al.</i> (2022)
Homobrassicin (38)	<i>B. oleracea</i>	NI.	(Mehta <i>et al.</i> , 1995)
3'-Hydroxyepi glucoisatisin (39)	<i>I. tinctoria</i>	Whole plants	Ahmad <i>et al.</i> (2008)
	<i>I. tinctoria</i>	NI.	Antoine <i>et al.</i> (2001)
4-Hydroxyglucobrassicin (40)	<i>B. oleracea</i>	NI.	Truscott <i>et al.</i> (1983)
3'-Hydroxyglucoisatisin (41)	<i>I. tinctoria</i>	Seeds	Antoine <i>et al.</i> (2001)

Compound	Source	Plant part	Reference
(<i>E</i>)-2-(4-Hydroxy-2-oxoindolin-3-ylidene)acetonitrile (42)	<i>I. indigotica</i>	Roots	Chen <i>et al.</i> (2012)
(-)-(<i>R</i>)-2-(4-Hydroxy-2-oxoindolin-3-yl)acetamide (43)	<i>I. indigotica</i>	Roots	Chen <i>et al.</i> (2012)
(-)-(<i>R</i>)-2-(4-Hydroxy-2-oxoindolin-3-yl)acetonitrile (44)			
(+)-(<i>S</i>)-2-(3-Hydroxy-4-methoxy-2-oxoindolin-3-yl)acetamide (45)			
(-)-(<i>S</i>)-2-(3-Hydroxy-4-methoxy-2-oxoindolin-3-yl)acetonitrile (46)			
(+)-(<i>S</i>)-2-[7-[1-(4-Hydroxyphenyl)-ethyl]-4-methoxy-1 <i>H</i> -indol-3-yl]acetonitrile (47)	<i>I. indigotica</i>	Roots	Chen <i>et al.</i> (2012)
(2 <i>E</i>)- <i>N</i> -(2-Hydroxyphenyl)-2-(1-hydroxy-3-oxoindolin-2-ylidene)acetamide (48)	<i>I. indigotica</i>	Leaves	Yang and Bao (2020)
(-)-(<i>2R,3R</i>)-3-Hydroxy-2 <i>H</i> -pyrrolo[2,3- <i>b</i>]indolo[5,5 <i>a</i> ,6- <i>b</i> , <i>a</i>]quinazoline-9(<i>8H</i>),7'-dione (49)	<i>I. indigotica</i>	Roots	Chen <i>et al.</i> Chen <i>et al.</i> (2012)
(+)-(<i>2S,3S</i>)-3-Hydroxy-2 <i>H</i> -pyrrolo[2,3- <i>b</i>]indolo[5,5 <i>a</i> ,6- <i>b</i> , <i>a</i>]quinazoline-9(<i>8H</i>),7'-dione (50)			
Indigotin (51)	<i>I. indigotica</i>	Leaves, Roots	Zou (2007)
Indirubin (52)	<i>Isatis folium</i>	Leaves	Lu <i>et al.</i> (2012)
3-Indoleacetic acid (53)	<i>B. oleracea</i> var. <i>capitata</i>	Heads	Weller <i>et al.</i> (1953)

Compound	Source	Plant part	Reference
Indole-3-acetonitrile (54)	<i>B. campestris</i> L. spp. <i>rapa</i> .	NI.	Kim <i>et al.</i> (2004)
Indole-3-acetonitrile-2- <i>S</i> - β -D-glucopyranoside (55)	<i>I. indigotica</i>	Roots	Yang <i>et al.</i> (2014)
Indole-3-acetonitrile-6- <i>O</i> - β -D-glucopyranoside (56)	<i>I. indigotica</i>	Roots	Li <i>et al.</i> (2003)
Indole-3-acetonitrile-4-methoxy-2- <i>S</i> - β -D-glucopyranoside (57)	<i>I. indigotica</i>	Roots	Yang <i>et al.</i> (2014)
1 <i>H</i> -Indole-3-carboxylic acid (58)	<i>I. tinctoria</i>	Roots	Zhang <i>et al.</i> (2022)
3-Indoleformic acid (59)	<i>I. indigotica</i>	Roots	Yang <i>et al.</i> (2014)
	<i>I. tinctoria</i>	Roots	Zhang <i>et al.</i> (2022)
2-(1 <i>H</i> -Indol-2-yl)-6-methoxy-4(3 <i>H</i>)-quinazolinone (60)	<i>I. tinctoria</i>	Roots	Zhang <i>et al.</i> (2019)
(<i>Z</i>)-2-(1 <i>H</i> -Indol-3-ylmethylene)-1,2-dihydro-3 <i>H</i> -indol-3-one (61)	<i>I. indigotica</i>	Roots	Chen <i>et al.</i> (2012)
2-(1 <i>H</i> -Indol-2-yl)-4(3 <i>H</i>)-quinolinone (62)	<i>I. tinctoria</i>	Roots	Zhang <i>et al.</i> (2019)
Isalexin (63)	<i>B. napus</i> var. <i>rapifera</i>	Tubers	Pedras <i>et al.</i> (2004)
Isatan A (64)	<i>I. indigotica</i>	Roots	Oberthur <i>et al.</i> (2004)
	<i>I. tinctoria</i>	NI. Whole plants	Oberthur <i>et al.</i> (2004) Ahmad <i>et al.</i> (2008)
Isatan B (65)	<i>I. tinctoria</i>	NI.	Oberthur <i>et al.</i> (2004)
Isatibisindosulfonic acid A 3- <i>O</i> - β -D-glucopyranoside (66)	<i>I. indigotica</i>	Roots	Meng <i>et al.</i> (2017)
Isatibisindosulfonic acid B (67)			

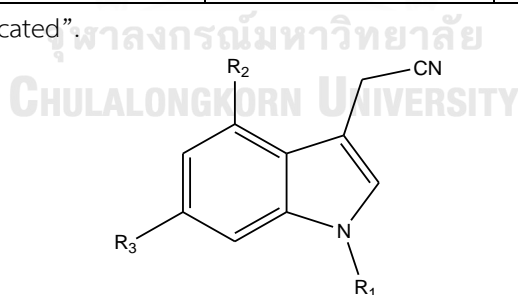
Compound	Source	Plant part	Reference
Isatidifoliumoside A (68)	<i>I. indigotica</i>	Leaves	Guo <i>et al.</i> (2020)
Isatidifoliumoside B (69)			
Isatidifoliumoside D (70)			
Isatigotindoledioside A (71)	<i>I. indigotica</i>	Roots	Meng <i>et al.</i> (2017)
Isatigotindoledioside B (72)			
Isatigotindoledioside C (73)			
Isatigotindoledioside D (74)			
Isatigotindoledioside E (75)			
Isatigotindoledioside F (76)			
Isatin (77)	<i>I. indigotica</i>	Roots	Zhang <i>et al.</i> (2019)
Isatindigobisindoloside A (78)	<i>I. indigotica</i>	Roots	Liu <i>et al.</i> (2015)
Isatindigobisindoloside B (79)			
Isatindigobisindoloside C (80)	<i>I. indigotica</i>	Roots	Liu <i>et al.</i> (2015)
Isatindigobisindoloside D (81)	<i>I. indigotica</i>	Roots	Zhang <i>et al.</i> (2019)
Isatindigobisindoloside E (82)	<i>I. indigotica</i>	Roots	Liu <i>et al.</i> (2015)
Isatindigobisindoloside F (83)			
Isatindigobisindoloside G (84)			
Isatindigodiphindoside (85)	<i>I. indigotica</i>	Roots	Meng <i>et al.</i> (2018)
Isatindigoside D (86)	<i>I. tinctoria</i>	Roots	Zhang <i>et al.</i> (2019)
Isatindigoside F (87)	<i>I. tinctoria</i>	Roots	Zhang <i>et al.</i> (2020)
Isatindigoside G (88)			
Isatindigoside H (89)	<i>I. indigotica</i>	Roots	Zhang <i>et al.</i> (2020)
Isatindigoside I (90)			
Isatindigoside J (91)			
Isatindigoside K (92)			
Isatindigoside L (93)			

Compound	Source	Plant part	Reference
Isatindigoside M (94)	<i>I. tinctoria</i>	Roots	Zhang <i>et al.</i> (2022)
Isatindigotindoloside B (95)	<i>I. tinctoria</i>	Roots	Zhang <i>et al.</i> (2019)
Isatindolignanoside A (96)	<i>I. indigotica</i>	Roots	Lingjie <i>et al.</i> (2018)
Isatindosulfonic acid B (97)	<i>I. indigotica</i>	Roots	Meng <i>et al.</i> (2017)
Isatindosulfonic acid C (98)			
Isatindosulfonic acid D (99)			
Isatindosulfonic acid E (100)			
Isatindosulfonic acid F (101)			
Isatisindigoticanine A (102)	<i>I. tinctoria</i>	Roots	Zhang <i>et al.</i> (2019)
Isatisindigoticanine F (103)	<i>I. tinctoria</i>	Roots	Zhang <i>et al.</i> (2019)
Isatisindigoticanine G (104)			
Isatisindigoticanine H (105)	<i>I. tinctoria</i>	Roots	Zhang <i>et al.</i> (2020)
Isatisindigoticanine I (106)			
Isatisindigoticanine J (107)	<i>I. indigotica</i>	Roots	Zhang <i>et al.</i> (2020)
Isatisindigoticanine K (108)			
Isatisindigoticanine L (109)			
Isatisindigoticanine M (110)	<i>I. tinctoria</i>	Roots	Zhang <i>et al.</i> (2022)
Isatisindigoticanine N (111)			
Isatisine A (112)	<i>I. indigotica</i>	Leaves	Liu <i>et al.</i> (2007)
1-Methoxybrassenin A (113)	<i>B. oleracea</i> var. <i>capitata</i>	NI.	Monde <i>et al.</i> (1991b)
1-Methoxybrassenin B (114)			
1-Methoxybrassinin (115)	<i>B. campestris</i> var. <i>pekinensis</i>	NI.	Takasugi <i>et al.</i> (1987)
4-Methoxybrassinin (116)	<i>B. oleracea</i>	NI.	Monde <i>et al.</i> (1990)

Compound	Source	Plant part	Reference
1-Methoxybrassinin (117)	<i>B. oleracea</i> var. <i>botrytis</i>	NI.	Pedras <i>et al.</i> (2006)
6-Methoxycamalexin (118)	<i>Capsella bursapastoris</i>	Leaves	Jimenez <i>et al.</i> (1997)
4-Methoxycyclobrassinon (119)	<i>B. napus</i>	Roots	Pedras (2008b)
4-Methoxydehydrocyclobrassinin (120)			
4-Methoxyglucobrassicin (121)	<i>B. oleracea</i>	NI.	Truscott <i>et al.</i> (1983)
4-Methoxy-3-indoleacetic acid (122)	<i>I. indigotica</i>	Roots	Yang <i>et al.</i> (2014)
<i>N</i> -Methoxy-indole-3-acetonitrile-2- <i>S</i> - β - <i>D</i> -glucopyranoside (123)	<i>I. indigotica</i>	Roots	Yang <i>et al.</i> (2014)
1-Methoxy-3-indoleformic acid (124)	<i>I. tinctoria</i>	Roots	Zhang <i>et al.</i> (2022)
	<i>I. indigotica</i>	Roots	Yang <i>et al.</i> (2014)
	<i>Wasabia japonica</i>	NI.	Somei <i>et al.</i> (2001)
1-Methoxyspirobrassinin (125)	<i>B. oleracea</i>	Stems	Gross <i>et al.</i> (1994)
1-Methoxyspirobrassinol (126)	<i>Raphanus sativus</i> var. <i>hortensis</i>	Roots	Monde <i>et al.</i> (1995)
(2 <i>R</i> ,3 <i>R</i>)-1-Methoxyspirobrassinol methyl ether (127)			
1-Methylbenzocamalexin (128)	<i>B. oleracea</i>	NI.	Pedras <i>et al.</i> (2010)
1-Methyl-6'-cyanobenzocamalexin (129)			
1-Methyl-6'-methoxybenzocamalexin (130)			
Methyl-1 <i>H</i> -methoxyindole-3-carboxylate (131)	<i>W. japonica</i>	NI.	Pedras <i>et al.</i> (1998)
Methyl quindoline-11-carboxylate (132)	<i>I. indigotica</i>	Leaves	Yang and Bao (2020)
Phaitanthrin A (133)	<i>I. indigotica</i>	Roots	Liu <i>et al.</i> (2016)
Phaitanthrin D (134)	<i>I. indigotica</i>	Leaves	Yang and Bao (2020)

Compound	Source	Plant part	Reference
	<i>Phaius mishensis</i>	NI.	Jao <i>et al.</i> (2008)
Rapalexin A (135)	<i>B. napus</i>	Leaves	Pedras <i>et al.</i> (2007)
Rapalexin B (136)			
Rutalexin (137)	<i>B. napus var. rapifera</i>	Tubers	Pedras <i>et al.</i> (2004)
Sinalbin A (138)	<i>Sinapis alba</i>	Leaves	Pedras <i>et al.</i> (2000)
Sinalbin B (149)			
Sinalexin (140)	<i>S. alba</i>	NI.	Soledade <i>et al.</i> (1997)
(S)-Spirobrassinin (141)	<i>Rhaphanus sativus</i> <i>var. hortensis</i>	NI.	Takasugi <i>et al.</i> (1987)
Sulfoglucobrassicin (142)	<i>I. tinctoria</i>	Whole plants	Ahmad <i>et al.</i> (2008)
Tryptanthrin (143)	<i>I. indigotica</i>	Leaves	Wei <i>et al.</i> (2019)
	<i>I. tinctoria</i>	Roots	Speranza <i>et al.</i> (2020)
Wasalexin A (144)	<i>W. japonica</i>	NI.	Pedras <i>et al.</i> (1999)
Wasalexin B (146)			

NI. refers to “not indicated”.



Arvelexin (**1**); R₁= H, R₂= OCH₃, R₃= H

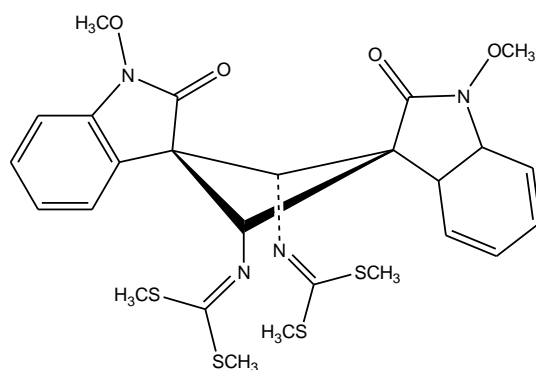
1-Methoxy-indole-3-acetonitrile (Caulilexin C) (**16**); R₁= OCH₃, R₂= H, R₃= H

2-[(4-β-D-Glucopyranosyloxy)-1-indol-3-yl] acetonitrile (**36**); R₁= H, R₂= O-Glu, R₃= H

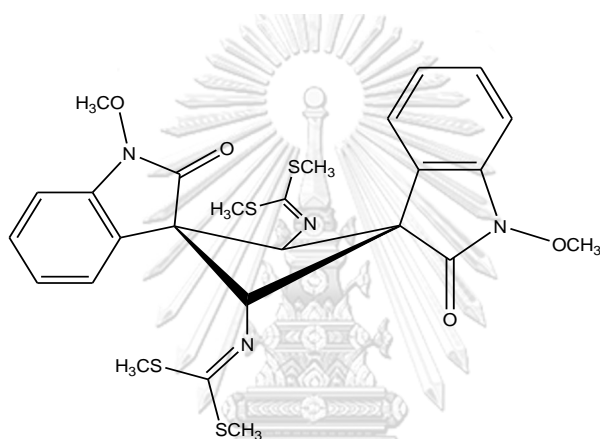
Indole-3-acetonitrile (**54**); R₁= H, R₂= H, R₃= H

Indole-3-acetonitrile-6-O-β-D-glucopyranoside (**56**); R₁= H, R₂= H, R₃= O-Glu

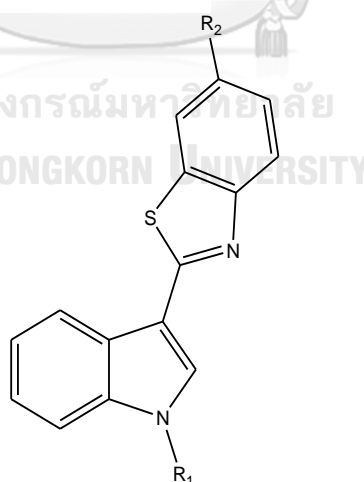
Isatindigotindoloside B (**97**); R₁= OCH₃, R₂= H, R₃= O-Glu



Biswasalexin A1 (3)



Biswasalexin A2 (4)

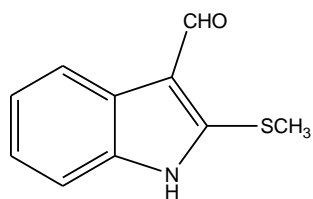


Benzocamalexin (2); $R_1 = R_2 = H$

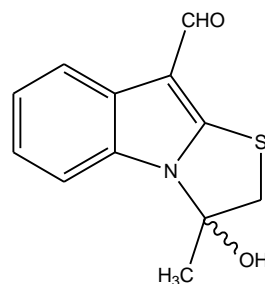
1-Methylbenzocamalexin (128); $R_1 = CH_3, R_2 = H$

1-Methyl-6'-cyanobenzocamalexin (129); $R_1 = CH_3, R_2 = CN$

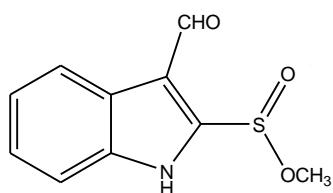
1-Methyl-6'-methoxybenzocamalexin (130); $R_1 = CH_3, R_2 = OCH_3$



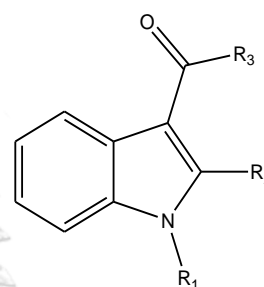
Brassicanal A (5)



Brassicanal B (6)

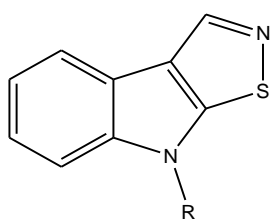
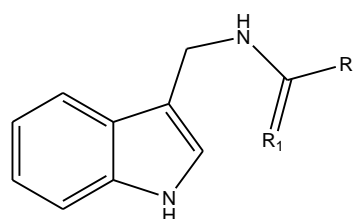


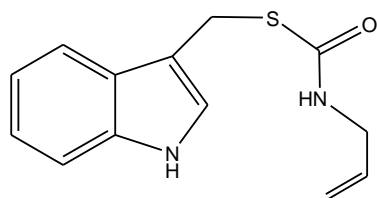
Brassicanal C (7)

Brassicanate A (8); $R_1 = \text{H}$, $R_2 = \text{SCH}_3$, $R_3 = \text{OCH}_3$ β -D-Glucopyranosyl indole-3-carboxylic acid (37); $R_1 = R_2 = \text{H}$, $R_3 = \text{O-Glu}$ 1*H*-Indole-3-carboxylic acid (58); $R_1 = R_2 = \text{H}$, $R_3 = \text{OH}$ 3-Indoleformic acid (59); $R_1 = \text{H}$, $R_2 = \text{SCH}_3$, $R_3 = \text{OH}$ Isatindigoside M (97); $R_1 = \text{OCH}_3$, $R_2 = \text{H}$, $R_3 = \text{O-Glu}$ Methyl-1*H*-methoxyindole-3-carboxylate (131); $R_1 = \text{OCH}_3$, $R_2 = \text{H}$, $R_3 = \text{OCH}_3$ 1-Methoxy-3-indoleformic acid (124); $R_1 = \text{OCH}_3$, $R_2 = \text{H}$, $R_3 = \text{OH}$ 

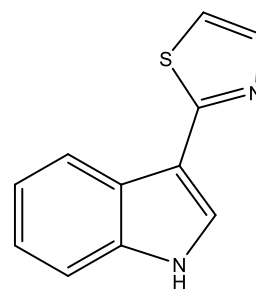
จุฬาลงกรณ์

CHULALONGKORN UNIVERSITY

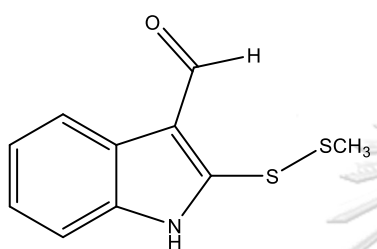
Brassilexin (9) $R = \text{H}$ Sinalexin (140) $R = \text{OCH}_3$ Brassinin (10); $R_1 = \text{S}$, $R_2 = \text{SCH}_3$ Brassitin (11); $R_1 = \text{O}$, $R_2 = \text{SCH}_3$ Caulilexin B (15); $R_1 = \text{O}$, $R_2 = \text{H}$



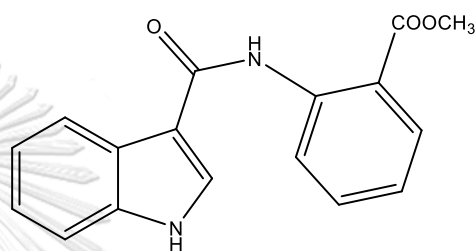
Brussalexin A (12)



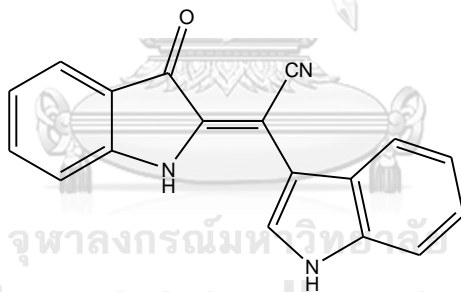
Camalexin (13)



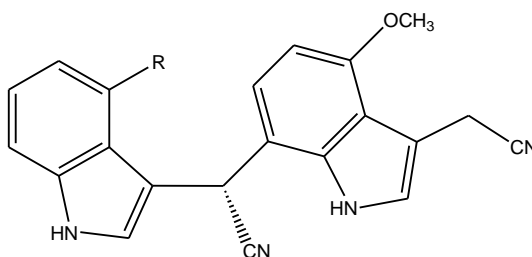
Caulilexin A (14)



Cephalandole B (17)



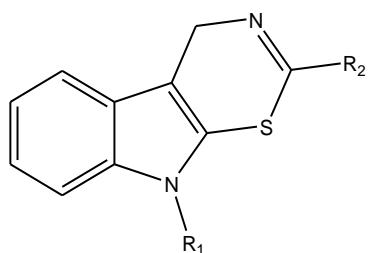
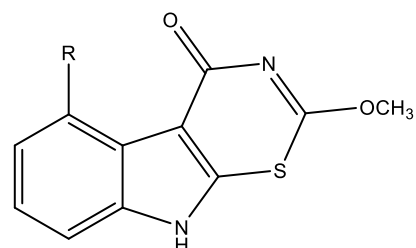
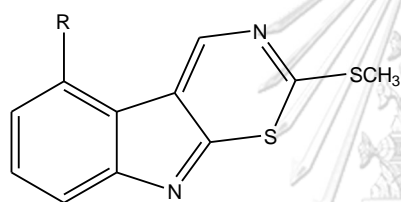
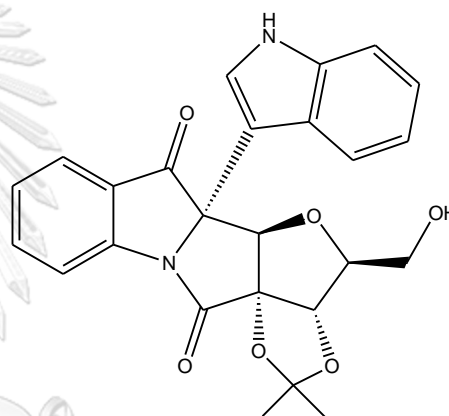
2-[Cyano(3-indolyl)methylene]-3-indolone (18)



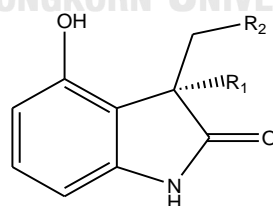
(-)-*R*-2-(3-Cyanomethyl-4-methoxy-1*H*-indol-7-yl)-2-(1*H*-indol-3-yl) acetonitrile (19); R= H

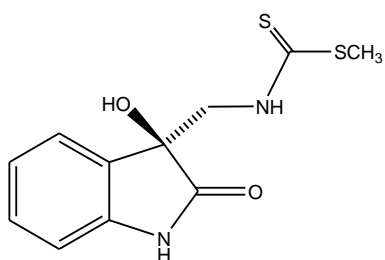
(-)-*R*-2-(3-Cyanomethyl-4-methoxy-1*H*-indol-7-yl)-2-(4-methoxy-1*H*-indol-3-yl) acetonitrile (20)

; R= OCH₃

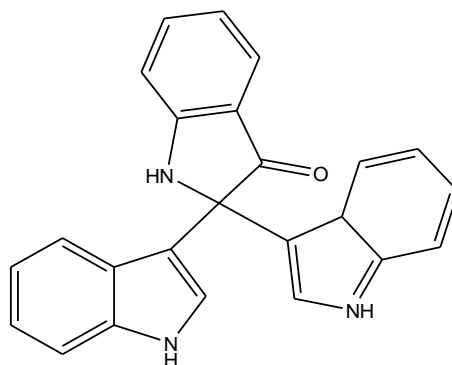
Cyclobrassinin (**21**); R₁ = H, R₂ = SCH₃Cyclobrassinin sulfoxide (**22**); R₁ = H, R₂ = S(O)CH₃Sinalbin A (**138**); R₁ = OCH₃, R₂ = S(O)CH₃Sinalbin B (**139**); R₁ = OCH₃, R₂ = SCH₃Cyclobrassinone (**23**); R = H4-Methoxycyclobrassinone (**119**); R = OCH₃Dehydrocyclobrassinin (**24**); R₁ = H4-Methoxydehydrocyclobrassinin (**121**); R₁ = OCH₃9α,13α-Dihydroxylisopropylidenyl-isatisine A (**25**)

CHULALONGKORN UNIVERSITY

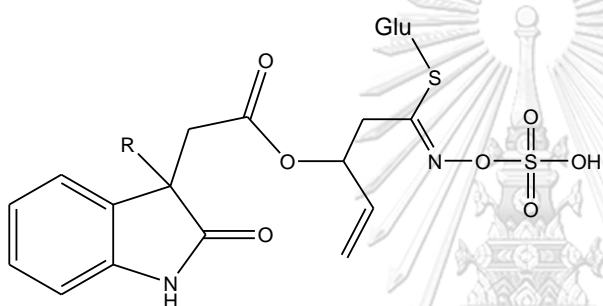
(+)-(S)-2-(3,4-Dihydroxy-2-oxoindolin-3-yl) acetonitrile (**26**); R₁ = OH, R₂ = CN(-)-(R)-2-(4-Hydroxy-2-oxoindolin-3-yl) acetamide (**43**); R₁ = H, R₂ = CONH₂(-)-(R)-2-(4-Hydroxy-2-oxoindolin-3-yl) acetonitrile (**45**);R₁ = H, R₂ = CN



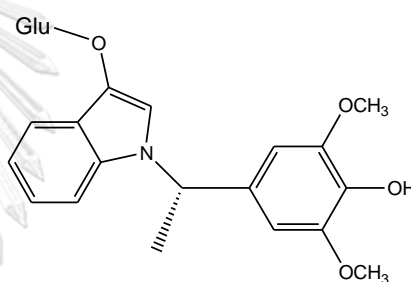
Dioxibrassinin (27)



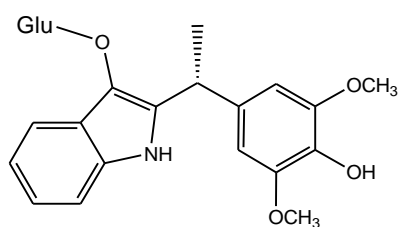
2,2-Di-(3-indolyl)-3-indolone (28)

Epiglucoisatisin (29); R= H, *S*-configurationGlucoisatisin (35); R= H, *R*-configuration

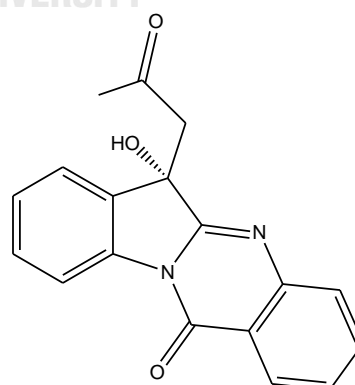
3'-Hydroxyepiglucoisatisin (39); R= OH



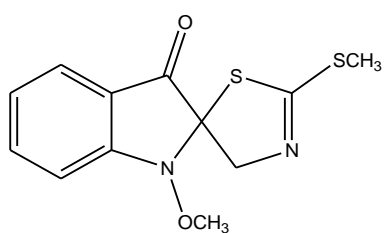
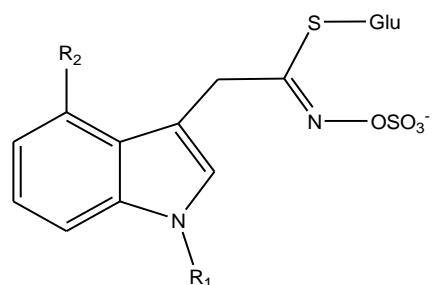
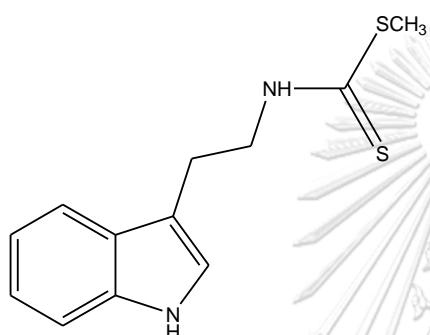
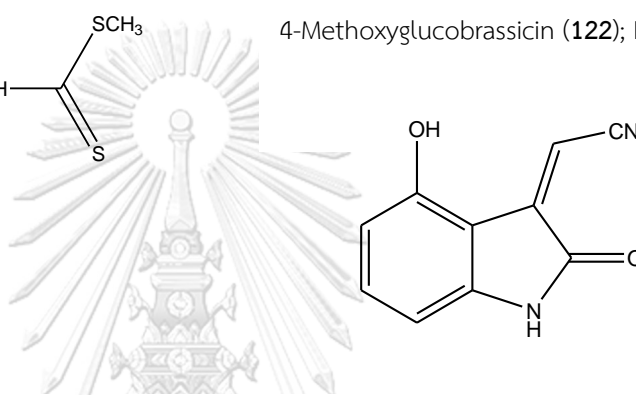
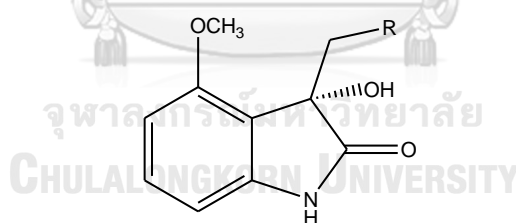
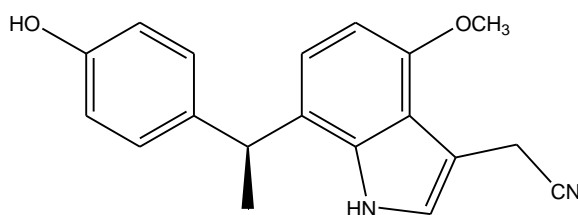
Epiisatidifolioside A (30)

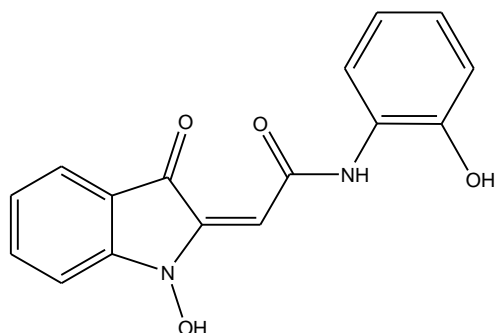


Epiisatidifolioside B (31)

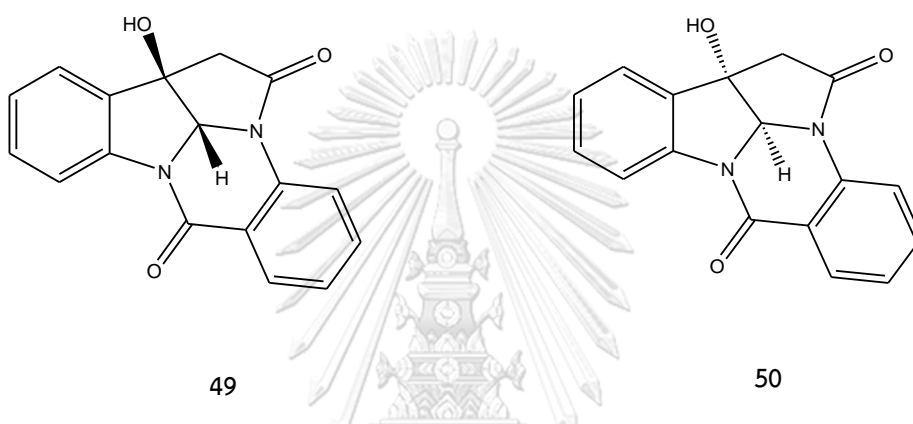


Epiphaitanthrin A (32)

Erucalexin (**33**)Glucobrassicin (**34**); $R_1 = R_2 = H$ 4-Hydroxyglucobrassicin (**40**); $R_1 = H, R_2 = OH$ 4-Methoxyglucobrassicin (**122**); $R_1 = H, R_2 = OCH_3$ Homobrassicin (**38**)*(E)*-2-(4-Hydroxy-2-oxoindolin-3-ylidene) acetonitrile (**42**)*(+)*-(*S*)-2-(3-Hydroxy-4-methoxy-2-oxoindolin-3-yl) acetamide (**45**); $R = CONH_2$ *(+)*-(*S*)-2-(3-Hydroxy-4-methoxy-2-oxoindolin-3-yl) acetonitrile (**46**); $R = CN$ *(+)*-(*S*)-2-[7-[1-(4-Hydroxyphenyl)-ethyl]-4-methoxy-1*H*-indol-3-yl] acetonitrile (**47**)

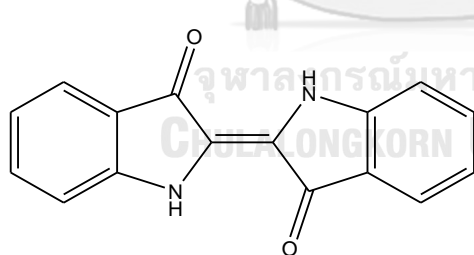


(2E)-N-(2-Hydroxyphenyl)-2-(1-hydroxy-3-oxoindolin-2-ylidene) acetamide (**48**)

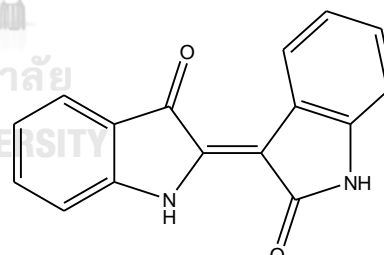


(-)-(2R,3R)-3-Hydroxy-2H-pyrrolo[2,3-b]indolo[5,5a,6-b,a]quinazoline-9(8H),7'-dione (**49**)

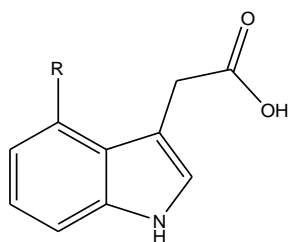
(+)-(2S,3S)-3-Hydroxy-2H-pyrrolo[2,3-b]indolo[5,5a,6-b,a]quinazoline-9(8H),7'-dione (**50**)



Indigotin (**51**)

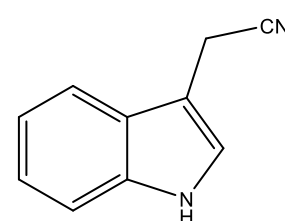


Indirubin (**52**)

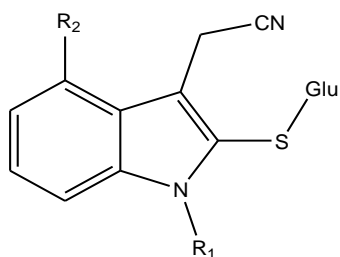


3-Indoleacetic acid (**53**); R= H

4-Methoxy-3-indoleacetic acid (**122**); R= OCH₃



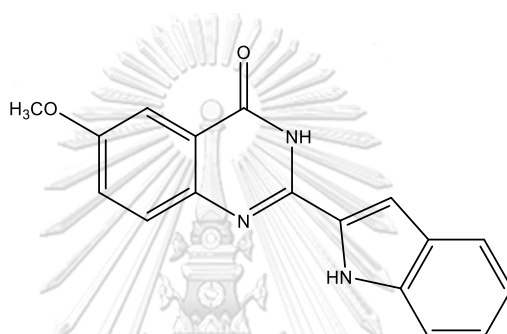
Indole-3-acetonitrile (**54**)



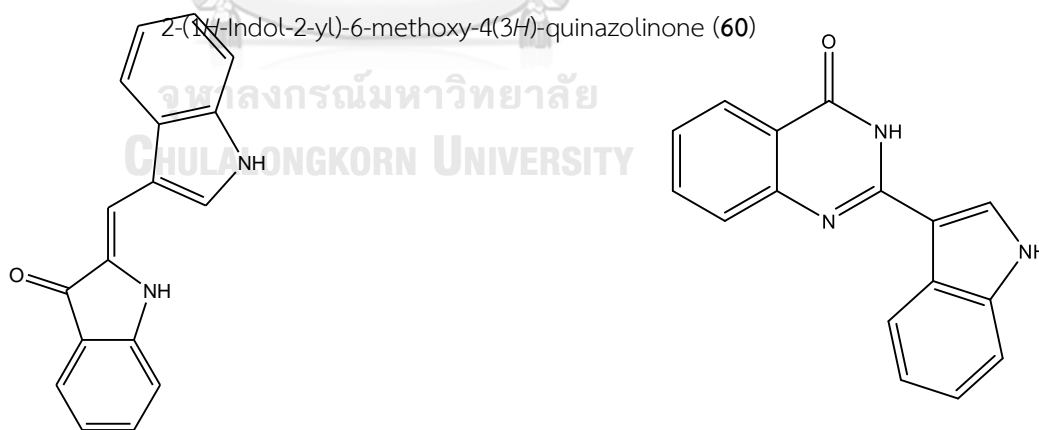
Indole-3-acetonitrile-2-*S*- β -D-glucopyranoside (**55**); $R_1 = R_2 = H$

Indole-3-acetonitrile-4-methoxy-2-*S*- β -D-glucopyranoside (**57**); $R_1 = H$, $R_2 = OCH_3$

N-Methoxy-indole-3-acetonitrile-2-*S*- β -D-glucopyranoside (**123**); $R_1 = OCH_3$, $R_2 = H$

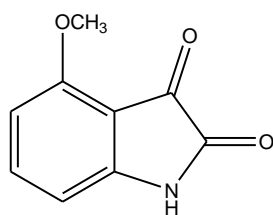


2-(1*H*-Indol-2-yl)-6-methoxy-4(3*H*)-quinazolinone (**60**)

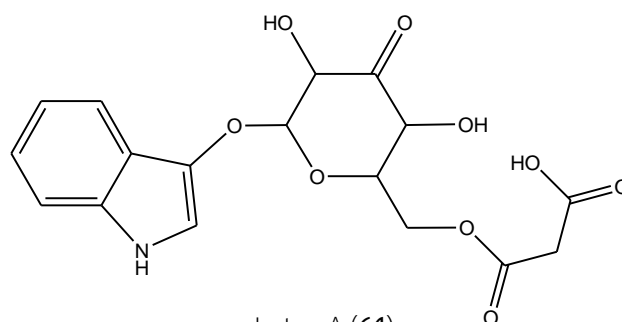


(*Z*)-2-(1*H*-Indol-3-yl-methylidene)-1,2-dihydro-3*H*-indol-3-one (**61**)

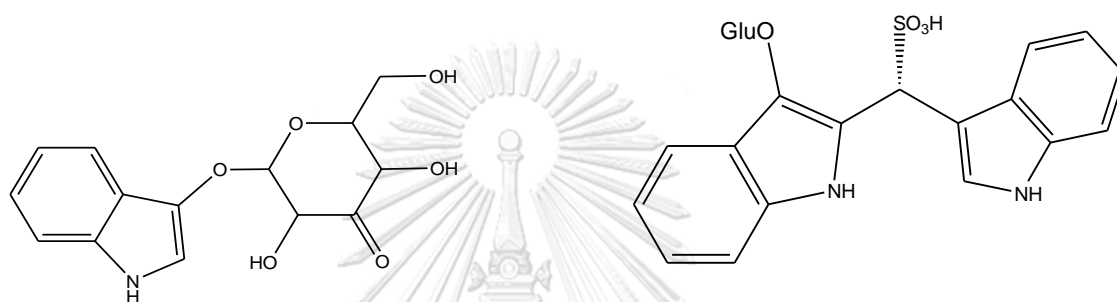
2-(1*H*-Indol-2-yl)-4(3*H*)-quinolinone (**62**)



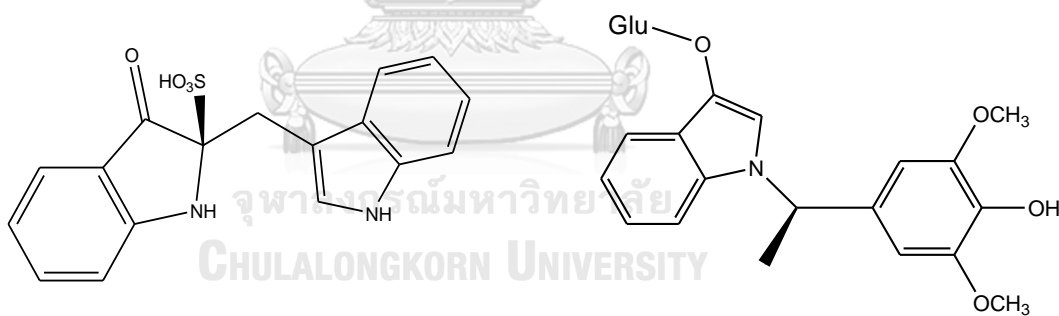
Isalexin (63)



Isatan A (64)

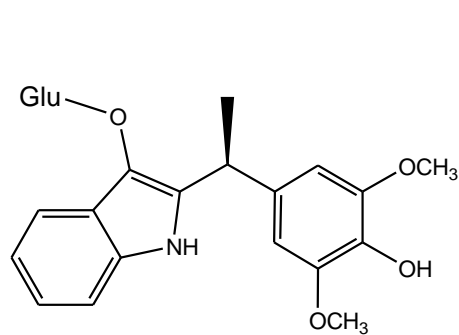


Isatan B (65)

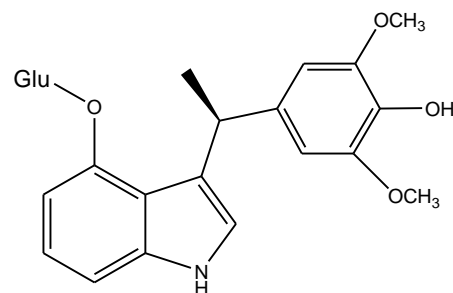
Isatibisindosulfonic acid A 3-*O*- β -D-glucopyranoside (66)

Isatibisindosulfonic acid B (67)

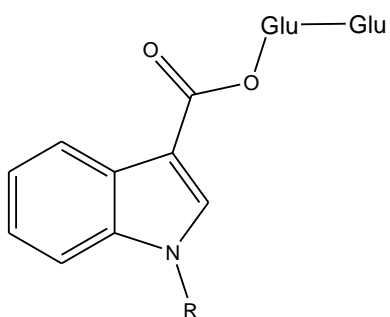
Isatidifoliumoside A (68)



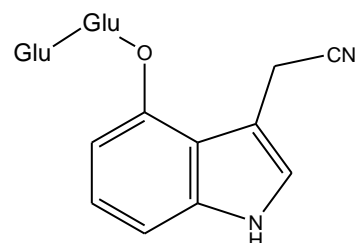
Isatidifoliumoside B (69)



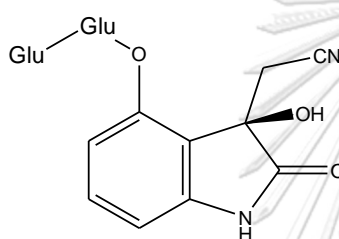
Isatidifoliumoside D (70)

Isatigotindoleoside A (71); R= OCH₃

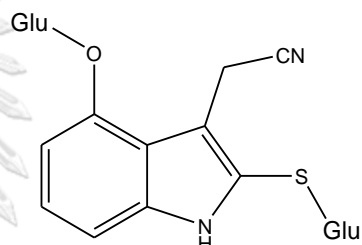
Isatigotindoleoside B (72); R= H



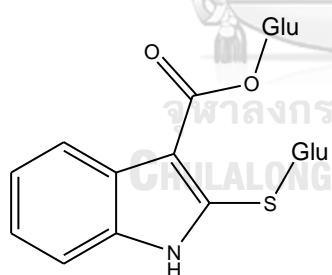
Isatigotindoleoside C (73)



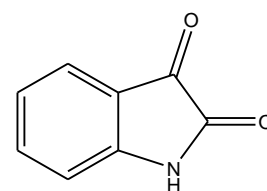
Isatigotindoleoside D (74)



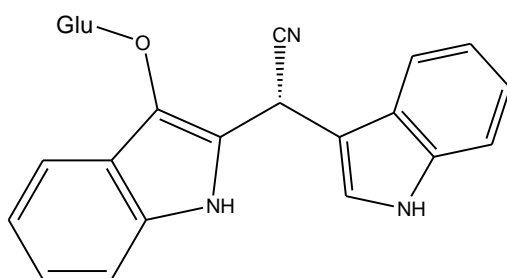
Isatigotindoleoside E (75)



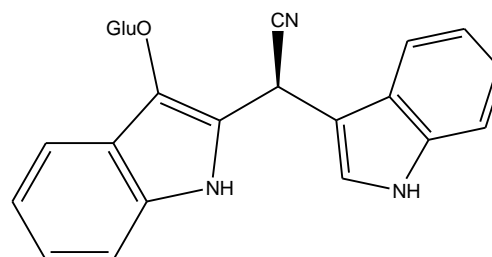
Isatigotindoleoside F (76)



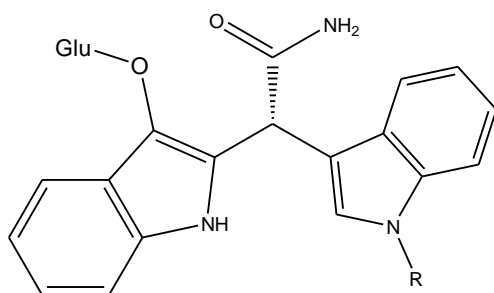
Isatin (77)



Isatindigobisindoloside A (78)

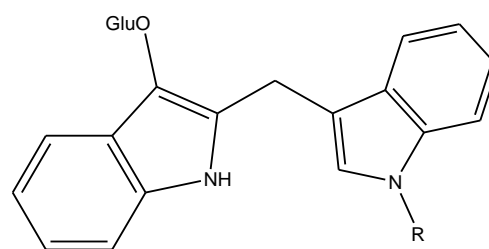


Isatindigobisindoloside B (79)



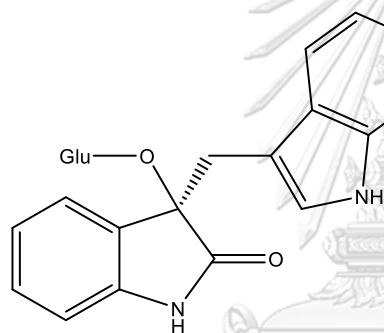
Isatindigobisindolose C (80)

Isatindigolose J (91)

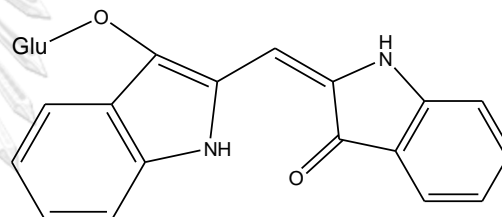


Isatindigobisindolose D (81)

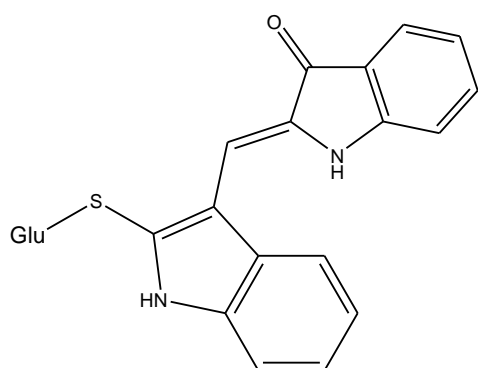
Isatindigolose H (93)



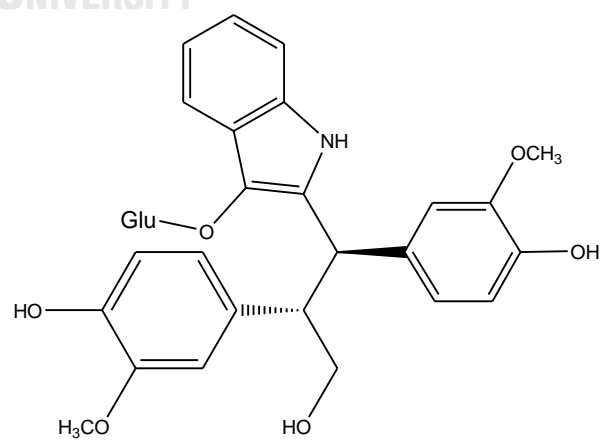
Isatindigobisindolose E (82)



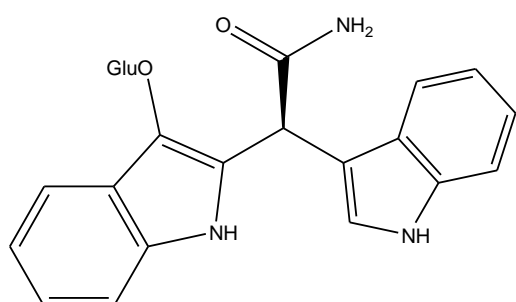
Isatindigobisindolose F (83)



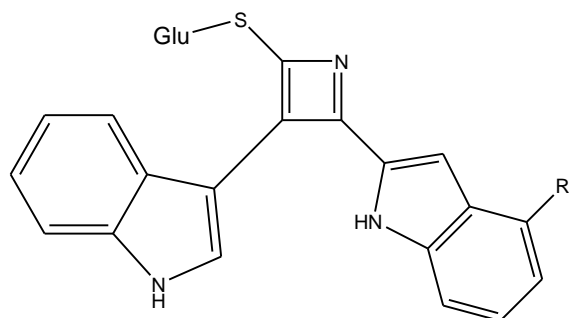
Isatindigobisindolose G (84)



Isatindigodiphindolide (85)

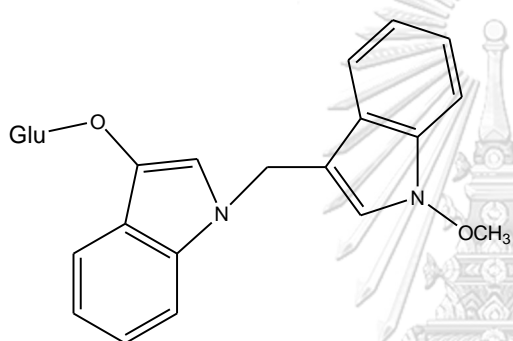


Isatindigoside D (86)

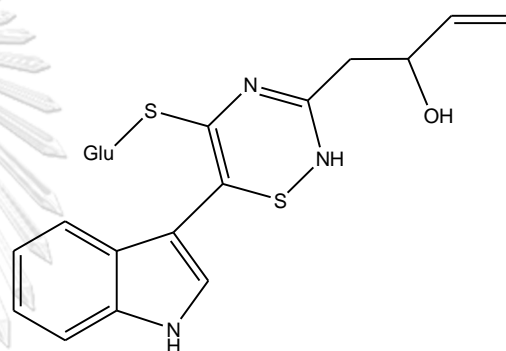


Isatindigoside F (87)

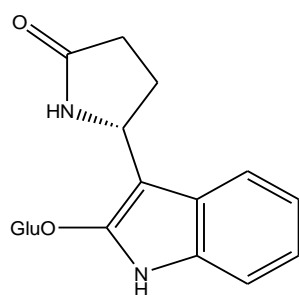
Isatindigoside G (88)



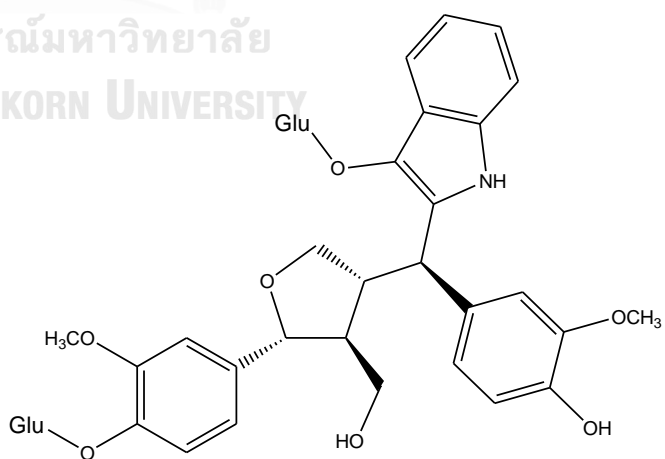
Isatindigoside I (90)



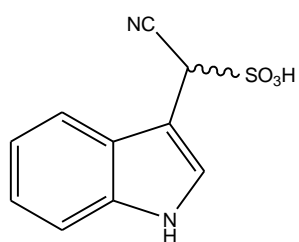
Isatindigoside K (92)



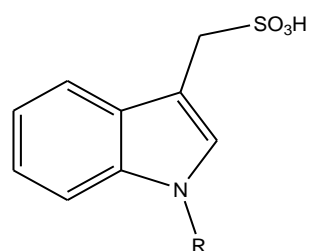
Isatindigoside L (93)



Isatindolignanose A (96)

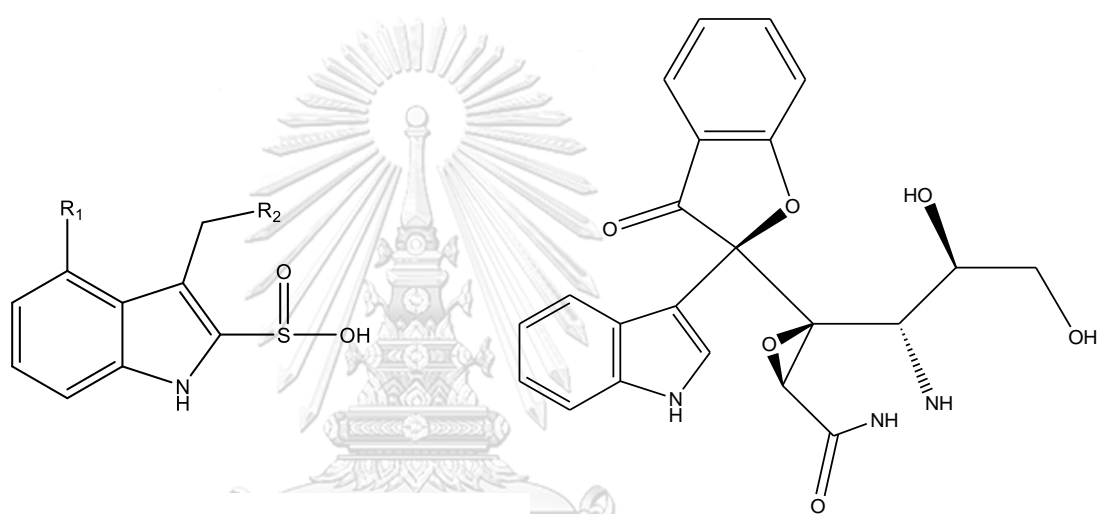


Isatindosulfonic acid B (97)



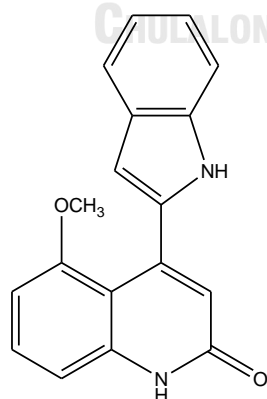
Isatindosulfonic acid C (98)

Isatindosulfonic acid E (100)

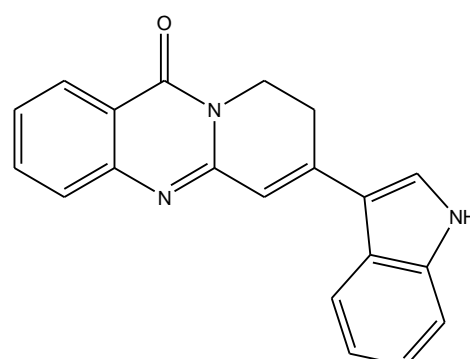
Isatindosulfonic acid D (99); R₁= OCH₃, R₂= CNIsatindosulfonic acid D (101); R₁= H, R₂= COOH

Isatisindigoticanine A (102)

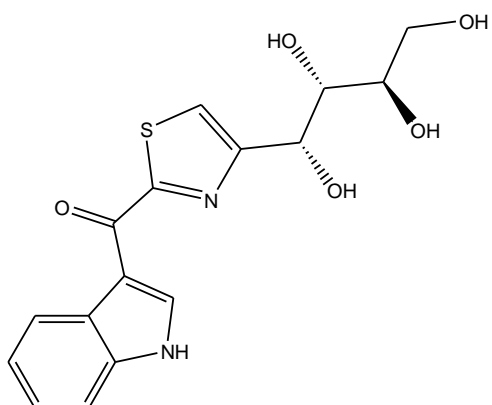
จุฬาลงกรณ์มหาวิทยาลัย
CHULALONGKORN UNIVERSITY



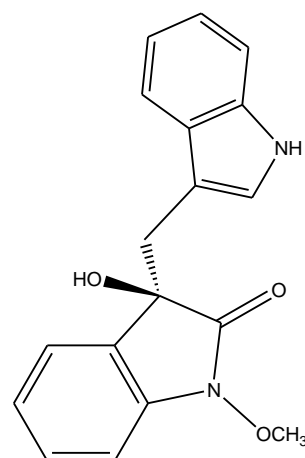
Isatisindigoticanine F (103)



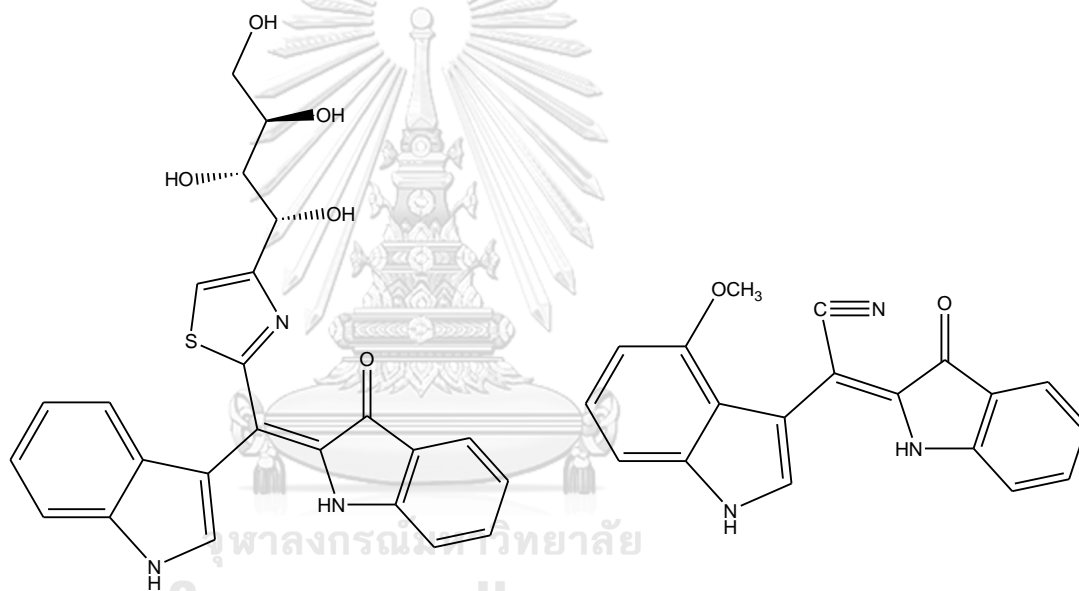
Isatisindigoticanine G (104)



Isatisindigoticanine H (105)

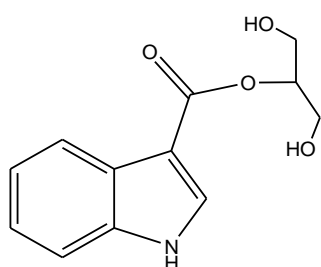


Isatisindigoticanine I (106)

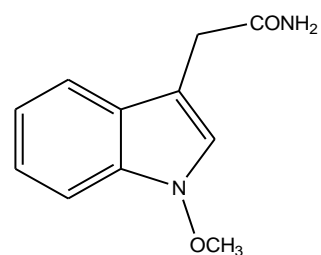


Isatisindigoticanine J (107)

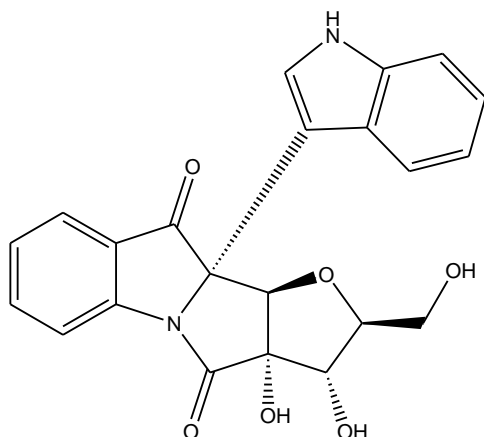
Isatisindigoticanine K (108)



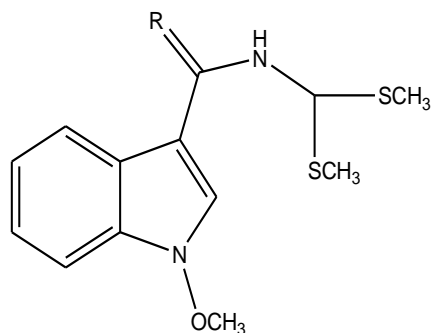
Isatisindigoticanine M (110)



Isatisindigoticanine N (111)

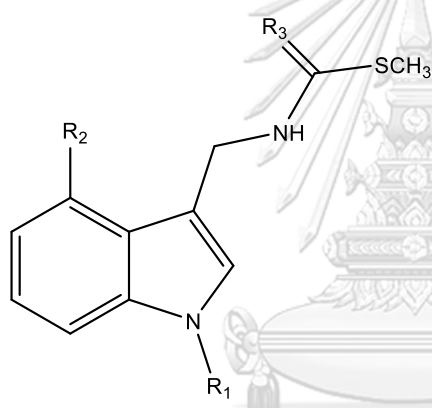
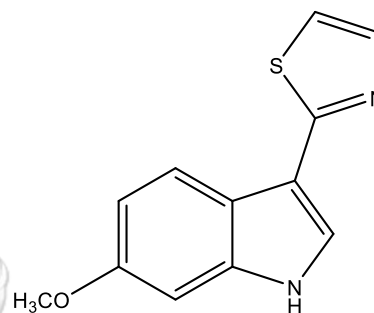


Isatisine A (112)

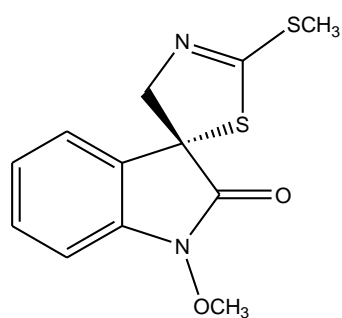


1-Methoxybrassenin A (113)

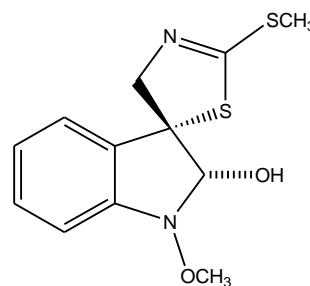
1-Methoxybrassenin B (114)

1-Methoxybrassinin (115); $R_1 = \text{OCH}_3$, $R_2 = \text{H}$, $R_3 = \text{S}$ 4-Methoxybrassinin (116); $R_1 = \text{H}$, $R_2 = \text{OCH}_3$, $R_3 = \text{S}$ 1-Methoxybrassitin (117); $R_1 = \text{OCH}_3$, $R_2 = \text{H}$, $R_3 = \text{O}$ 

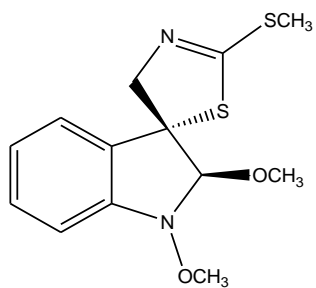
6-Methoxycamalexin (118)



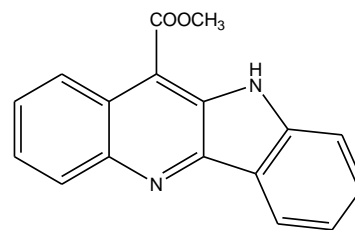
1-Methoxyspirobrassinin (125)



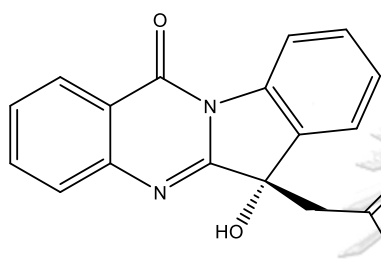
1-Methoxyspirobrassinol (126)



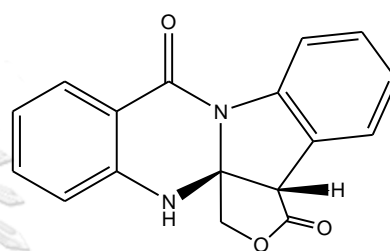
(2*R*,3*R*)-1-Methoxyspirobrassinol methyl ether (127)



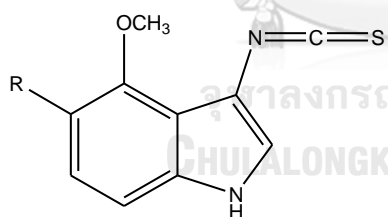
Methyl quindoline-11-carboxylate (132)



Phaitanthrin A (133)

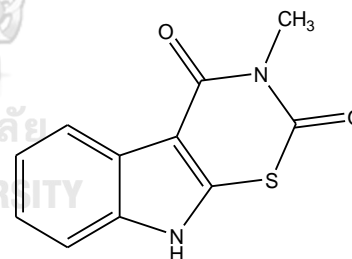


Phaitanthrin D (134)

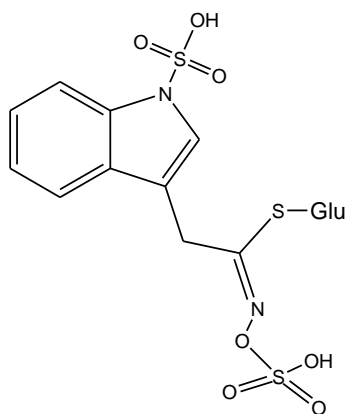


Rapalexin A; R= H (135)

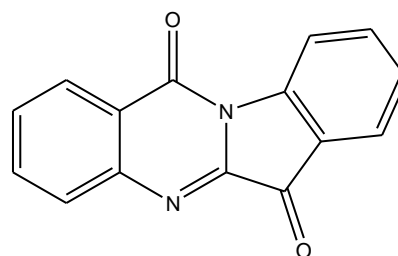
Rapalexin B; R= OH (136)



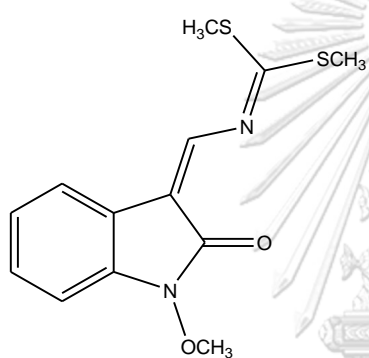
Rutalexin (137)



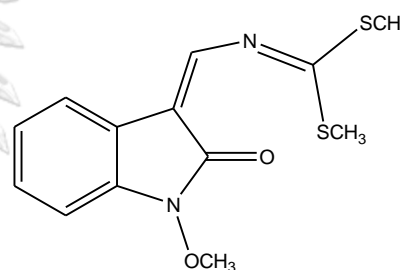
Sulfolucobrassicin (142)



Tryptanthrin (143)



Wasalexin A (144)



Wasalexin B (145)

Table 2. Chemical constituents of plants in the genus *Capparis*

Compounds	Source	Plant part	Reference
Alkaloids			
14- <i>N</i> -Acetylisocodonocarpine (146) 15- <i>N</i> -Acetylcapparisine (147)	<i>Capparis decidua</i>	Root barks	Forster <i>et al.</i> (2016)
Berberine (148)	<i>C. dongvanensis</i>	Leaves	Khang <i>et al.</i> (2021)
Cadabicine (149)	<i>C. decidua</i>	NI.	Ahmad <i>et al.</i> (1986)
	<i>C. spinosa</i>	Root barks	Khanfar <i>et al.</i> (2003)

Compounds	Source	Plant part	Reference
Capparidisine (150)	<i>C. decidua</i>	NI.	Ahmad <i>et al.</i> (1986)
Capparidisinine (151)	<i>C. decidua</i>	Root barks	Forster <i>et al.</i> (2016)
Cappariloside A (152)	<i>C. spinosa</i>	Fruits	Calis <i>et al.</i> (1999)
Cappariloside B (153)			
Capparin A (154)	<i>C. sinaica</i>	Fruits	Zhou <i>et al.</i> (2010)
Capparin B (155)	<i>C. himalayensis</i>	NI.	Li <i>et al.</i> (2008)
Capparisine (156)	<i>C. decidua</i>	Root barks	Ahmad <i>et al.</i> (1986)
Capparisine A (157)	<i>C. spinosa</i>	Fruits	Yang <i>et al.</i> (2010)
Capparisine B (158)			
Capparisine C (159)			
Capparispine (160)	<i>C. spinosa</i>	Roots	Fu <i>et al.</i> (2008)
Codonocarpine (161)	<i>C. decidua</i>	Root barks	Forster <i>et al.</i> (2016)
Flazin (162)	<i>C. spinosa</i>	Fruits	Zhou <i>et al.</i> (2010)
4-Hydroxy-1 <i>H</i> -indole-3-carboxaldehyde (163)	<i>C. spinosa</i>	Aerial parts	Zhou <i>et al.</i> (2010)
2-(5-Hydroxymethyl-2-formylpyrrol-1-yl) propionic acid lactone (164)	<i>C. spinosa</i>	Fruits	(Yang <i>et al.</i> , 2010)
3-Hydroxy-3-methyl-4-methoxyoxindole (165)	<i>C. tomentosa</i>	Roots	Akoto <i>et al.</i> (2008)
<i>N</i> -(3'-Maleimidyl)-5-hydroxymethyl-2-pyrrole formaldehyde (166)	<i>C. spinosa</i>	Fruits	Yang <i>et al.</i> , 2010
Stachydrine (167)	<i>C. tomentosa</i>	Roots	Akoto <i>et al.</i> (2008)

Compounds	Source	Plant part	Reference
Tetrahydroquinoline acid (168)	<i>C. spinosa</i>	Stems and Fruits	Zhang <i>et al.</i> (2014)
Long-chain hydrocarbons			
Nonadecan-1-ol (169)	<i>C. dongvanensis</i>	Leaves	Khang <i>et al.</i> (2021)
Octadecanoic acid (170)	<i>C. spinosa</i>	Root barks	Khanfar <i>et al.</i> (2003)
Tetracontane (171)	<i>C. dongvanensis</i>	Leaves	Khang <i>et al.</i> (2021)
1-Tetradecanol (172)	<i>C. spinosa</i>	Root barks	Khanfar <i>et al.</i> (2003)
Flavonoids			
Ginkgetin (173)	<i>C. spinosa</i>	Fruits	H. F. Zhou <i>et al.</i> (2011)
Isoginkgetin (174)	<i>C. spinosa</i>	Fruits	H. F. Zhou <i>et al.</i> (2011)
Isorhamnetin-3-O-rutinoside (175)	<i>C. spinosa</i>	Root barks	Khanfar <i>et al.</i> (2003)
Isoquercetin (176)	<i>C. sinaica</i>	NI.	Ibrahim <i>et al.</i> (2013)
Kaempferol (177)	<i>C. cartilaginea</i>	Leaves	Al-Mahweety and Alyahawi (2020)
	<i>C. spinosa</i>	Buds	Wiese <i>et al.</i> (2013)
	<i>C. spinosa</i>	Fruits	Zhou <i>et al.</i> (2010)
Kaempferol-3-O-rutinoside (178)	<i>C. spinosa</i>	Fruits	H. F. Zhou <i>et al.</i> (2011)
	<i>C. spinosa</i>	Buds	Wiese <i>et al.</i> (2013)

Compounds	Source	Plant part	Reference
Oroxylin A (179)	<i>C. himalayensis</i>	NI.	Li <i>et al.</i> (2008)
Quercetin (180)	<i>C. sinaica</i> <i>C. spinosa</i>	Fruits Buds	Zhou <i>et al.</i> (2010) Wiese <i>et al.</i> (2013)
Rutin (181)	<i>C. sinaica</i>	Fruits	Zhou <i>et al.</i> (2010)
Sakuranetin (182)	<i>C. spinosa</i>	Fruits	H. F. Zhou <i>et al.</i> (2011)
Thevetiaflavone (183)	<i>C. spinosa</i>	Fruits	Zhou <i>et al.</i> (2010)
Wogonin (184)	<i>C. himalayensis</i>	NI.	Li <i>et al.</i> (2008)
Glucosinolates and isothiocyanates			
Glucobrassicin (34)	<i>C. spinosa</i>	NI.	Ahmed <i>et al.</i> (1972)
Glucocapparin (185)	<i>C. spinosa</i>	NI.	Matthaus and Ozcan (2002)
Glucoiberin (186)	<i>C. spinosa</i>	NI.	Ahmed <i>et al.</i> (1972)
3-Methyl-3-butenylisothiocyanate (187)	<i>C. flexuosa</i>	NI.	Gramosa <i>et al.</i> (1997)
3-Methyl-2-butenyl- β -glucoside (189)	<i>C. spinosa</i>	Root barks	Khanfar <i>et al.</i> (2003)
Neoglucobrassicin (190)	<i>C. spinosa</i>	Buds	Wiese <i>et al.</i> (2013)
Phenolic acids			
Caffeic acid (191)	<i>C. spinosa</i>	Buds	Wiese <i>et al.</i> (2013)
4-Coumaric acid (192)	<i>C. spinosa</i>	Root barks	Khanfar <i>et al.</i> (2003)
3,4-Dihydroxybenzoic acid (193)			

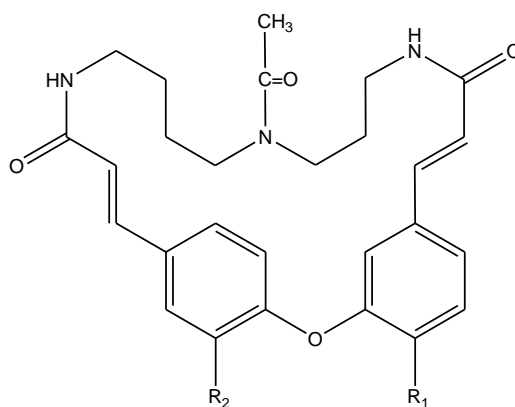
Compounds	Source	Plant part	Reference
Ferulic acid (194)	<i>C. spinosa</i>	Nl.	Aliyazicioglu <i>et al.</i> (2013)
Gallic acid (195)	<i>C. spinosa</i>	Buds	Wiese <i>et al.</i> (2013)
Salicylic acid (196)	<i>C. dongvanensis</i>	Leaves	Khang <i>et al.</i> (2021)
Vanillic acid (197)	<i>C. spinosa</i>	Fruits	Zhou <i>et al.</i> (2010)
Steroids			
5 α ,6 α -Epoxycholestan-3 β -ol (198) 5 β ,6 β -Epoxycholestan-3 β -ol (199)	<i>C. ovata</i>	Buds, Fruits, Flowers, Leaves and Stems	Gazioglu <i>et al.</i> (2020)
β -Sitosterol (200)	<i>C. decidua</i>	Stems	Rathee <i>et al.</i> (2012)
	<i>C. dongvanensis</i>	Leaves	Khang <i>et al.</i> (2021)
	<i>C. cartilaginea.</i>	Leaves	Khang <i>et al.</i> (2021)
	<i>C. spinosa</i>	Root barks	Khanfar <i>et al.</i> (2003)
	<i>C. ovata</i>	Buds, Fruits, Flowers, Leaves and Stems	Gazioglu <i>et al.</i> , 2020)
β -Sitosterol 3- <i>O</i> - β -D-glucopyranoside (201)	<i>C. dongvanensis</i>	Leaves	Khang <i>et al.</i> (2021)

Compounds	Source	Plant part	Reference
	<i>C. spinosa</i>	Root barks	Khanfar <i>et al.</i> (2003)
Stigmasterol (202)	<i>C. ovata</i>	Buds, Fruits, Flowers, Leaves and Stems	Gazioglu <i>et al.</i> (2020)
Terpenoids			
Capparisol A (203)	<i>C. spinosa</i>	Root barks	Khanfar <i>et al.</i> (2003)
Dihydroxy-lup-20(29)-en-28-oic acid (204)	<i>C. cartilaginea</i>	Leaves	Al-Mahweety and Alyahawi (2020)
(+)-(6 <i>S</i> ,9 <i>S</i>)-9- <i>O</i> - β -D-Glucopyranosyloxy-6-hydroxy-3-oxo- α -ionol (205) (-)-(6 <i>S</i> ,9 <i>S</i>)-9- <i>O</i> - β -D-Glucopyranosyloxy-6,13-dihydroxy-3-oxo- α -ionol (206)	<i>C. spinosa</i>	Root barks	Khanfar <i>et al.</i> (2003)
Lupeol (207)	<i>M. siamensis</i>	Leaves and Twigs	Nobsathian <i>et al.</i> (2018)
Olean-12-en-3 β ,28-diol 3 β -pentacosanoate (208)	<i>C. ovata</i>	Buds, Fruits, Flowers, Leaves and Stems	Gazioglu <i>et al.</i> (2020)
Oleanolic acid (209)	<i>C. ovata</i>	Buds, Fruits, Flowers, Leaves and Stems	Gazioglu <i>et al.</i> (2020)
Simiarenol (210)	<i>C. spinosa</i>	Root barks	Khanfar <i>et al.</i> (2003)
Taraxerol (211)	<i>C. ovata</i>	Buds, Fruits, Flowers, Leaves and Stems	Gazioglu <i>et al.</i> (2020)

Compounds	Source	Plant part	Reference
Ursolic acid (212)	<i>C. spinosa</i>	Root barks	Khanfar <i>et al.</i> (2003)
Miscellaneous			
Benzoic acid (213)	<i>C. dongvanensis</i>	Leaves	Calis <i>et al.</i> (1999) Khang <i>et al.</i> (2021)
Bismethyl-octylphthalate (214)	<i>C. ovata</i>	Buds, Fruits, Flowers, Leaves and Stems	Gazioglu <i>et al.</i> (2020)
Guanosine (215)	<i>C. spinosa</i>	Fruits	Zhou <i>et al.</i> (2010)
(+)- <i>R</i> -2-(4-Hydroxy-2-oxo-2,3-dihydrobenzofuran-3-yl) acetonitrile (216) (+)- <i>S</i> -2-(4-Hydroxy-2-oxo-2,3-dihydrobenzofuran-3-yl) acetonitrile (217)	<i>C. spinosa</i>	Fruits and Stems	Zhang <i>et al.</i> (2014)
Nicotinamide (218)	<i>C. spinosa</i>	Root barks	Khanfar <i>et al.</i> (2003)
<i>Para</i> -hydroxybenzaldehyde (219)	<i>C. spinosa</i>	Root barks	Khanfar <i>et al.</i> (2003)
Phthalic acid (220)	<i>C. decidua</i>	Root barks	Forster <i>et al.</i> (2016)
Tryptophan (221)	<i>C. dongvanensis</i>	Leaves	Khang <i>et al.</i> (2021)

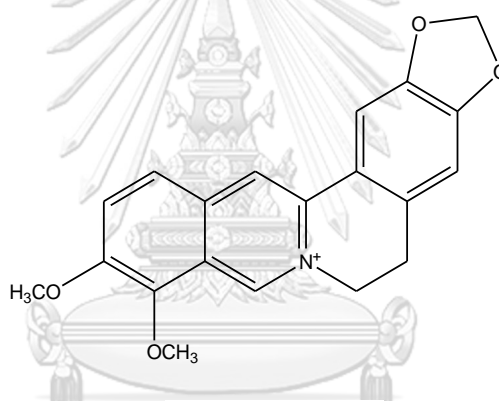
Nl. refers to “not indicated”.

Alkaloids

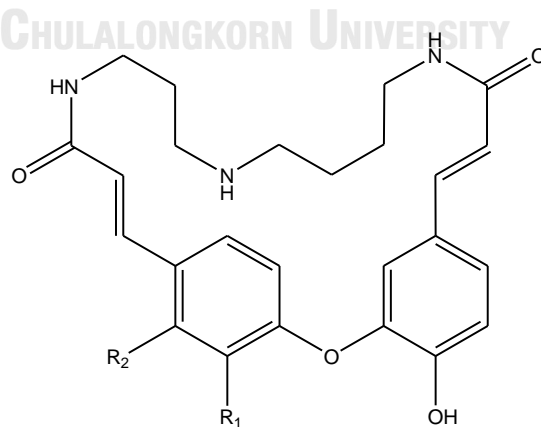


14-*N*-Acetylcodonocarpine (**146**); $R_1 = \text{OCH}_3$, $R_2 = \text{OH}$

15-*N*-Acetylcodonocarpine (**147**); $R_1 = \text{OH}$, $R_2 = \text{OCH}_3$

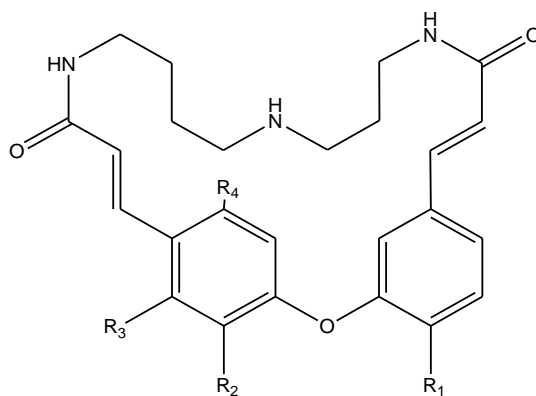


Berberine (**148**)



Cadabicine; $R_1 = R_2 = \text{H}$ (**149**)

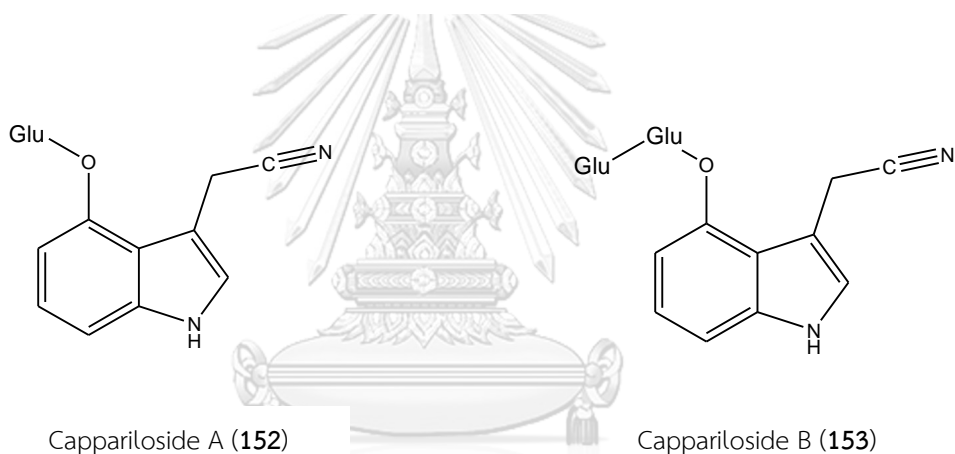
Capparisidine; $R_1 = R_2 = \text{OCH}_3$ (**150**)



Capparidisinine; $R_1 = \text{OCH}_3$, $R_2 = \text{OH}$, $R_3 = \text{OCH}_3$, $R_4 = \text{OCH}_3$ (**151**)

Capparisine; $R_1 = \text{OH}$, $R_2 = \text{H}$, $R_3 = \text{OCH}_3$, $R_4 = \text{H}$ (**156**)

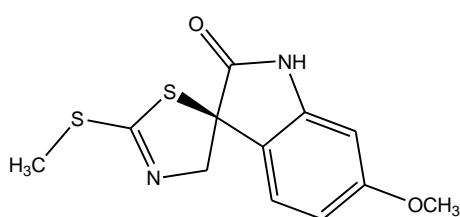
Codonocarpine; $R_1 = \text{OH}$, $R_2 = \text{OCH}_3$, $R_3 = \text{H}$, $R_4 = \text{H}$ (**161**)



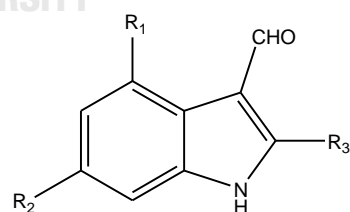
Cappariloside A (**152**)

Cappariloside B (**153**)

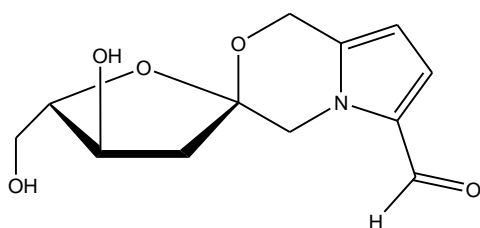
จุฬาลงกรณ์มหาวิทยาลัย
CHULALONGKORN UNIVERSITY



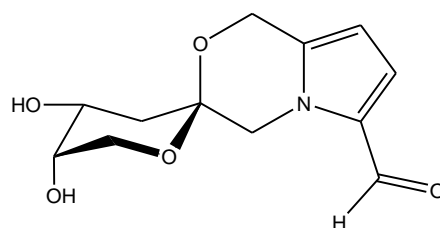
Capparin A (**154**)



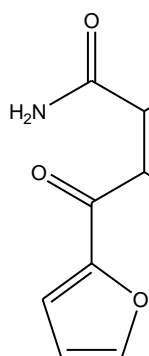
Capparine B (**155**); $R_1 = \text{H}$, $R_2 = \text{OCH}_3$, $R_3 = \text{SCH}_3$
4-Hydroxy-1*H*-indole-3-carbaldehyde (**163**);
 $R_1 = \text{OH}$, $R_2 = R_3 = \text{H}$



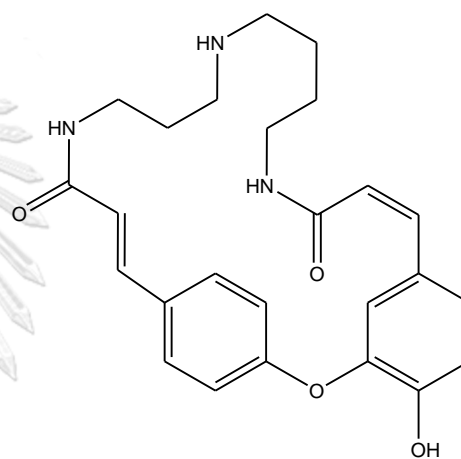
Capparisine A (157)



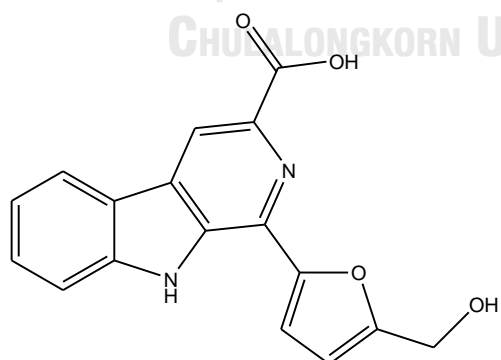
Capparisine B (158)



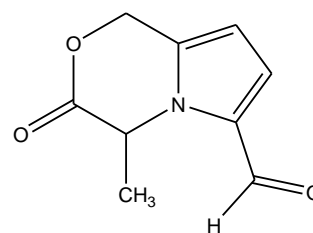
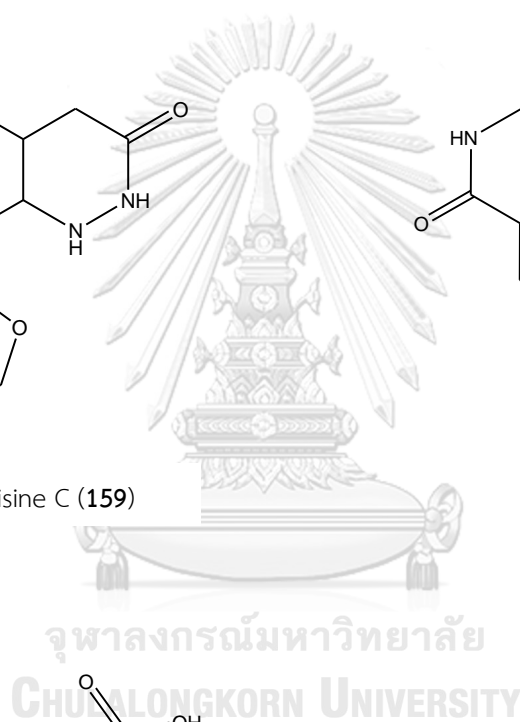
Capparisine C (159)

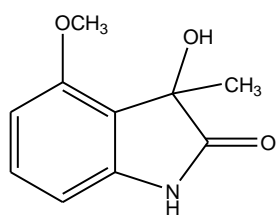


Capparispine (160)

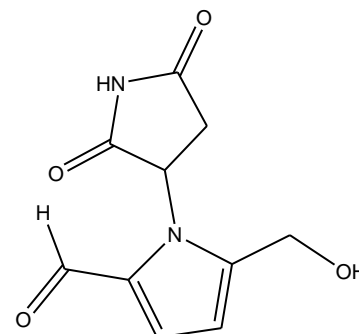
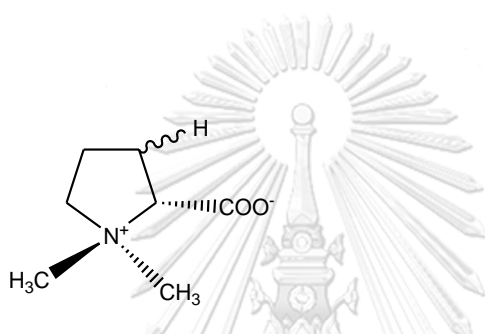


Flazin (162)

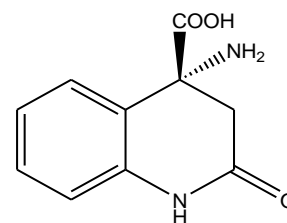
2-(5-Hydroxymethyl-2-formylpyrrol-1-yl)
propionic acid lactone (164)



3-Hydroxy-3-methyl-4-methoxyoxindole (165)

*N*-(3'-Maleimidyl)-5-hydroxymethyl-2-pyrrole formaldehyde (166)

Stachydrine; R= H (167)

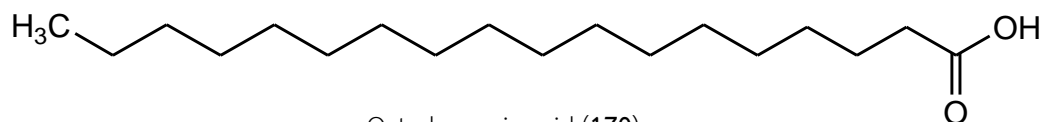


Tetrahydroquinoline acid (168)

Long chain hydrocarbons



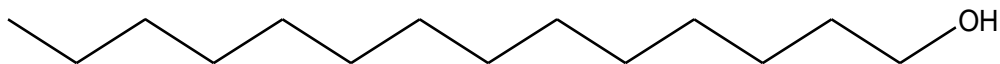
Nonadecan-1-ol (169)



Octadecanoic acid (170)

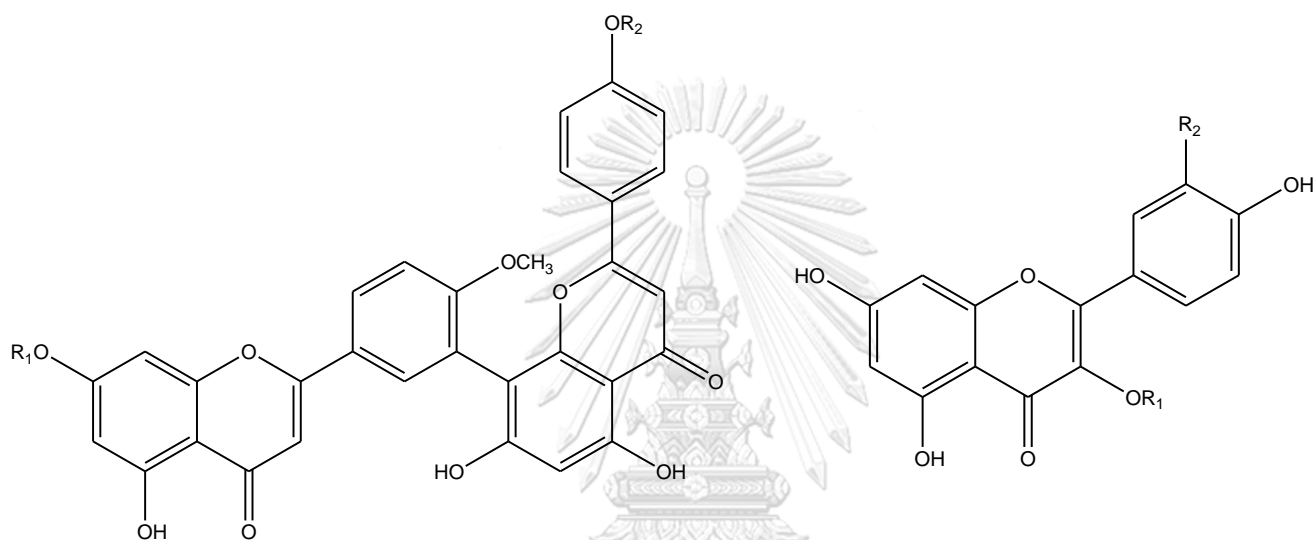
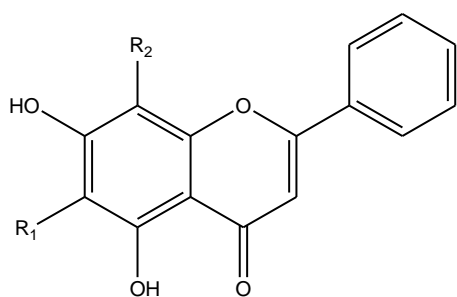
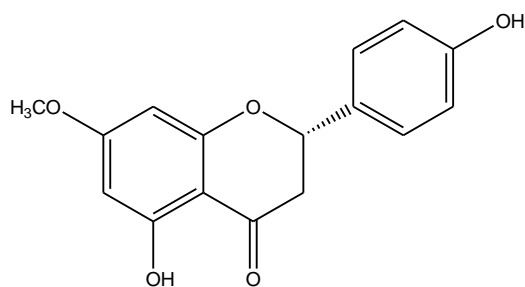


Tetracontane (171)

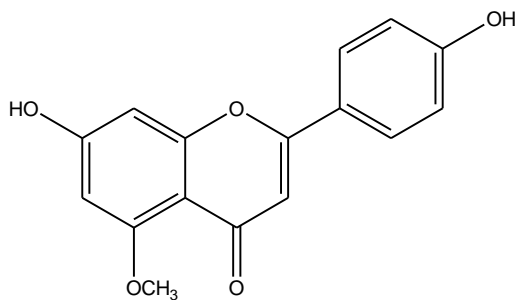


1-Tetradecanol (172)

Flavonoids

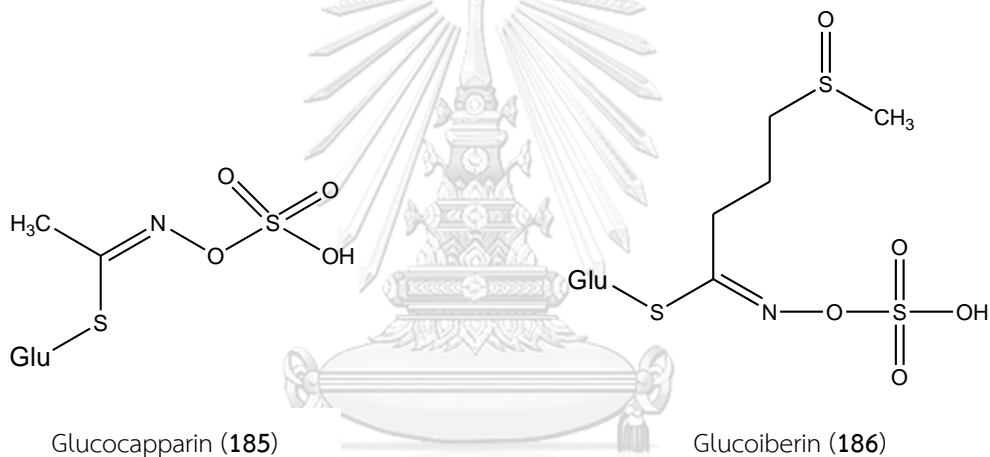
Ginkgetin (173); $R_1 = \text{CH}_3$, $R_2 = \text{H}$ Isoginkgetin (174); $R_1 = \text{H}$, $R_2 = \text{CH}_3$ Isorhamnetin-3-O-rutinoside (175); $R_1 = \text{rutinoside}$, $R_2 = \text{OCH}_3$ Isoquercetin (176); $R_1 = \text{Glu}$, $R_2 = \text{OH}$ Kaempferol (177); $R_1 = R_2 = \text{H}$ Kaempferol-3-O-rutinoside (178); $R_1 = \text{rutinoside}$, $R_2 = \text{H}$ Quercetin (180); $R_1 = \text{H}$, $R_2 = \text{OH}$ Rutin (181); $R_1 = \text{rutinoside}$, $R_2 = \text{OH}$ Oroxylin A (179); $R_1 = \text{OCH}_3$, $R_2 = \text{H}$ Wogonin (184); $R_1 = \text{H}$, $R_2 = \text{OCH}_3$ 

Sakuranetin (182)



Thevetiaflavone (183)

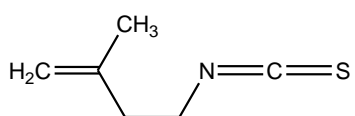
Glucosinolates and isothiocyanates



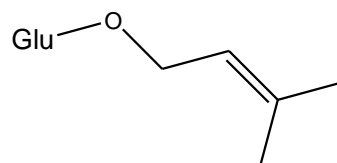
Glucocapparin (185)

Glucoiberin (186)

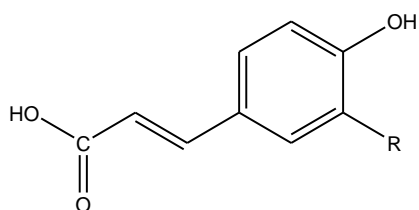
จุฬาลงกรณ์มหาวิทยาลัย
CHULALONGKORN UNIVERSITY



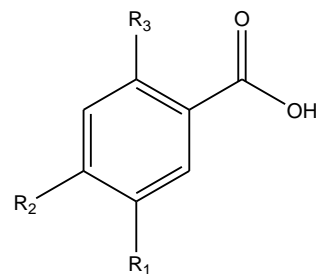
3-Methyl-3-butenylisothiocyanate (187)

3-Methyl-2-butenyl- β -glucoside (188)

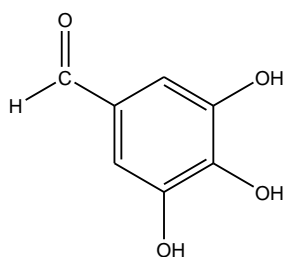
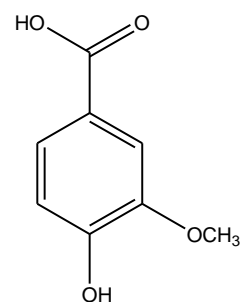
Phenolic acids



Caffeic acid (**191**); R = OH
 4-Coumaric acid (**192**); R = H
 Ferulic acid (**194**); R = OCH₃

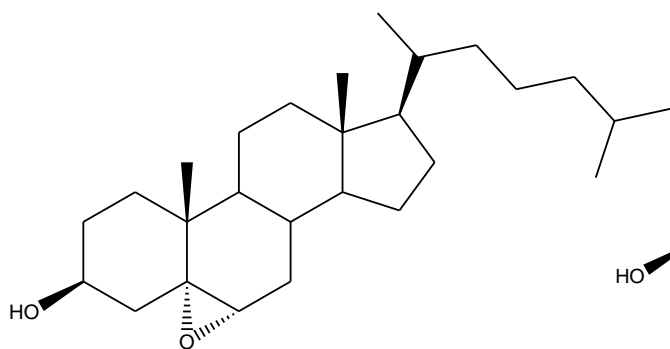
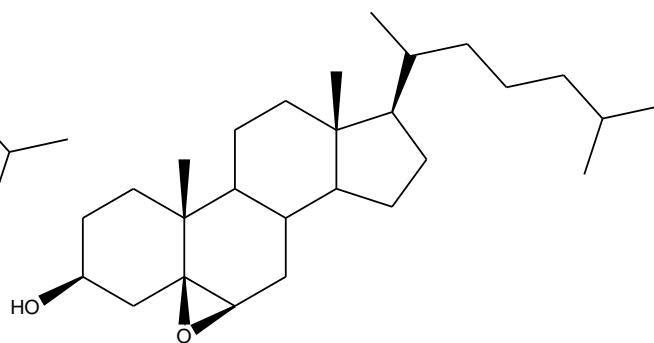


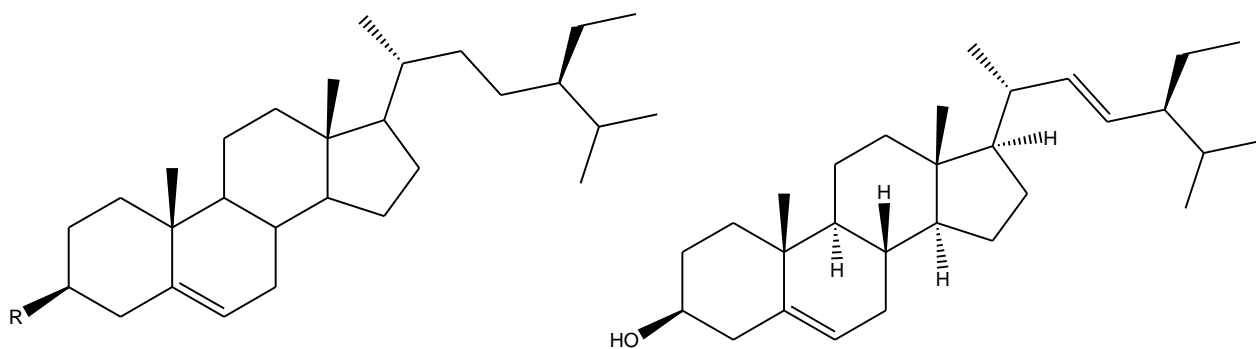
3,4-Dihydroxybenzoic acid (**193**); R₁ = R₂ = OH, R₃ = H
 Salicylic acid (**196**); R₁ = R₂ = H, R₃ = OH

Gallic acid (**195**)Vanillic acid (**197**)

จุฬาลงกรณ์มหาวิทยาลัย
 CHULALONGKORN UNIVERSITY

Steroids

5 α ,6 α -Epoxycholestan-3 β -ol (**198**)5 β ,6 β -Epoxycholestan-3 β -ol (**199**)

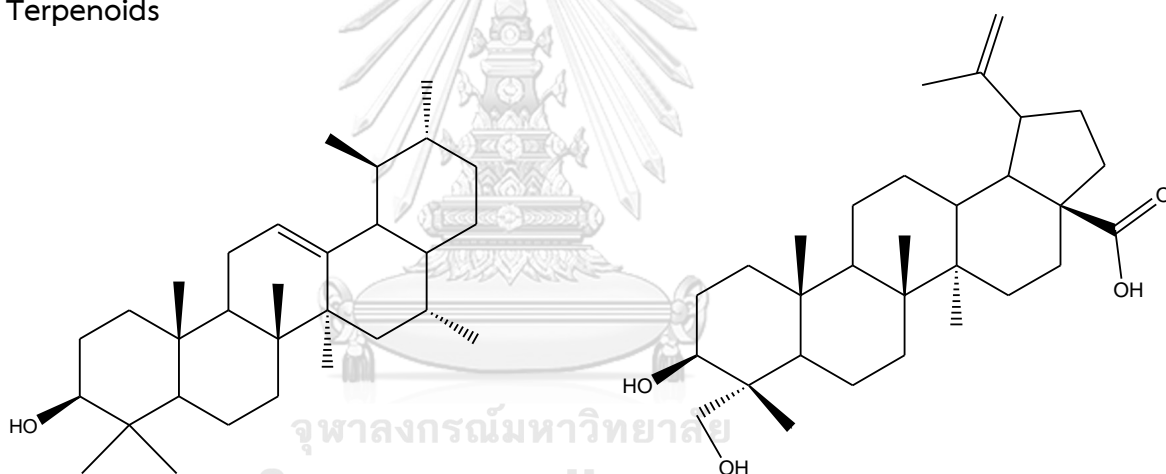


β -Sitosterol (200); R= OH

β -Sitosterol 3-O- β -D-glucopyranoside (201); R= O-Glu

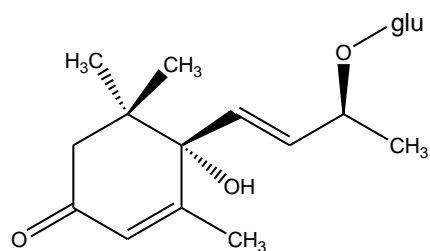
Stigmasterol (202)

Terpenoids

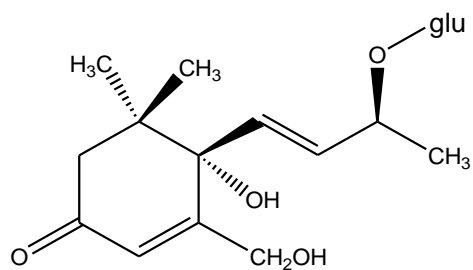


Capparisol A (203)

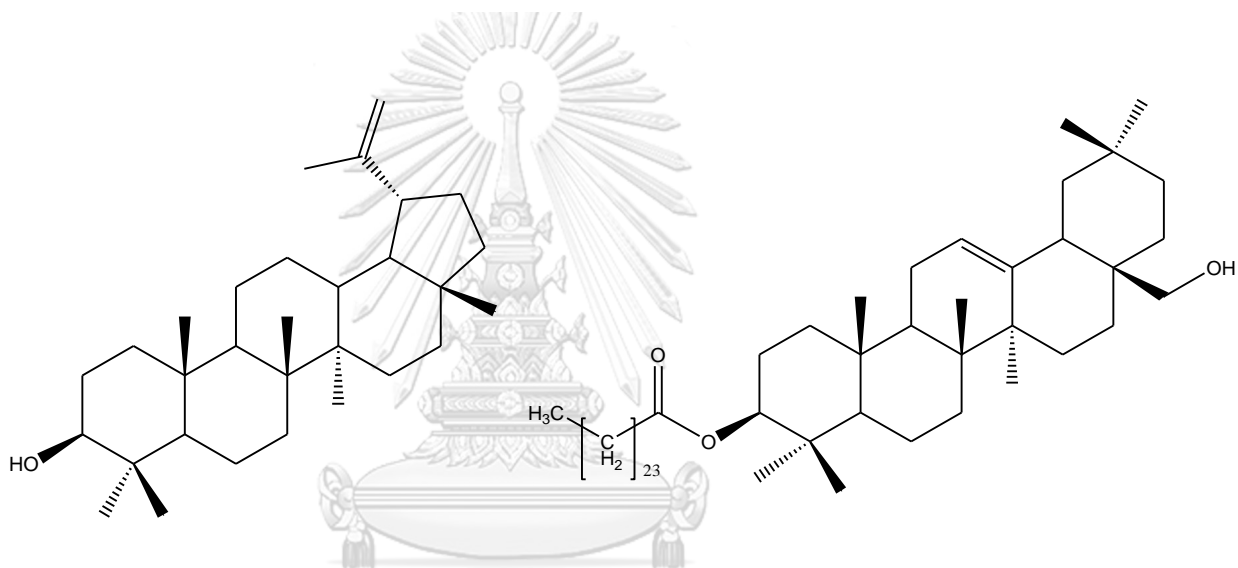
Dihydroxy-lup-20(29)-en-28-oic acid (204)



(+)-(6S,9S)-9-O- β -D-Glucopyranosyloxy-6-hydroxy-3-oxo- α -ionol (205)

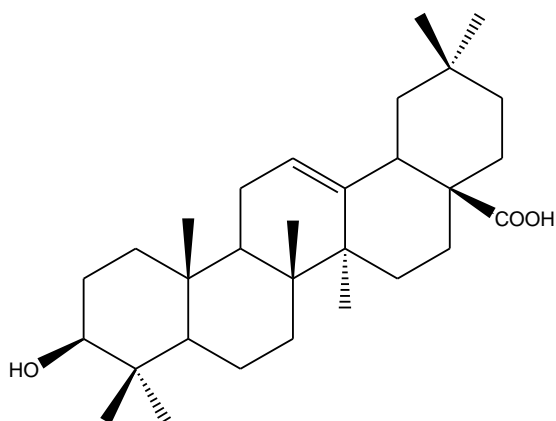


(-)-(6*S*,9*S*)-9-*O*- β -D-Glucopyranosyloxy-6,13-dihydroxy-3-oxo- α -ionol (206)

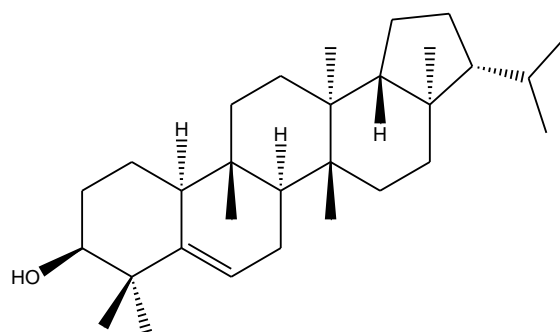


Lupeol (207)

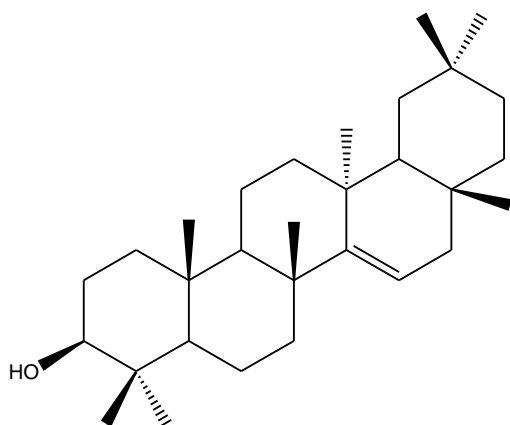
Olean-12-en-3 β ,28-diol 3 β -pentacosanoate (208)



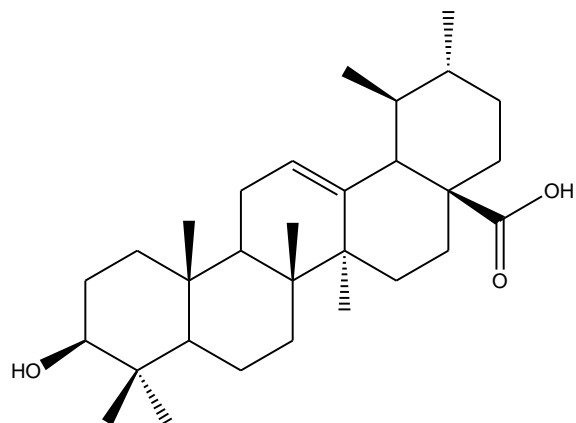
Oleanolic acid (209)



Simiarenol (210)

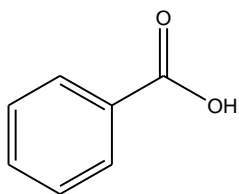


Taraxerol (211)

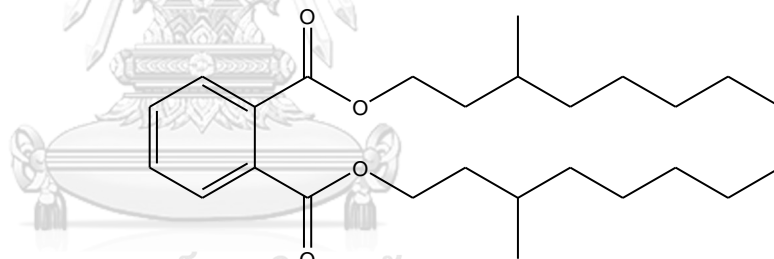


Ursolic acid (212)

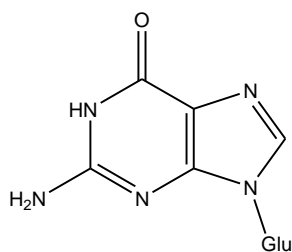
Miscellaneous



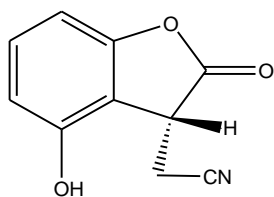
Benzoic acid (213)



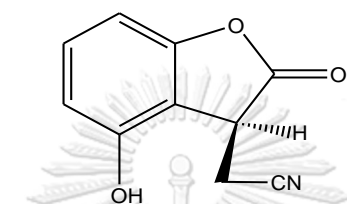
bismethyl-octylphthalate (214)



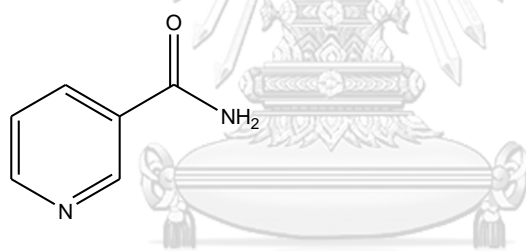
Guanosine (215)



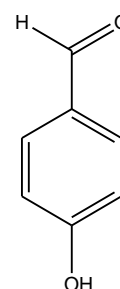
(+)-R-2-(4-Hydroxy-2-oxo-2,3-dihydrobenzofuran-3-yl) acetonitrile (216)



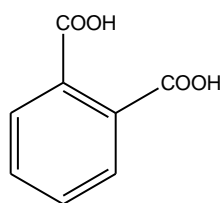
(+)-S-2-(4-Hydroxy-2-oxo-2,3-dihydrobenzofuran-3-yl) acetonitrile (217)



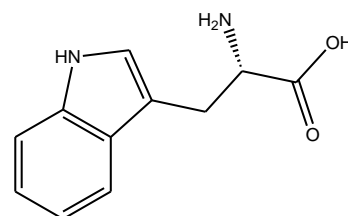
Nicotinamide (218)



para-Hydroxybenzaldehyde (219)



Phthalic acid (220)



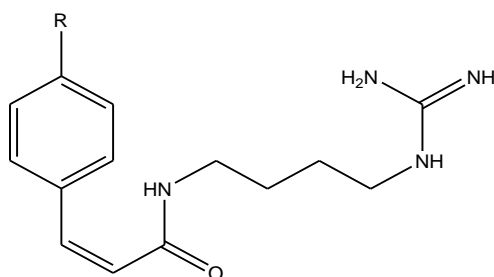
Tryptophan (221)

Table 3. Chemical constituents of plants in the genus *Maerua*

Compound	Source	Plant part	Reference
Alkaloids			
Cappariloside A (152)	<i>M. siamensis</i>	Leaves and	Nobsathian <i>et al.</i> (2018)
Cappariloside B (153)		Twigs	
<i>cis</i> -Cinnamoyl-4-aminobutylguanidine (222)	<i>M. edulis</i>	Leaves	Stevenson <i>et al.</i> (2018)
<i>trans</i> -Cinnamoyl-4-aminobutylguanidine (223)			
4-Hydroxy- <i>E</i> -cinnamoyl-4-aminobutylguanidine (224)			
4-Hydroxy- <i>Z</i> -cinnamoyl-4-aminobutylguanidine (225)			
Stachydrine (167)	<i>M. crassifolia</i>	Aerial parts	Bishay <i>et al.</i> (1990)
	<i>M. edulis</i>	Leaves	Stevenson <i>et al.</i> (2018)
Flavonoids			
Chrysoeriol (226)	<i>M. siamensis</i>	Leaves and Twigs	Nobsathian <i>et al.</i> (2018)
Kaempferol (177)	<i>M. crassifolia</i>	Aerial parts	Bishay <i>et al.</i> (1990)
Kaempferol-3- <i>O</i> -galactorhamnoside (227)			
Quercetin (180)	<i>M. crassifolia</i>	Aerial parts	Ibraheim (1995)
Quercetin-3- <i>O</i> -arabinopyranoside (228)	<i>M. crassifolia</i>	Aerial parts	Bishay <i>et al.</i> (1990)
Quercetin-3- <i>O</i> - β -D-galactoside (229)			
Rutin (181)			
Lignan			
Lyoniresinol-3- <i>O</i> -glucopyranoside (230)	<i>M. crassifolia</i>	Aerial parts	Bishay <i>et al.</i> (1990)
Steroids			

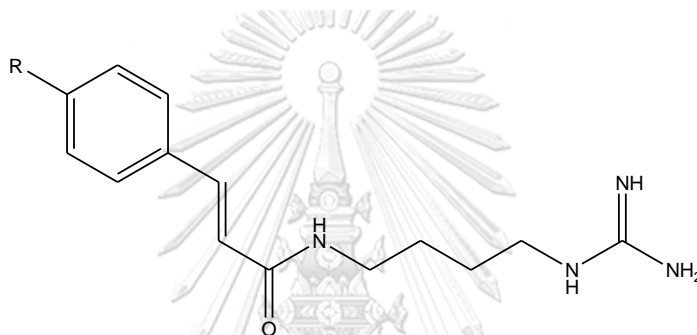
Compound	Source	Plant part	Reference
Lupeol (207)	<i>M. siamensis</i>	Leaves and Twigs	Nobsathian <i>et al.</i> (2018)
Terpenoids			
Betulin (231)	<i>M. oblongifolia</i>	Aerial parts	Abdel-Mogib (1999)
Betulinaldehyde (232)			
Glochidone (233)	<i>M. siamensis</i>	Leaves and Twigs	Nobsathian <i>et al.</i> (2018)
Hexahydrofarnesyl acetone (234)	<i>M. oblongifolia</i>	Aerial parts	Abdel-Mogib (1999)
Ionol glucoside (235)	<i>M. crassifolia</i>	Aerial parts	Ibraheim (1995)
Lup-20(29)-en-3 β ,30-diol (236)	<i>M. oblongifolia</i>	Aerial parts	Abdel-Mogib (1999)
Phytol (237)	<i>M. oblongifolia</i>	Aerial parts	Abdel-Mogib (1999)
Miscellaneous			
Cinnamic acid (238)	<i>M. siamensis</i>	Leaves and Twigs	Nobsathian <i>et al.</i> (2018)
3,4-Dihydroxybenzoic acid (193)			
Guaiacyl glycerol (239)	<i>M. crassifolia</i>	Aerial parts	Ramadan <i>et al.</i> (1999)
6- <i>N</i> -Methyl-9- β -D-glucoside adenine (240)	<i>M. crassifolia</i>	Aerial parts	Ramadan <i>et al.</i> (1999)
3,4,5-Trimethoxyphenol-1- <i>O</i> - β -D-glucopyranoside (241)			
Vanillin (242)	<i>M. siamensis</i>	Leaves and Twigs	Nobsathian <i>et al.</i> (2018)

Alkaloids



cis-Cinnamoyl-4-aminobutylguanidine (**222**); R= H

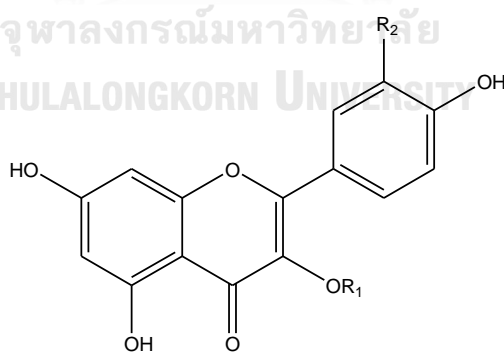
4-Hydroxy-*Z*-cinnamoyl-4-aminobutylguanidine (**225**); R= OH



trans-Cinnamoyl-4-aminobutylguanidine (**223**); R= H

4-Hydroxy-*E*-cinnamoyl-4-aminobutylguanidine (**224**); R= OH

Flavonoids



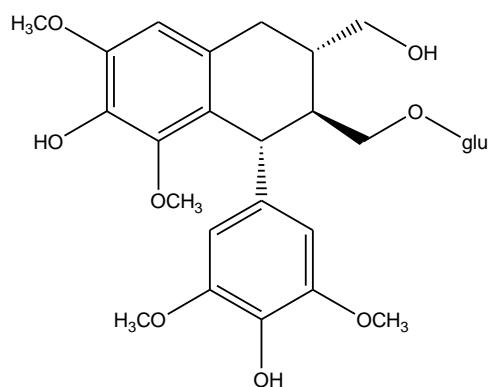
Chrysoeriol (**226**); R₁= H, R₂= OCH₃

Kaempferol-3-*O*-galactorhamnoside (**227**); R₁= galactose—rhamnose, R₂ = H

Quercetin-3-*O*-arabinopyranoside (**228**); R₁= arabinose, R₂= OH

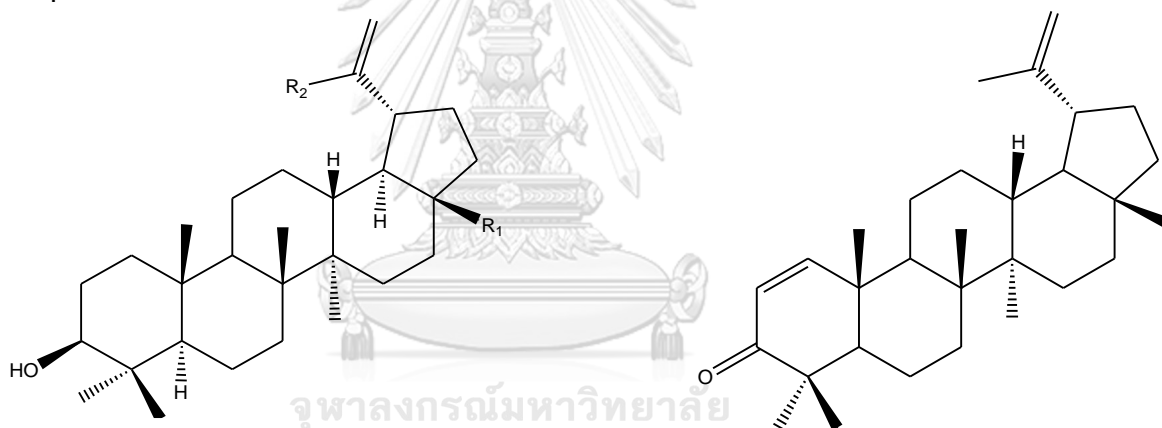
Quercetin-3-*O*-β-D-galactoside (**229**); R₁= β-D-galactose, R₂= OH

Lignans

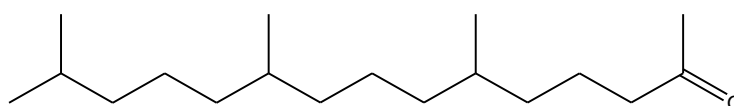


Lyoniresinol-3-O-glucopyranoside (230)

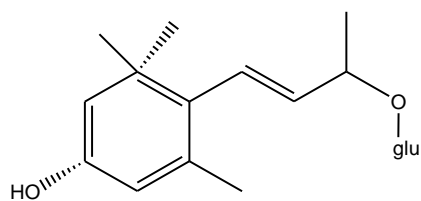
Terpenoids

Betulin (231); $R_1 = \text{CH}_2\text{OH}$, $R_2 = \text{CH}_3$ Betulinaldehyde (232) $R_1 = \text{CHO}$, $R_2 = \text{CH}_3$ Lup-20(29)-en-3 β ,30-diol (236); $R_1 = \text{CH}_3$, $R_2 = \text{CH}_2\text{OH}$

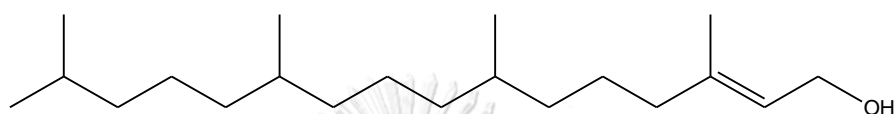
Glochidone (233)



Hexahydrofarnesyl acetone (234)

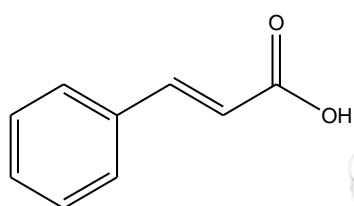


Ionolglucoside (235)

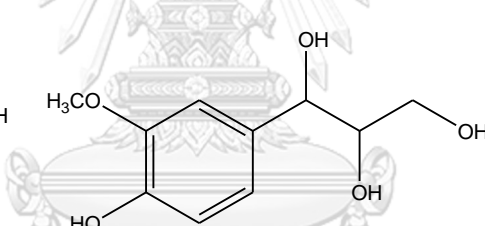


Phytol (237)

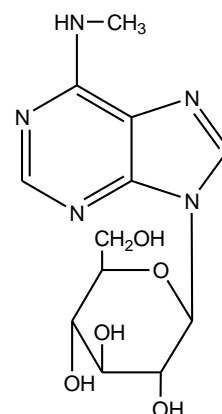
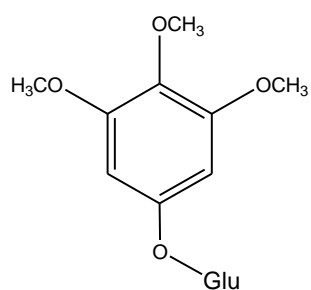
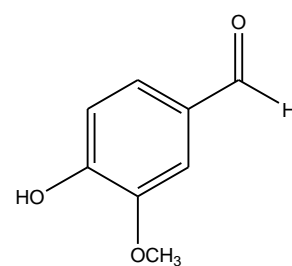
Miscellaneous



Cinnamic acid (238)



Guaiacyl glycerol (239)

6-N-Methyl-9- β -D-glucoside adenine (240)3,4,5-Trimethoxyphenol-1- O - β -D-glucopyranoside (241)

Vanillin (242)

CHAPTER III

EXPERIMENTAL

3.1 Source of plant materials

The stems of *Capparis micracantha* were collected from Saraburi province in March 2019, while the roots of *Maerua siamensis* were collected from Sikhio district, Nakhon Ratchasima in April 2019. Voucher specimens of these plants have been deposited at department of Pharmacognosy and Pharmaceutical Botany, Faculty of Pharmaceutical Sciences, Chulalongkorn University, Thailand.

3.2 General techniques

3.2.1 Solvents

organic solvents used in this study were commercial grade and were distilled before used.

3.2.2 Analytical normal-phase thin-layer chromatography (TLC)

Technique	:	One dimensional, ascending
Absorbent	:	Silica gel 60 F254 (Merck, Darmstadt, Germany)
Layer thickness	:	0.2 mm
Distance	:	5 cm
Temperature	:	Room temperature (30-32 °C)
Detection	:	<ol style="list-style-type: none"> 1. Ultraviolet light (wavelengths of 254 and 365 nm) 2. Spraying with $Ce_2(SO_4)_3$ reagent and heating at 110-130 °C for 5 min

3.2.3 Analytical reversed-phase thin-layer chromatography (RP-18)

Technique	:	One dimensional ascending
Absorbent	:	Silica gel 60 RP-18 F ₂₅₄ S (Merck) No. 1.05559
Layer thickness	:	0.2 mm
Distance	:	5 cm
Temperature	:	Room temperature (30-32 °C)

Detection : as described in section 3.2.2

3.2.4 Column chromatography

3.2.4.1 Flash Column Chromatography

Adsorbent : Silica gel 60, 230–400 mesh (Merck)

Packing method : Dry packing

Sample loading : The sample was dissolved in a small amount of organic solvent. Then, a small quantity of silica was mixed with the sample and dried. After that, the mixture was placed on top of the column.

Detection : Fractions were examined as described in section 3.2.2.

3.2.4.2 Medium Performance Liquid Column Chromatography (MPLC)

Adsorbent : Silica gel 60 (70–230 or 230–400 mesh) and v LiChroprep[®] RP-18 (25–40 μm) (Merck)

Packing method : Dry packing

Sample loading : The sample was dissolved in a small amount of organic solvent. Then, a small quantity of silica was mixed with the sample and dried. After that, the mixture was placed on top of the column.

Detection : Fractions were examined as described in section 3.2.2.

3.2.4.3 Conventional column chromatography

Adsorbent : Silica gel 60 (70–230 or 230–400 mesh) (Merck)

Packing method : Dry packing

Sample loading : The sample was dissolved in a small amount of organic solvent. Then, a small quantity of silica was mixed with the sample and dried. After that, the mixture was placed on top of the column.

Detection : Fractions were examined as described in section 3.2.2.

3.2.4.4 Gel filtration chromatography

Adsorbent : Sephadex LH-20 (GE Healthcare, Amersham, UK)

Packing method : Sephadex gel was allowed to swell in mobile phase for 24 hours, then poured into the column.

Sample loading : The sample was dissolved in a small amount of mobile phase, then placed on top of the column.

Detection : Fractions were examined as described in section 3.2.2.

3.3 Spectroscopy

3.3.1 Ultraviolet absorption spectra

Ultraviolet (UV) spectra were obtained on a Milton Roy Spectronic 3000 Array spectrophotometer (Rochester, NY, USA) at Pharmaceutical Research Instrument Center, Faculty of Pharmaceutical Sciences, Chulalongkorn University.

3.3.2 Infrared spectra

Fourier Transform Infrared (FT-IR) spectra was recorded on a Thermo scientific Nicolet™ iS50 FT-IR spectrometer (Thermo Fisher scientific, Waltham, MA, USA) at the National Nanotechnology Center (NANOTEC, Thailand) or a Perkin Elmer FT-IR 1760X spectrometer (Boston, MA, USA) spectrometer (Scientific and Technological Equipment Center, Chulalongkorn University).

3.3.3 Mass spectrometer

High Resolution-Electron Spray Ionization-Mass Spectrometry (HR-ESI-MS) spectra were obtained on a Bruker APEX II mass spectrometer (Karlsruhe, Germany) at Kaohsiung Medical University (Taiwan), or an Agilent 6540 UHD Accurate-Mass Q-TOF mass spectrometer (CA, USA) at the Science Lab Center, Faculty of Science, Naresuan University.

3.3.4 Proton and carbon-13 nuclear magnetic resonance (^1H - and ^{13}C -NMR) spectroscopy

^1H -NMR (600 MHz) and ^{13}C -NMR (150 MHz) spectra were recorded on a Varian VNMRS-600 spectrometer (Lexington, MA, USA) Kaohsiung Medical University and ^1H NMR (400 MHz) and ^{13}C NMR (100 MHz) spectra were recorded on a Bruker Advance NEO 400 MHz NMR spectrometer (Karlsruhe, Germany) at the Faculty of Pharmaceutical Sciences, Chulalongkorn University.

3.3.5 Circular dichroism

Circular dichroism was measured on a JASCO J-815CD/ORD spectropolarimeter (Kyoto, Japan) at Pharmaceutical Research Instrument Center, Faculty of Pharmaceutical Sciences, Chulalongkorn University.

3.3.6 Polarimetry

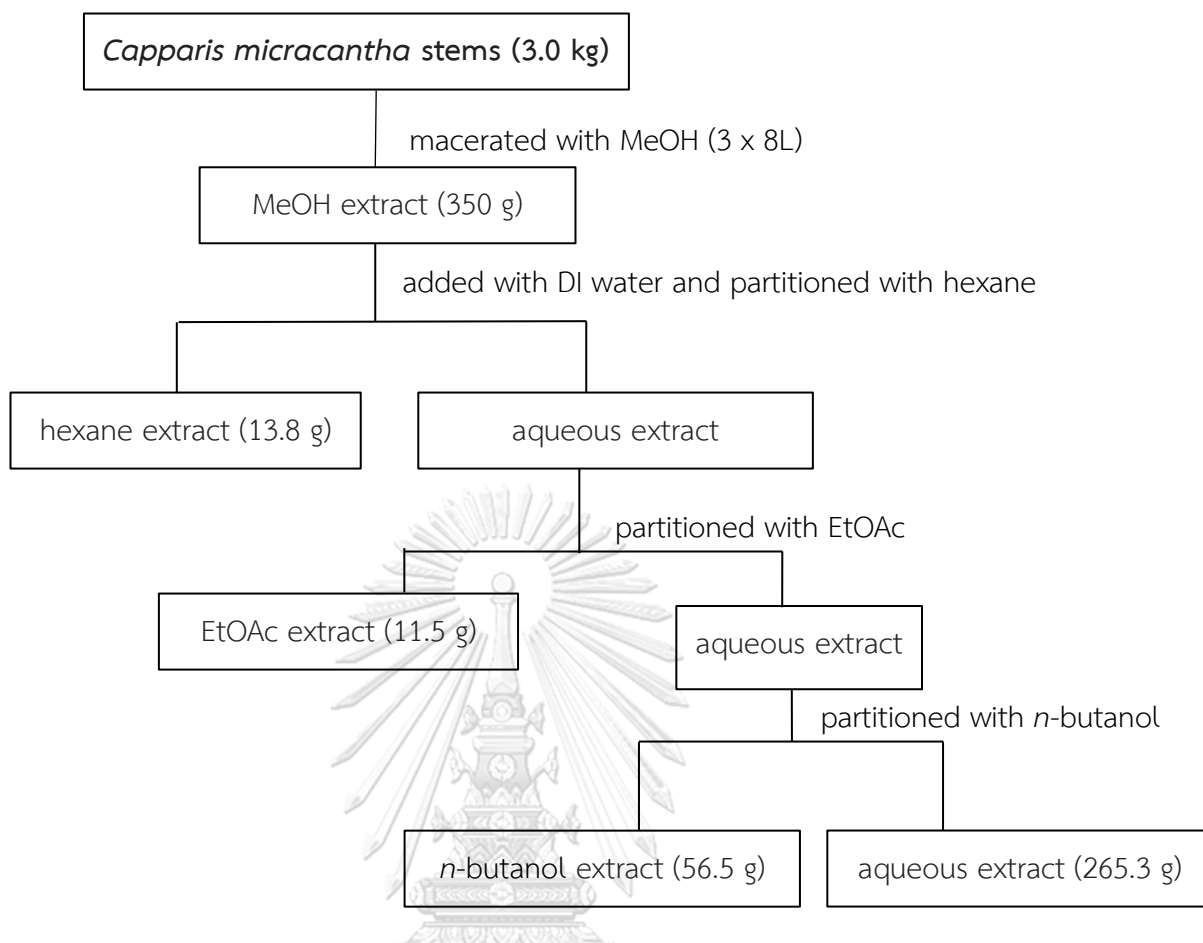
3.3.6.1 Optical rotation

Specific rotation values were measured using a JASCO P-2000 polarimeter (Kyoto, Japan) at Pharmaceutical Research Instrument Center, Faculty of Pharmaceutical Sciences, Chulalongkorn University.

3.4. Extraction and isolation

3.4.1 Extraction of *Capparis micracantha* stems

Dried stems of *C. micracantha* (3.0 kg) were cut into small pieces and macerated with methanol (MeOH) 3×8 L, for three days each. The methanol extract was evaporated under reduced pressure to obtain crude MeOH extract (350 g, 11.67 % yield, based on dried weight of stems). The extract was redissolved in MeOH added with deionized (DI) water, then partitioned with hexane (6 L), ethyl acetate (EtOAc, 8 L), and *n*-butanol (8 L) successively to give hexane extract (13.8 g, 0.46% yield), EtOAc extract (11.5 g, 0.38% yield), *n*-butanol extract (56.5 g, 1.9 % yield) and aqueous extract (265.3 g, 8.84 % yield). (**Scheme 1.**)



Scheme 1. Extraction of *Capparis micracantha* stems.

3.4.2 Isolation of compounds from the EtOAc extract of *Capparis micracantha* stems (CMSE)

The EtOAc extract (11.45 g) was divided into 4 portions and each portion was separated by MPLC using silica gel as stationary phase. The column was eluted with *n*-hexane-acetone (4:1 to 0:1) and washed by CH₂Cl₂-MeOH (1:1). Each fraction was collected about 50 mL of eluate. All fractions were combined according to their TLC pattern to give 8 major fractions: CMSE-1 (0.7 g), CMSE-2 (1.2 g), CMSE-3 (1.8 g), CMSE-4 (1.6 g), CMSE-5 (2.7 g), CMSE-6 (2.4 g), CMSE-7 (1.5 g), and CMSE-8 (2.5g).

3.4.2.1 Isolation of compound 1 (methyl 6-methoxy-3-indolecarbonate)

Fraction CMSE-4 was combined with CMSE-5 and separated by MPLC using silica gel as stationary phase. The mobile phase was *n*-hexane-acetone (4:1 to 0:1). The eluates were combined into 8 fractions (Fr.4-1 to 4-8). Fraction 4-3 (99.8 mg) was purified by size exclusion chromatography (Sephadex LH-20), eluted with CH₂Cl₂-MeOH (1:1) to give 4 subfractions (fr.4-3-1 – 4-3-4). Subfraction 4-3-4 (10 mg) was further repurified by Sephadex LH-20 column (MeOH) to obtain 10 subfractions. **Compound 1** (1.2 mg) was obtained from subfraction 4-3-4-5 as a yellow amorphous solid (**Scheme 2**).

3.4.2.2 Isolation of compound 2 (vanillic acid)

Fraction 4-5 (147.2 mg) was subjected to silica gel column chromatography (Si-CC), eluted with CH₂Cl₂-acetone (30:1 to 0:1) to gain 8 subfractions (fr.4-5-1 – 4-5-8). Subfraction 4-5-2 (49 mg) was further separated by Si-CC with *n*-hexane-EtOAc (3:2) as the mobile phase to afford 6 subfractions (fr.4-5-2-1 – 4-5-2-6). Subfraction 4-5-2-3 was further purified by recrystallization in CH₂Cl₂-MeOH to obtain **compound 2** (4.1 mg) as a white amorphous solid (**Scheme 2**).

3.4.2.3 Isolation of compound 3 [(-)-syringaresinol]

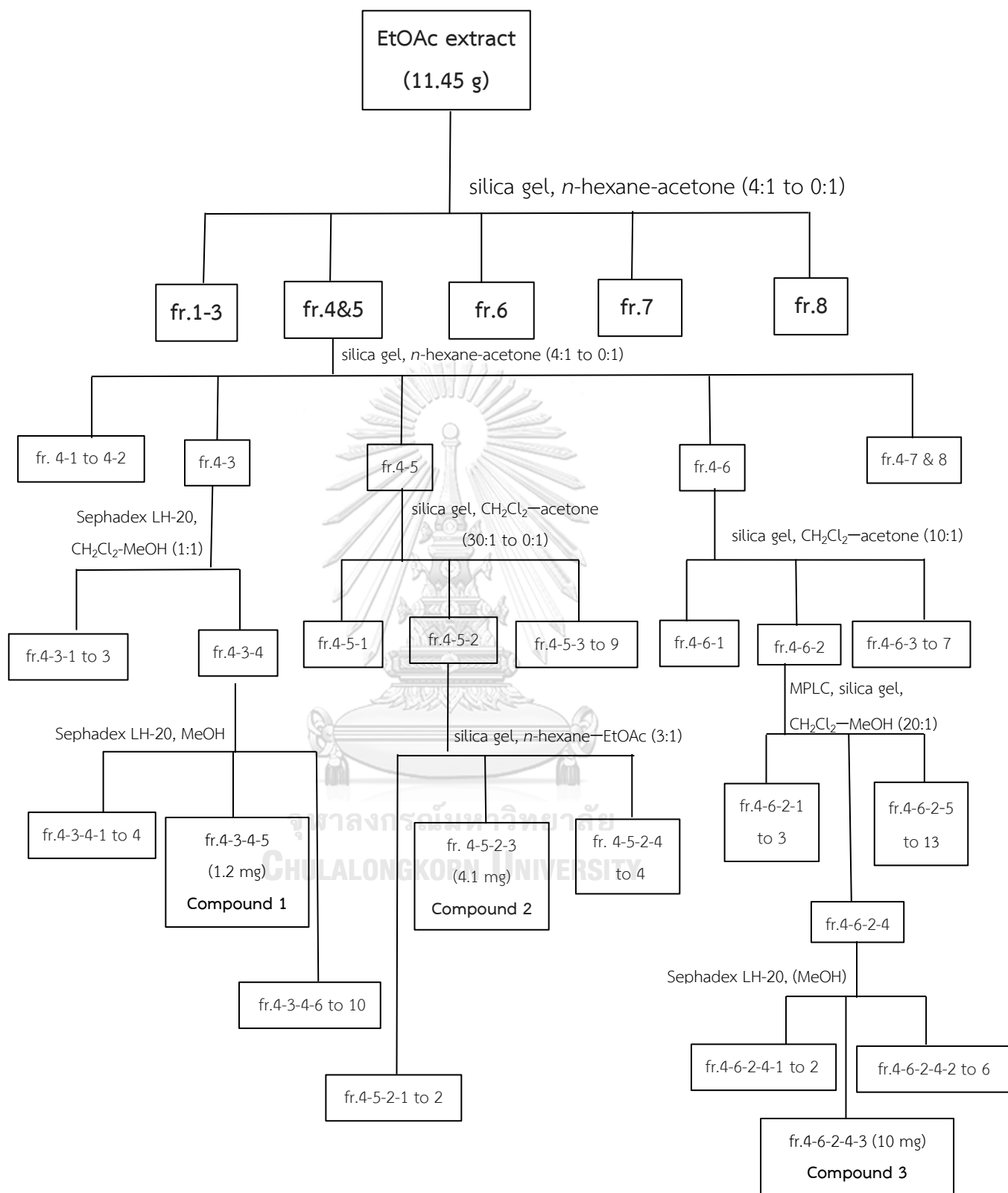
Fraction 4-6 (537.8 mg) was separated by MPLC using silica gel as stationary phase and CH₂Cl₂-acetone (10:1) as mobile phase to yield 7 subfractions (Fr.4-6-1 – 4-6-7). Subfraction 4-6-2 (81.3 mg) was subjected to Si-CC using CH₂Cl₂-MeOH (20:1) as the solvent system to obtain 13 subfractions (fr.4-6-2-1 – 4-6-2-13). Subfraction 4-6-2-4 (38.5 mg) was further separated on a Sephadex LH-20 column (MeOH) to obtain 6 subfractions (fr.4-6-2-4-1 – 4-6-2-4-6). Subfraction 4-6-2-4-3 yielded **compound 3** (10.0 mg) as a white amorphous solid (**Scheme 2**).

3.4.2.4 Isolation of compound 4 [(+)-ampelopsin A]

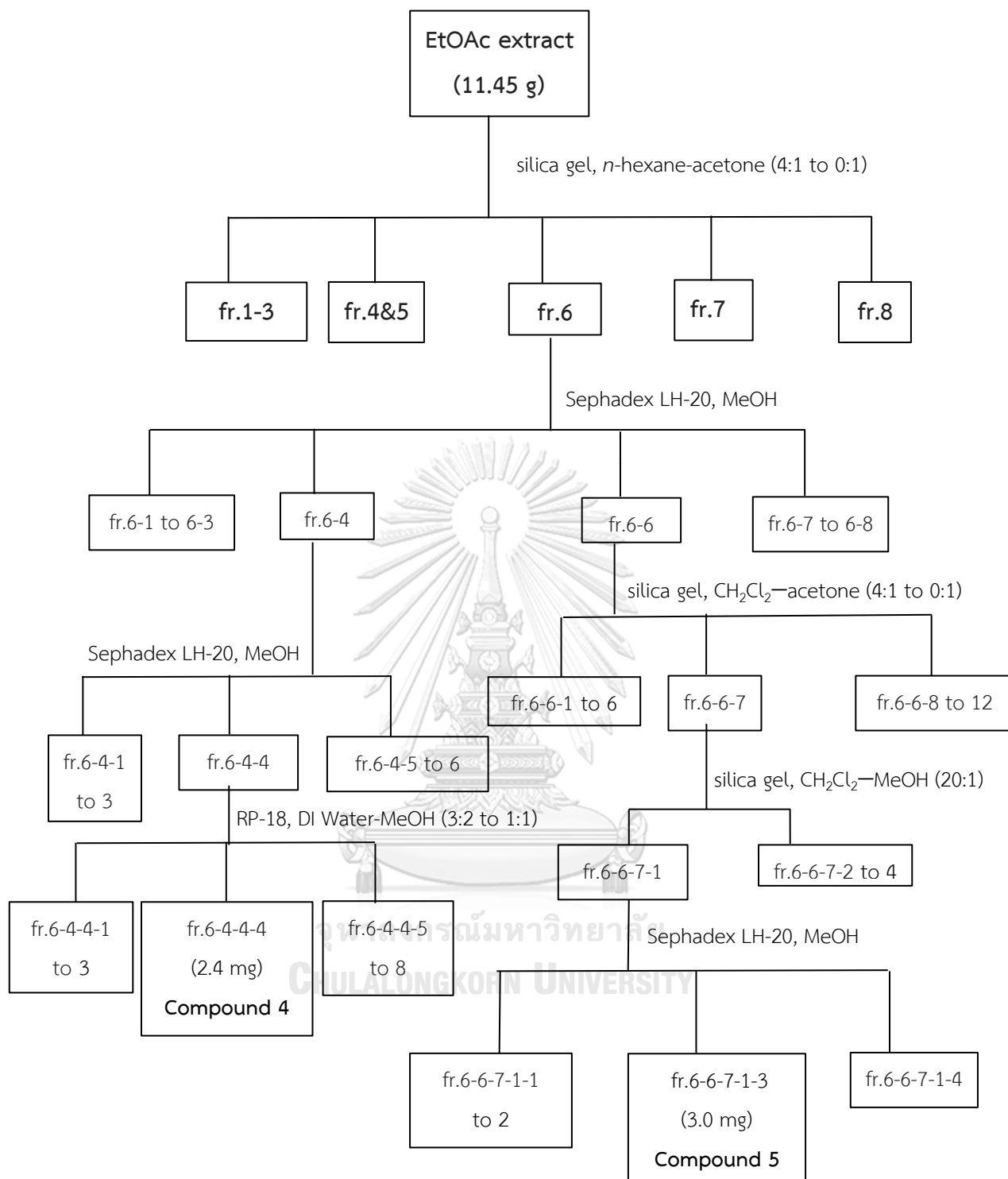
Fraction CMSE 6 (2.4 g) was subjected to Sephadex LH-20 column eluted with MeOH to give 8 fractions (fr.6-1 – 6-8). Fraction 6-4 (32.5 mg) was repurified on Sephadex LH-20 column (MeOH) to yield 6 subfractions (fr.6-4-1 – 6-4-6). Subfraction 6-4-4 (32.8 mg) was further separated by MPLC using reverse phase (RP-18) column as stationary phase. After eluting with DI water–MeOH (3:2 to 1:1), 8 subfractions (fr.6-4-4-1 – 6-4-4-8) were afforded. **Compound 4** (2.4 mg) was purified from subfraction 6-4-4-4 (**Scheme 3**).

3.4.2.5 Isolation of compound 5 [(-)-pauciflorol E]

Fraction 6-6 (162.0 mg) was loaded on MPLC [silica gel, CH₂Cl₂–acetone (4:1 to 0:1)] to gain 12 subfractions. Subfractions 6-6-7 (7.9 mg) was purified by Si-CC using CH₂Cl₂–MeOH (20:1) to obtain 4 subfractions (fr.6-6-7-1 – 6-6-7-4). Subfractions 6-6-7-1 (5.1 mg) was further purified by Sephadex LH-20 (MeOH) to give 4 subfractions. **Compound 5** (3.0 mg) was obtained from subfraction 6-6-7-1-3 as a green amorphous solid (**Scheme 3**).



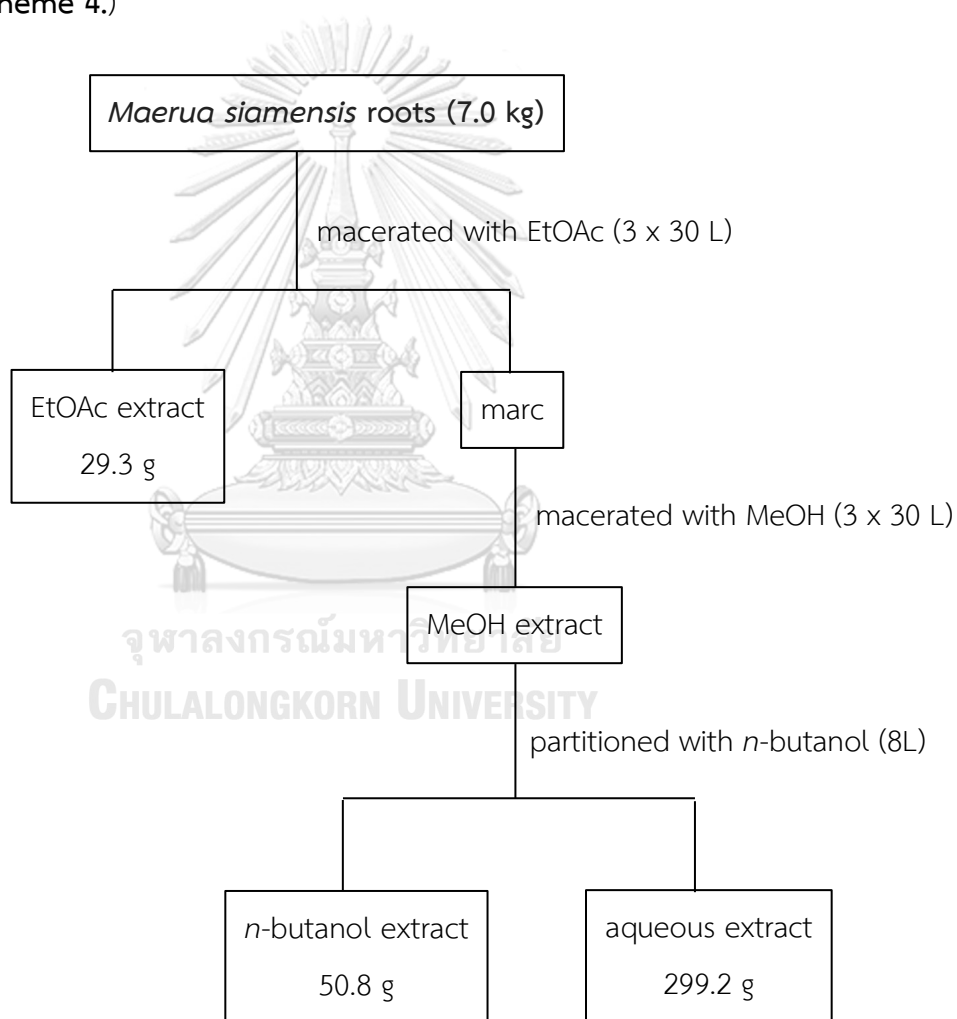
Scheme 2. Isolation of compounds 1 – 3 from the EtOAc extract of *C. micracantha*



Scheme 3. Isolation of compounds 4 – 5 from the EtOAc extract of *C. micracantha*

3.4.3 Extraction of *Maerua siamensis* roots

Dried roots of *M. siamensis* (7.0 kg) were cut into small pieces and extracted with EtOAc (3×30 L), for three days each. The extract was evaporated under vacuum to yield EtOAc extract (29.3 g, 0.42 % yield). The marc was further macerated with MeOH (3× 30 L), for three days each. After evaporation, the MeOH extract (350 g, 5.0 % yield) was redissolved in MeOH, added with DI water and partitioned with *n*-butanol (8 L) to give *n*-butanol extract (50.8 g, 0.73 % yield) and aqueous extracts (299.2 g, 4.27 % yield). (Scheme 4.)



Scheme 4. Extraction of *Maerua siamensis* roots

3.4.4 Isolation of compounds from EtOAc extract of *Maerua siamensis* roots

The EtOAc extract (29.3 g) was separated by a silica gel MPLC column using *n*-hexane-acetone (15:1 to 6:1) as mobile phase. The flow rate was 15 mL/min. Each collected fraction was 50 mL. Based on TLC pattern, 9 major fractions were obtained as follows: MSRE-1 (5.30 g), MSRE-2 (4.17 g), MSRE-3 (1.10 g), MSRE-4 (0.20 g), MSRE-5 (0.18 g), MSRE-6 (0.27 g), MSRE-7 (0.25 g), MSRE-8 (2.14 g), and MSRE-9 (1.06 g).

3.4.4.1 Isolation of compound 6 [(+)-maeruanitrile A] and compound 7 (maeruanitrile B)

Fraction MRSE-8 (2.14 g) was subjected to MPLC [silica gel, CH₂Cl₂–acetone (120:1 to 20:1)] to give 12 fractions (fr.8-1 – 8-12). Fraction 8-2 (66.6 mg) was separated using MPLC [silica gel, *n*-hexane–CH₂Cl₂–acetone (8:1:1 to 4:1:1)] to gain 12 subfractions (fr.8-2-1 – 8-2-12). Subfraction 8-2-4 (28.60 mg) was purified in two steps using *n*-hexane–CH₂Cl₂–acetone system [8:1:1 to 4:1:1 and 4:1:1 to 2:1:1] to yield 14 subfractions (fr.8-2-4B-1–8-2-4B-14). Subfraction 8-2-4B-14 was subjected to Si-CC eluted with *n*-hexane–CH₂Cl₂–acetone (2:1:1) to afford **compound 6** (2.4 mg) as a reddish-brown amorphous solid from subfraction 8-2-4B-14-4, and **compound 7** (1.4 mg) as a reddish-brown amorphous solid from subfraction 8-2-4B-14-8 (**Scheme 5**).

3.4.4.2 Isolation of compound 8 (maeroxime A)

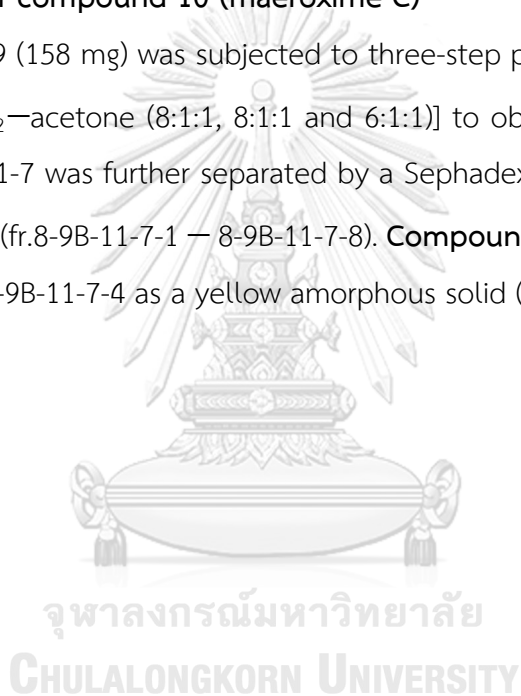
Fraction MRSE-6 (274.50 mg) was loaded on MPLC [silica gel, *n*-hexane-acetone (3:1)], to yield 10 fractions (fr.6-1 – 6-10). Fraction 6-5 (38.2 mg) was further separated by MPLC using C-18 reversed phase silica gel as stationary phase and DI water–acetonitrile (1:2) as mobile phase to gain 13 subfractions (Fr.6-5-1 – 6-5-13). Subfraction 6-5-2 (8 mg) was purified by preparative reversed phase TLC using DI water–acetonitrile (1:4) as mobile phase to afford **compound 8** (2.4 mg) as a reddish-brown amorphous solid from fraction 6-5-2-2 (**Scheme 6**).

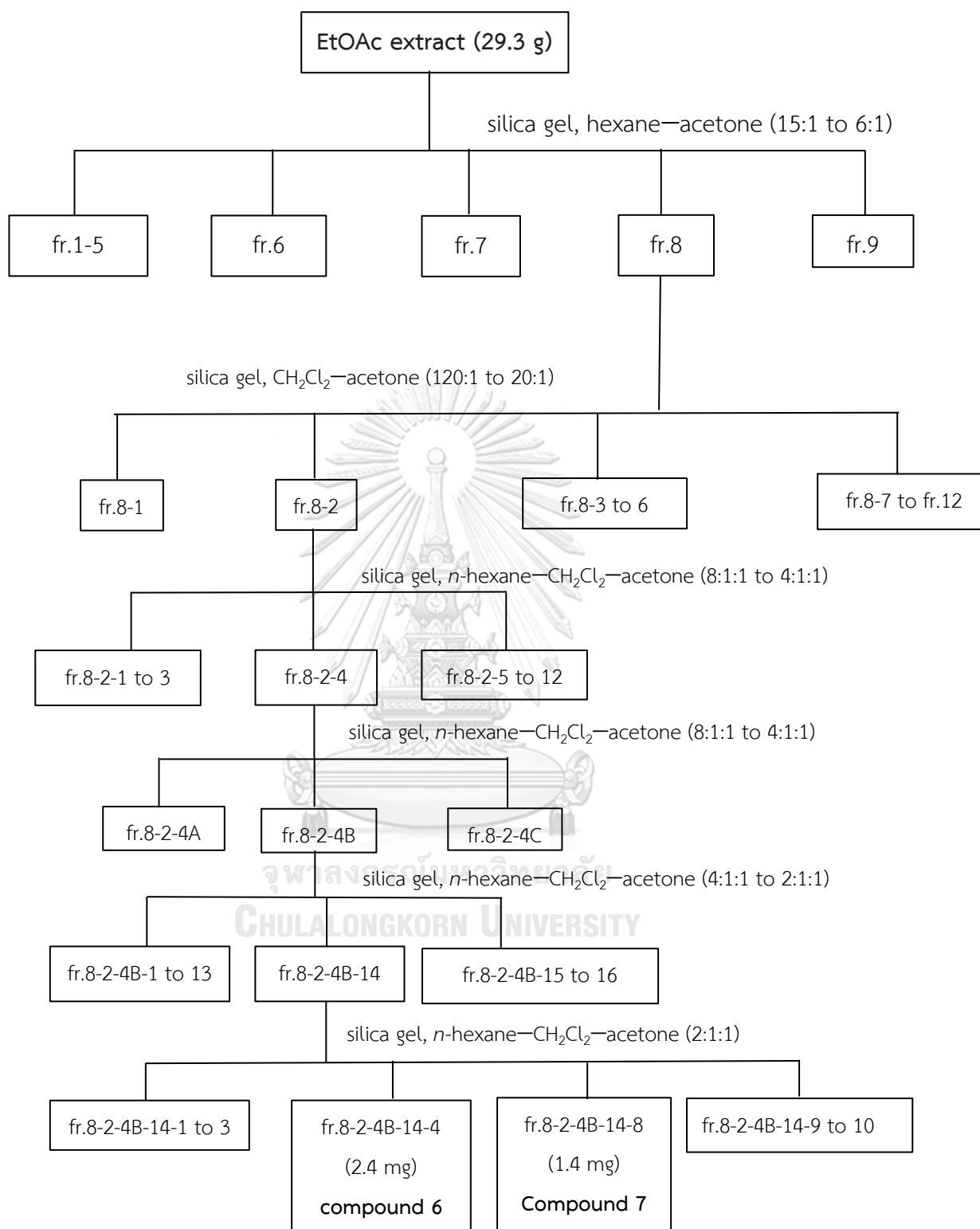
3.4.4.3 Isolation of compound 9 (maeroxime B)

Fraction MRSE-8 (2.14 g) was subjected to MPLC [silica gel, CH₂Cl₂–acetone (120:1 to 20:1)] to give 12 fractions (fr.8-1 – 8-12). Fraction 8-6 (31.90 mg) was undergone three-step purification by Si-CC using with *n*-hexane–acetone (10:1 to 6:1) and *n*-hexane–acetone (6:1), and *n*-hexane–acetone (3:1) to obtain **compound 9** (fraction 8-6-13-3A, 1.0 mg) as an orange-brown amorphous solid (**Scheme 7**).

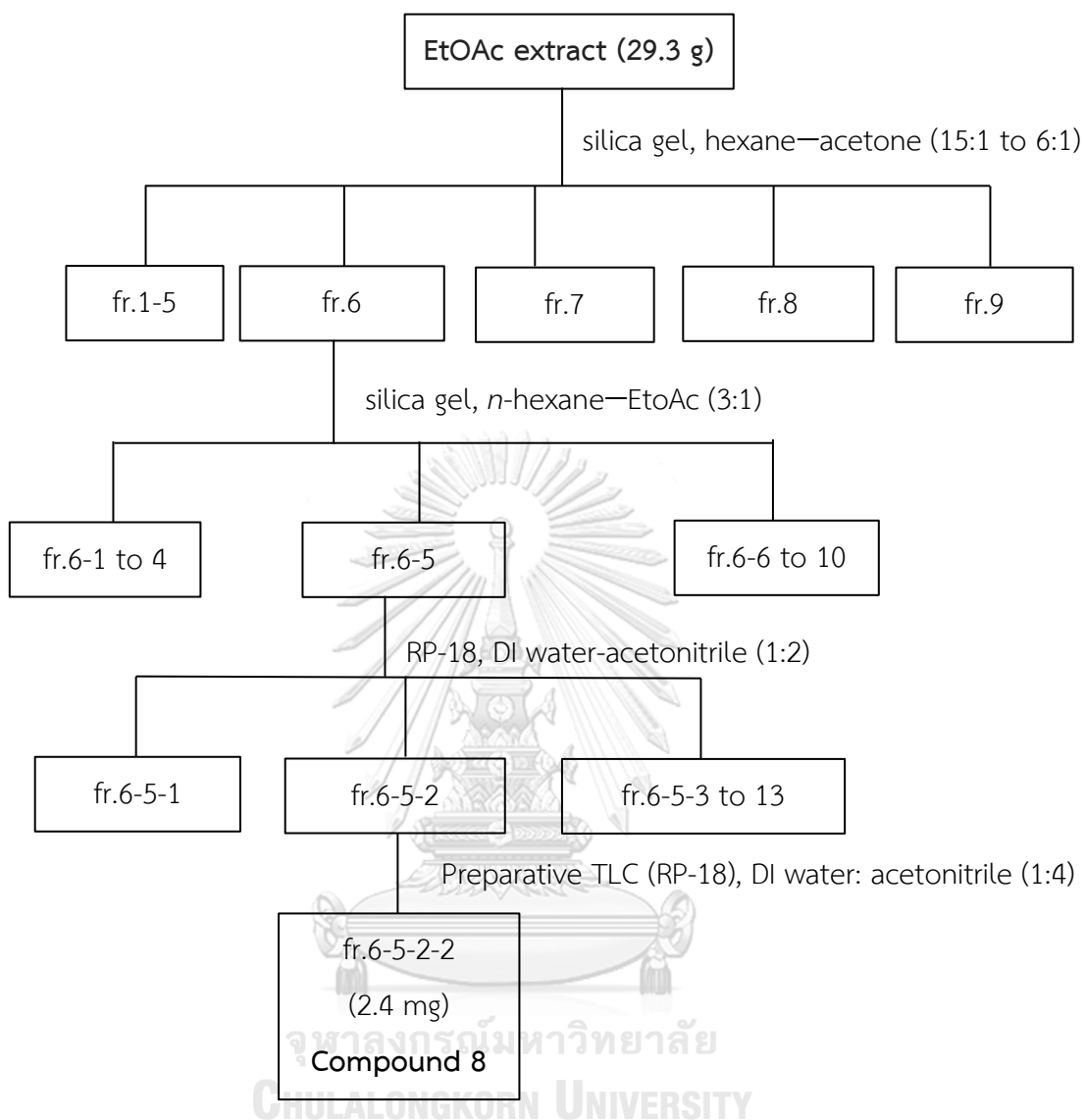
3.4.4.4 Isolation of compound 10 (maeroxime C)

Fraction 8-9 (158 mg) was subjected to three-step purification by MPLC [Si-CC, *n*-hexane–CH₂Cl₂–acetone (8:1:1, 8:1:1 and 6:1:1)] to obtain subfraction 8-9B-11-7. Subfraction 8-9B-11-7 was further separated by a Sephadex LH-20 column (MeOH) to give 8 subfractions (fr.8-9B-11-7-1 – 8-9B-11-7-8). **Compound 10** (3.5 mg) was obtained from subfraction 8-9B-11-7-4 as a yellow amorphous solid (**Scheme 8**).

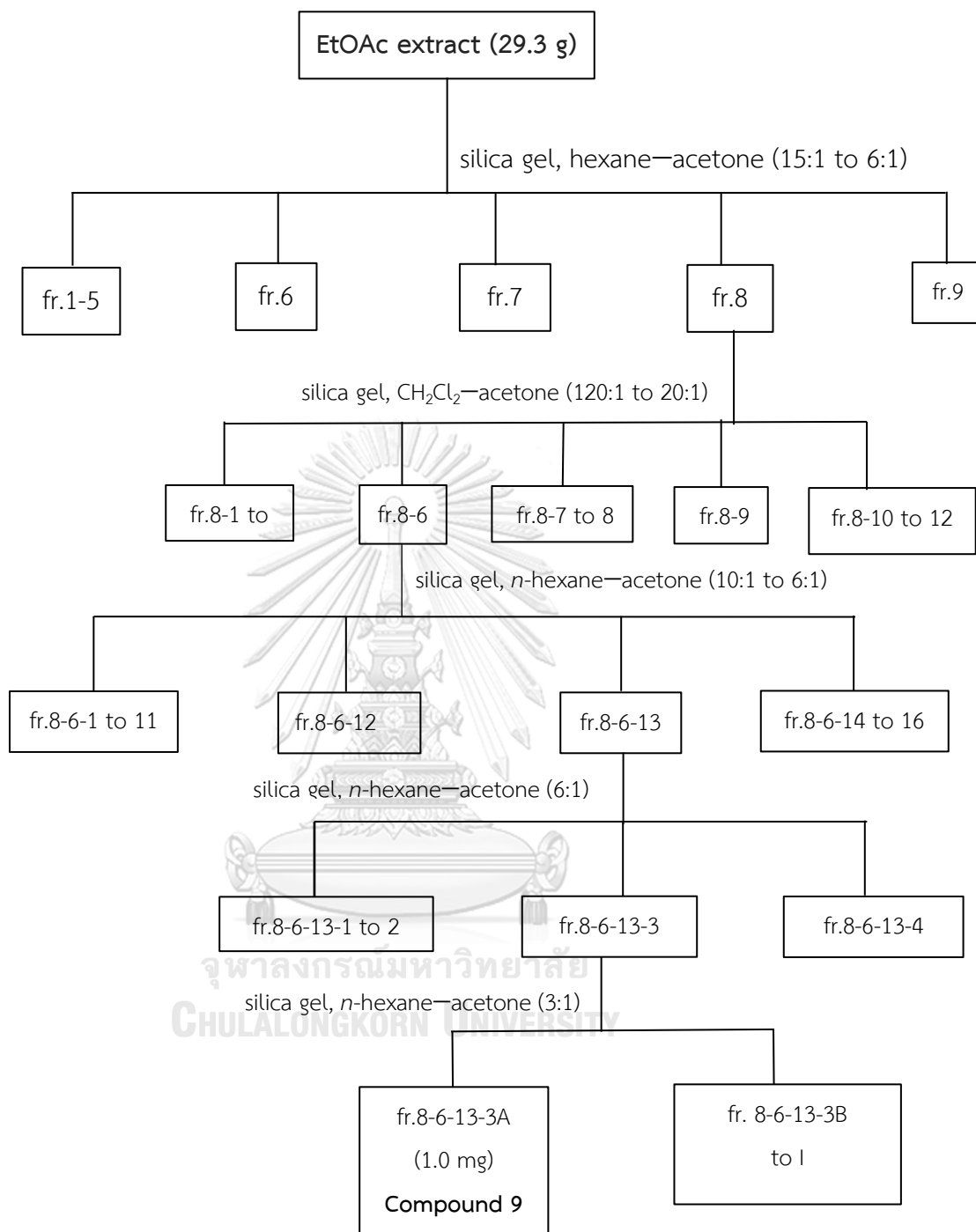




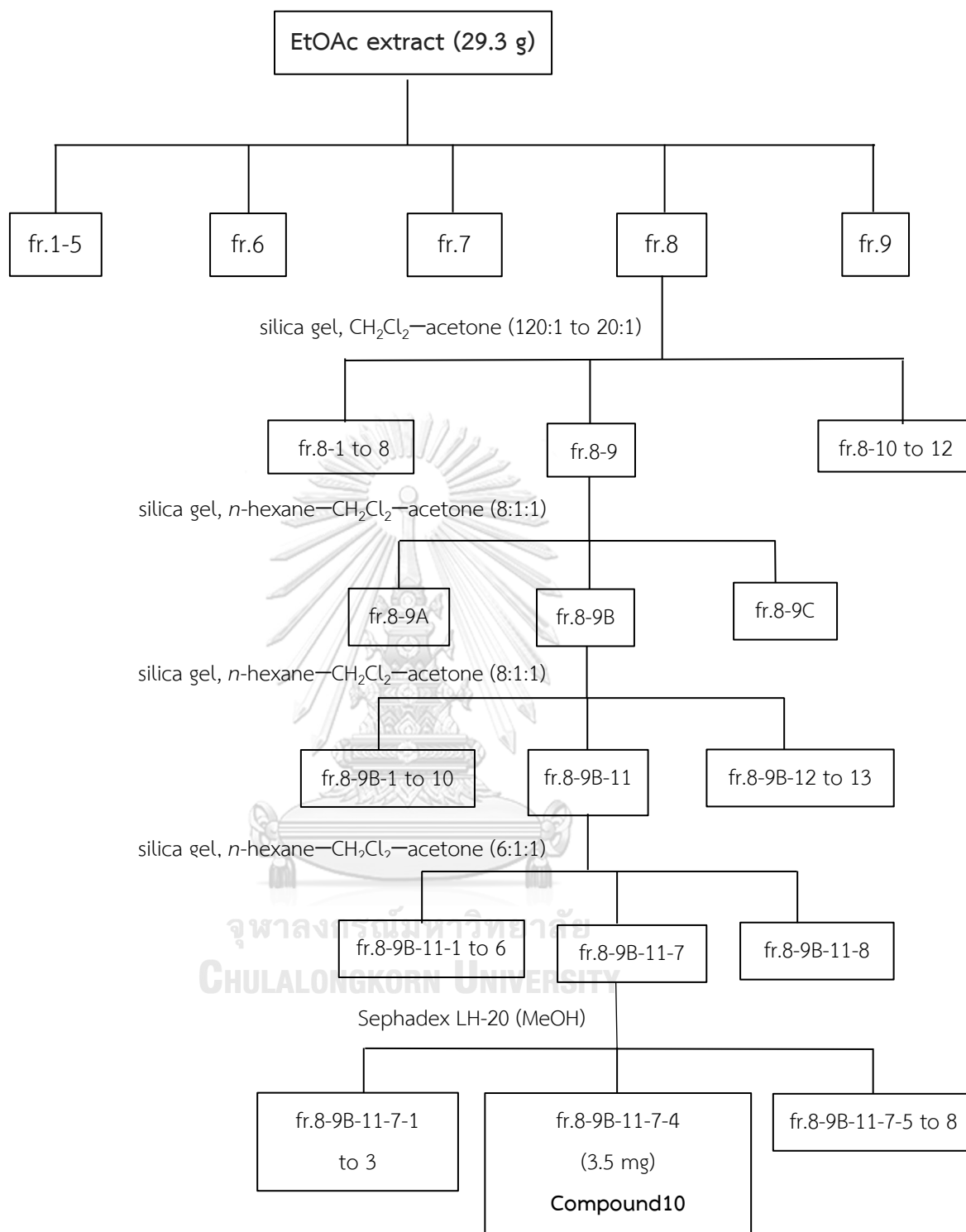
Scheme 5. Isolation of compound **6** — **7** from the EtOAc extract of *M. siamensis*



Scheme 6. Isolation of compound 8 from the EtOAc extract of *M. siamensis*



Scheme 7. Isolation of compound **9** from the EtOAc extract of *M. siamensis*



Scheme 8. Isolation of compound **10** from the EtOAc extract of *M. siamensis*

3.4.5 Isolation of compounds from *n*-butanol extract of *M. siamensis* roots

The *n*-butanol extract (50.8 g) was divided into 4 portions and loaded on Sephadex LH-20 (MeOH). All fractions were combined to yield 5 major fractions—MSRB-A (26.5 g), MSRB-B (20.8 g), MSRB-C (5.7 g), MSRB-D (5.7g) and MSRB-E (5.2 g).

3.4.5.1 Isolation of compounds 11 (maeruabisindole A)

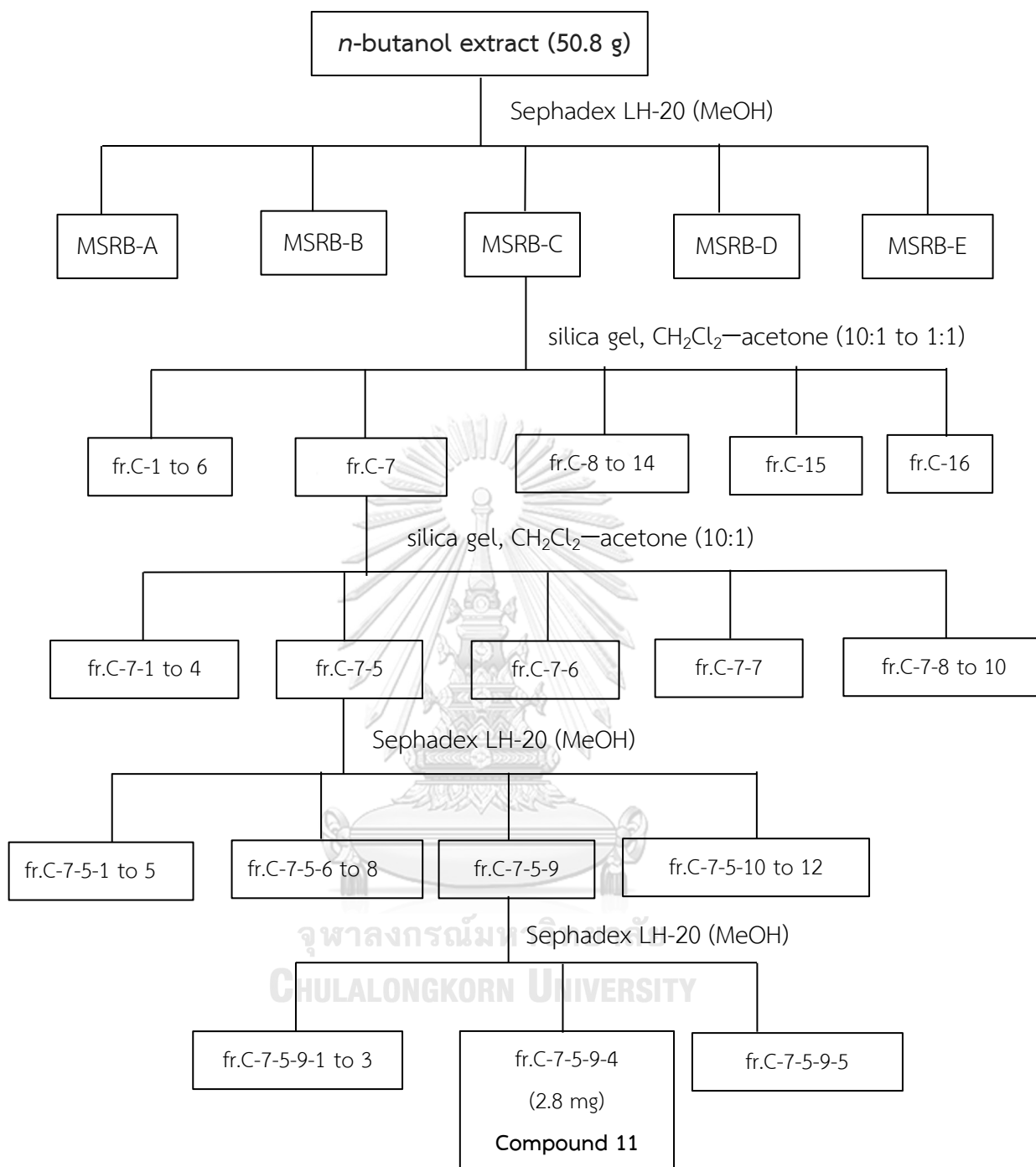
Fraction MSRB-C (5.7 g) was done with a separation on MPLC [silica gel, CH₂Cl₂-acetone (10:1 to 1:1)] to gain 16 subfractions (fr.C-1 – C-16). Subfraction MSRB-C-7 was further purified using MPLC [silica gel, CH₂Cl₂-acetone (10:1)] to obtain 10 subfractions (fr.C-7-1 – C-7-10). Subfraction C-7-5 (283.5 mg) was separated into two steps by Sephadex LH-20 (MeOH) to yield **compound 11** (subfraction MSRB-C-7-5-9-4, 1.1 mg) as a pale green amorphous solid (**Scheme 9**).

3.4.5.2 Isolation of compounds 12 (maeruabisindole B)

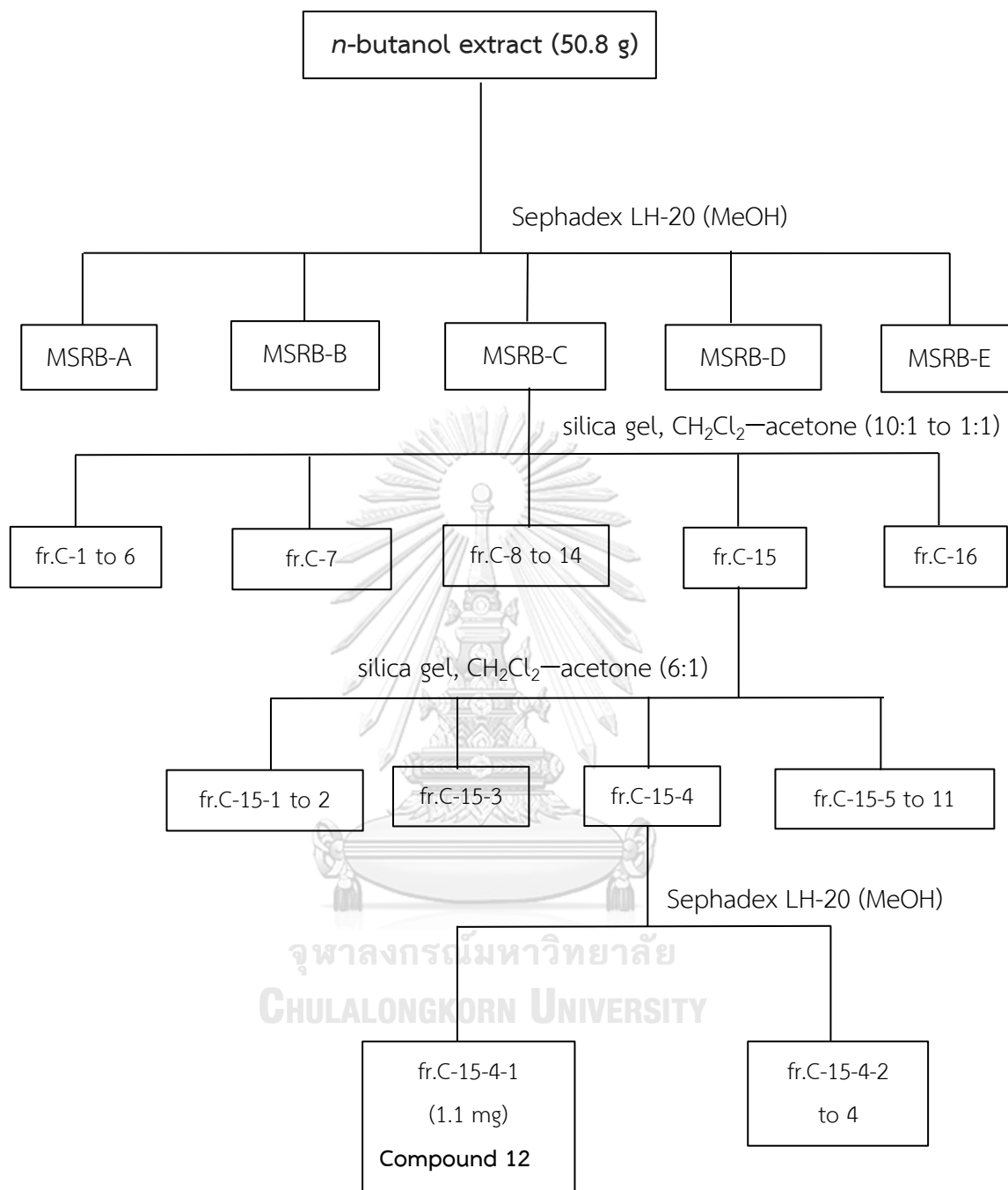
Fraction MSRB-C-15 (3.58 g) was separated by MPLC [Si-CC, CH₂Cl₂-acetone (6:1)] to yield 11 subfractions (fr.C-15-1 – C-15-11). Fraction C-15-4 (8.6 mg) was further purified by Sephadex LH-20 (MeOH) to obtain 4 subfractions (fr.C-15-4-1 – C-15-4-4). **Compound 12** (1.1 mg) was yielded as a pale green amorphous solid from subfraction MSRB-C-15-4-1 (**Scheme 10**).

3.4.5.3 Isolation of compounds 13 (maeruabisindole C)

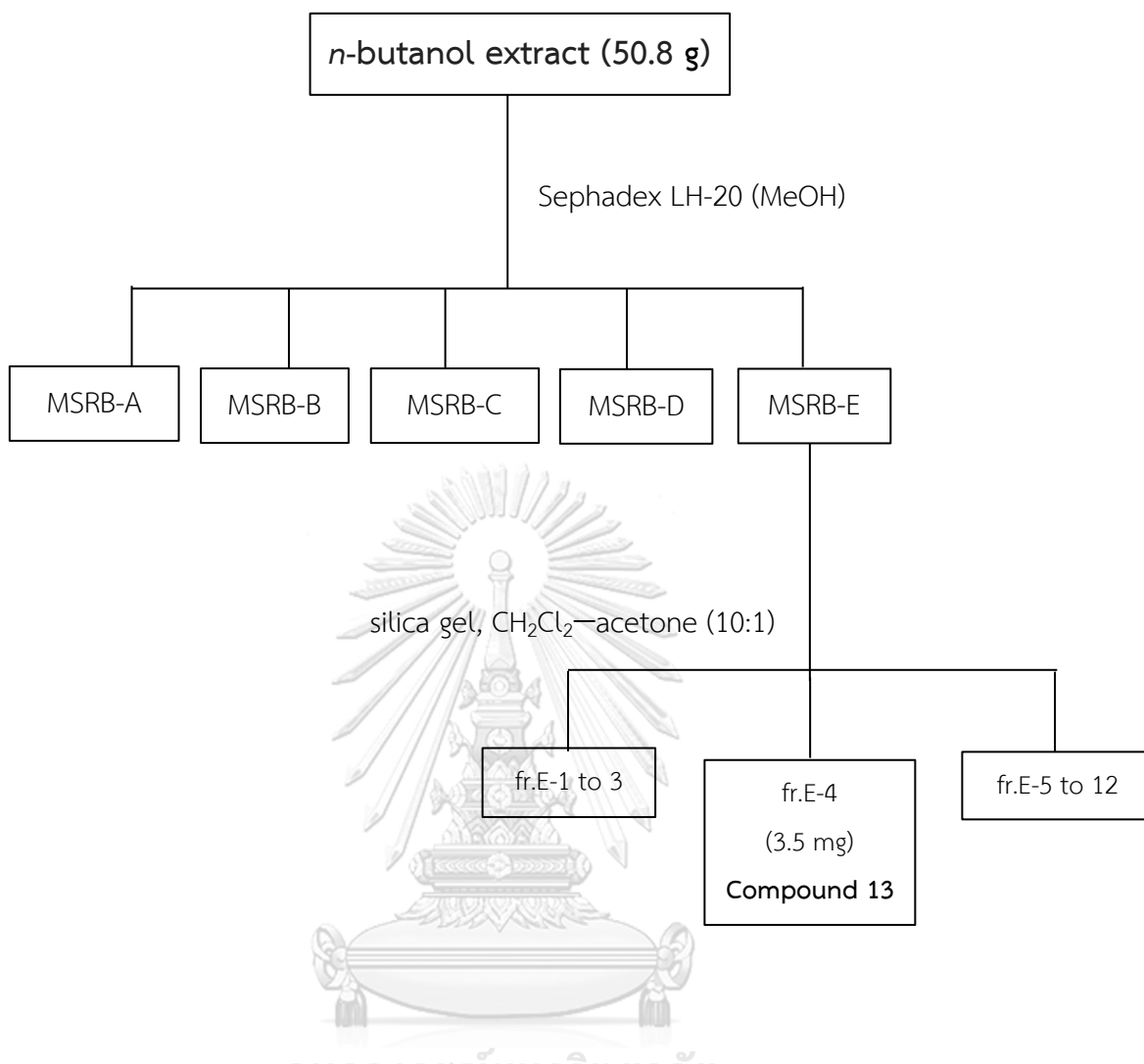
Fraction MSRB-E (2.31g) was separated by MPLC column [silica gel, CH₂Cl₂-acetone (10:1 to 1:1) to obtain 12 subfractions (fr.E-1 – E-12). **Compound 13** (3.5 mg) was obtained as a dark green amorphous solid from subfraction MSRB-E-4 (**Scheme 11**).



Scheme 9. Isolation of compound **11** from the butanol extract of *M. siamensis*



Scheme 10. Isolation of compounds **12** from the butanol extract of *M. siamensis*



Scheme 11. Isolation of compound **13** from the butanol extract of *M. siamensis*

3.5 Physical and spectral data of isolated compounds

3.5.1 Compound 1 (methyl 6-methoxy-3-indolecarbonate)

Compound 1 was obtained as a yellow amorphous solid, soluble in acetone (1.2 mg, 0.00004% based on dried weight of stems).

HR-ESI-MS : $[M+H]^+$ at m/z 206.0817 (calculated for $C_{11}H_{12}NO_3$, 206.0818); **Figure 5**

FT-IR : ν_{\max} (ATR) cm^{-1} : 3307, 2947, 2836, 1678, 1532, 1442, 1277, 1153;

Figure 6

1H -NMR : δ ppm, 400 MHz, acetone- d_6 ; see **Table 4; Figure 7-8**

^{13}C -NMR : δ ppm, 100 MHz, acetone- d_6 ; see **Table 4; Figure 9**

3.5.2 Compound 2 (vanillic acid)

Compound 2 was obtained as a white amorphous solid, soluble in acetone (4.1 mg, 0.00014% based on dried weight of stems).

HR-ESI-MS : $[M+H]^+$ at m/z 169.0504 (calculated for $C_8H_8O_4$, 169.0501); **Figure 15**

FT-IR : ν_{\max} (ATR) cm^{-1} : 3484, 2923, 1674, 1595, 1522, 1433, 1217, 1237, 1202, 1111, 763, 503; **Figure 16**

1H -NMR : δ ppm, 400 MHz, acetone- d_6 ; see **Table 5; Figure 17**

^{13}C -NMR : δ ppm, 100 MHz, acetone- d_6 ; see **Table 5; Figure 18**

3.5.3 Compound 3 [(-)-syringaresinol]

Compound 3 was obtained as a white amorphous solid, soluble in acetone (10 mg, 0.00033% based on dried weight of stems).

HR-ESI-MS : $[M+Na]^+$ at m/z 441.1540 (calculated for $C_{22}H_{26}NO_8Na$, 441.1520); **Figure 23**

$[\alpha]_D^{25}$: -31.0° (c 0.01, MeOH)

FT-IR : ν_{\max} (ATR) cm^{-1} : 3397, 2939, 2835, 1610, 1515, 1459, 1424, 1332, 1212, 1108; **Figure 24**

$^1\text{H-NMR}$: δ ppm, 400 MHz, acetone- d_6 ; see **Table 6; Figure 25-26**

$^{13}\text{C-NMR}$: δ ppm, 100 MHz, acetone- d_6 ; see **Table 6; Figure 27**

3.5.4 Compound 4 [(+)-ampelopsin A]

Compound 4 was obtained as a red amorphous solid, soluble in MeOH and acetone (2.4 mg, 0.00008% based on dried weight of stems).

HR-ESI-MS : $[\text{M}+\text{H}]^+$ at m/z 471.1455 (calculated for $\text{C}_{28}\text{H}_{22}\text{NO}_7$, 471.1444); **Figure 33**

$[\alpha]_D^{25}$: $+98^\circ$ (c 0.10, MeOH)

FT-IR : ν_{max} (ATR) cm^{-1} : 3314, 1597, 1513, 1451, 1339, 1234, 1173, 1151, 1135, 1007, 834; **Figure 34**

$^1\text{H-NMR}$: δ ppm, 400 MHz, acetone- d_6 ; see **Table 7; Figure 35-36**

$^{13}\text{C-NMR}$: δ ppm, 100 MHz, acetone- d_6 ; see **Table 7; Figure 37-38**

3.5.5 Compound 5 [(-)-pauciflorol E]

Compound 5 was obtained as a green amorphous solid, soluble in acetone (3.0 mg, 0.0001% based on dried weight of stems).

HR-ESI-MS : $[\text{M}+\text{H}]^+$ ion at m/z 469.1320 (calculated for $\text{C}_{28}\text{H}_{20}\text{NO}_7$, 469.1287); **Figure 45**

$[\alpha]_D^{25}$: -166° (c 0.10, MeOH)

FT-IR : ν_{max} (ATR) cm^{-1} : 3339, 2924, 2852, 1656, 1596, 1531, 1447, 1374, 1333, 1261, 1175, 1158, 1110, 1010, 835; **Figure 46**

$^1\text{H-NMR}$: δ ppm, 400 MHz, acetone- d_6 ; see **Table 8; Figure 47-49**

$^{13}\text{C-NMR}$: δ ppm, 100 MHz, acetone- d_6 ; see **Table 8; Figure 50-51**

3.5.6 Compound 6 [(+)-maeruanitrile A]

Compound 6 was obtained as a reddish-brown amorphous solid, soluble in acetone (2.4 mg, 0.00003% based on dried weight of roots).

- HR-ESI-MS : $[M+Na]^+$ at m/z 241.0585 (calculated for $C_{11}H_{10}N_2O_3Na$, 241.0584);
Figure 58
- $[\alpha]_D^{25}$: $+3.0^\circ$ (c 0.001, MeOH)
- UV : λ_{max} (MeOH) nm (log ϵ): 218 (5.49), 268 (4.66), 322 (4.04); **Figure 57**
- CD : (c 0.000045, MeOH) nm (mdeg): 240 (+8.20), 265.5 (−9.64), 283.0 (0.07);
Figure 60
- FT-IR : ν_{max} (ATR) cm^{-1} : 3291, 2256, 1789, 1629, 1462, 1342, 1722; **Figure 59**
- 1H -NMR : δ ppm, 600 MHz, acetone- d_6 ; see **Table 9**; **Figure 61**
- ^{13}C -NMR : δ ppm, 150 MHz, acetone- d_6 ; see **Table 9**; **Figure 62**

3.5.7 Compound 7 (maeruanitrile B)

Compound 7 was obtained as a reddish-brown amorphous solid, soluble in acetone (1.4 mg, 0.00002% based on dried weight of roots).

- HR-ESI-MS : $[M+Na]^+$ at m/z 271.0511 (calculated for $C_{12}H_{12}N_2O_2SNa$, 271.0517);
Figure 69
- UV : λ_{max} (MeOH) nm (log ϵ): 228 (4.85), 300 (4.39), 342 (3.77); **Figure 68**
- FT-IR : ν_{max} (ATR) cm^{-1} : 3163, 2924, 2850, 2360, 2249, 1626, 1451, 1298, 1208, 1160, 1022; **Figure 70**
- 1H -NMR : δ ppm, 600 MHz, CD_3OD ; see **Table 10**; **Figure 71**
- ^{13}C -NMR : δ ppm, 150 MHz, CD_3OD ; see **Table 10**; **Figure 72**

3.5.8 Compound 8 (maeroxime A)

Compound 8 was obtained as a reddish-brown amorphous solid, soluble in acetone (2.4 mg, 0.00003% based on dried weight of roots).

- HR-ESI-MS : $[M+H]^+$ at m/z 265.0999 (calculated for $C_{13}H_{16}N_2O_2S$, 265.1010);
Figure 81

UV : λ_{\max} (MeOH) nm (log ϵ): 212 (5.12), 217 (5.26), 225 (4.80), 269 (4.15);

Figure 80

FT-IR : ν_{\max} (ATR) cm^{-1} : 3369, 2923, 2852, 1714, 1627, 1501, 1457, 1337, 1198, 1093; **Figure 82**

$^1\text{H-NMR}$: δ ppm, 400 MHz, $\text{DMSO-}d_6$; see **Table 11**; **Figure 83-84**

$^{13}\text{C-NMR}$: δ ppm, 100 MHz, $\text{DMSO-}d_6$; see **Table 11**; **Figure 85**

3.5.9 Compound 9 (maeroxime B)

Compound 9 was obtained as an orange-brown amorphous solid, soluble in acetone (1.0 mg, 0.00001% based on dried weight of roots).

HR-ESI-MS : $[\text{M}+\text{H}]^+$ at m/z 279.0780 (calculated for $\text{C}_{13}\text{H}_{14}\text{N}_2\text{O}_3\text{S}$, 279.0803); **Figure 96**

UV : λ_{\max} (MeOH) nm (log ϵ): 212 (4.69), 280 (3.25), 314 (4.18); **Figure 94**

FT-IR : ν_{\max} (ATR) cm^{-1} : 3283, 2924, 2851, 1718, 1617, 1521, 1421, 1241, 1197, 1074, 1032; **Figure 95**

$^1\text{H-NMR}$: δ ppm, 400 MHz, $\text{DMSO-}d_6$; see **Table 12**; **Figure 97**

$^{13}\text{C-NMR}$: δ ppm, 100 MHz, $\text{DMSO-}d_6$; see **Table 12**; **Figure 98**

3.5.10 Compound 10 (maeroxime C)

Compound 10 was obtained as a yellow amorphous solid, soluble in acetone (3.5 mg, 0.00005% based on dried weight of roots).

HR-ESI-MS : $[\text{M}+\text{H}]^+$ at m/z 279.0782 (calculated for $\text{C}_{13}\text{H}_{14}\text{N}_2\text{O}_3\text{S}$, 279.0803); **Figure 106**

UV : λ_{\max} (MeOH) nm (log ϵ): 208 (4.80), 272 (4.47), 316 (4.15); **Figure 105**

FT-IR : ν_{\max} (ATR) cm^{-1} : 3306, 2956, 2924, 2854, 1729, 1618, 1461, 1378, 1283, 1074, 1037; **Figure 107**

$^1\text{H-NMR}$: δ ppm, 400 MHz, $\text{DMSO-}d_6$; see **Table 13**; **Figure 108**

$^{13}\text{C-NMR}$: δ ppm, 100 MHz, $\text{DMSO-}d_6$; see **Table 13**; **Figure 109**

3.5.11 Compound 11 (maeruabisindole A)

Compound 11 was obtained as a pale green amorphous solid, soluble in MeOH (1.1 mg, 0.00002% based on dried weight of roots).

HR-ESI-MS : $[\text{M}+\text{H}]^+$ at m/z 390.1298 (calculated for $\text{C}_{22}\text{H}_{20}\text{N}_3\text{O}_2\text{S}$, 390.1271);

Figure 116

UV : λ_{max} (MeOH) nm (log ϵ): 210 (3.72), 270 (4.03), 315 (3.95), 355 (3.49), 365 (3.44); **Figure 115**

FT-IR : ν_{max} (ATR) cm^{-1} : 3384, 2919, 2850, 1625, 1559, 1508, 1458, 1420, 1325, 1286, 1246, 1228, 1196, 1162, 1089, 1029; **Figure 117**

$^1\text{H-NMR}$: δ ppm, 400 MHz, $\text{DMSO-}d_6$; see **Table 14**; **Figure 118-119**

$^{13}\text{C-NMR}$: δ ppm, 100 MHz, $\text{DMSO-}d_6$; see **Table 14**; **Figure 120-121**

3.5.12 Compound 12 (maeruabisindole B)

Compound 12 was obtained as a pale green amorphous solid, soluble in MeOH (1.1 mg, 0.00002% based on dried weight of roots).

HR-ESI-MS : $[\text{M}+\text{H}]^+$ at m/z 406.1224 (calculated for $\text{C}_{22}\text{H}_{20}\text{N}_3\text{O}_3\text{S}$, 406.1220); **Figure 130**

UV : λ_{max} (MeOH) nm (log ϵ): 210 (4.47), 230 (4.15), 310 (3.93), 340 (3.31), 355 (3.31); **Figure 129**

FT-IR : ν_{max} (ATR) cm^{-1} : 3396, 2921, 2851, 1602, 1465, 1377, 1258, 1172, 1117, 1025; **Figure 131**

$^1\text{H-NMR}$: δ ppm, 400 MHz, CD_3OD ; see **Table 15**; **Figure 132-133**

$^{13}\text{C-NMR}$: δ ppm, 100 MHz, CD_3OD ; see **Table 15**; **Figure 134**

3.5.13 Compound 13 (maeruabisindole C)

Compound 13 was obtained as a dark green amorphous solid, soluble in acetone (3.5 mg, 0.00005% based on dried weight of roots).

HR-ESI-MS : $[M-H]^-$ at m/z 326.0968 (calculated for $C_{20}H_{12}N_3O_2$, 326.0935); **Figure 141**

UV : λ_{max} (MeOH) nm (log ϵ): 210 (4.07), 285 (2.93), 355 (2.21), 365 (2.36); **Figure 142**

FT-IR : ν_{max} (ATR) cm^{-1} : 3359, 3192, 2921, 2851, 2212, 1658, 1632, 1468, 1412, 1279, 1135, 702, 632; **Figure 143**

1H -NMR : δ ppm, 400 MHz, acetone- d_6 ; see **Table 16**; **Figure 144-145**

^{13}C -NMR : δ ppm, 100 MHz, acetone- d_6 ; see **Table 16**; **Figure 146-147**

3.6 Evaluation of inhibitory activity on nitric oxide (NO) production and cytotoxicity

RAW 264.7 macrophage cells (ATCC, TIB-71) were cultivated in DMEM (Dulbecco's Modified Eagle Medium, Gibco, Thermo Fisher Scientific, Waltham, MA, USA) including 10% fetal bovine serum (FBS), and penicillin (100 U/mL) and streptomycin (100 μ g/mL) in a humidified atmosphere (37°C, 5%CO₂). Indomethacin was used as positive control.

Briefly, cells were placed in 96-well plate (5×10^4 cells/well) and pre-treated with various concentrations of compounds for 24 h. Then, the cells were added with 100 ng/mL LPS and further incubated for 24 h. After that, the supernatants were collected for NO production assay and the cytotoxicity was determined by MTT assay.

Cells were pre-treated with various concentrations of samples for 24 h. Cells were induced with 100 ng/mL LPS for 24 h. The culture supernatant was collected for NO production analysis using Griess reagent kit (Invitrogen, Thermo Fisher Scientific, Waltham, MA, USA), and cells were further examined for their viability.

Ninety μ L of supernatant was mixed with 10 μ L of Griess reagent and incubated for 30 min at room temperature, then the NO concentration was measured at 540 nm

using the microplate reader (Synergy H1, BioTeK, Santa Clara, CA, USA) and calculated using NaNO₂ standard curve (Kim *et al.*, 2020). Percentage of NO production was calculated from **equation 1**.

$$\% \text{ NO production} = \frac{A}{B} \times 100 \quad \text{equation 1}$$

A = concentration of nitric oxide in cells induced by LPS with sample pre-treatment

B = concentration of nitric oxide in cells induced by LPS without sample pre-treatment

The NO inhibitory activity was indicated as half maximal inhibitory concentration (IC₅₀) calculated by GraphPad Prism 9.

For MTT assay, MTT solution (1 mg/mL) was added to each well and incubated for 4 h at 37°C. After removal of the MTT solution, cells were added with DMSO to dissolve formazan product. The absorbance was measured at 570 nm using a microplate reader (Eaknai *et al.*, 2022).

3.7 Statistical analysis

The results were expressed as mean ± standard error of the mean (SEM) from three independent experiments. The mean differences of IC₅₀ values of samples vs that of indomethacin (positive control) were analyzed by one-way analysis of variance (ANOVA) (GraphPad Prism 9). Statistical significance was defined as $p < 0.05$.

CHAPTER IV

RESULTS AND DISCUSSION

In this study, eight compounds were isolated from the EtOAc extract of the stems of *Capparis micracantha* and five compounds were obtained from the *n*-butanol extract of the roots of *Maerua siamensis*. They were purified by chromatographic techniques and their chemical structures were identified or elucidated by spectroscopic techniques including IR, UV, MS and NMR spectroscopy. The extracts and all isolated compounds were tested for their inhibitory effect on nitric oxide production.

4.1 Identification of compounds isolated from *Capparis micracantha* stems

4.1.1 identification of compound 1 (methyl 6-methoxy-3-indolecarbonate)

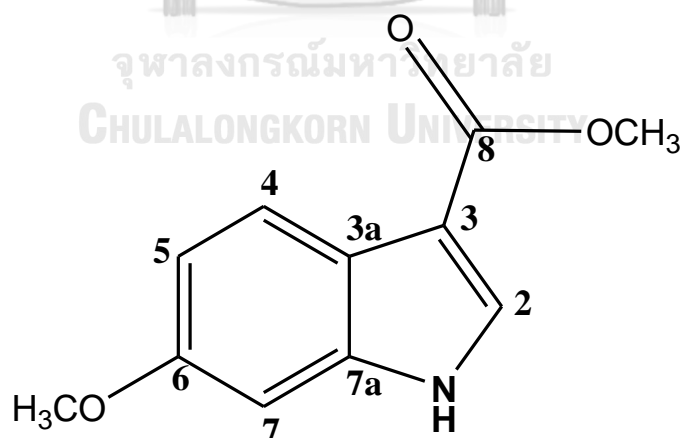
Compound **1** was obtained as a yellow amorphous solid. Its pseudo-molecular $[M+H]^+$ ion was observed in the high resolution ESI mass spectrum at m/z 206.0818 (calculated for $C_{11}H_{12}NO_3$, 206.0817) (**Figure 5**), suggesting a molecular formula of $C_{11}H_{11}NO_3$, with seven degrees of unsaturation. The IR spectrum showed NH absorption peak at 3307 cm^{-1} and conjugated ester carbonyl peak at 1679 cm^{-1} (**Figure 6**).

The ^1H NMR spectrum of compound **1** (400 MHz, acetone- d_6) (**Figure 7-8** and **Table 4**) displayed the signals of one carboxymethyl group at δ_{H} 3.82 (3H, s, 8-COOCH₃) and one methoxy group at δ_{H} 3.81 (3H, s, 6-OCH₃), an ABX system of a 1,2,4 trisubstituted aromatic ring at δ_{H} 6.86 (1H, *dd*, $J = 8.7, 2.4$ Hz, H-5), 7.03 (1H, *d*, $J = 2.4$ Hz, H-7) and 7.92 (1H, *d*, $J = 8.7$ Hz, H-4), an olefinic methine proton at δ_{H} 7.90 (1H, *s*, H-2) and a broad NH proton at δ_{H} 10.76 (1H, *br s*, NH-1). These data were indicative of an indole nucleus with two substituents.

Its ^{13}C NMR data (100 MHz, acetone- d_6) (**Figure 9** and **Table 4**) and ^1H - ^{13}C HSQC spectrum (**Figure 10**) showed resonances of eleven carbon atoms including a methoxy carbon 55.8 (6-OCH₃), a carboxymethyl group at δ_{C} 50.9 (8-COOCH₃) and 168.4 (C-8), three aromatic methine carbons at δ_{C} 95.9 (C-7), 112.4 (C-5) and 122.5 (C-4), an olefinic

methane carbon at δ_C 131.5 (C-2), and four quaternary carbons at δ_C 108.6 (C-3), 121.2 (C-3a), 138.5 (C-7a) and 157.9 (C-6)..

The ^1H - ^1H COSY spectrum (**Figure 13**) exhibited cross peak between the signals of H-4 at δ_H 7.92 and H-5 at δ_H 6.86, confirming their *ortho*-coupling. The assignment of H-4 signal was confirmed by its long-range ^1H - ^{13}C HMBC correlation (**Figure 11-12** and **Table 4**) to that of C-3. The methoxy substitution at C-6 was confirmed by ^1H - ^1H NOESY cross peaks (**Figure 14**) between both H-5 and H-7 signals with that of 6-OCH₃, as well as HMBC cross peak of this methoxy protons with the signal of C-6. Additionally, the olefinic H-2 signal at δ_H 7.90 showed HMBC cross peaks with the signals of C-3a and C-7a, establishing a substituent at position 3 of the indole nucleus. Then spectroscopic data indicated an indole moiety with a methoxy substitution at C-6 and an ester carbonyl substitution at C-3. These NMR data helped identify compound **1** as methyl 6-methoxy-3-indolecarbonate, which has previously been found in the roots and rhizomes of *Clematis manshurica* (family Ranunculaceae), which are used as an anti-inflammatory, analgesic and antitumor herb in traditional Chinese medicine (Shi *et al.*, 2006).



Methyl 6-methoxy-3-indolecarbonate

Table 4. ^1H - and ^{13}C -NMR data of compound **1** (400 MHz, in acetone- d_6) and methyl 6-methoxy-3-indolecarbonate (300 MHz, in CDCl_3)

Position	Compound 1		Methyl 6-methoxy-3-indolecarbonate*		HMBC correlation with
	δ_{H} (mult., J in Hz)	δ_{C}	δ_{H} (mult., J in Hz)	δ_{C}	
NH-1	10.76 (<i>br</i>)	-	-	-	-
2	7.90 (<i>s</i>)	131.5	7.82 (<i>s</i>)	129.9	C-3, C-3a, C-7a
3	-	108.6	-	108.8	-
3a	-	121.2	-	119.9	-
4	7.92 (<i>d</i> , 8.7)	122.5	8.06 (<i>d</i> , 9.0)	122.1	C-3, C-3a, C-6
5	6.86 (<i>dd</i> , 8.7, 2.4)	112.4	6.95 (<i>dd</i> , 9.0, 2.4)	111.8	C-3a, C-6, C-7
6	-	157.9	-	157.1	-
7	7.03 (<i>d</i> , 2.4)	95.9	6.89 (<i>d</i> , 2.4)	94.9	C-3a, C-5, C-6
7a	-	138.5	-	136.9	-
8	-	168.4	-	165.7	-
6-OCH ₃	3.81 (<i>s</i>)	55.8	3.91 (<i>s</i>)	55.6	C-6
8-COOCH ₃	3.82 (<i>s</i>)	50.9	3.86 (<i>s</i>)	51.1	C-8

*Shi *et al.* (2006).

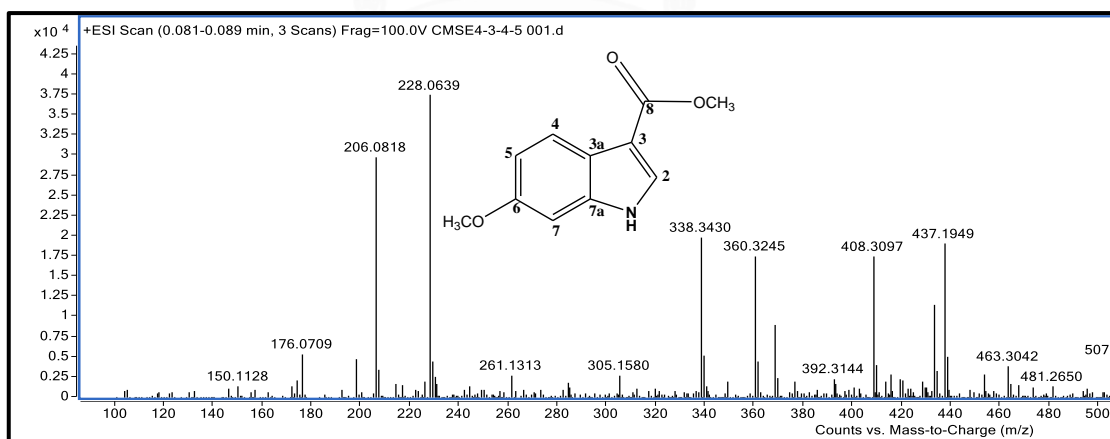


Figure 5. HR-ESI mass spectrum of compound **1**

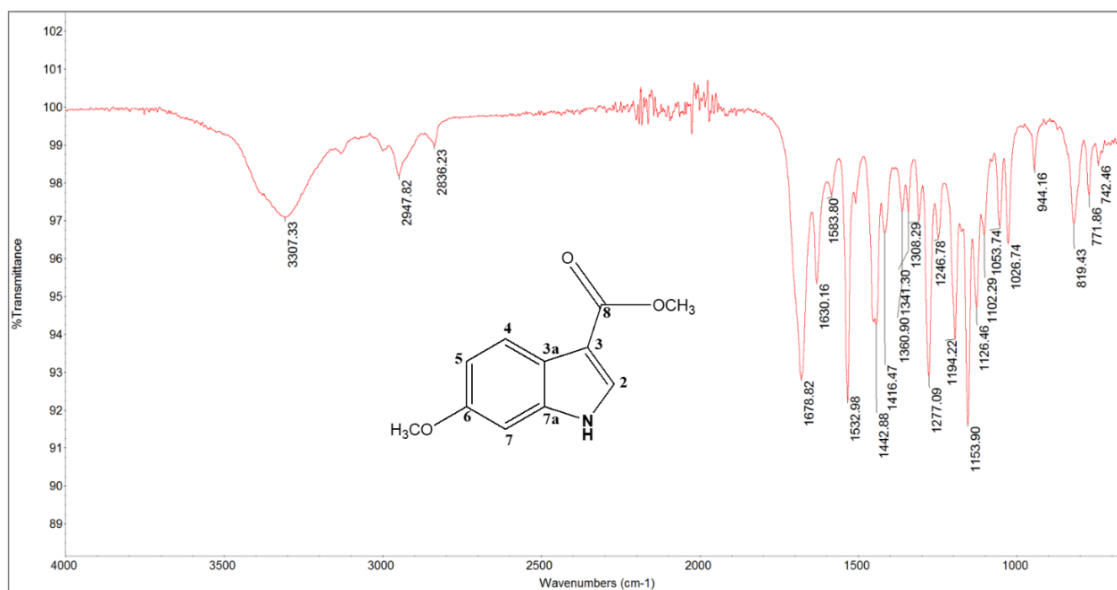


Figure 6. IR spectrum of compound 1

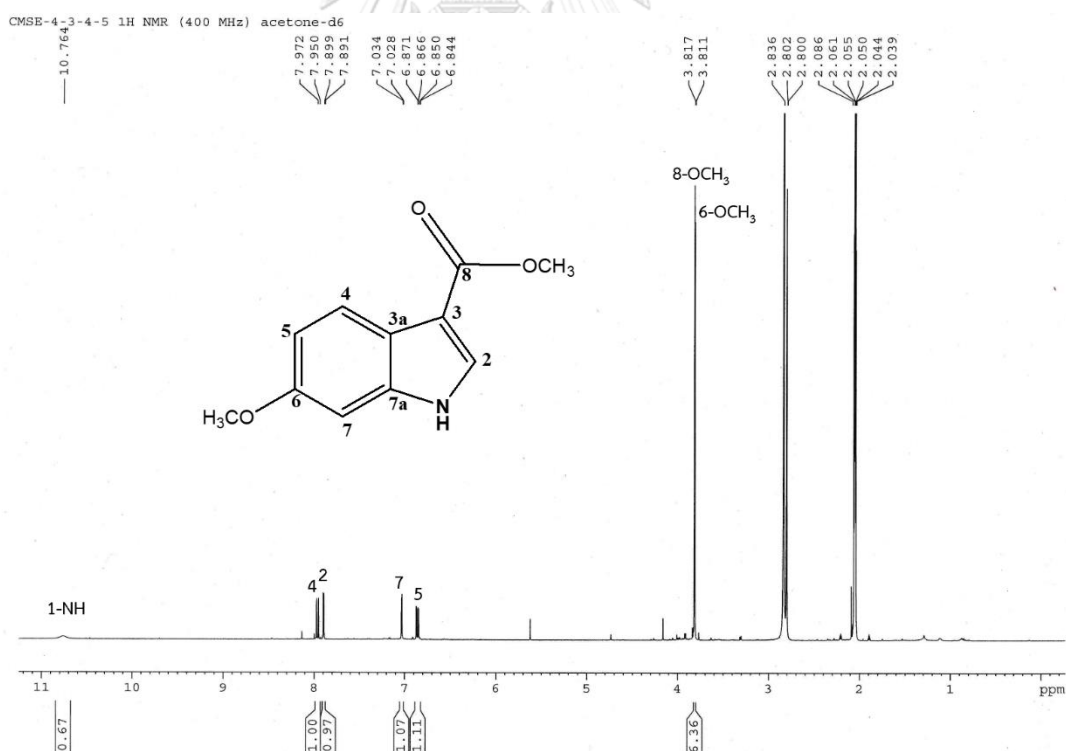
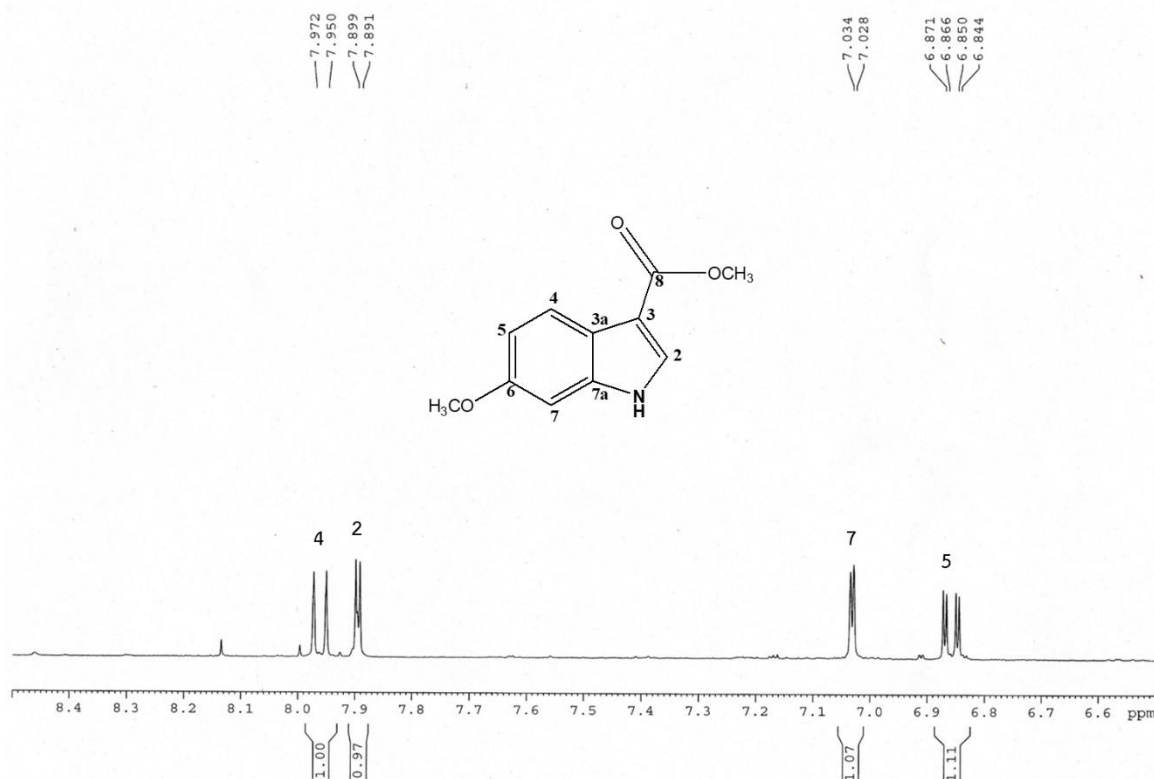
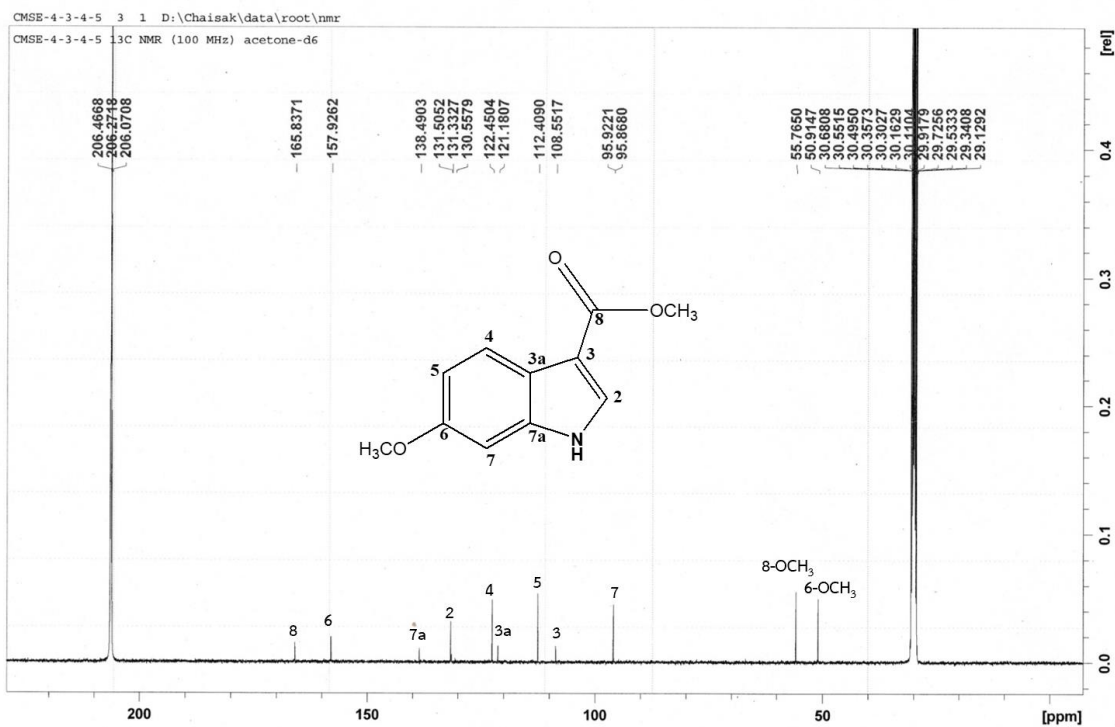


Figure 7. ¹H-NMR spectrum of compound 1 (400 MHz, acetone-d₆)

CMSE-4-3-4-5 1H NMR (400 MHz) acetone-d6

Figure 8. ^1H -NMR spectrum of compound 1 (expansion between δ_{H} 6.5-8.5 ppm)Figure 9. ^{13}C -NMR spectrum of compound 1 (100 MHz, acetone- d_6)

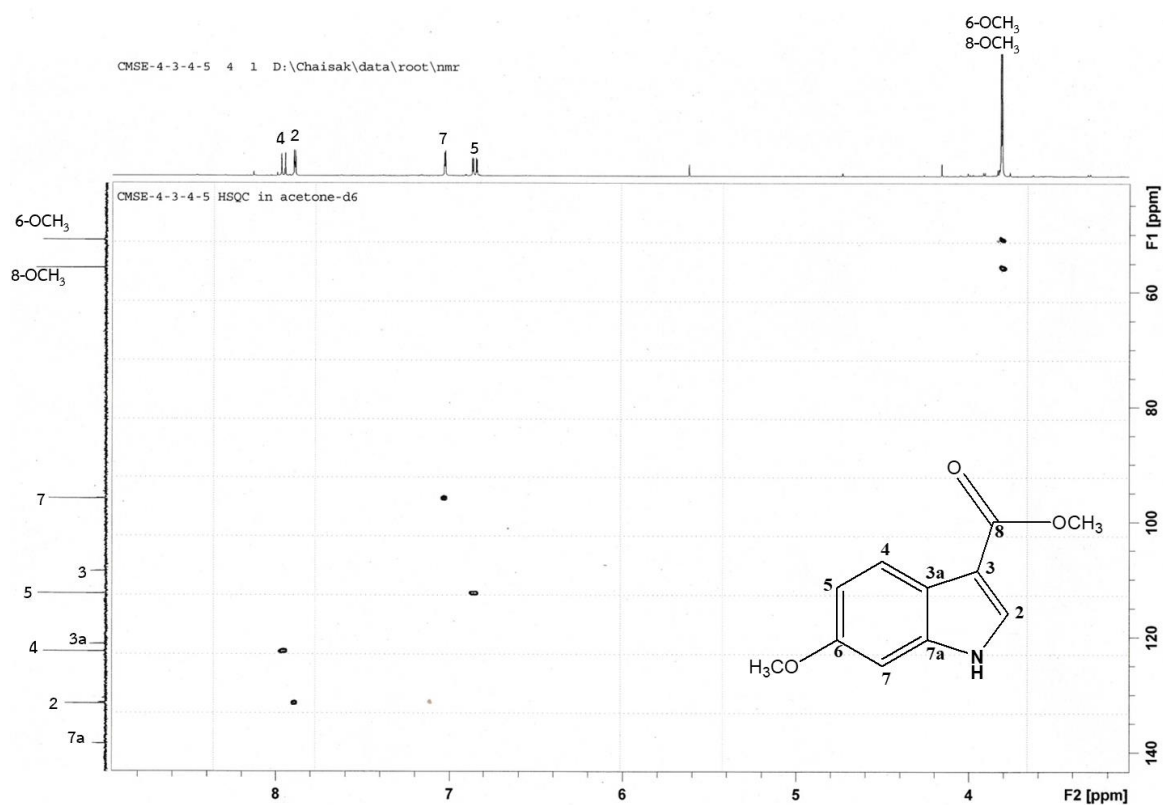


Figure 10. ^1H - ^{13}C HSQC spectrum of compound 1

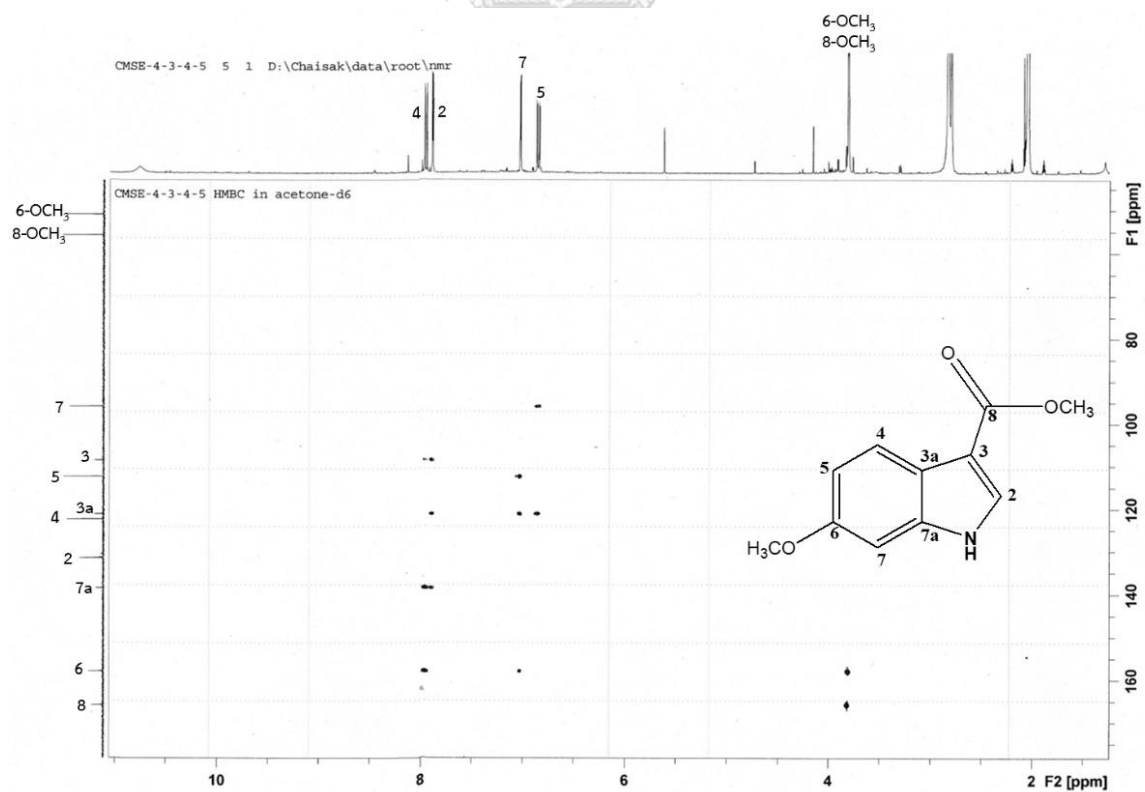


Figure 11. ^1H - ^{13}C HMBC spectrum of compound 1

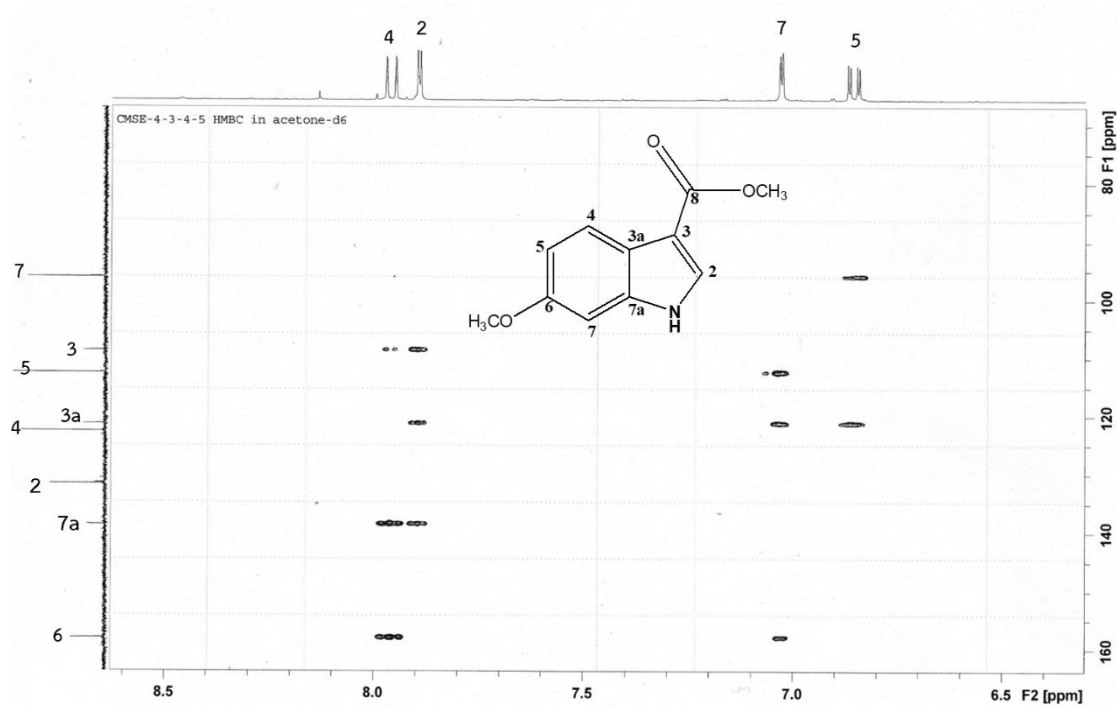


Figure 12. ^1H - ^{13}C HMBC spectrum of compound 1
(expansion between δ_{H} 6.3-8.6 ppm, δ_{C} 70-160 ppm)

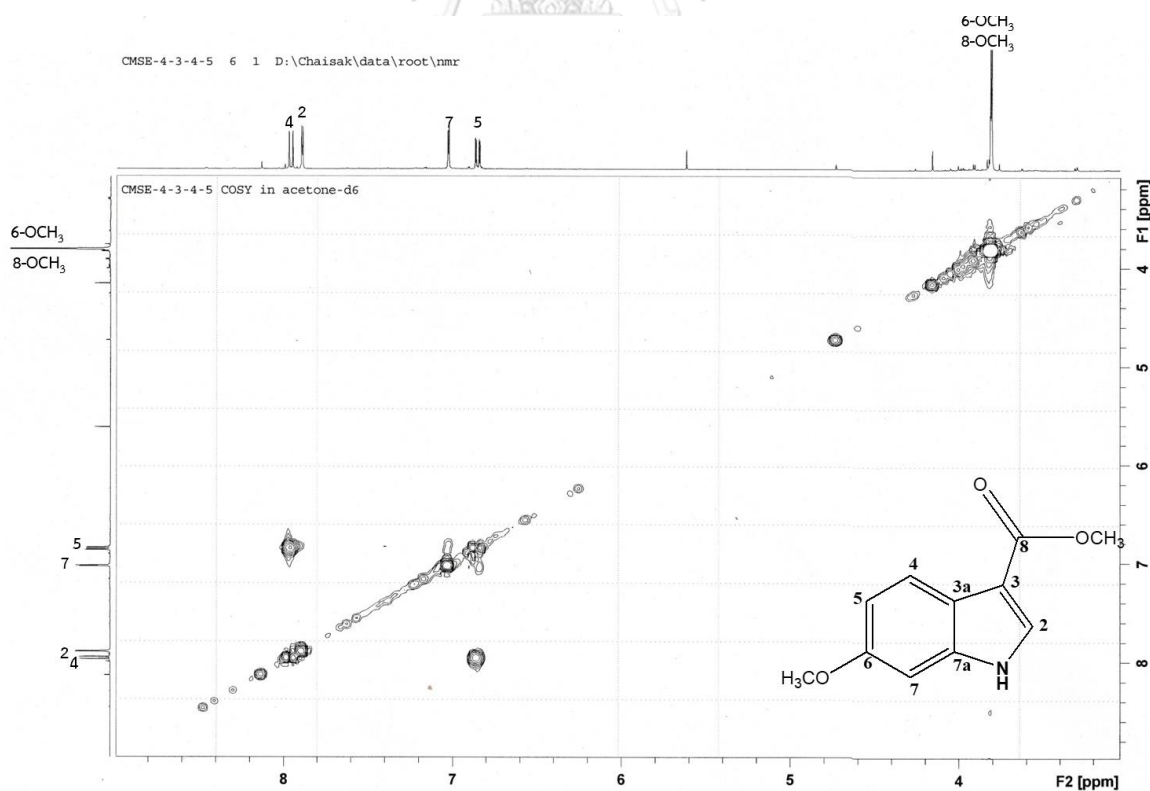


Figure 13. ^1H - ^1H COSY spectrum of compound 1

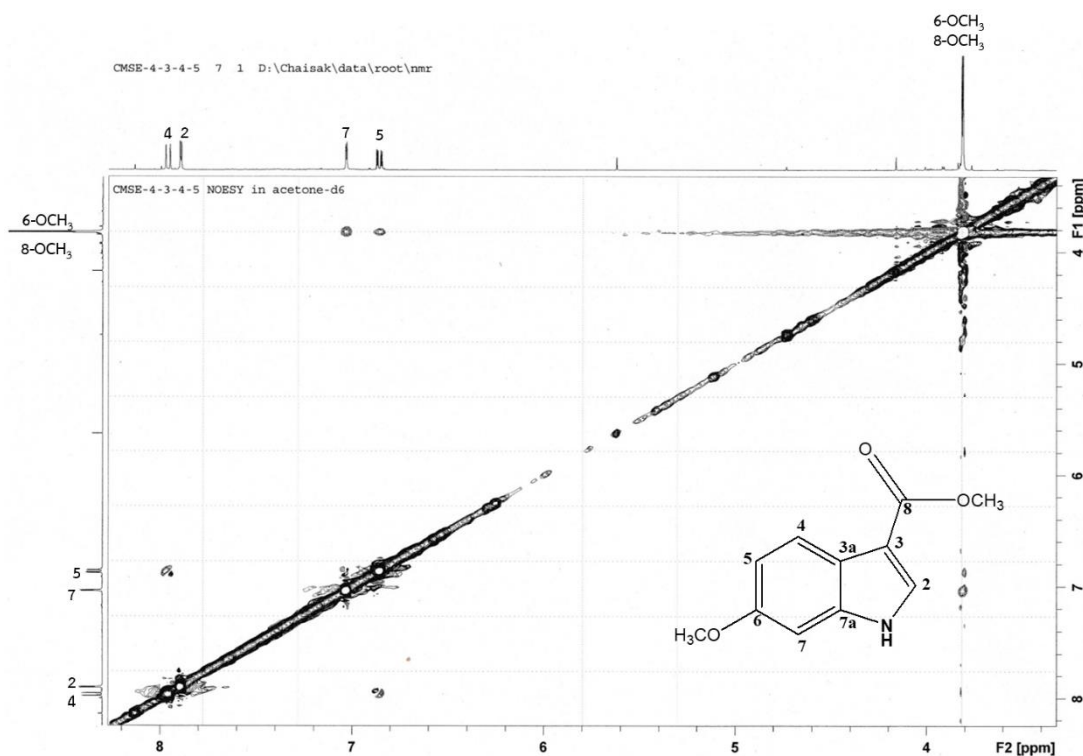


Figure 14. ^1H - ^1H NOESY spectrum of compound 1

4.1.2 Identification of compound 2 (vanillic acid)

Compound 2 was obtained as a white amorphous solid soluble in acetone. Its HR-ESI mass spectrum (Figure 15) revealed a pseudo-molecular $[\text{M}+\text{H}]^+$ ion peak at m/z 169.0504, in accordance with the molecular formula $\text{C}_8\text{H}_8\text{O}_4$ (calculated for $\text{C}_8\text{H}_9\text{O}_4$, 169.0501). The IR spectrum (Figure 16) displayed absorption peaks of hydroxyl group at 3483 cm^{-1} and conjugated carboxyl group at 1674 cm^{-1} .

In the ^1H NMR spectrum (400 MHz, acetone- d_6) (Figure 17 and Table 5), an ABX system of three aromatic protons were observed at δ_{H} 6.91 (1H, *d*, $J = 8.2$ Hz, H-5), 7.56 (1H, *d*, $J = 2.0$ Hz, H-2) and 7.59 (1H, *dd*, $J = 8.2, 2.0$ Hz, H-6). A three-proton resonance of one methoxy group was also located at δ_{H} 3.90 (3H, *s*, 3-OCH₃).

Its ^{13}C NMR spectrum (100 MHz, acetone- d_6) (Figure 18 and Table 5) exhibited eight carbon signals including those of three methines at δ_{C} 113.5 (C-2), 115.6 (C-5) and 124.9 (C-6), three quaternary carbons at δ_{C} 123.0 (C-1), 148.1 (C-3) and 152.1 (C-4), a carboxylic acid carbonyl at δ_{C} 167.6 (C-7) and a methoxy carbon at δ_{C} 56.4 (3-OCH₃).

These spectroscopic data of compound **2** was indicative of its chemical structure as a 1,3,4-trisubstituted benzene ring, One substituent is a carboxylic acid group which could be located at position 1, based on the long-range ^1H - ^{13}C HMBC cross peaks from the proton signals of both H-2 and H-6 to that of C-7 (**Figure 20**). A methoxy substituent at position 3 was confirmed by ^1H - ^1H NOESY correlation (**Figure 22**) observed between the proton signals of H-2 and 3-OCH₃. Therefore, the third substituent group, which is a hydroxy group, could be placed at position 4 of the benzene ring. These data helped identify compound **2** as vanillic acid. This aromatic compound has been isolated from several plants; for example, from the roots of *Lepidium meyenii* (family Brassicaceae) (Bai *et al.*, 2015), the aerial parts of *Alyssum alyssoides* (family Brassicaceae) (Tsiftoglou *et al.*, 2019) and the aerial parts of *Matthiola incana* (family Brassicaceae). Recently, vanillic acid has been reported to exhibit anti-inflammatory activity in osteoarthritis through inhibition of inflammatory cytokines such as interleukin 1 β (IL-1 β) and tumor necrosis factor α (TNF- α) in human chondrocytes (Ziadlou *et al.*, 2020).

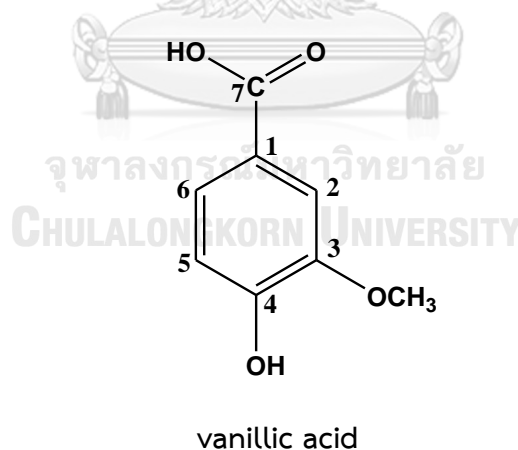


Table 5. ^1H - and ^{13}C -NMR data of compound **2** (400 MHz, in acetone- d_6) and vanillic acid (500 MHz, in CD_3OD)

Position	Compound 2		vanillic acid*		HMBC correlation with
	δ_{H} (mult., J in Hz)	δ_{C}	δ_{H} (mult., J in Hz)	δ_{C}	
1	-	123.0	-	123.8	-
2	7.56 (d, 2.0)	113.5	7.57 (d, 2.0)	115.3	C-1, C-3, C-4, C-6, C-7
3	-	148.1	-	147.6	-
4	-	152.1	-	151.6	-
5	6.91 (d, 8.2)	115.6	7.12 (d, 8.2)	112.2	C-1, C-3, C-4
6	7.59 (dd, 8.2, 2.0)	124.9	7.63-7.65 (dd, 8.2, 2.0)	125.2	C-2, C-7
7	-	167.6	-	169.0	-
3-OCH ₃	3.90 (s)	56.4	3.91 (s)	55.4	C-3

*Chang *et al.* (2009).

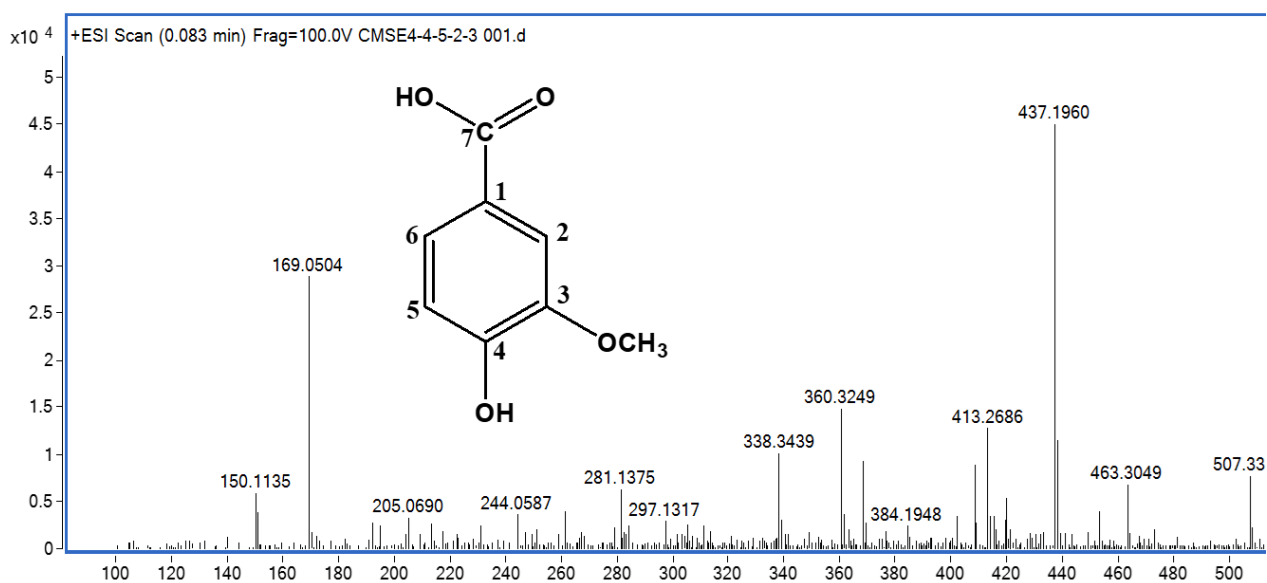


Figure 15. HR-ESI mass spectrum of compound **2**

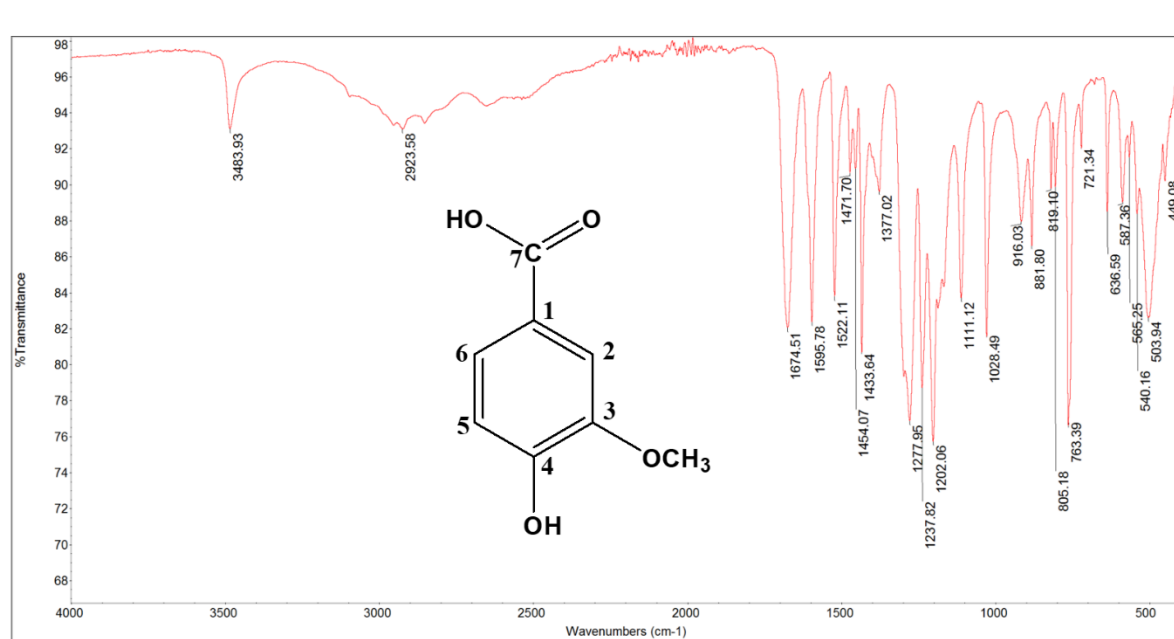
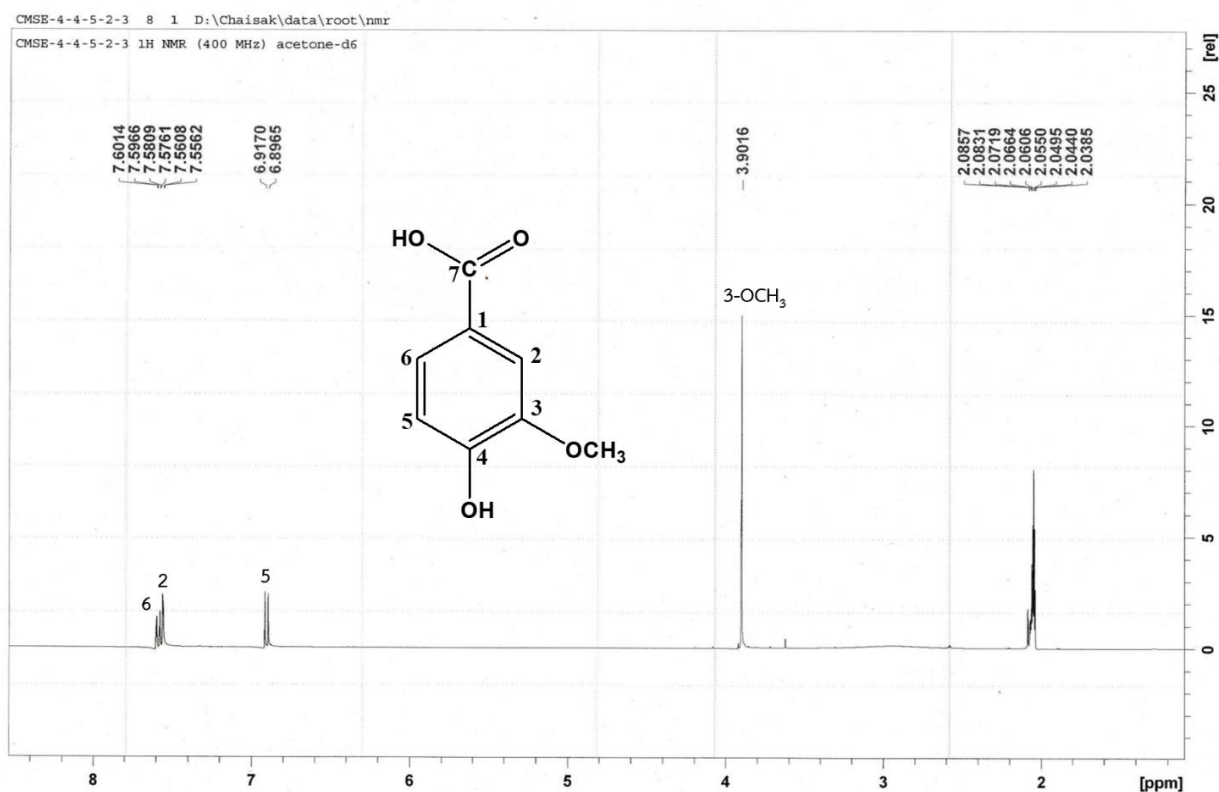


Figure 16. IR spectrum of compound 2

Figure 17. ¹H-NMR spectrum of compound 2 (400 MHz, acetone-d₆)

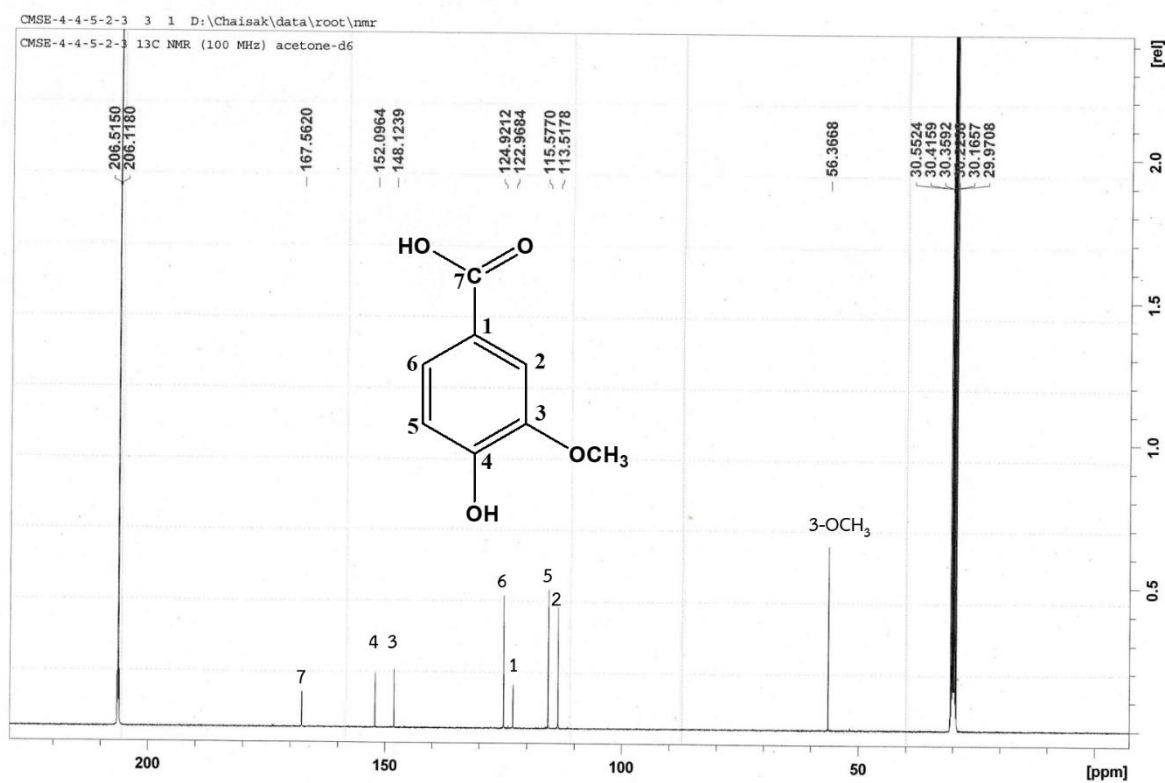


Figure 18. ¹³C-NMR spectrum of compound 2 (100 MHz, acetone d₆)

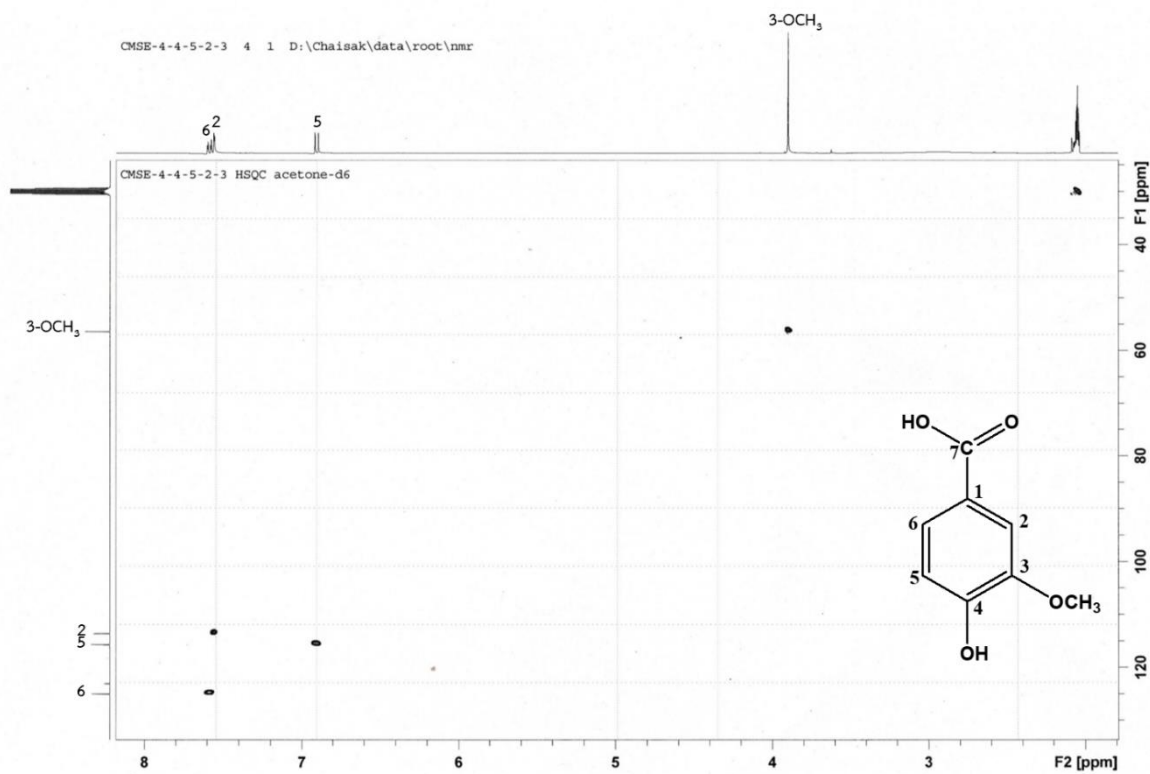
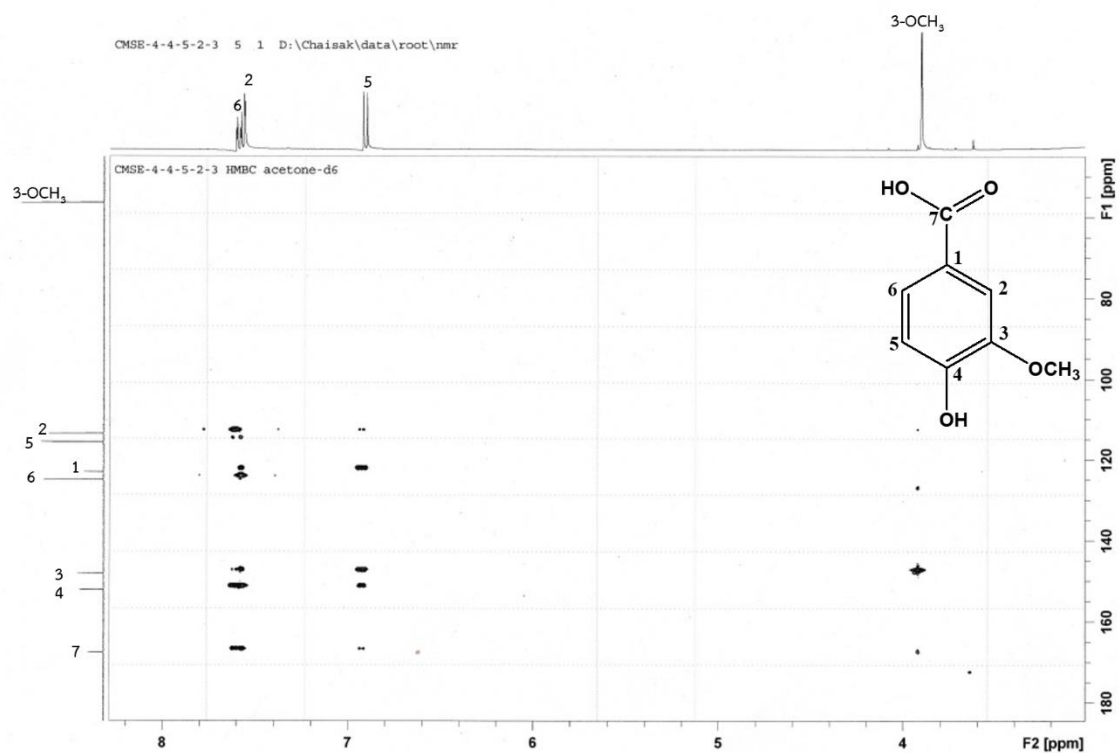
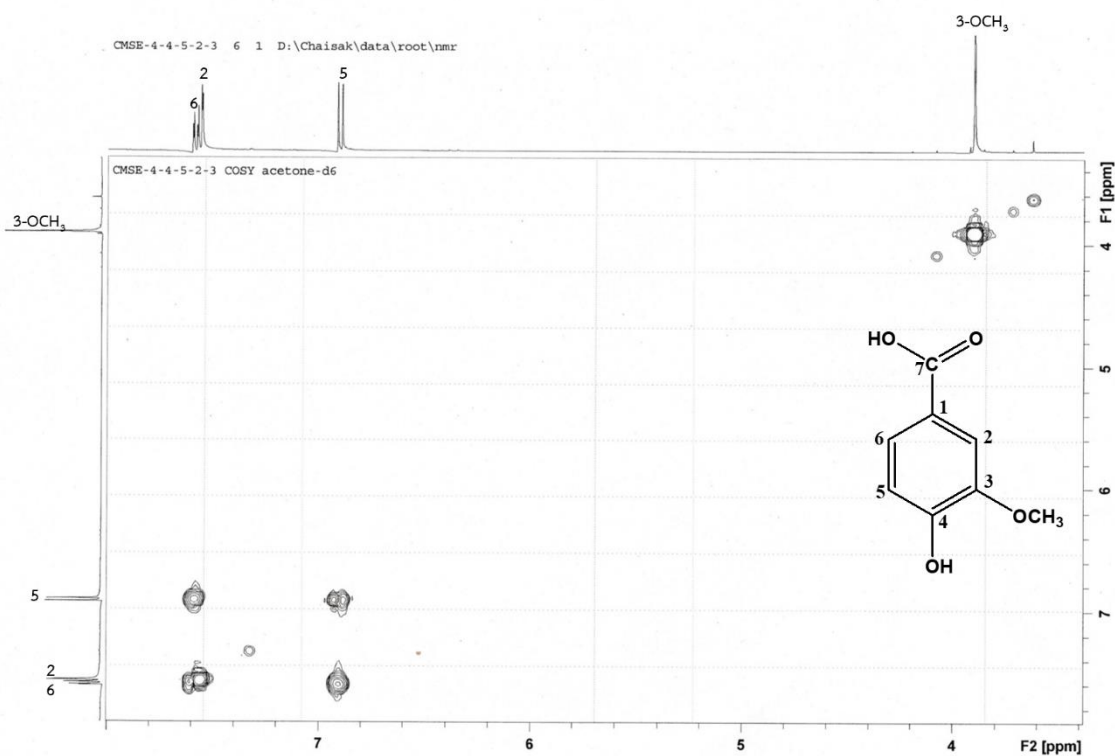


Figure 19. ¹H-¹³C HSQC spectrum of compound 2

Figure 20. ^1H - ^{13}C HMBC spectrum of compound 2Figure 21. ^1H - ^1H COSY spectrum of compound 2

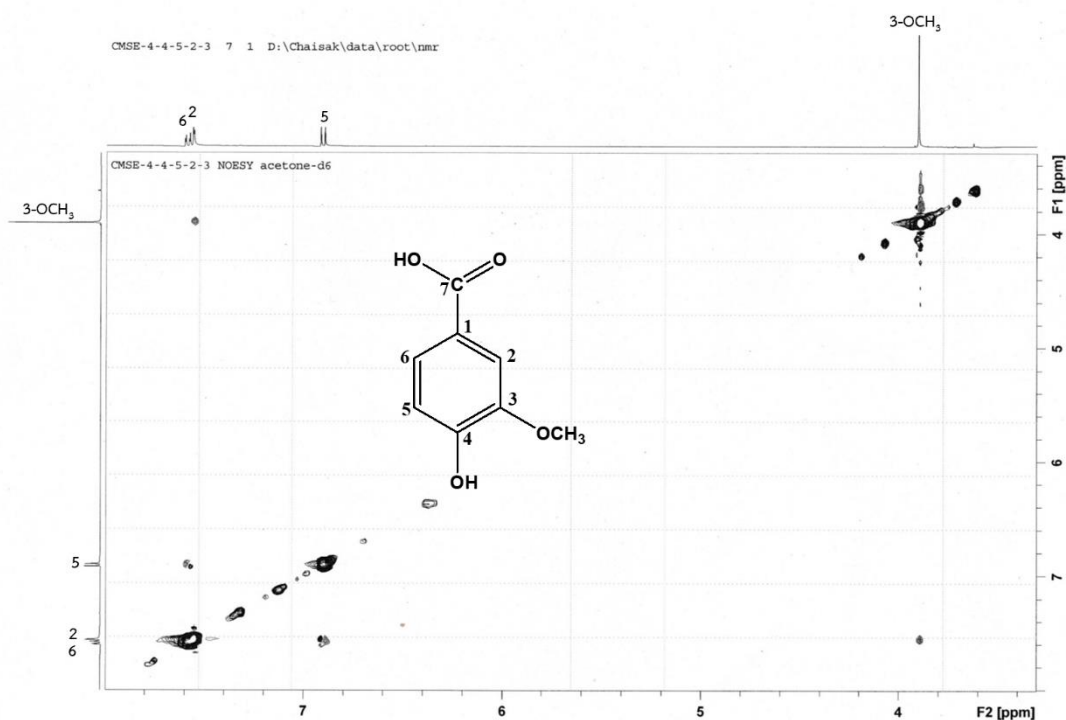


Figure 22. ^1H - ^1H NOESY spectrum of compound 2

4.1.3 Identification of compound 3 [(-)-syringaresinol]

Compound 3 was obtained as a white amorphous solid, which gave a quenching spot under short-wave UV light (254 nm) and appeared as a black spot after spraying with $\text{Ce}_2(\text{SO}_4)_3$ and heated. Its molecular formula was deduced as $\text{C}_{22}\text{H}_{26}\text{O}_8$, based on a pseudo-molecular $[\text{M}+\text{Na}]^+$ ion peak observed at m/z 441.1540 in the HR-ESI mass spectrum (calculated for $\text{C}_{22}\text{H}_{26}\text{NO}_8\text{Na}$, 441.1520) (Figure 23). The IR spectrum of compound 3 (Figure 24) showed hydroxyl absorption peak at 3397 cm^{-1} . In the ^{13}C -NMR (100 MHz, CDCl_3) (Figure 27) and ^1H - ^{13}C HSQC spectra (Figure 28), only eight carbon signals were observed, suggesting its symmetrical structure. The signals were those of four methoxy carbons which resonated at δ_{C} 56.4 (3'/3''- OCH_3 and 5'/5''- OCH_3), two methine carbons at δ_{C} 54.3 (C-1 and C-5), two oxymethines at δ_{C} 86.1 (C-2 and C-6), two oxymethylenes at δ_{C} 71.8 (C-4 and C-8), four aromatic methine carbons at δ_{C} 102.8 (C-2'/2'' and C-6'/6'') and eight aromatic quaternary carbons at δ_{C} 132.1 (C-1'/1''), 134.3 (C-4'/4'') and 147.1 (C-3'/3'' and C-5'/5'').

Its ^1H NMR spectrum (400 MHz, CDCl_3) (**Figure 25-26** and **Table 6**) displayed resonances of methine protons at δ_{H} 3.09 (2H, *m*, H-1, H-5), oxymethylene protons at δ_{H} 3.91 (2H, *s*, H_b-4/8), δ_{H} 4.23 (2H, *ddd*, $J = 9.2, 6.8, 2.2$ Hz, H_a-4/8), oxymethine protons at δ_{H} 4.73 (2H, *d*, $J = 4.4$ Hz H-2, H-6), *meta*-coupled aromatic protons at δ_{H} 6.59 (4H, *d*, $J = 2.8$ Hz, H-2'/2'' and H-6'/6''), methoxy groups at δ_{H} 3.91 (6H, *s*, 3'/3''-OCH₃) and 3.91 (6H, *s*, 5'/5''-OCH₃) and hydroxy protons at δ_{H} 5.51 (2H, *s*, 4'/4''-OH).

In ^1H - ^{13}C HMBC spectrum (**Figure 29-30**), correlations between δ_{H} 4.74 (H-2 and H-6) with C-4/8 (δ_{C} 71.8), C-2'/2'' and C-6'/6'' (δ_{C} 102.8) indicated the connection of two phenylpropanoid subunits. In addition, ^1H - ^1H NOESY cross peaks (**Figure 32**) of H-2'/2''/6'/6'' with 3'/3''/5'/5''-OCH₃ helped establish the substitution of methoxy groups at positions 3', 3'', 5' and 5'', hence hydroxy groups at positions 4' and 4''. Moreover, the ^1H - ^1H COSY cross peaks (**Figure 31**) indicated the connection of H-2/6, H-1/5 and H-4/8.

These spectroscopic data suggested the chemical structure of compound **3** as a tetrahydrofuran lignan, compared to the previously reported (Chen *et al.*, 1998).

Therefore, compound **3** was identified as (-)-syringaresinol, which was firstly isolated from the stems of *Annona cherimola* (family Annonaceae). Later, it has been found in the orchid plants such as *Dendrobium secundum* and *Dendrobium heterocarpum* (Sritularak *et al.*, 2011; Warinhomhoun *et al.*, 2021). (-)-syringaresinol showed inhibitory activity on nitric oxide production and LPS-induced NF- κ B activation in a BV2 microglia cells (Zhang *et al.*, 2022).

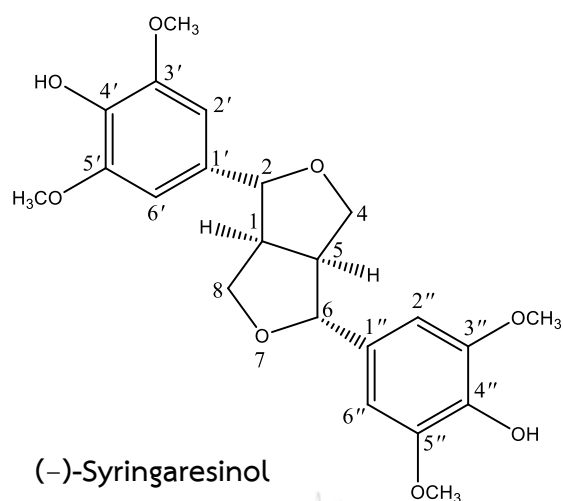


Table 6. ^1H - and ^{13}C -NMR data of compound **3** (400 MHz, in CDCl_3) and (-)-syringaresinol (400 MHz, in CDCl_3)

Position	Compound 3		(-)-syringaresinol*		HMBC correlation with
	δ_{H} (mult., <i>J</i> in Hz)	δ_{C}	δ_{H} (mult., <i>J</i> in Hz)	δ_{C}	
1/5	3.09 (<i>m</i>)	54.3	3.11 (<i>m</i>)	54.3	C-1'/1'', C-2/6
2/6	4.73 (<i>d</i> , 4.4)	86.1	4.74 (<i>d</i> , 4.3)	86.1	C-1/5
4/8	4.23 (<i>ddd</i> , 9.2, 6.8, 2.2) 3.91 (<i>s</i>)	71.8	4.29 (<i>d</i> , 9.6, 8.8) 3.91 (<i>d</i> , 9.6, 3.6)	71.8	C-1/5, C-2/6
1'/1''	-	132.1	-	132.1	-
2'/2''	6.59 (<i>d</i> , 2.8)	102.8	6.59 (<i>s</i>)	102.8	C-2/6, C-1'/1'', C-3'/3'', C-4'/4'', C-6'/6''
3'/3''	-	147.1	-	147.2	-
4'/4''	-	134.3	-	134.4	-
5'/5''	-	147.2	-	147.2	-
6'/6''	6.59 (<i>d</i> , 2.8)	102.8	6.59 (<i>s</i>)	102.8	C-2/6, C-1'/1'', C-2'/2'', C-4'/4'', C-5'/5''
4'/4''-OH	5.51 (<i>s</i>)	-	-	-	C-4'/4'', C-3'/3'', C-5'/5''
3'/3''-OCH ₃	3.91 (<i>s</i>)	56.4	3.91 (<i>s</i>)	56.4	C-3/3'
5'/5''-OCH ₃	3.91 (<i>s</i>)	56.4	3.91 (<i>s</i>)	56.4	C-5/5'

*Chen, *et al.* (1998).

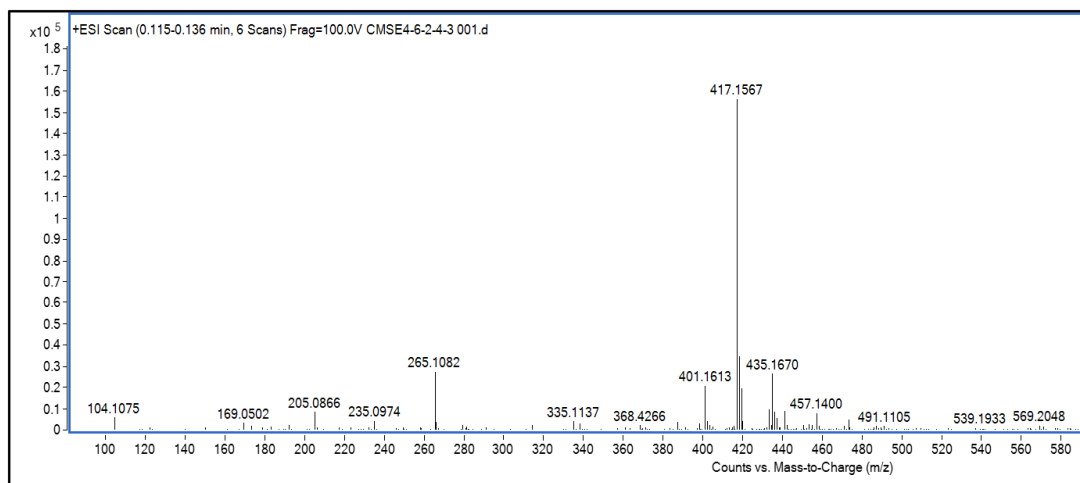


Figure 23. HR-ESI mass spectrum of compound 3

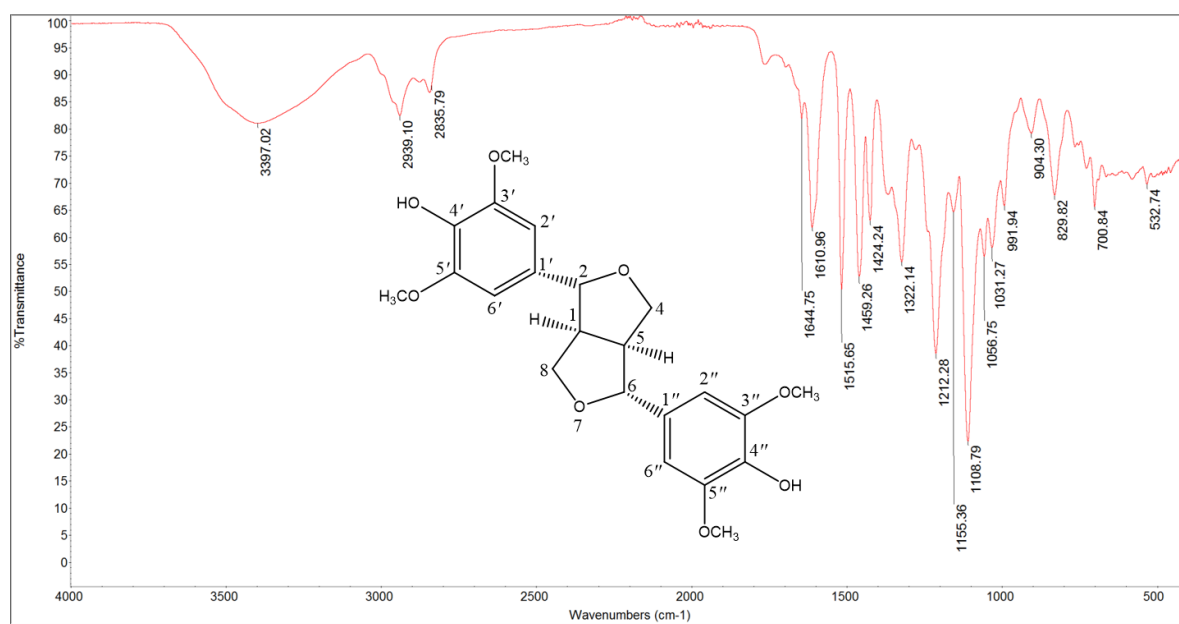


Figure 24. IR spectrum of compound 3

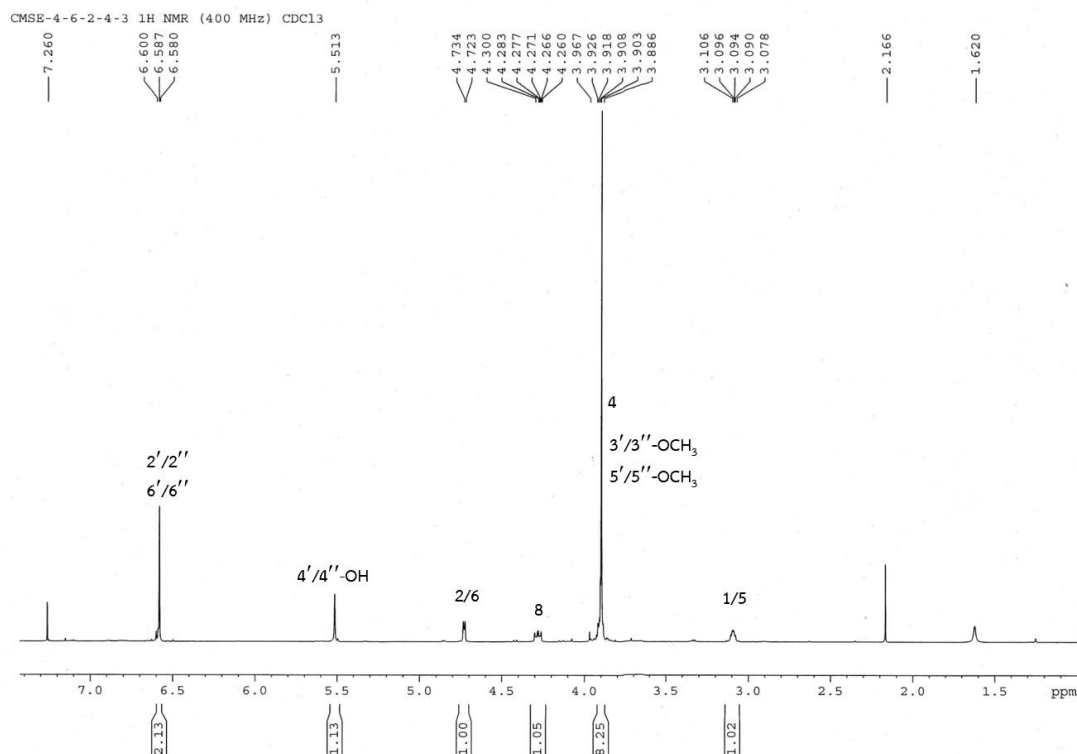


Figure 25. ¹H-NMR spectrum of compound **3** (400 MHz, CDCl₃)

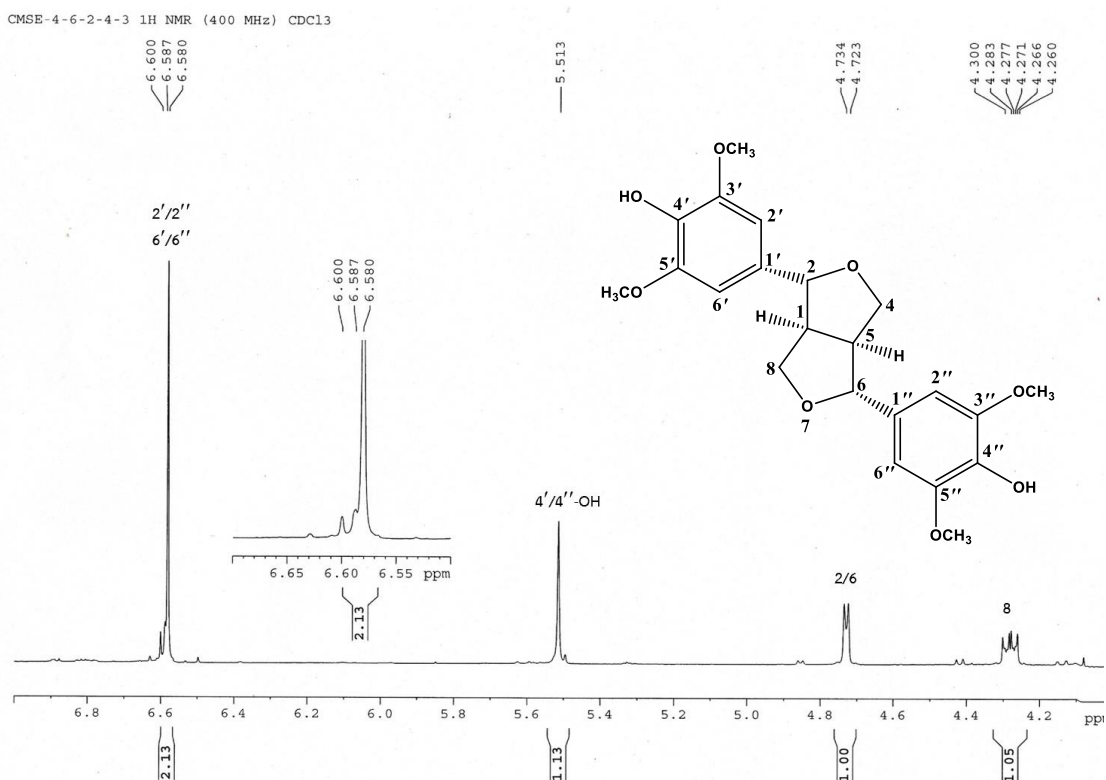
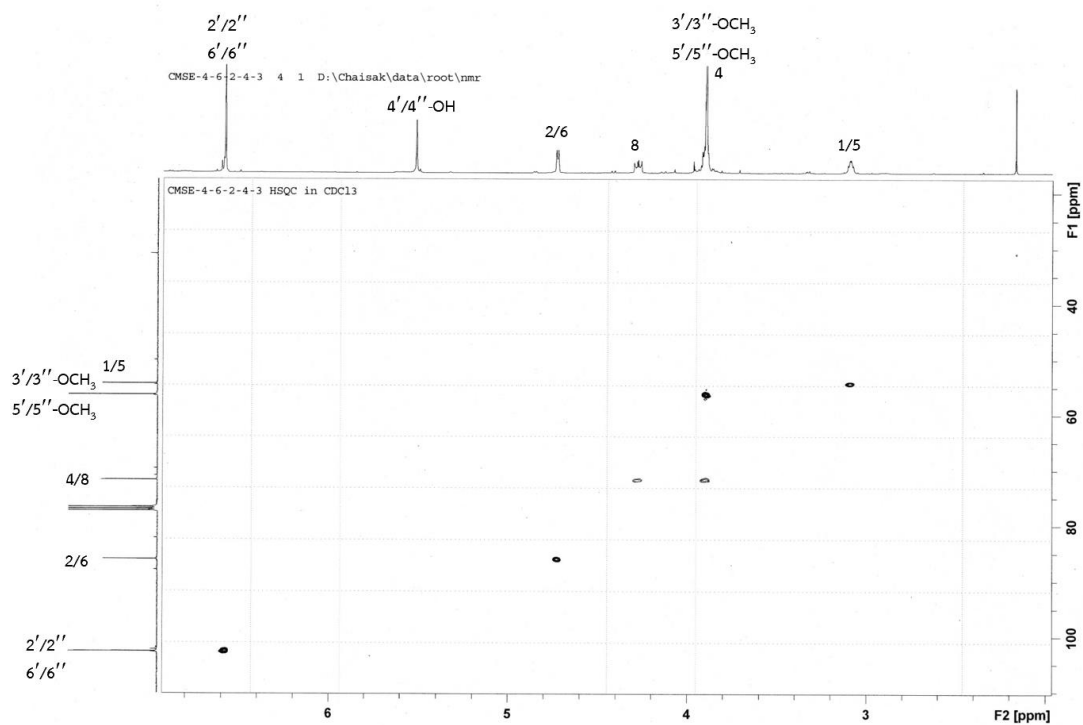
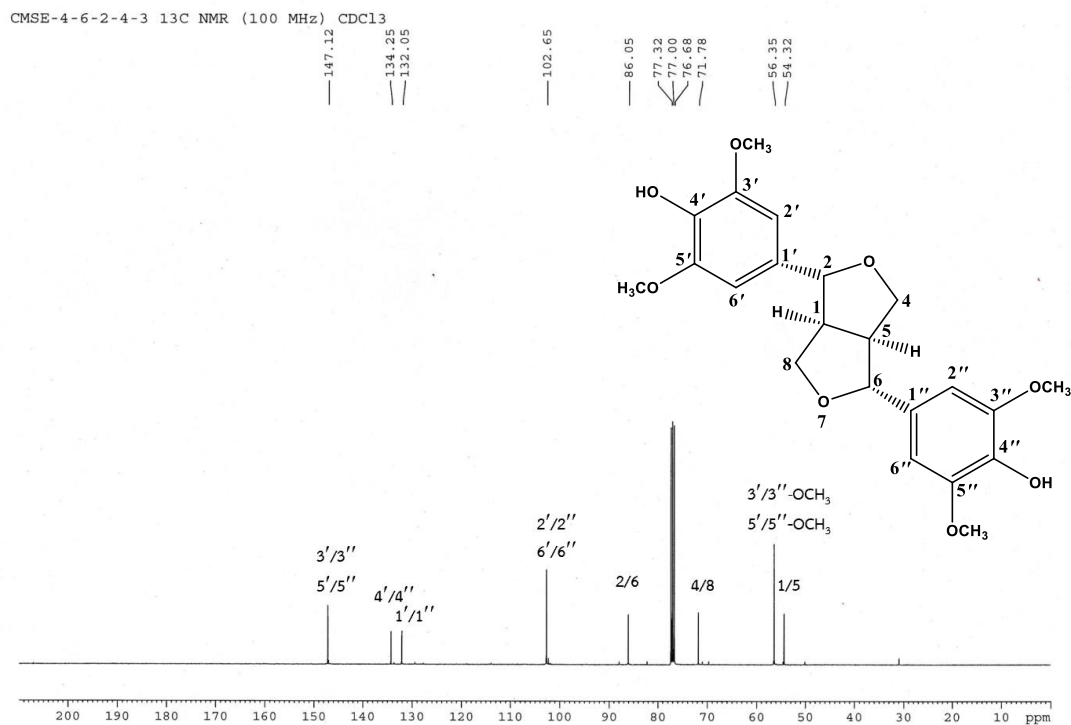


Figure 26. ¹H-NMR spectrum of compound **3** (expansion between δ_{H} 4.2-6.9 ppm)



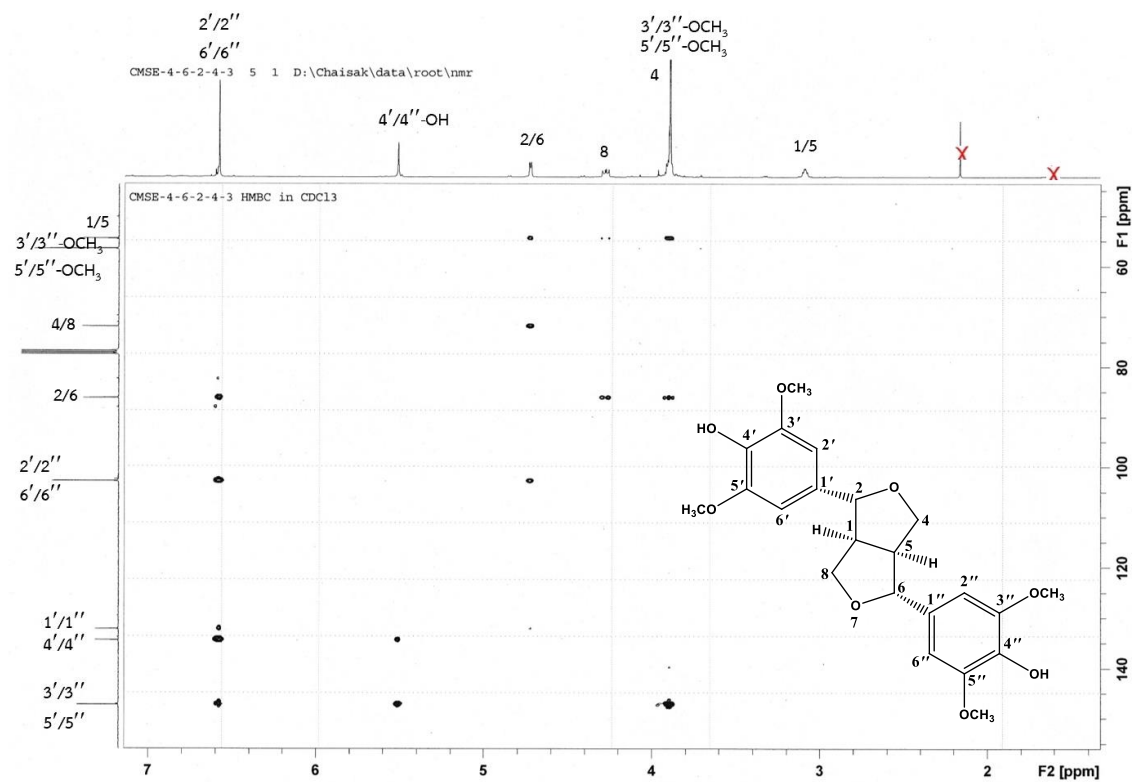


Figure 29. ^1H - ^{13}C HMBC spectrum of compound 3

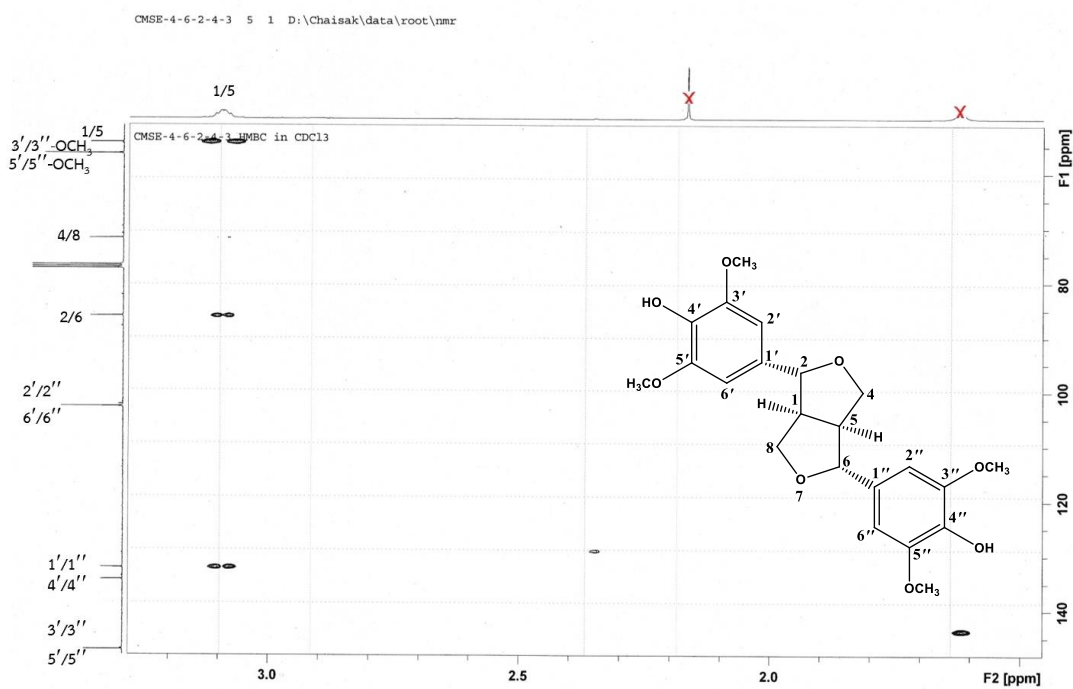
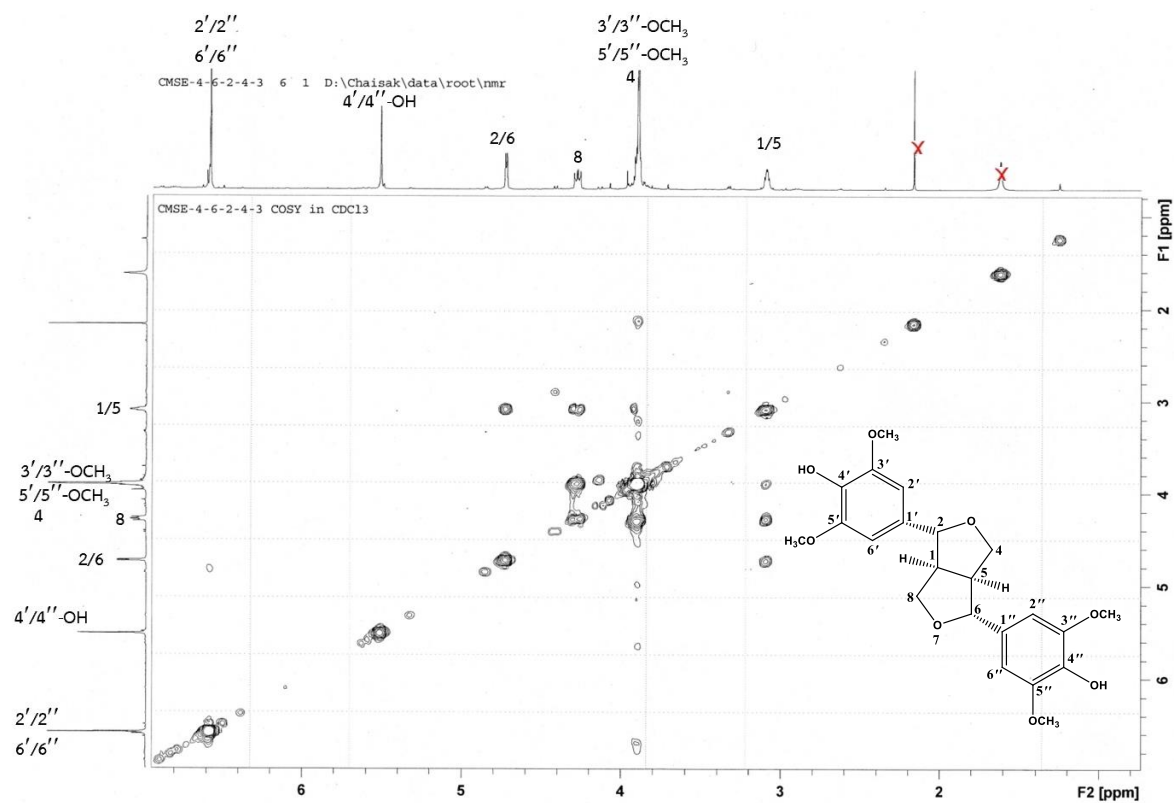
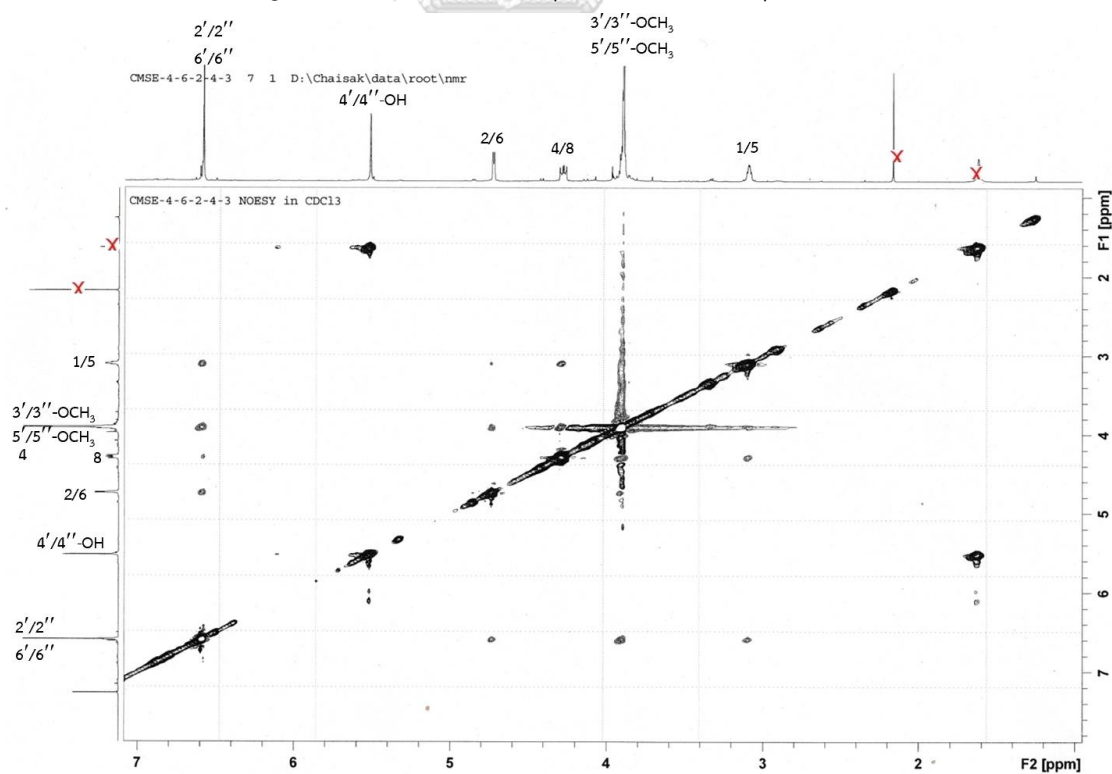


Figure 30. ^1H - ^{13}C HMBC spectrum of compound 3
(expansion between δ_{H} 1.0-3.3 ppm, δ_{C} 55-145 ppm)

Figure 31. ¹H-¹H COSY spectrum of compound 3Figure 32. ¹H-¹H NOESY spectrum of compound 3

4.1.4 Identification of compound 4 [(+)-ampelopsin A]

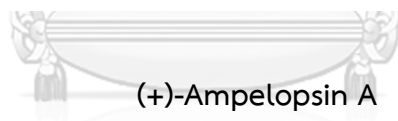
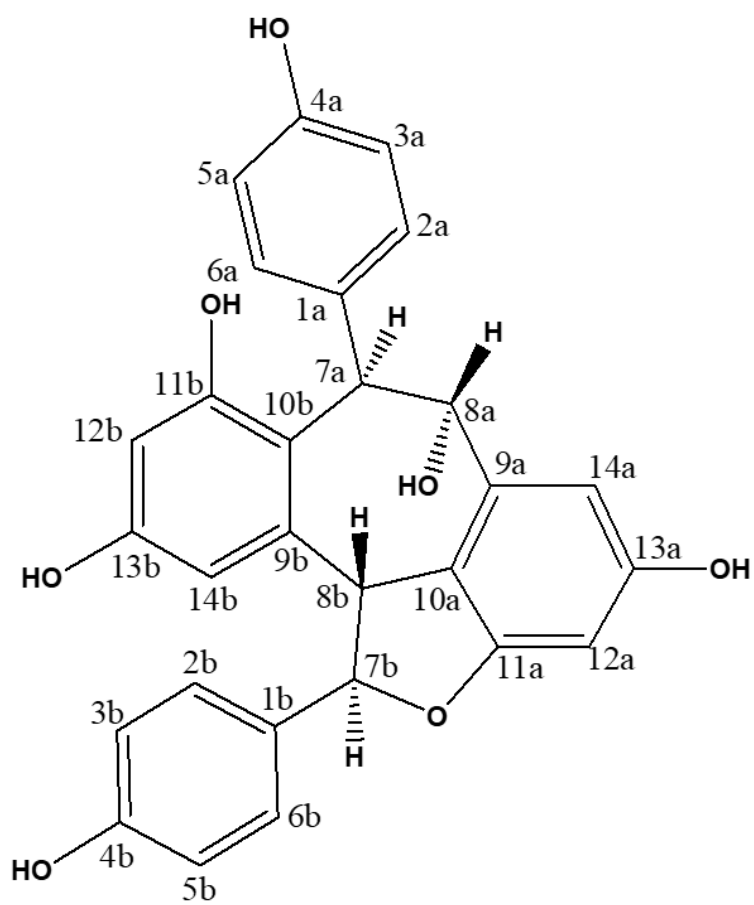
Compound **4** was obtained as a red amorphous solid. Its molecular formula was determined as $C_{28}H_{22}O_7$ (eighteen degrees of unsaturation) based on an observed pseudo-molecular $[M+H]^+$ ion peak at m/z 471.1455 (calculated for $C_{28}H_{23}O_7$, 471.1444) in the HR-ESI mass spectrum (**Figure 33**). The IR spectrum of this compound showed hydroxyl absorption peak at 3397 cm^{-1} (**Figure 34**).

The ^1H NMR spectrum (400 MHz, CD_3OD) of compound **4** (**Figure 35-36** and **Table 7**) displayed the resonances of two pairs of *ortho*-coupled protons of two *para*-disubstituted benzene rings at δ_{H} 6.83 (2H, *d*, $J = 8.4$ Hz, H-2a/6a) and 6.59 (2H, $J = 8.4$ Hz, H-3a/5a), and δ_{H} 6.70 (2H, *d*, $J = 8.4$ Hz, H-3b/5b) and 7.02 (2H, *d*, $J = 8.4$ Hz, H-2b/6b), two pairs of *meta*-coupled protons at δ_{H} 6.12 (1H, *d*, $J = 2.4$ Hz, H-12a) and 6.53 (1H, *d*, $J = 2.4$ Hz, H-14a), and δ_{H} 6.11 (1H, *d*, $J = 2.4$ Hz, H-14b) and 6.32 ppm (1H, *d*, $J = 2.4$ Hz, H-12b). These data implied the presence of four aromatic rings. Two pairs of vicinal aliphatic methine protons were also observed at δ_{H} 5.38 ppm (2H, *s*, H-7a/8a) and δ_{H} 4.03 (1H, *d*, $J = 11.6$ Hz, H-8b) and 5.70 (1H, *d*, $J = 11.6$ Hz, H-7b). The number of carbon atoms in the molecular formula and the number of aromatic rings were deduced from ^1H NMR data corresponding to the basic structure of a stilbenoid dimer.

Twenty-four carbon resonances (100 MHz, CD_3OD) were appeared in ^{13}C NMR spectrum (**Figure 37-38** and **Table 7**). These carbon signals could be differentiated, with the aid of ^1H - ^{13}C HSQC spectrum (**Figure 39**), into those of twelve quaternary carbons including six oxygen-substituted ones at δ_{C} 71.9 (C-8a), 119.2 (C-10b), 129.0 (C-10a), 133.3 (C-1b), 139.9 (C-9a), 143.6 (C-9b), 156.4 (C-4a), 157.7 (C-11b), 159.3 (C-4b), 159.5 (C-13a/13b) and 160.6 (C-11a), eight aromatic methine carbons at δ_{C} 97.7 (C-12a), 101.8 (C-12b), 105.6 (C-14b), 111.0 (C-14a), 115.8 (C-3a/5a and C-3b/5b) and 129.2 (C-2a/6a and C-2b/6b) and four aliphatic methine carbons at δ_{C} 44.2 (C-7a), 50.0 (C-8b), 71.9 (C-8a) and 89.4 (C-7b).

Two aromatic rings of one stilbenoid subunit was connected via the methine carbons 7a and 8a, as confirmed by long-range ^1H - ^{13}C HMBC cross peaks (**Figure 40-42** and **Table 7**) of H-7a (δ_{H} 5.38) with C-2a/6a (δ_{C} 129.2) and C-9a (δ_{C} 139.9) and of H-

8a (δ_{H} 5.38) with C-10a (δ_{C} 120.0) and C-14a (δ_{C} 111.0). HMBC correlations were also observed between H-7a signal with carbon signals of another stilbenoid subunit at C-9b (δ_{C} 143.6), C-10b (δ_{C} 119.2) and C-11b (δ_{C} 157.7). The second stilbenoid subunit displayed HMBC cross peaks between H-7b (δ_{H} 5.70) and C-2b/6b (δ_{C} 129.2) and C-9b (δ_{C} 143.6), as well as between H-8b (δ_{H} 4.03 ppm) and C-9a and C-10a. These data suggested that the compound comprised two resveratrol subunits which were connected via a seven-membered ring and a furan ring, with a hydroxyl substituent at position 8a. The configuration of H-7a, H-8a, H-7b and H-8b was assigned based on comparison of the optical rotation of this compound (+228.0° (c 0.1, MeOH)) with previous study (+98.0° (c 0.1, MeOH)) (Oshima *et al.*, 1990). Therefore, compound **4** was identified as (+)-ampelopsin A, which has been previously isolated from the roots of *Ampelopsis brevipedunculata* var. *hancei* (Oshima *et al.*, 1990) and *Vitis vinifera* (family Vitaceae). It was reported to possess neuroprotective ability by increasing the function of the central or peripheral nervous system (Hong *et al.*, 2021). The compound also demonstrated anti-inflammatory effect against lipopolysaccharide (LPS)-induced arthritis (Wang *et al.*, 2011).



จุฬาลงกรณ์มหาวิทยาลัย
CHULALONGKORN UNIVERSITY

Table 7. ^1H - and ^{13}C -NMR data of compound **4** (400 MHz, in CD_3OD) and (+)-ampelopsin A (500 MHz, in acetone- d_6)

Position	Compound 4		(+)-ampelopsin A*		HMBC correlation with
	δ_{H} (mult., J in Hz)	δ_{C}	δ_{H} (mult., J in Hz)	δ_{C}	
1a	-	131.0	-	130.6	-
2a	6.83 (<i>d</i> , 8.4)	129.2	6.90 (<i>d</i> , 8.3)	128.6	C-4a, C-6a, C-7a
3a	6.59 (<i>d</i> , 8.4)	115.8	6.65 (<i>d</i> , 8.3)	115.4	C-1a, C-4a, C-5a
4a	-	156.4	-	158.2	-
5a	6.59 (<i>d</i> , 8.4)	115.8	6.65 (<i>d</i> , 8.3)	115.4	C-1a, C-3a, C-4a
6a	6.83 (<i>d</i> , 8.4)	129.2	6.90 (<i>d</i> , 8.3)	128.6	C-2a, C-4a, C-7a
7a	5.38 (<i>d</i> , 4.8)	44.2	5.45 (<i>d</i> , 5.0)	43.7	C-1a, C-2a, C-6a, C-9a, C-9b
8a	5.38 (<i>d</i> , 4.8)	71.9	5.42 (<i>d</i> , 5.0)	71.2	C-1a, C-10b, C-14a
9a	-	139.9	-	139.8	-
10a	-	120.0	-	118.1	-
11a	-	160.6	-	159.9	-
12a	6.12 (<i>d</i> , 2.4)	97.7	6.16 (<i>d</i> , 2.3)	97.2	C-10a, C-14a
13a	-	159.5	-	158.6	-
14a	6.53 (<i>d</i> , 2.4)	111.0	6.62 (<i>d</i> , 2.3)	110.4	C-8a, C-10a, C-12a
1b	-	133.3	-	132.3	-
2b	7.02 (<i>d</i> , 8.4)	129.2	7.12 (<i>d</i> , 8.3)	129.8	C-6b
3b	6.70 (<i>d</i> , 8.4)	116.4	6.78 (<i>d</i> , 8.3)	115.9	C-1b, C-4b C-5b,
4b	-	159.3	-	157.0	-
5b	6.70 (<i>d</i> , 8.4)	116.4	6.78 (<i>d</i> , 8.3)	115.9	C-1b, C-3b, C-4b
6b	7.02 (<i>d</i> , 8.4)	129.2	7.12 (<i>d</i> , 8.3)	129.8	C-2b
7b	5.70 (<i>d</i> , 11.6)	89.4	5.77 (<i>d</i> , 11.7)	88.3	C-2, C-6, C-9b
8b	4.03 (<i>d</i> , 11.6)	50.0	4.17 (<i>d</i> , 11.7)	49.4	C-1b, C-9a, C-10a
9b	-	143.6	-	142.8	-
10b	-	119.2	-	118.2	-
11b	-	157.7	-	155.8	-
12b	6.32 (<i>d</i> , 2.4)	101.8	6.43 (<i>d</i> , 2.3)	101.6	C-11b, C13b
13b	-	159.5	-	159.5	-
14b	6.11 (<i>d</i> , 2.4)	105.6	6.24 (<i>d</i> , 2.3)	105.4	C-8b, C-10b, C-12b

* Oshima, *et al.* (1990).

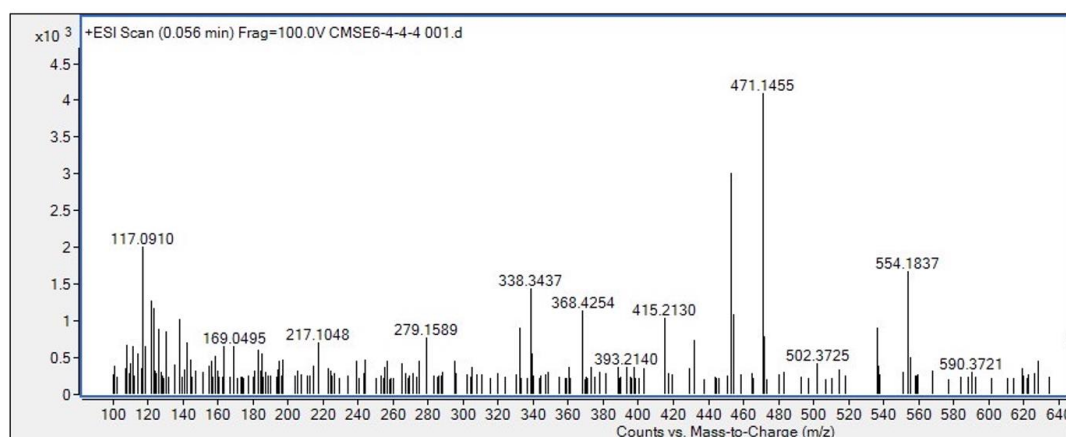


Figure 33. HR-ESI mass spectrum of compound 4

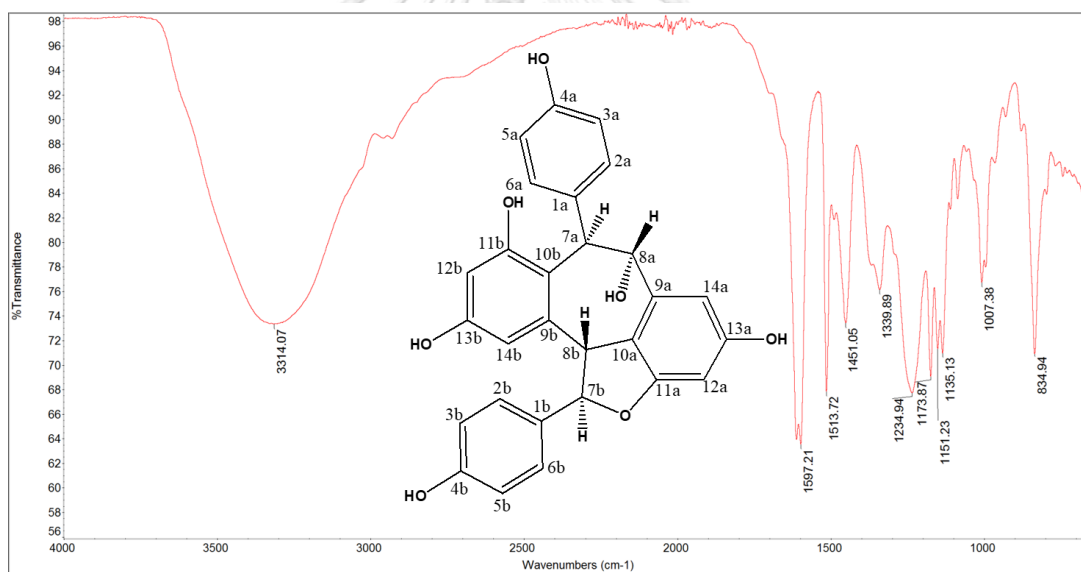


Figure 34. IR spectrum of compound 4

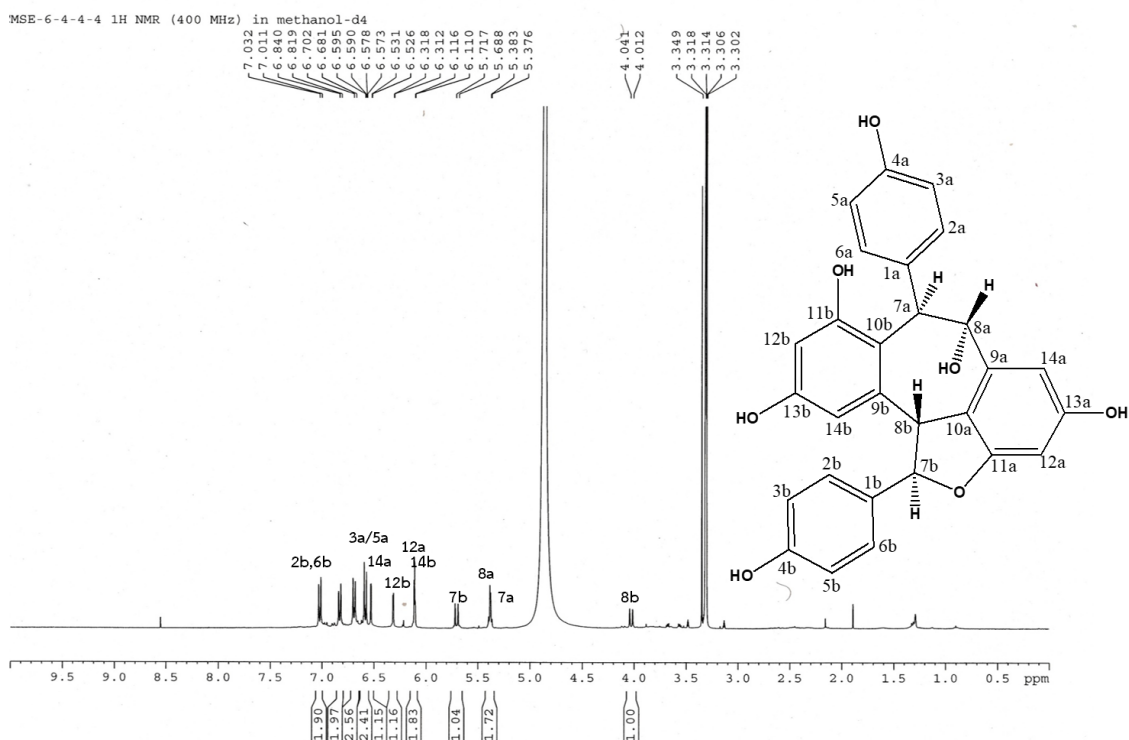


Figure 35. $^1\text{H-NMR}$ spectrum of compound **4** (400 MHz, CD_3OD)

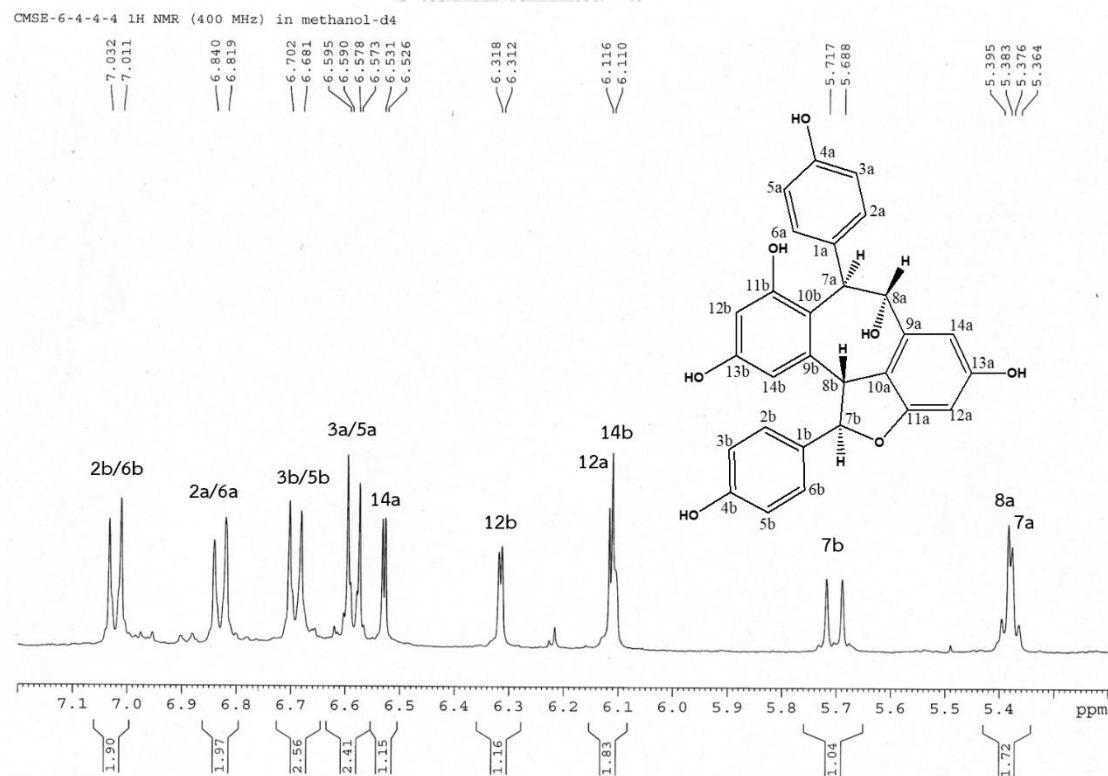
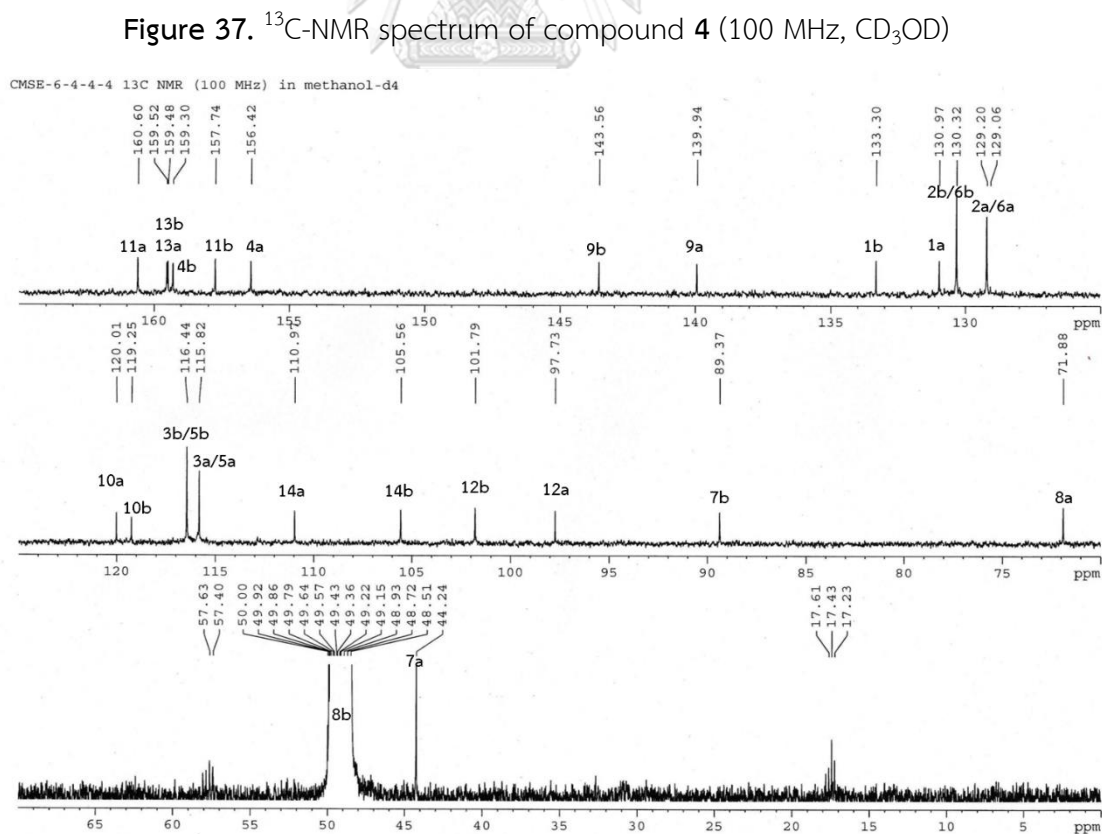
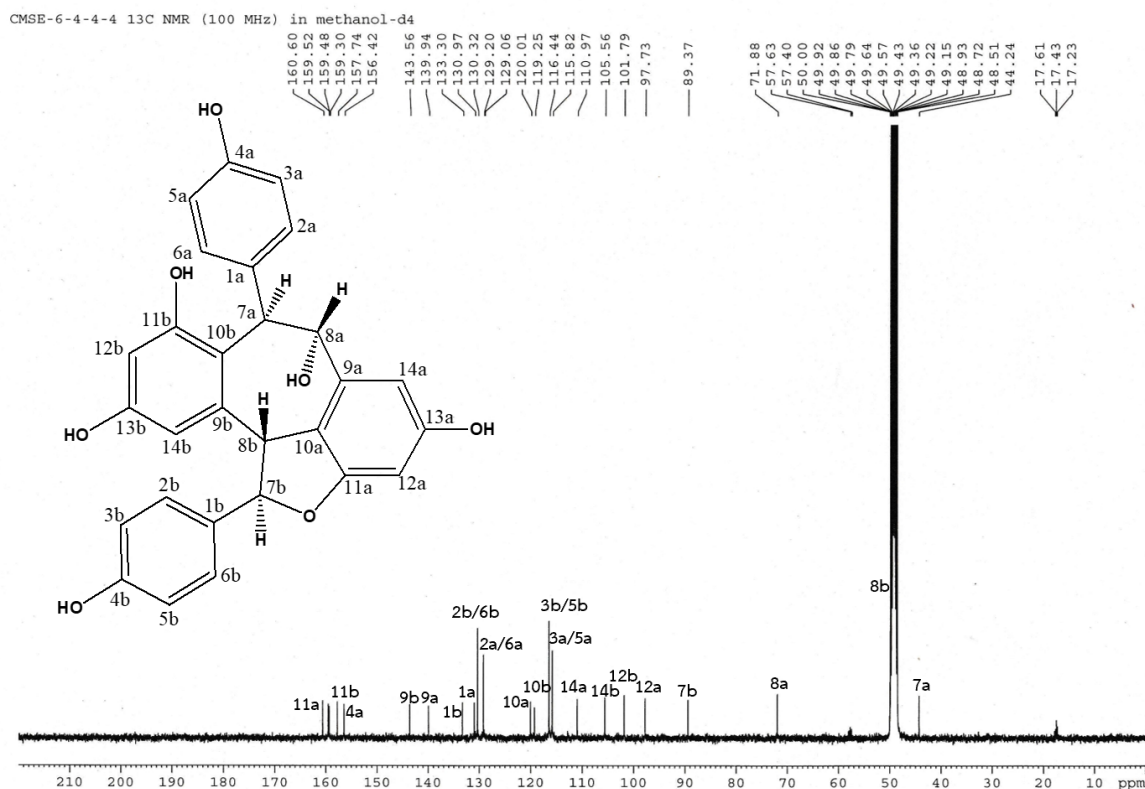
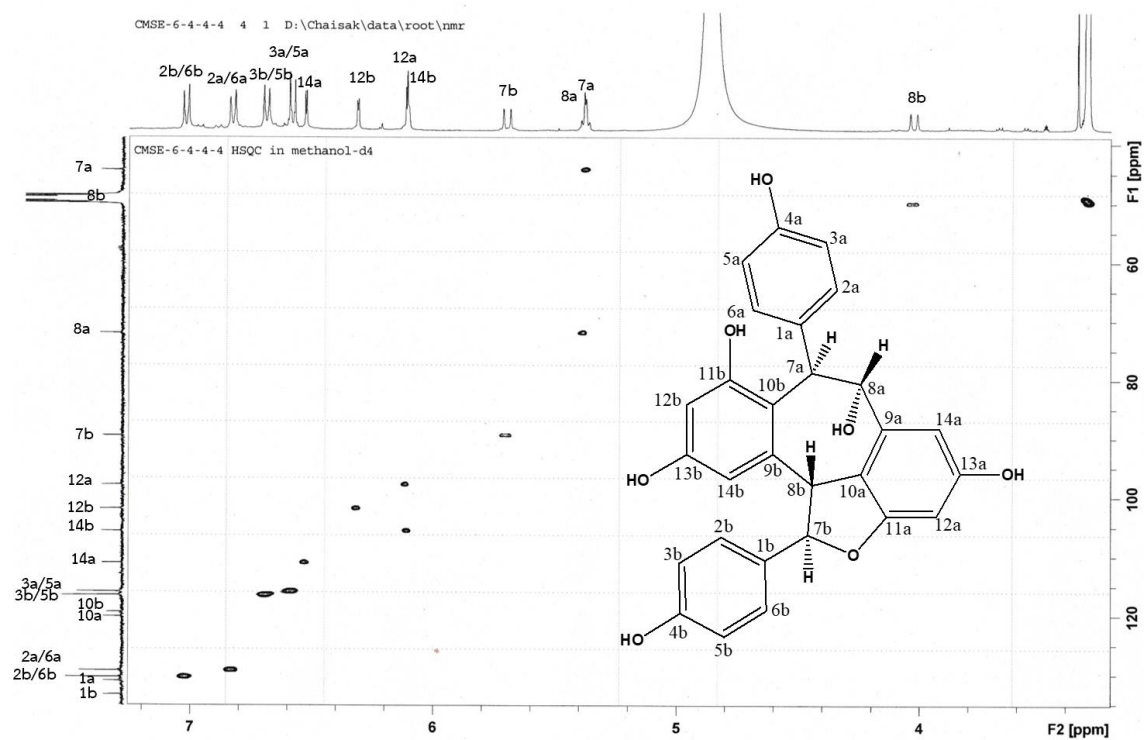
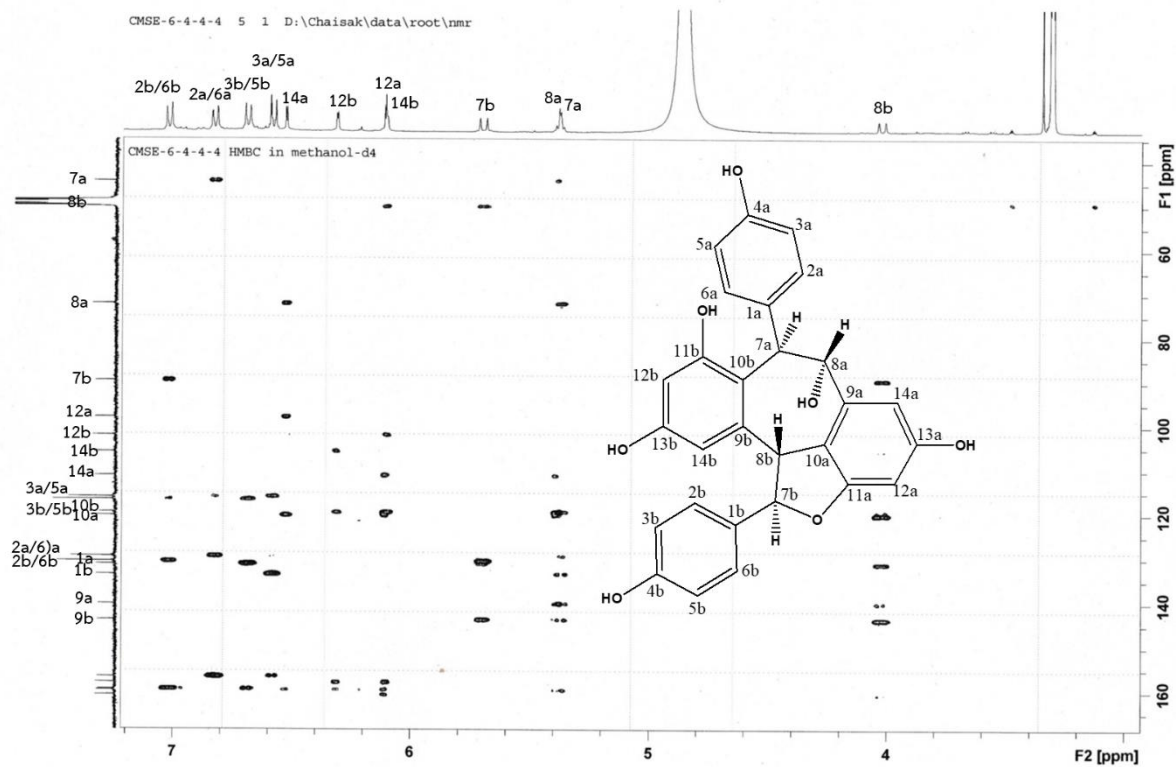
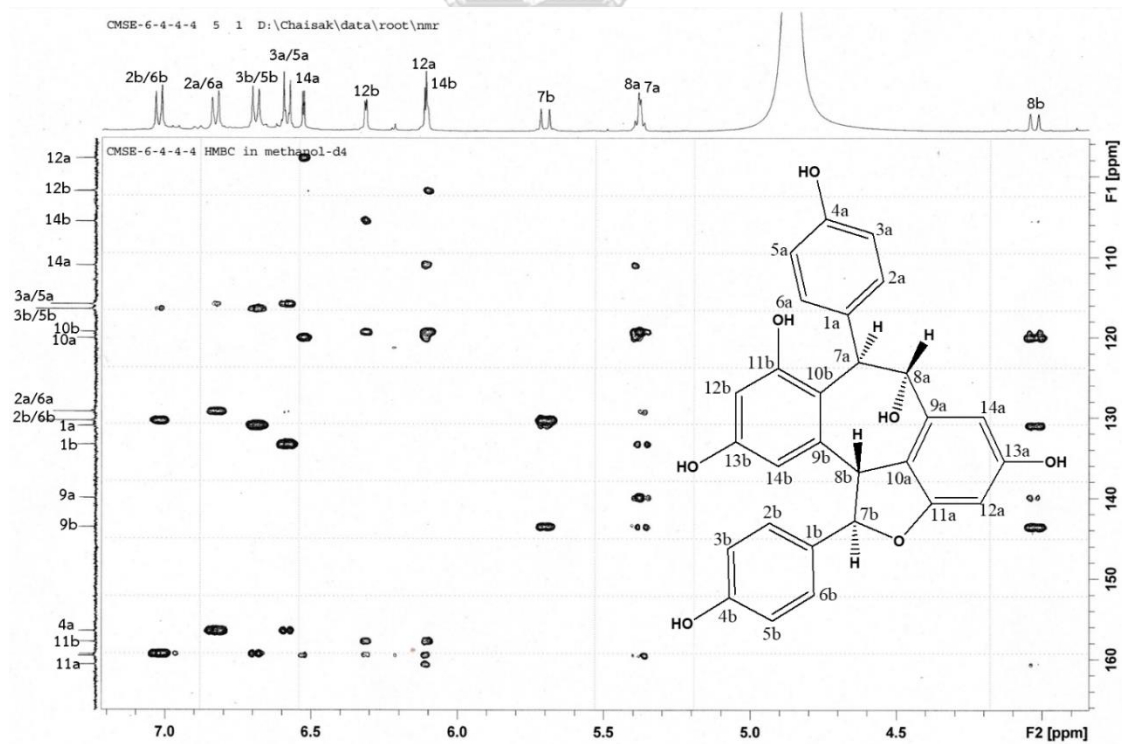
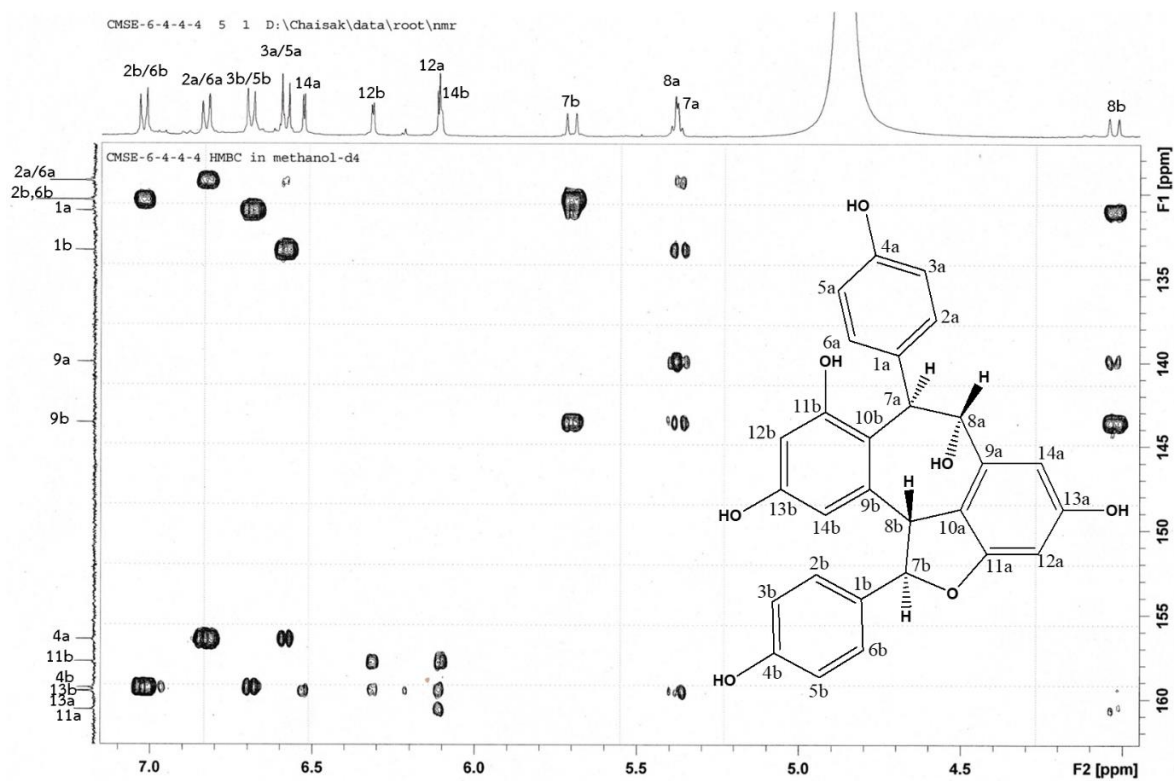
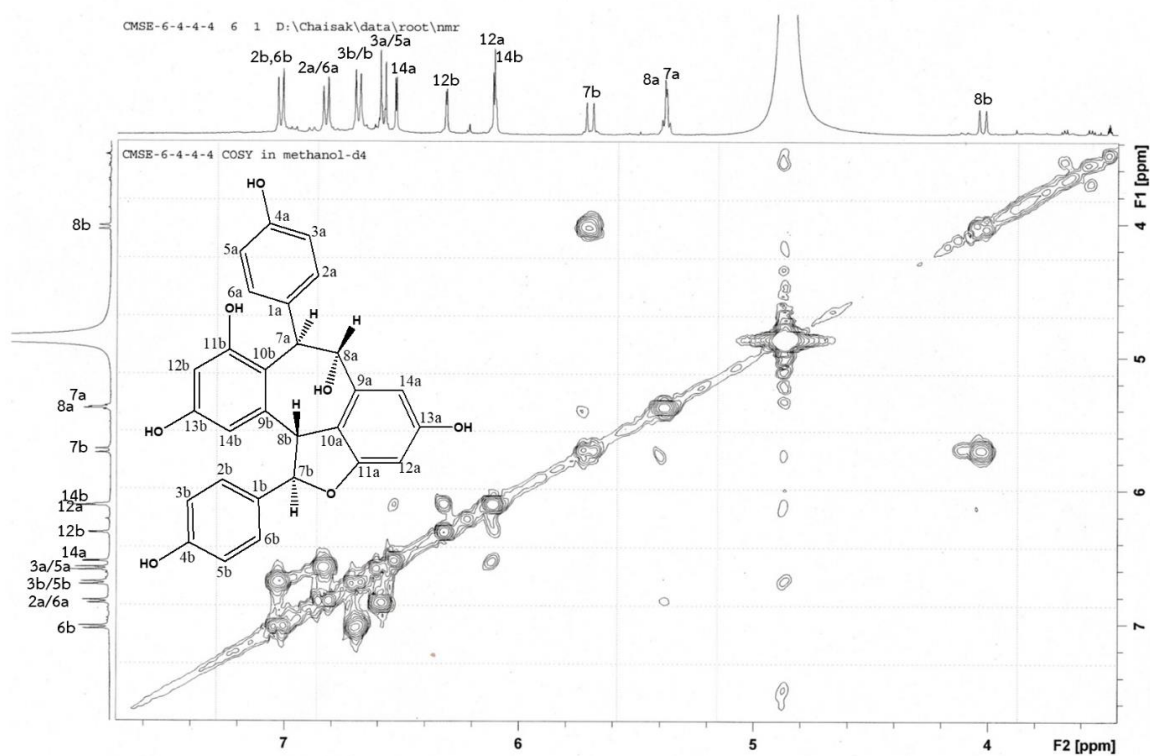
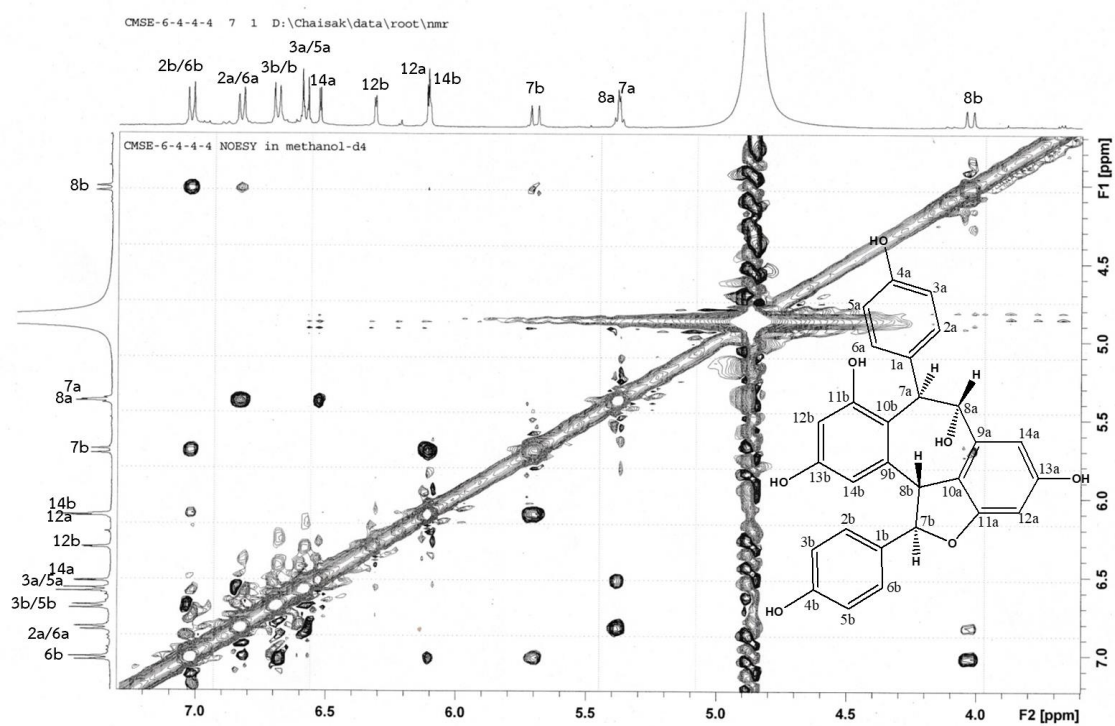


Figure 36. $^1\text{H-NMR}$ spectrum of compound **4** (expansion between δ_{H} 5.2-7.2 ppm)



Figure 39. ^1H - ^{13}C HSQC spectrum of compound 4Figure 40. ^1H - ^{13}C HMBC spectrum of compound 4



Figure 43. ^1H - ^1H COSY spectrum of compound 4Figure 44. ^1H - ^1H NOESY spectrum of compound 4

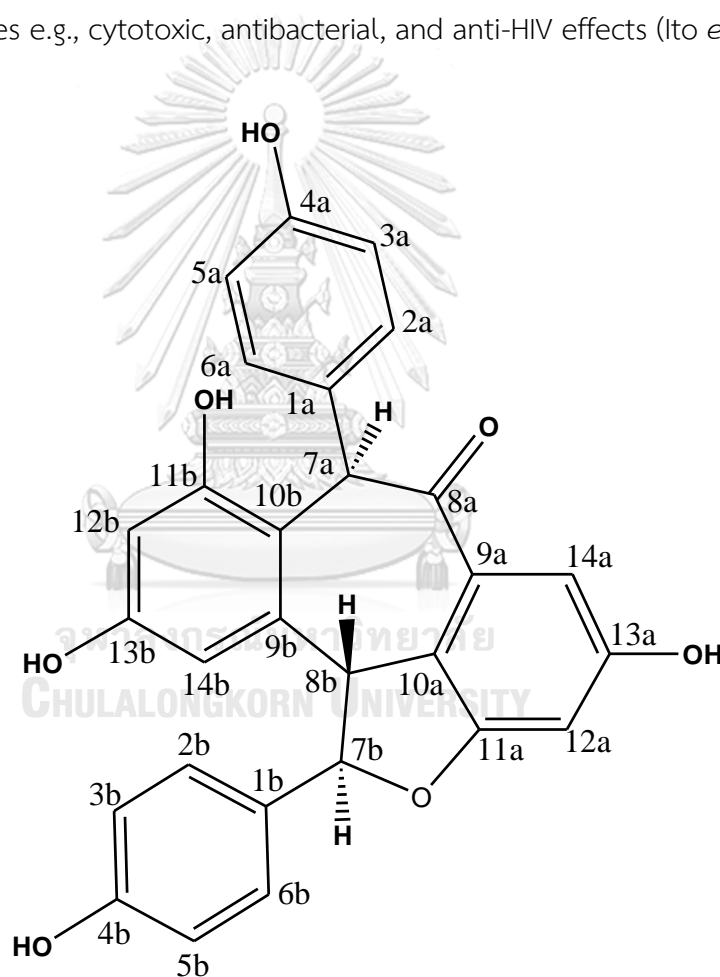
4.1.5 Identification of compound 5 [(-)-pauciflorol E]

Compound **5** was obtained as a yellow amorphous solid. Its molecular formula was established as $C_{28}H_{20}O_7$ (nineteen degrees of unsaturation) based on the pseudo-molecular $[M+H]^+$ ion peak in the high-resolution ESI mass spectrum (**Figure 45**) at m/z 469.1320 (calculated for $C_{28}H_{21}O_7$, 469.1287). The IR spectrum (**Figure 46**) showed absorption bands of hydroxyl (3339 cm^{-1}) and conjugated keto carbonyl (1656 cm^{-1}) functionalities. These data suggested the similarity between this compound and compound **4**, except the presence of a keto carbonyl group instead of a hydroxyl group.

The ^1H NMR spectrum (400 MHz, acetone d_6) (**Figure 47-49** and **Table 8**) exhibited signals of two *para*-disubstituted benzene rings at δ_{H} 6.77 (2H, *dd*, $J = 8.6, 1.2$ Hz, H-2a/6a) and 6.70 (2H, $J = 8.6$ Hz, H-3a/5a), and at δ_{H} 6.83 (2H, *d*, $J = 8.6$ Hz, H-3b/5b) and 7.18 (2H, *d*, $J = 8.6$ Hz, H-2b/6b), two pairs of *meta*-coupled protons at δ_{H} 6.45 (1H, *d*, $J = 2.4$ Hz, H-12a) and 7.12 (1H, *d*, $J = 2.4$ Hz, H-14a), and at δ_{H} 6.39 (1H, *br s*, H-14b) and 6.49 (1H, *d*, $J = 2.0$ Hz, H-12b). These data were similar to those of compound **4**. The rest were signals of an aliphatic methine proton at δ_{H} 6.05 (1H, *br s*, H-7a) and a set of mutually coupled aliphatic methine protons at δ_{H} 5.94 (1H, *d*, $J = 10.8$ Hz, H-7b) and 4.52 (1H, *d*, $J = 10.8$ Hz, H-8b).

Twenty-four carbon resonances representing 28 carbon atoms were observed in the ^{13}C NMR spectrum (100 MHz, acetone- d_6) (**Figure 50-51** and **Table 8**). Most of these signals were similar to those of compound **4** except for the presence of a keto carbonyl resonance at δ_{C} 195.6 (C-8a) instead of a methine carbon as compound **4**. The position of this C-8a carbonyl carbon could be confirmed with ^1H - ^{13}C HMBC cross peaks (**Figure 53-54**) of the methine H-7a signal (δ_{H} 6.05) and the aromatic H-14a proton (δ_{H} 7.12) with the signal of keto carbonyl at δ_{C} 195.6. In addition, HMBC spectrum also showed correlations of H-7a with C-10b (δ_{C} 114.3), C-2a/6a (δ_{C} 128.4), C-9a (δ_{C} 134.1) and C-9b (δ_{C} 142.5), confirming their connectivity as same as the compound **4**. Furthermore, significant long-range HMBC cross peaks were observed between H-8b signal (δ_{H} 4.53) with C-14b (δ_{C} 105.8), C-10b, C-10a (δ_{C} 124.4), C-1b (δ_{C}

130.5) and C-9a (δ_C 134.1), as well as from H-7b signal (at δ_H 5.94) to C-2b/6b (δ_C 129.9) and C-9b. ^1H - ^1H NOESY experiment (Figure 56) confirmed a relative configuration between H-7b and H-8b as *trans*, from the observed cross peaks between H-7b and H-14b signals, and between H-8b and H-2b/6b signals. Therefore, compound **5** was identified as a resveratrol dimer pauciflorol E, previously found as a constituent of the stem bark of *Vatica pauciflora* (family Dipterocarpaceae). The optical rotation of this compound was -166.0° (c 0.1, MeOH) compared with previous study (-228.0° (c 0.1, MeOH)) (Ito *et al.*, 2004). Resveratrol and its oligomers have been reported to display several bioactivities e.g., cytotoxic, antibacterial, and anti-HIV effects (Ito *et al.*, 2004).



(-)-Pauciflorol E

Table 8. ^1H - and ^{13}C -NMR data of compound **5** (400 MHz, in acetone- d_6) and (-)-pauciflorol E (300 MHz, in acetone- d_6)

Position	Compound 5		(-)-pauciflorol E *		HMBC correlation with
	δ_{H} (mult., J in Hz)	δ_{C}	δ_{H} (mult., J in Hz)	δ_{C}	
1a	-	128.7	-	128.2	-
2a	6.77 (dd, 8.6, 1.2)	128.4	6.77 (dd, 8.5, 1.1)	128.0	C-4a, C-6a, C-7a
3a	6.70 (d, 8.6)	116.3	6.70 (d, 8.5)	115.8	C-1a, C-5a
4a	-	156.5		156.8	-
5a	6.70 (d, 8.6)	116.3	6.70 (d, 8.5)	115.8	C-1a, C-3a
6a	6.77 (dd, 8.6, 1.2)	128.4	6.77 (dd, 8.5, 1.1)	128.0	C-2a, C-4a, C-7a
7a	6.05 (br s)	55.2	6.06 (br s)	54.8	C-2a, C-6a, C-8a, C-9a, C-9b, C-10b
8a	-	195.6	-	195.3	-
9a	-	134.1	-	133.7	-
10a	-	124.4	-	123.9	-
11a	-	160.9	-	160.4	-
12a	6.45 (d, 2.4)	102.6	6.45 (d, 2.4)	102.2	C-10a
13a	-	158.5	-	158.5	-
14a	7.12 (d, 2.4)	106.9	7.12 (d, 2.4)	106.5	C-10a, C-12a
1b	-	130.5	-	130.5	-
2b	7.18 (d, 8.6)	129.9	7.19 (d, 8.5)	129.5	C-4b, C-6b, C-7b
3b	6.83 (d, 8.6)	116.2	6.83 (d, 8.5)	115.9	C-1b, C-5b
4b	-	158.4	-	158.2	-
5b	6.83 (d, 8.6)	116.2	6.83 (d, 8.5)	115.9	C-1b, C-3b
6b	7.18 (d, 8.6)	129.9	7.19 (d, 8.5)	129.5	C-2b, C-4b, C-7b
7b	5.94 (d, 10.8)	88.9	5.94 (d, 10.8)	88.4	C-2b, C-6b, C-8b, C-9b
8b	4.52 (d, 10.8)	51.2	4.52 (d, 10.8)	50.8	C-9a, C-10a, C-1b, C-7b, C-9b, C-10b, C-14b
9b	-	142.5	-	142.0	-
10b	-	114.3	-	113.9	-
11b	-	158.9	-	159.0	-
12b	6.49 (d, 2.0)	102.1	6.49 (d, 2.4)	101.7	C-10b, C-14b
13b	-	157.8	-	158.0	-

Position	Compound 5		(-)-pauciflorol E *		HMBC correlation with
	δ_H (mult., <i>J</i> in Hz)	δ_C	δ_H (mult., <i>J</i> in Hz)	δ_C	
14b	6.39 (<i>br s</i>)	105.8	6.39 (<i>br s</i>)	105.3	C-8b, C-10b, C-12b
4a-OH	-	-	8.42 (<i>br s</i>)	-	-
4b-OH	-	-	8.71 (<i>br s</i>)	-	-
11-OH	-	-	8.94 (<i>br s</i>)	-	-
13a-OH	-	-	8.84 (<i>br s</i>)	-	-
13b-OH	-	-	8.57 (<i>br s</i>)	-	-

* Ito, *et al.* (2004).

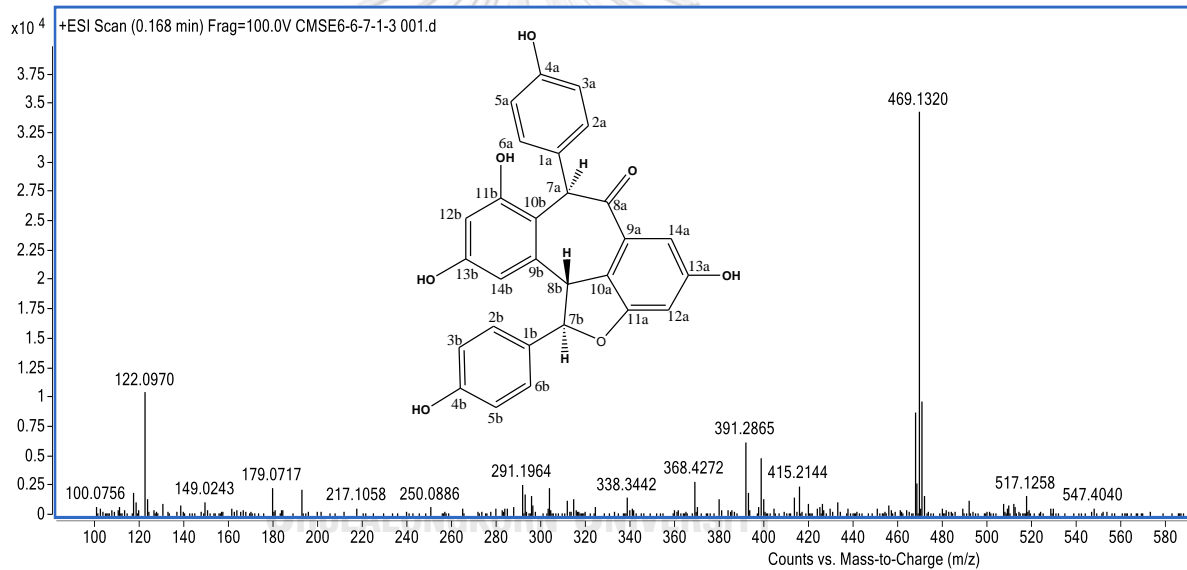


Figure 45. HR-ESI mass spectrum of compound 5

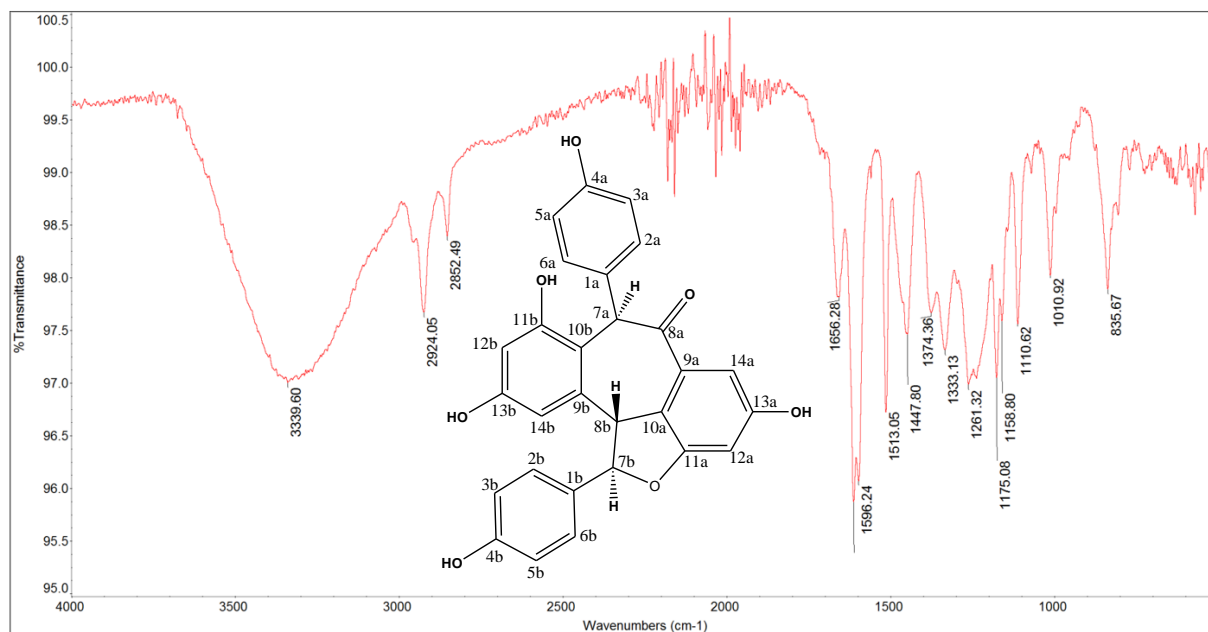
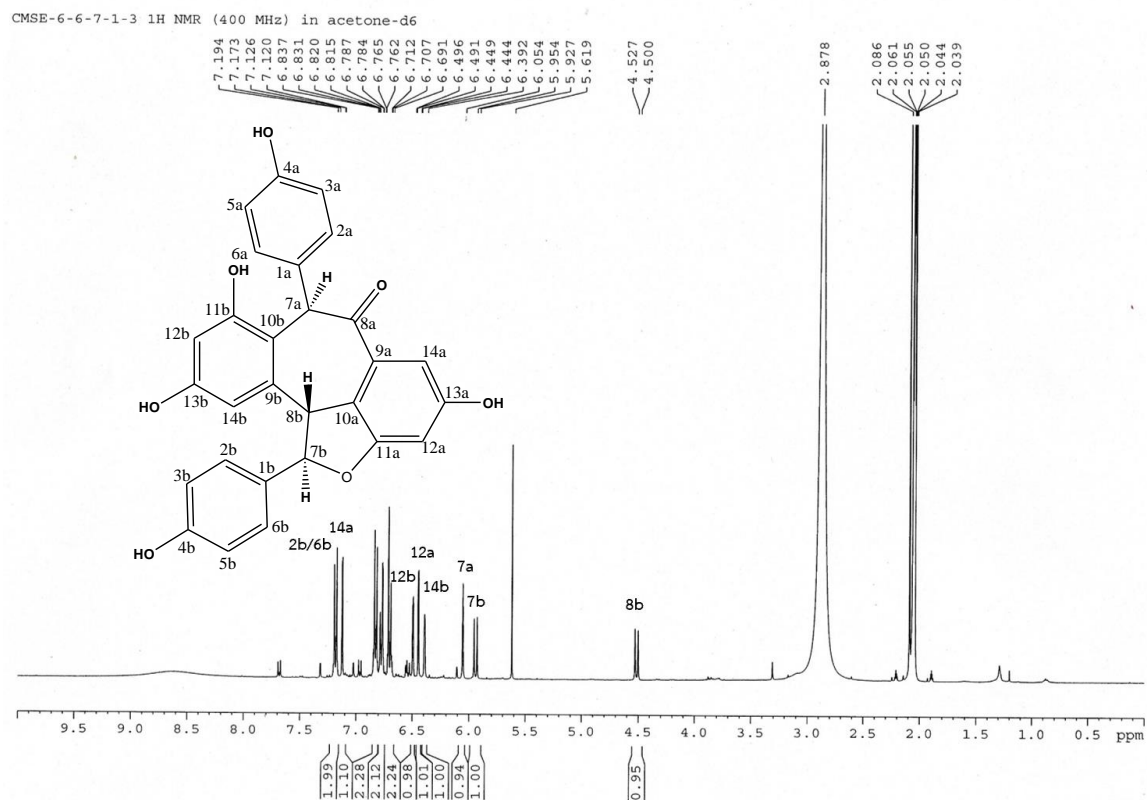


Figure 46. IR spectrum of compound 5

Figure 47. ¹H-NMR spectrum of compound 5 (400 MHz, acetone-d₆)

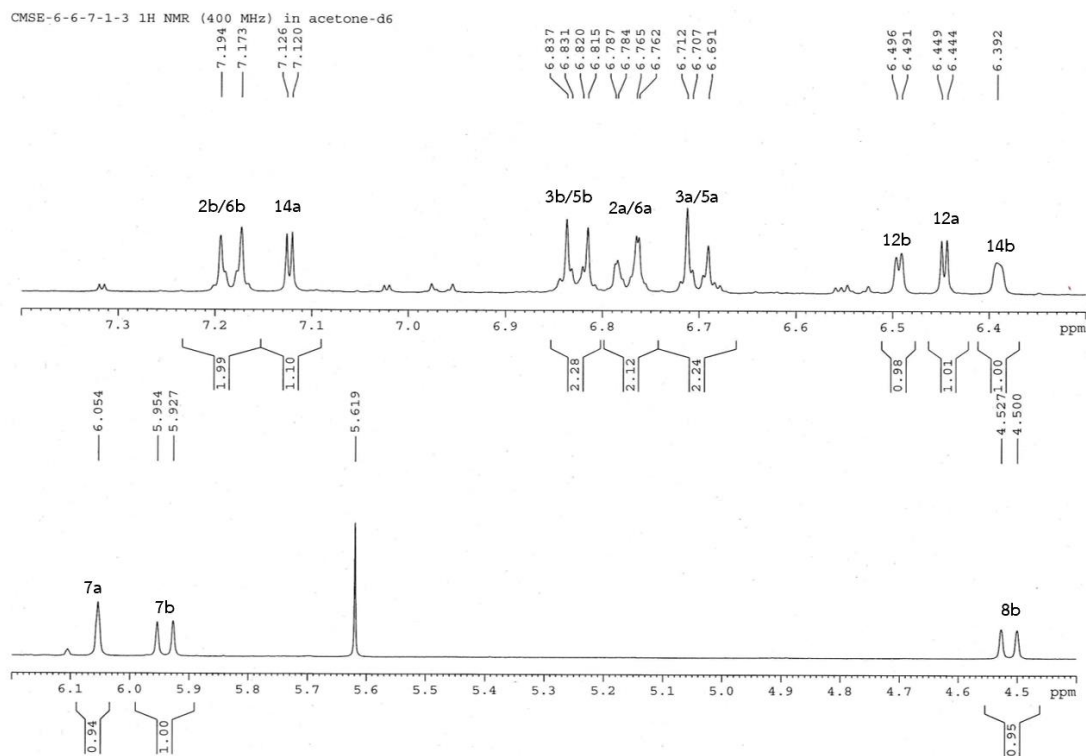


Figure 48. $^1\text{H-NMR}$ spectrum of compound **5** (expansion between δ_{H} 4.4-7.5 ppm)

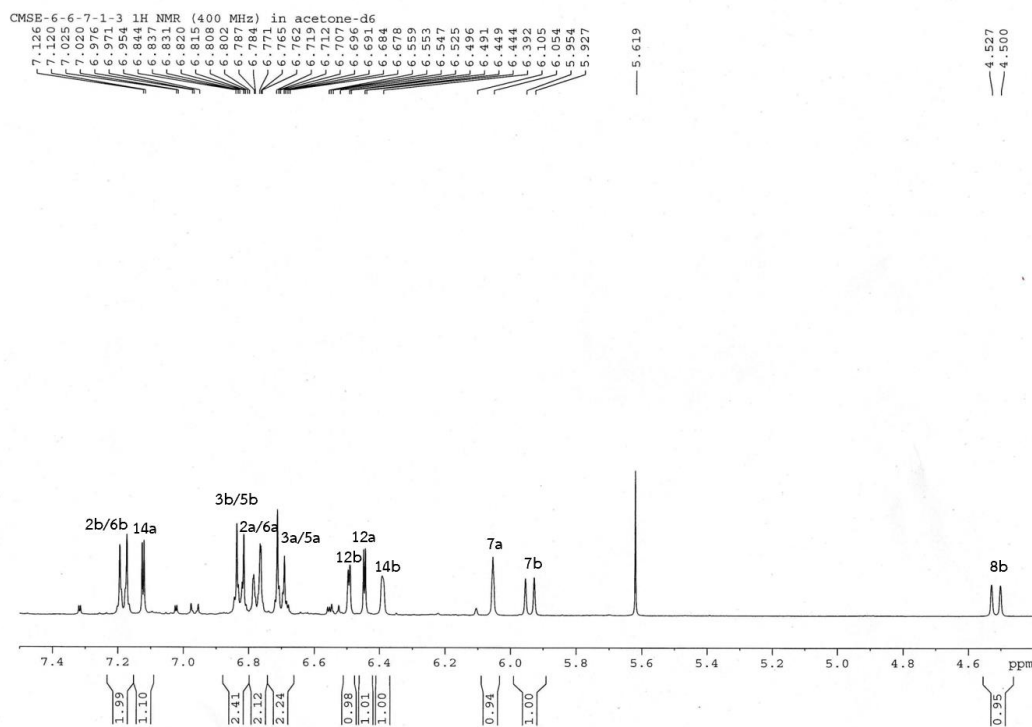


Figure 49. $^1\text{H-NMR}$ spectrum of compound **5** (expansion between δ_{H} 4.4-7.4 ppm)

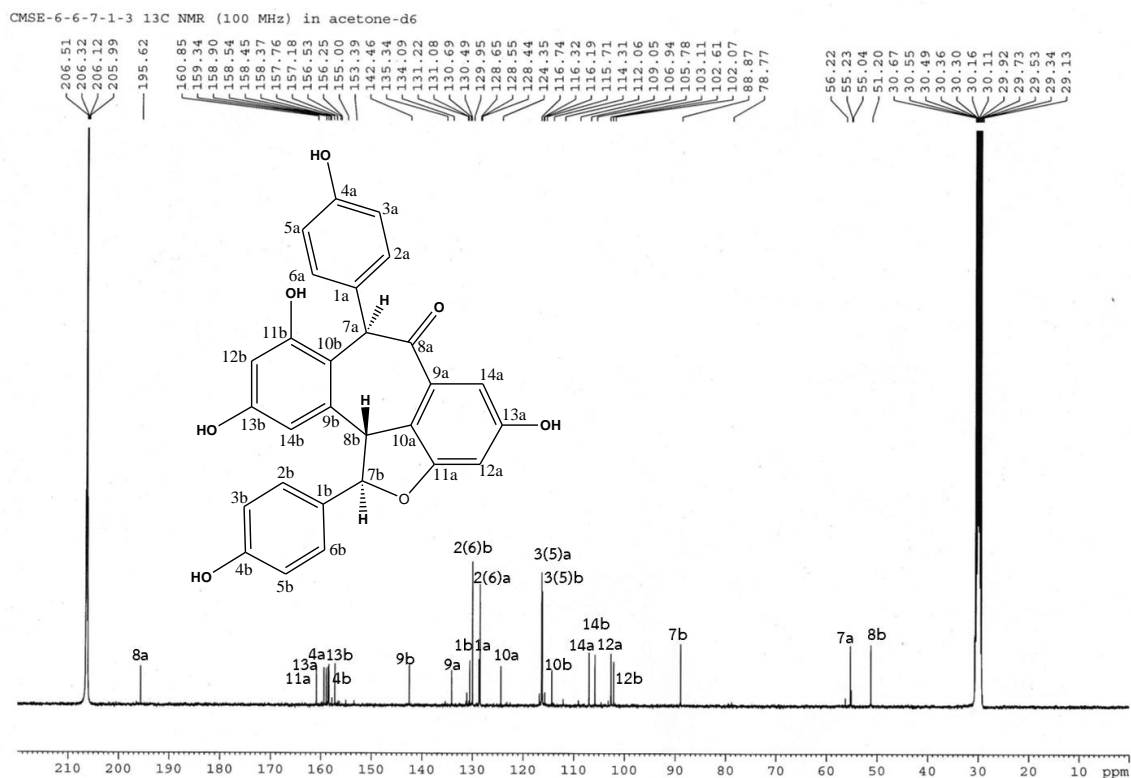


Figure 50. ^{13}C -NMR spectrum of compound 5 (100 MHz, acetone- d_6)

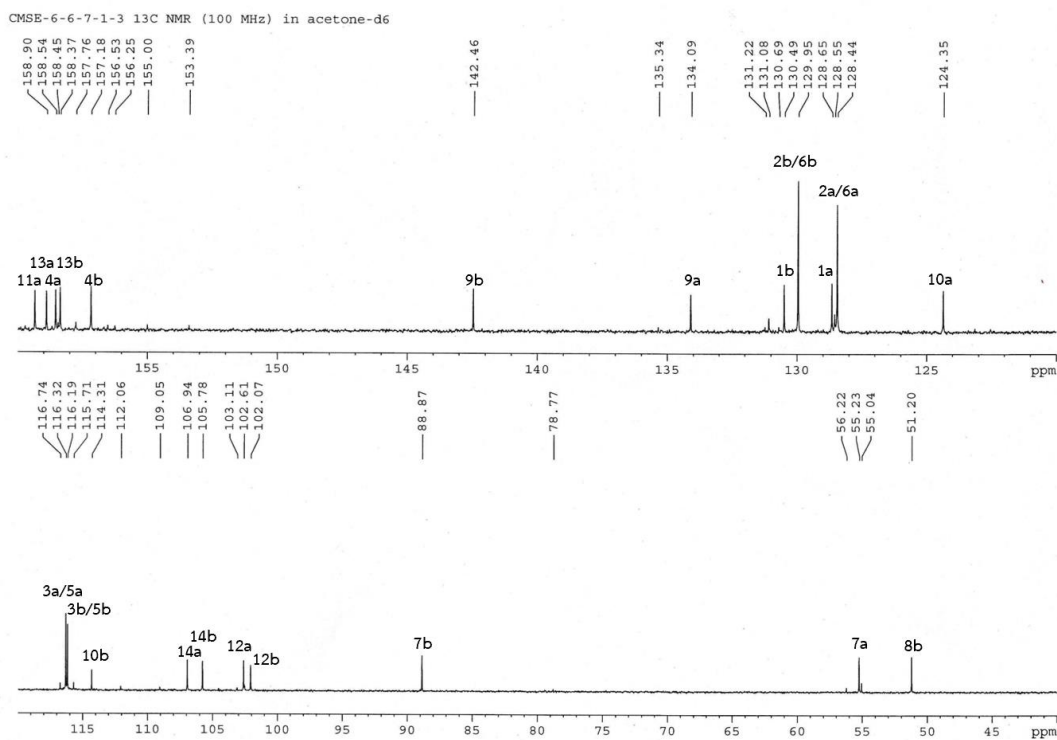


Figure 51. ^{13}C -NMR spectrum of compound 5 (expansion between δ_{C} 40-160 ppm)

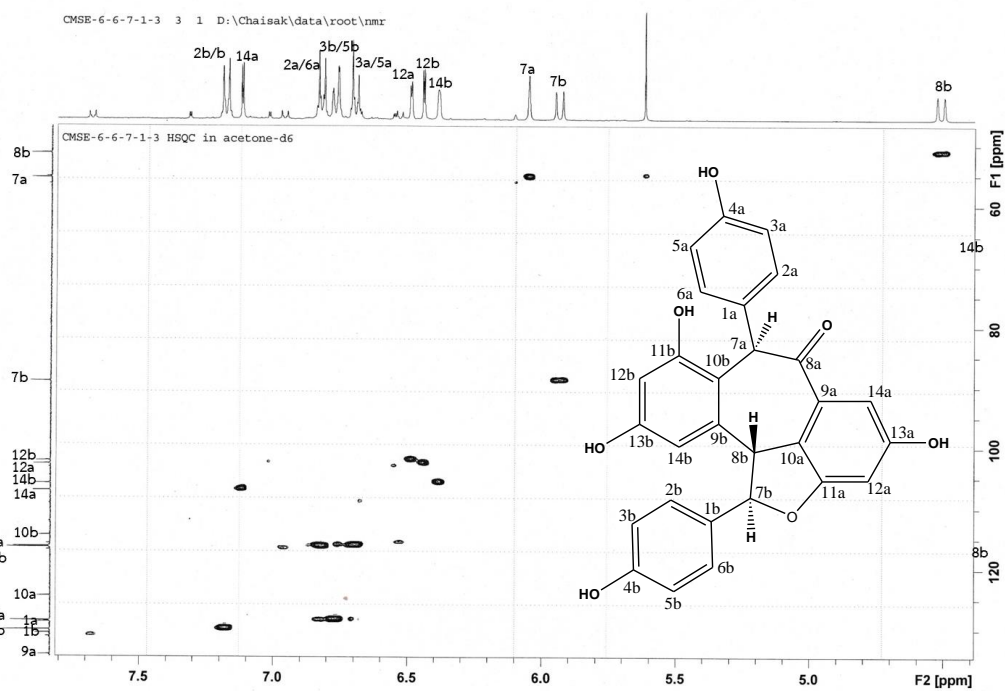


Figure 52. ^1H - ^{13}C HSQC spectrum of compound 5

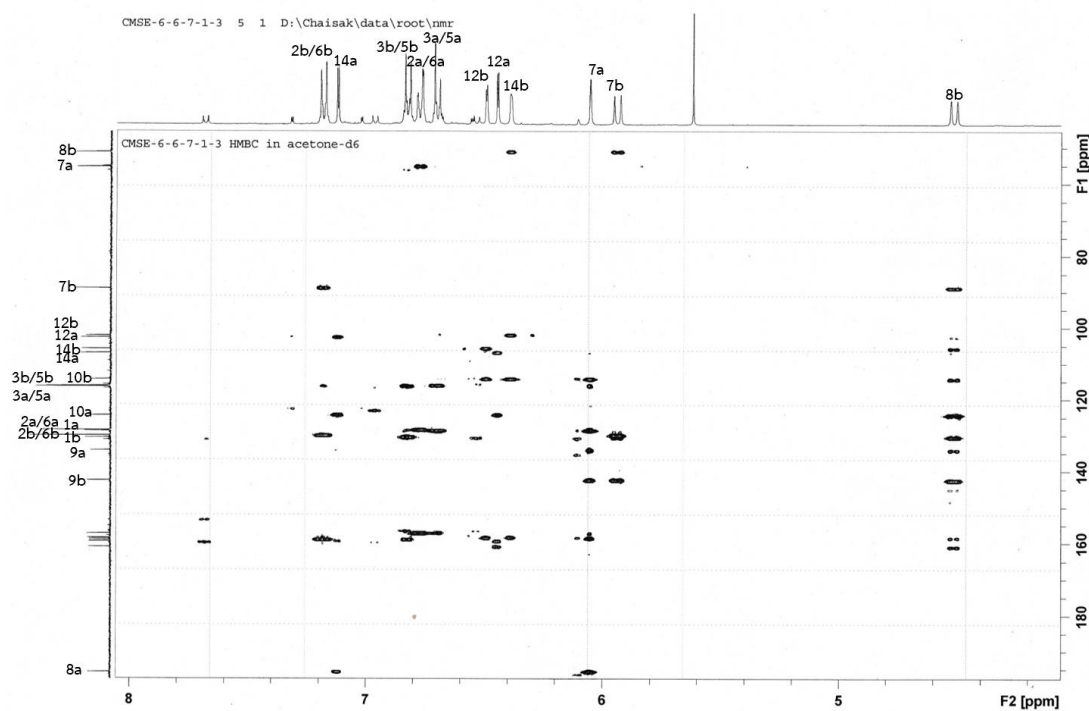


Figure 53. ^1H - ^{13}C HMBC spectrum of compound 5
(expansion between δ_{H} 4.2-8.0 ppm, δ_{C} 50-200 ppm)

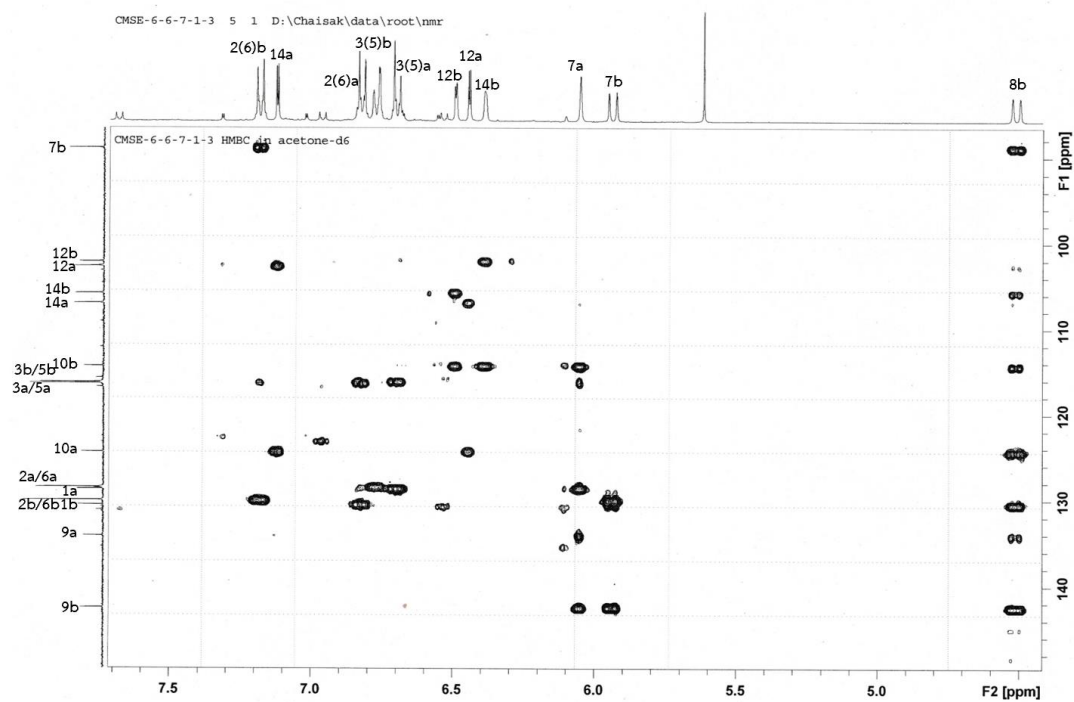


Figure 54. ^1H - ^{13}C HMBC spectrum of compound 5
(expansion between δ_{H} 4.5-7.6 ppm, δ_{C} 90-150 ppm)

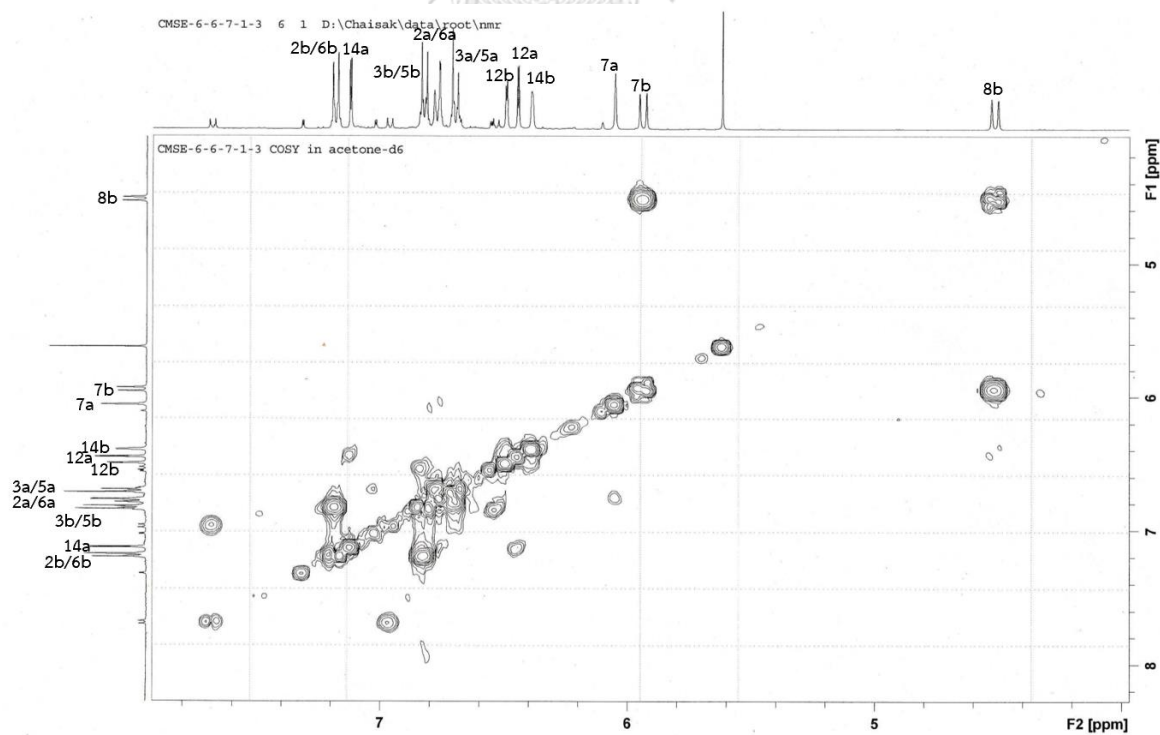


Figure 55. ^1H - ^1H COSY spectrum of compound 5

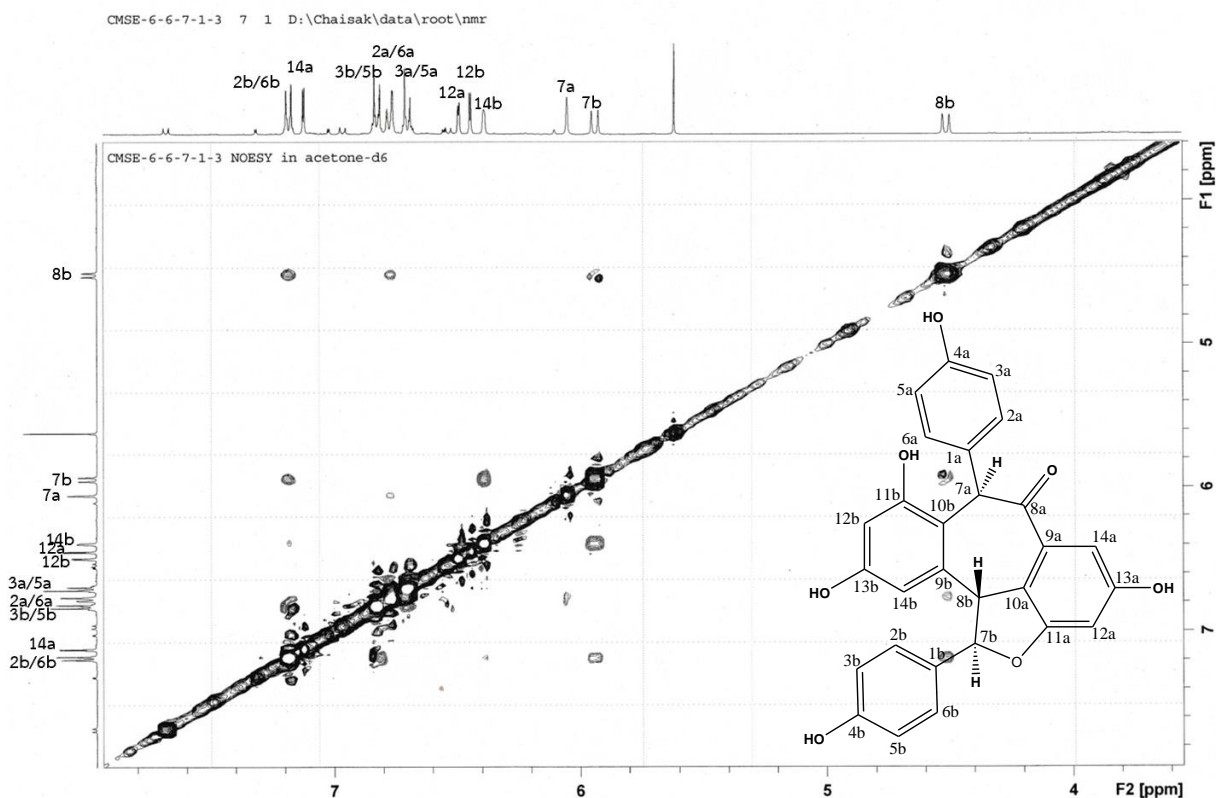


Figure 56. ^1H - ^1H NOESY spectrum of compound 5
(expansion between δ_{H} 3.5-8.0 ppm)

4.2 Structure elucidation of compounds isolated from *Maerua siamensis* roots

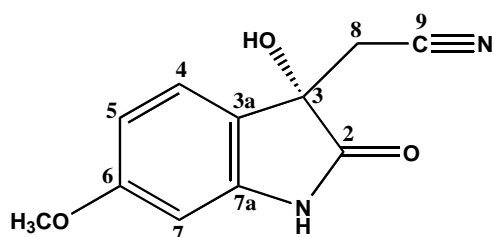
4.2.1 Structure elucidation of compound 6 [(+)-(maeruanitrile A)]

Compound 6 was obtained as a reddish-brown amorphous solid with a $[\alpha]_{\text{D}}^{25}$ value of $+3.0^\circ$ (c 0.001, MeOH). Its high-resolution ESI mass spectrum (Figure 58) displayed a sodium-adduct pseudo-molecular $[\text{M}+\text{Na}]^+$ ion peak at m/z 241.0585 (calculated for $\text{C}_{11}\text{H}_{10}\text{N}_2\text{O}_3\text{Na}$, 241.0584), corresponding to a molecular formula of $\text{C}_{11}\text{H}_{10}\text{N}_2\text{O}_3$ with eight degrees of unsaturation. The IR spectrum of this compound (Figure 59) exhibited an absorption band of nitrile group at 2256 cm^{-1} , hydroxyl and amide N-H bands at 3291 cm^{-1} , aromatic ring at 1630 and 1463 cm^{-1} , and γ -lactam carbonyl at 1722 cm^{-1} . UV absorption peaks (Figure 57) were observed at λ_{max} 218, 268 and 322 nm . These data are characteristic of oxindole moiety (Kinashi *et al.*, 1976).

The $^1\text{H-NMR}$ spectrum of compound **6** (Table 9 and Figure 61) showed resonances of an ABX system of a benzene ring at δ_{H} 7.48 (1H, *d*, $J = 8.4$ Hz, H-4), 6.63 (1H, *dd*, $J = 8.4, 2.4$ Hz, H-5) and 6.53 (1H, *d*, $J = 2.4$ Hz, H-7), methylene protons at δ_{H} 3.09 (1H, *d*, $J = 16.8$ Hz, H-8a) and 2.89 (1H, *d*, $J = 16.8$ Hz, H-8b), a methoxy group at δ_{H} 3.81 (3H, *s*, 6-OCH₃) and a hydroxyl group at δ_{H} 5.44 ppm (1H, *s*).

Its $^{13}\text{C-NMR}$ spectrum (Table 9 and Figure 62) showed eleven carbon resonances including those of an amide carbonyl carbon at δ_{C} 178.2 (C-2), a methoxy carbon at δ_{C} 56.5 (6-OCH₃), a methylene carbon at δ_{C} 28.0 (C-8), a nitrile carbon at δ_{C} 117.7 (C-9), three aromatic methine carbons at δ_{C} 98.8 (C-7), 108.4 (C-4) and 126.9 (C-4), an aliphatic quaternary carbon at δ_{C} 73.8 (C-3) and three aromatic quaternary carbons at δ_{C} 122.8 (C-3a), 144.7 (C-7a) and 163.4 (C-6).

The positions of aromatic protons on the benzene ring of this oxindole molecule were confirmed by two-dimensional NMR experiments. Long-range $^1\text{H-}^{13}\text{C}$ HMBC correlations (Figure 64-65) between H-4 signal (δ_{H} 7.48) and the aliphatic quaternary carbon at δ_{C} 73.8 (C-3) and the downfield aromatic methine carbon at δ_{C} 163.4 ppm (C-6), whereas H-7 signal showed three-bond HMBC cross peaks with those of C-3a (δ_{C} 122.8) and C-5 (δ_{C} 108.4). The assignment of a methoxy group at position 6 of the indole ring was supported by an observed HMBC cross peak between 6-OCH₃ signal and C-6, as well as $^1\text{H-}^1\text{H}$ NOESY correlations between this methoxy protons and both H-5 and H-7 signals (Figure 67). An acetonitrile group could be located at C-3, based on HMBC cross peaks of its methylene protons (H-8) with C-2 (δ_{C} 178.2), C-3 and C-3a. A hydroxyl group could also be located at C-3 based on its downfield shift and HMBC correlations from 3-OH signal (at δ_{H} 5.44 ppm) to C-3 and C-3a. The configuration at position 3 was confirmed by comparison of its ECD spectra (Figure. 60) with that of a known compound, (+)-*S*-2-(3-hydroxy-4-methoxy-2-oxindolin-3-yl) acetonitrile, from *Isatis indigotica* (Chen *et al.*, 2012). Therefore, the chemical structure of compound **6** was established as (+)-*S*-2-(3-hydroxy-6-methoxy-2-oxindolin-3-yl) acetonitrile, and was named (+)-maeruanitrile A.



(+)-maeruanitrile A.

Table 9. ^1H -, ^{13}C -NMR and HMBC data of compound **6** (400 MHz, acetone- d_6)

Position	Compound 6		
	δ_{H} (mult., J in Hz)	δ_{C}	HMBC correlation with
NH-1	9.52, <i>br s</i>	-	-
2	-	178.2	-
3	-	73.8	-
3a	-	122.8	-
4	7.48 (<i>d</i> , 8.4)	126.9	C-3, C-6
5	6.63 (<i>dd</i> , 8.4, 2.4)	108.4	C-3a, C-6, C-7
6	-	163.4	-
7	6.53 (<i>d</i> , 2.4)	98.8	C-3a, C-5, C-6, C-7a
7a	-	144.7	-
8a	3.09 (<i>d</i> , 16.8)	28.0	C-2, C-3, C-3a, C-9
8b	2.89 (<i>d</i> , 16.8)		
9-CN	-	117.8	-
3-OH	5.44, (<i>s</i>)		C-3, C-3a
6-OCH ₃	3.81, (<i>s</i>)	56.5	C-6

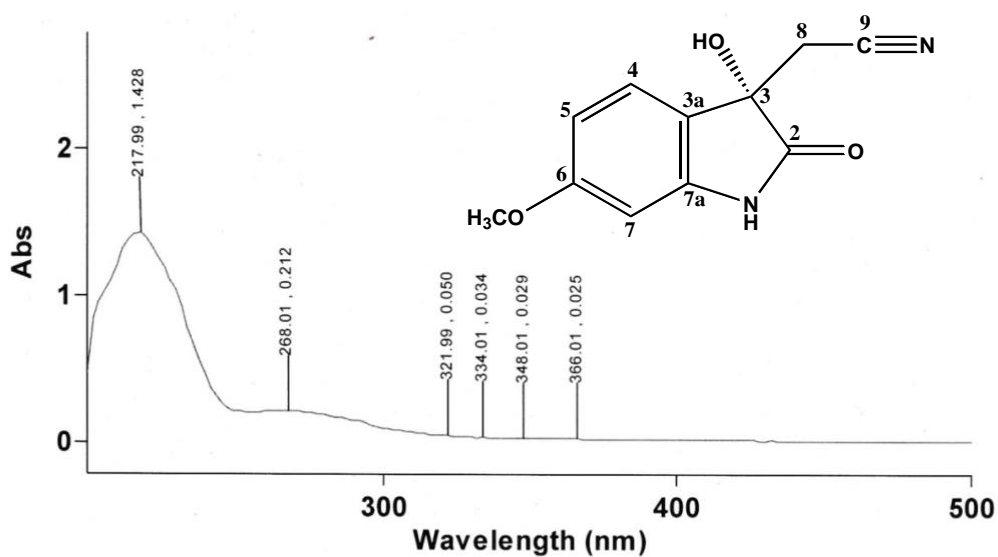
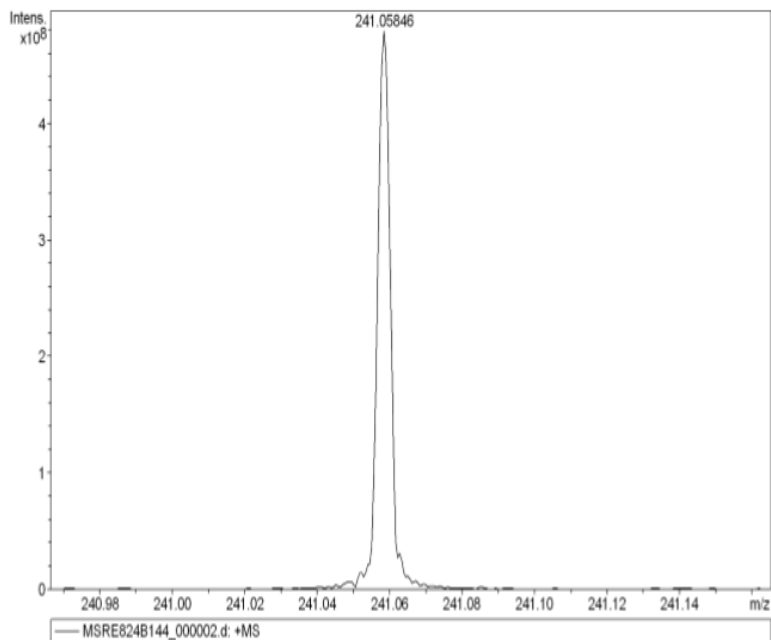


Figure 57. UV spectrum of compound 6

Mass Spectrum SmartFormula Report

Analysis Info

Analysis Name	D:\Data\7\MSRE824B144_000002.d	11/14/2019 3:43:09 PM
Method	broadband first signal	Operator: YU HSIAO-CHING
Sample Name	MSRE-8-2-4B-14-4	Instrument: BRUKER FT-MS solariX
Comment	ESI Positive	



Meas. m/z	#	Formula	Score	m/z	err [mDa]	err [ppm]	mSigma	rdb	e ⁻ Conf	N-Rule
241.05846	1	C 11 H 10 N 2 Na O 3	100.00	241.05836	-0.09	-0.39	9.4	7.5	even	ok

Figure 58. HR-ESI mass spectrum of compound 6

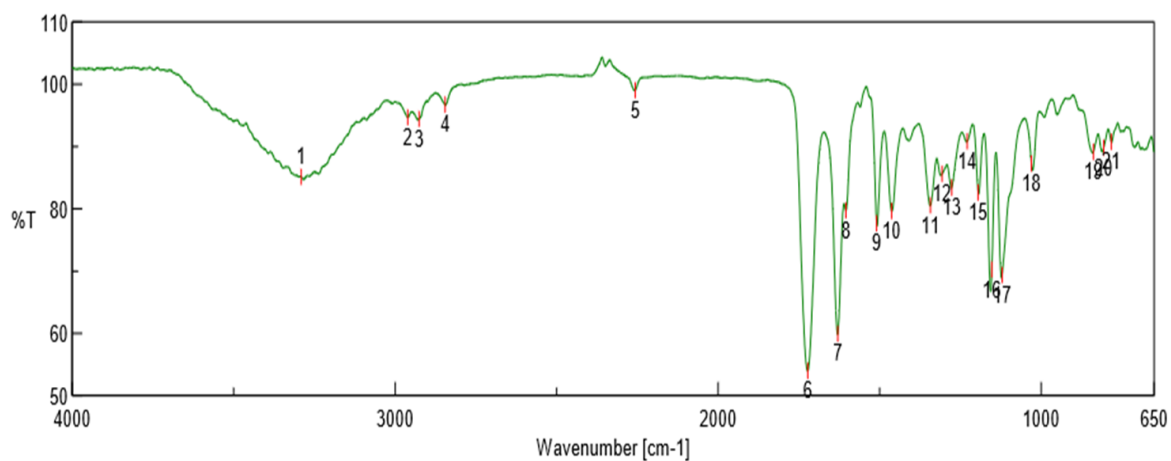


Figure 59. IR spectrum of compound 6

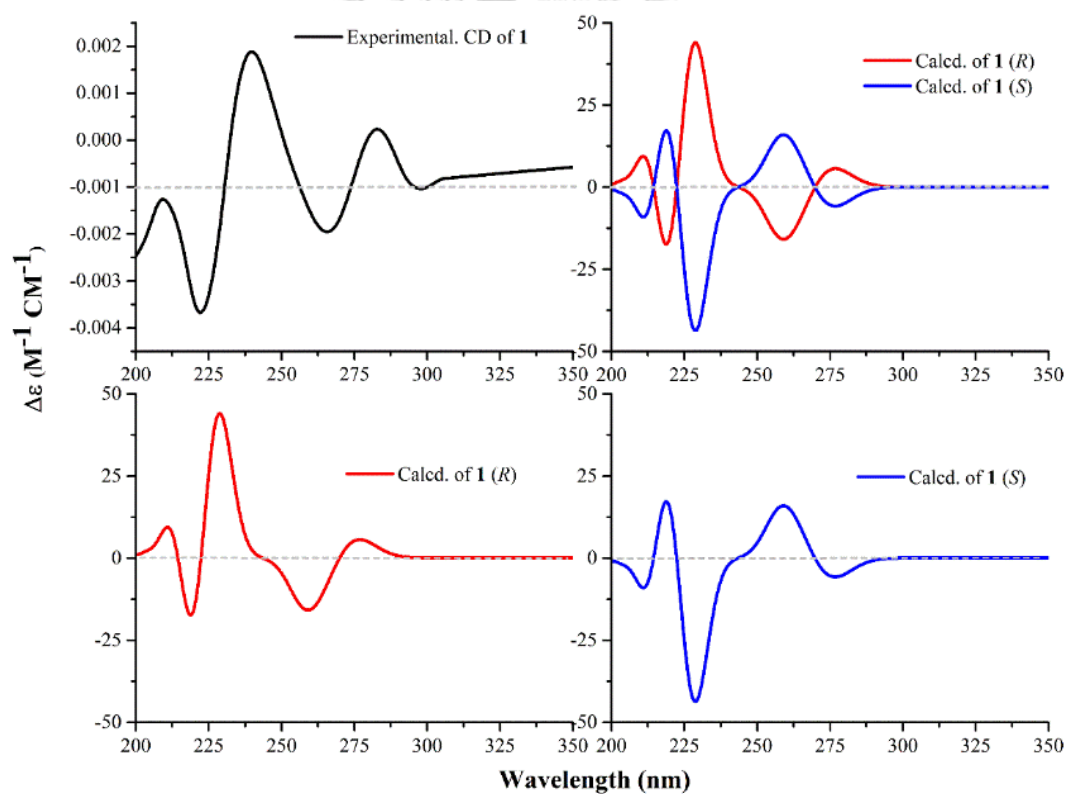
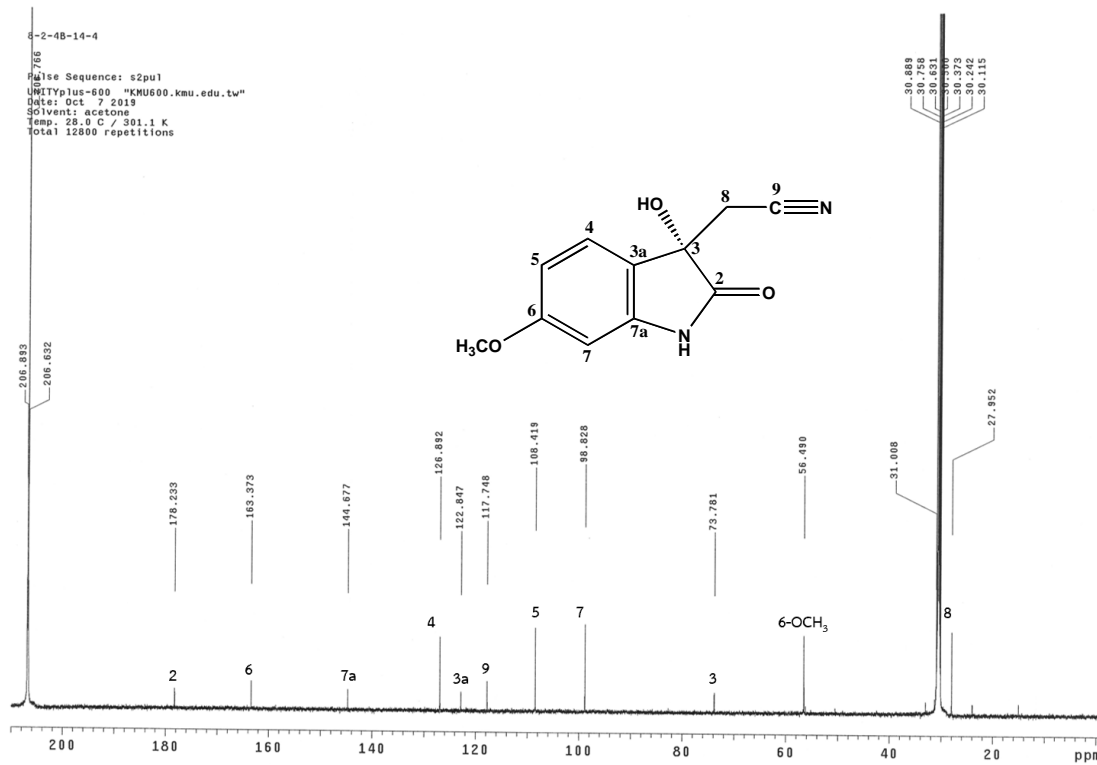
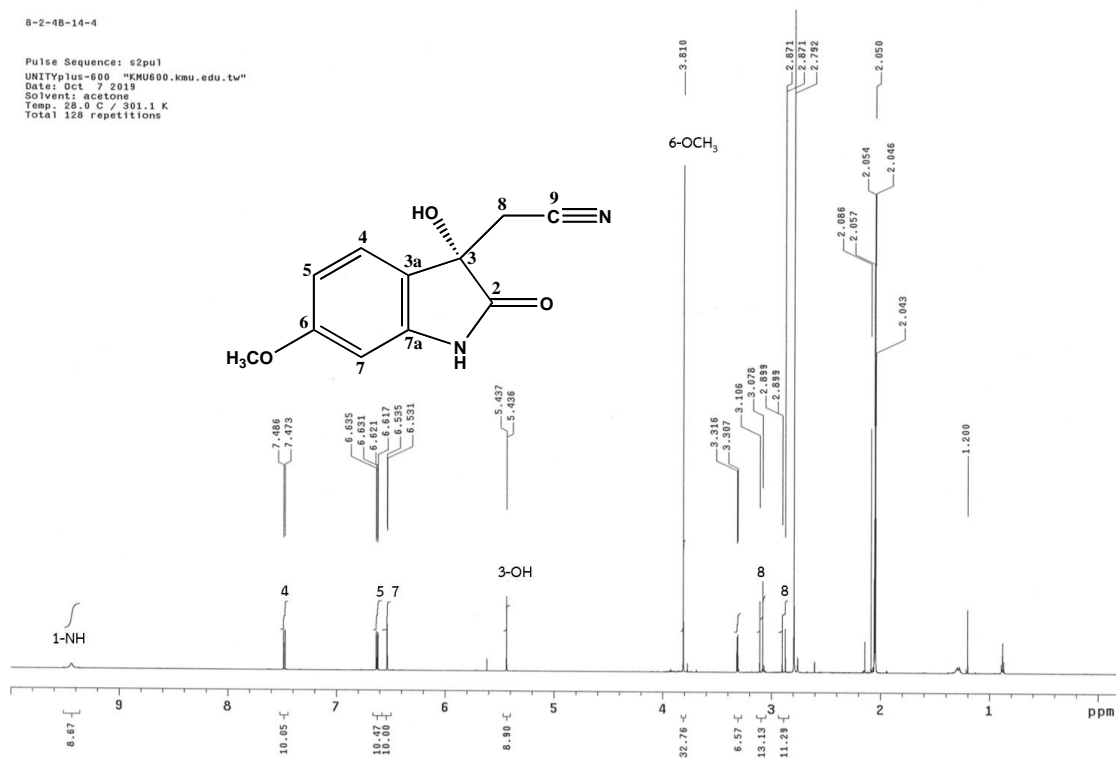


Figure 60. The CD spectrum in MeOH of compound **1** (upper left) and The ECD spectrum of compound **1**; calculated for *R* configuration (lower left), calculated for *S* configuration (lower right) and overlaid ECD spectrum (upper right).



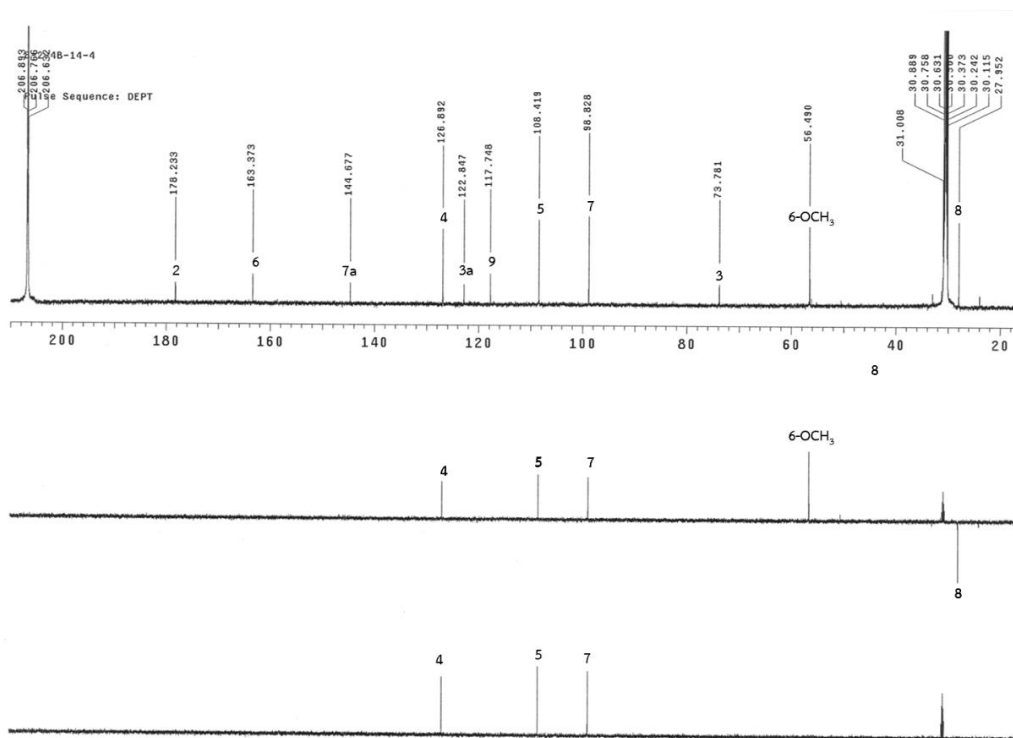


Figure 63. ^{13}C -NMR, DEPT135 and DEPT90 spectrum of compound 6

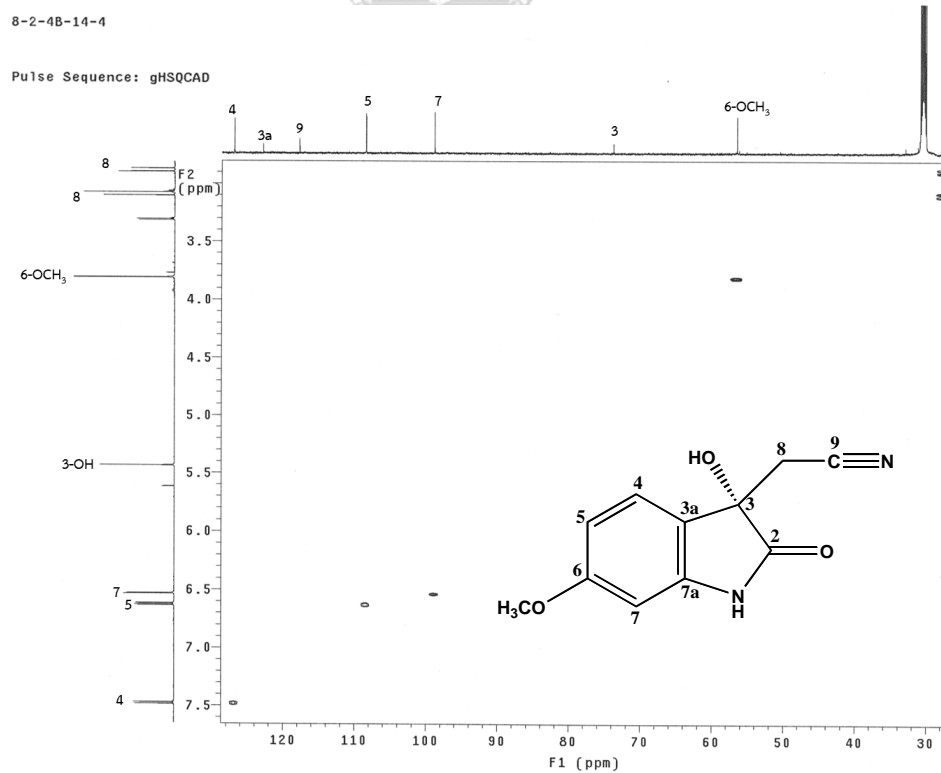


Figure 64. ^1H - ^{13}C HSQC spectrum of compound 6

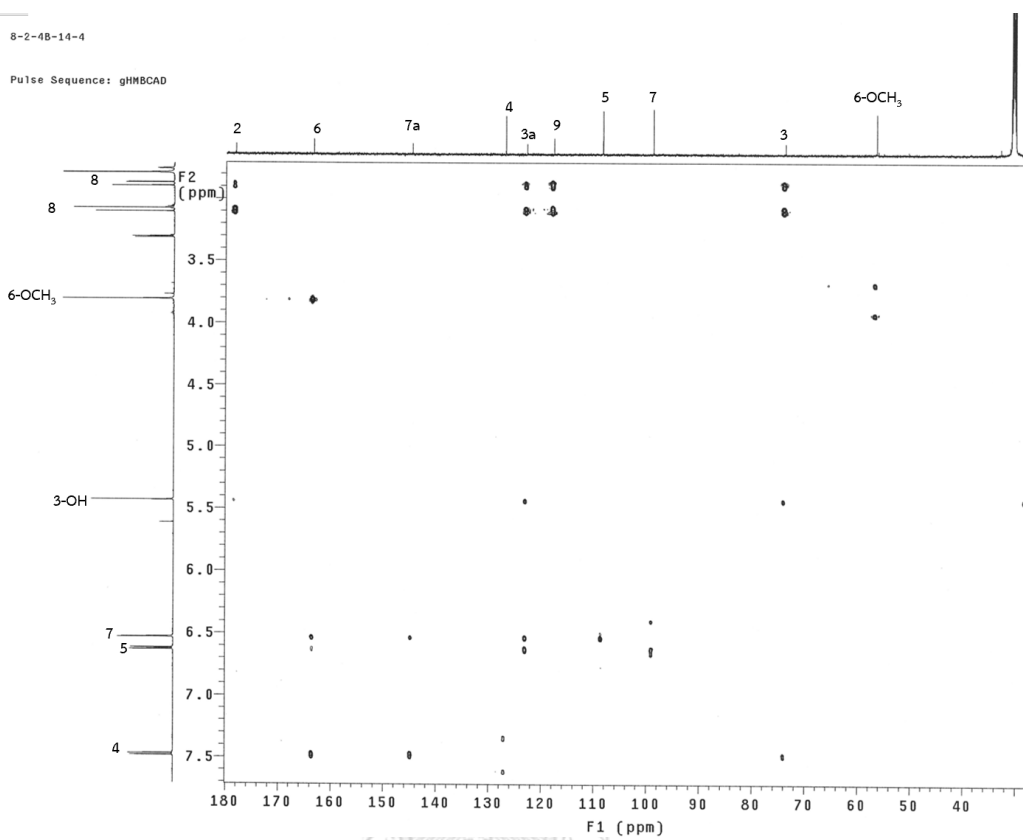


Figure 65. ^1H - ^{13}C HMBC spectrum of compound 6

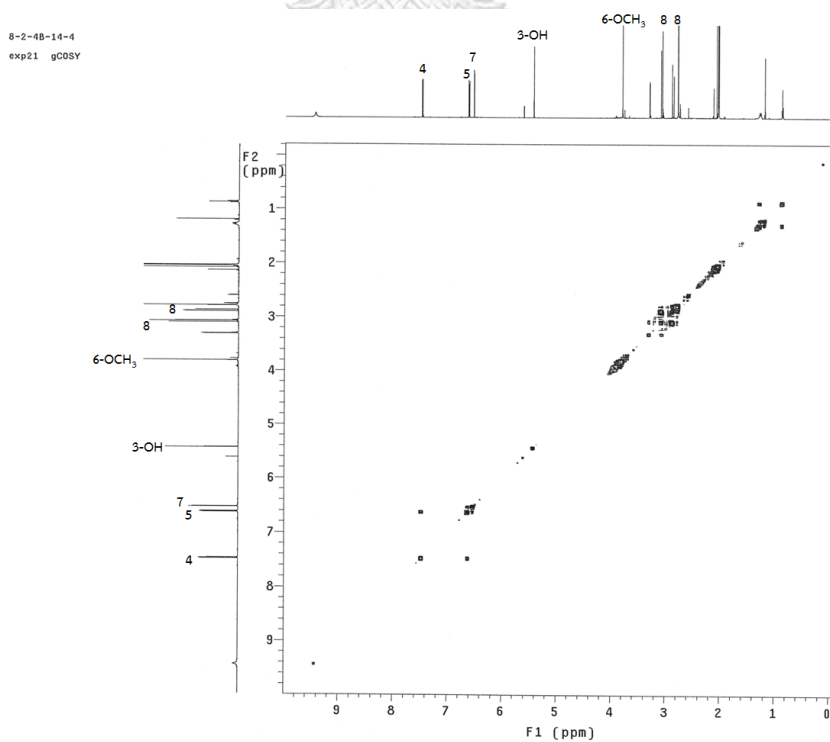


Figure 66. ^1H - ^1H COSY spectrum of compound 6

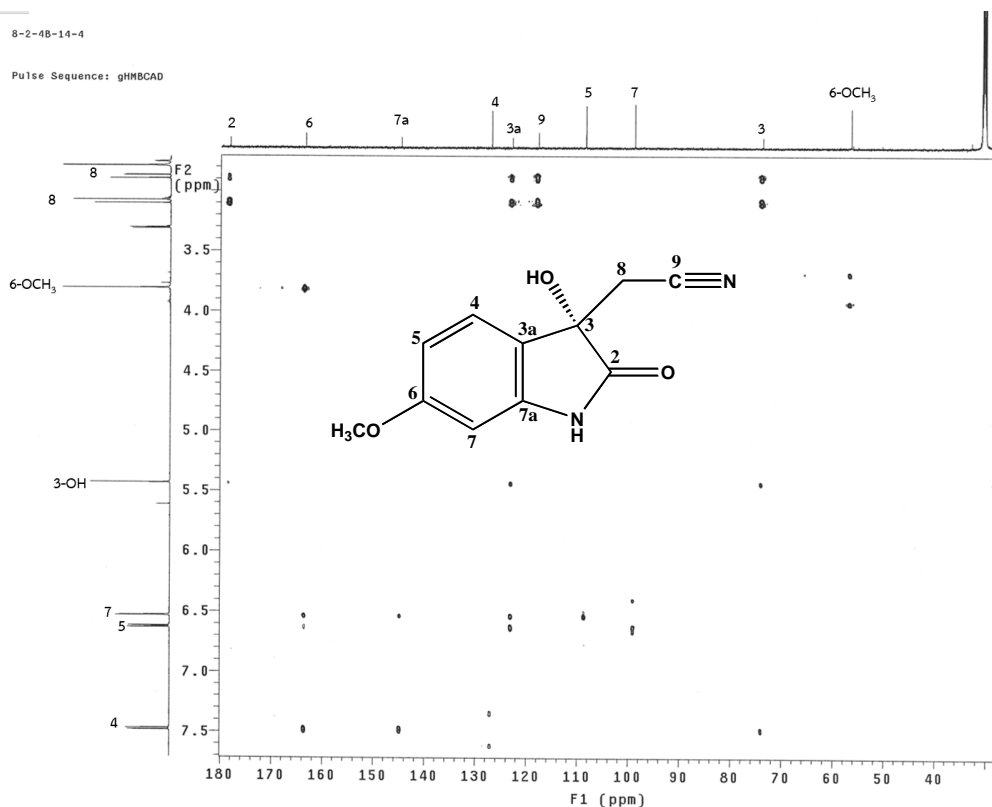


Figure 67. ^1H - ^1H NOESY spectrum of compound 6

4.2.2 Structure elucidation of compound 7 (maeruanitrile B)

Compound 7 was obtained as a reddish-brown amorphous solid. Its molecular formula was deduced as $\text{C}_{12}\text{H}_{12}\text{N}_2\text{O}_2\text{S}$ (nine degrees of unsaturation), based on the sodium-adduct pseudo-molecular $[\text{M}+\text{Na}]^+$ ion at m/z 271.0511 (calculated for $\text{C}_{12}\text{H}_{12}\text{N}_2\text{O}_2\text{SNa}$, 271.0512) in the HR-ESI mass spectrum (Figure 69). Its IR spectrum (Figure 70) showed strong absorption peaks of sulfoxide at 1022 cm^{-1} , nitrile group at 2250 cm^{-1} hydroxyl and amine groups at 3163 cm^{-1} and aromatic ring at 1626 and 1451 cm^{-1} . The UV spectrum (Figure 68) exhibited absorption maxima at λ_{max} 228, 300 and 342 nm .

Its ^1H -NMR data (Table 10 and Figure 71) showed ABX coupling protons of a benzene ring at δ_{H} 7.63 (1H, *d*, $J = 9.0\text{ Hz}$, H-4), 6.98 (1H, *d*, $J = 2.4\text{ Hz}$, H-7) and 6.87 (1H, *dd*, $J = 9.0, 2.4\text{ Hz}$, H-5), methylene protons of an acetonitrile group at δ_{H} 4.18 (1H, *d*, $J = 18.0\text{ Hz}$, H-8a) and 4.13 (1H, *d*, $J = 16.0\text{ Hz}$, H-8b), a methoxy singlet at δ_{H} 3.86 (3H, 6-OCH₃) and a methylsulfinyl singlet at δ_{H} 2.16 (3H, 2-SOCH₃).

Twelve signals were observed in the ^{13}C -NMR spectrum of this compound (Table 10 and Figure 72). These were signals of six quaternary carbons of the indole nucleus at δ_{C} 160.6 (C-6), 140.3 (C-7a), 132.5 (C-2), 121.4 (C-3a), 110.8 (C-3) and 118.9 (C-9), three aromatic methines at δ_{C} 121.4 (C-4), 113.4 (C-5) and 95.3 (C-7), one methylene carbon of an acetonitrile group at δ_{C} 13.0 (C-8), a methoxy carbon at δ_{C} 55.9 (6-OCH₃) and a methylsulfoxide carbon at δ_{C} 40.4 (2-SOCH₃).

The substitution pattern on aromatic ring of this indole derivative is similar to that of compound 6, as confirmed by long-range ^1H - ^{13}C HMBC correlations (Figure 76-77) between H-4 signal (δ_{H} 7.63) with C-3 (δ_{C} 110.8), C-6 (δ_{C} 160.6) and C-7a (δ_{C} 140.3), as well as from H-7 signal (at δ_{H} 6.98) to those of C-3a (δ_{C} 121.4) and C-5 (δ_{C} 113.4). In addition, correlations between both H-5 and H-7 signals to that of 6-methoxy protons could also be observed in its ^1H - ^1H NOESY spectrum (Figure 79). An acetonitrile group could be located at position 3 based on HMBC cross peaks of its methylene protons (δ_{H} 4.18 and 4.13) with C-2 (δ_{C} 132.5), C-3 (δ_{C} 110.8) and C-3a signals (δ_{C} 121.4). Finally, a methylsulfoxide group could be attached at C-2, which was confirmed by a HMBC cross peak of its methyl signal (at δ_{H} 2.16) to this carbon signal.

These spectroscopic data indicated that compound 7 was similar to indole-3-acetonitrile, isolated from fruits of *Capparis spinosa* (Calis *et al.* (1999), except the presence of an additional methoxy group at C-6 of this new compound. A glycoside with similar indole nucleus, indole-3-acetonitrile-2-*S*- β -glucopyranoside, has been isolated from the roots of *Isatis indigotica* (Yang *et al.*, 2014) of family Brassicaceae, which is closely related taxonomically to family Capparaceae. Thus, the chemical structure of compound 7 was established as 2-(6-methoxy-2-(methylsulfinyl)-1*H*-indol-3-yl) acetonitrile, and it was trivially named as maeruanitrile B.

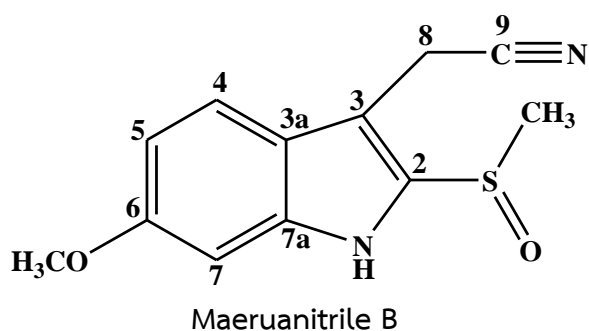


Table 10. ^1H -, ^{13}C NMR and HBMBC data of compound 7 (400 MHz, CD_3OD)

Position	δ_{H} , (mult., J in Hz)	δ_{C}	HMBC correlation with
NH-1	-		-
2	-	132.5	-
3	-	110.8	-
3a	-	121.4	-
4	7.63 (<i>d</i> , 9.0)	121.4	C-3, C-6, C-7a
5	6.87 (<i>dd</i> , 9.0, 2.4)	113.4	C-4, C-3a, C-7
6	-	160.6	-
7	6.98 (<i>d</i> , 2.4)	95.3	C-3a, C-5, C-7a
7a	-	140.3	-
8a	4.18 (<i>d</i> , 18.0)	13.0	C-2, C-3, C-3a
8b	4.13 (<i>d</i> , 18.0)		
9-CN	-	118.9	-
2-SOCH ₃	2.16 (<i>s</i>)	40.4	C-2
6-OCH ₃	3.86 (<i>s</i>)	55.9	C-6

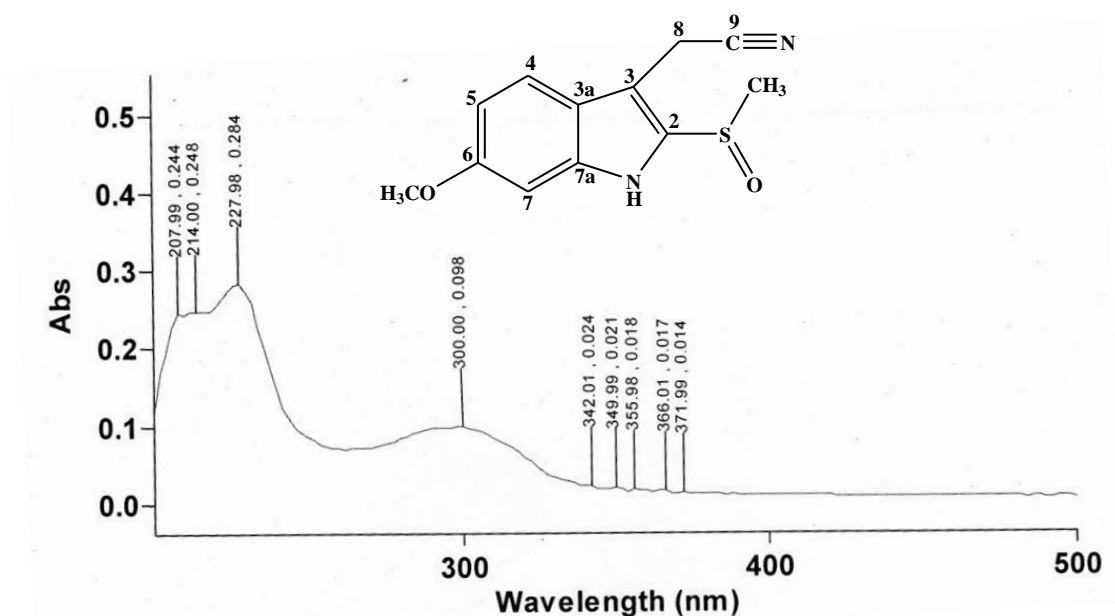


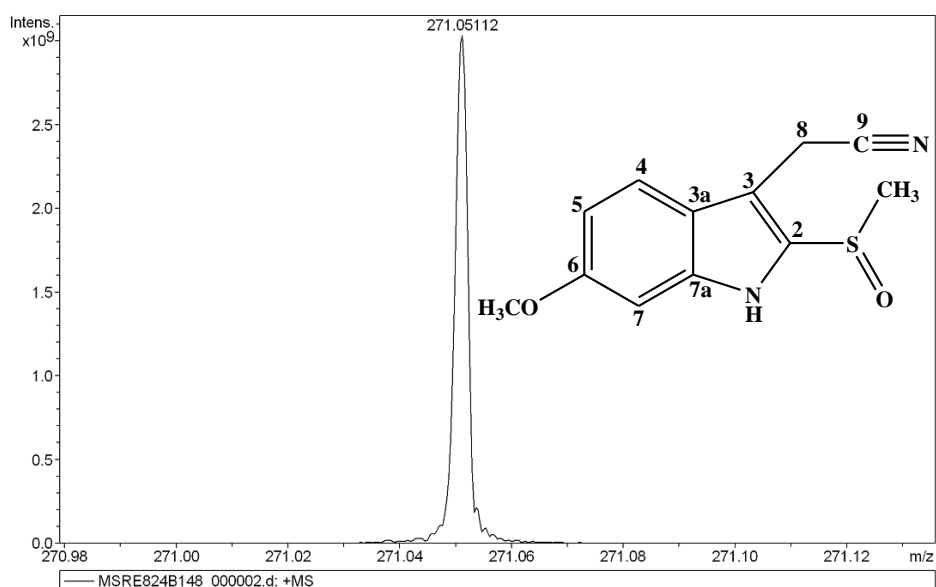
Figure 68. UV spectrum of compound 7

Mass Spectrum SmartFormula Report

Analysis Info

Analysis Name D:\Data\7\MSRE824B148_000002.d
 Method broadband first signal
 Sample Name MSRE-8-2-4B
 Comment ESI Positive

6/30/2020 3:26:08 PM
 Operator: YU HSIAO-CHING
 Instrument: BRUKER FT-MS solariX



Meas. m/z	#	Formula	Score	m/z	err [mDa]	err [ppm]	mSigma	rdb	e ⁻ Conf	N-Rule
271.05112	1	C 12 H 12 N 2 Na O 2 S	100.00	271.05117	0.05	0.19	38.1	7.5	even	ok

Figure 69. HR-ESI mass spectrum of compound 7

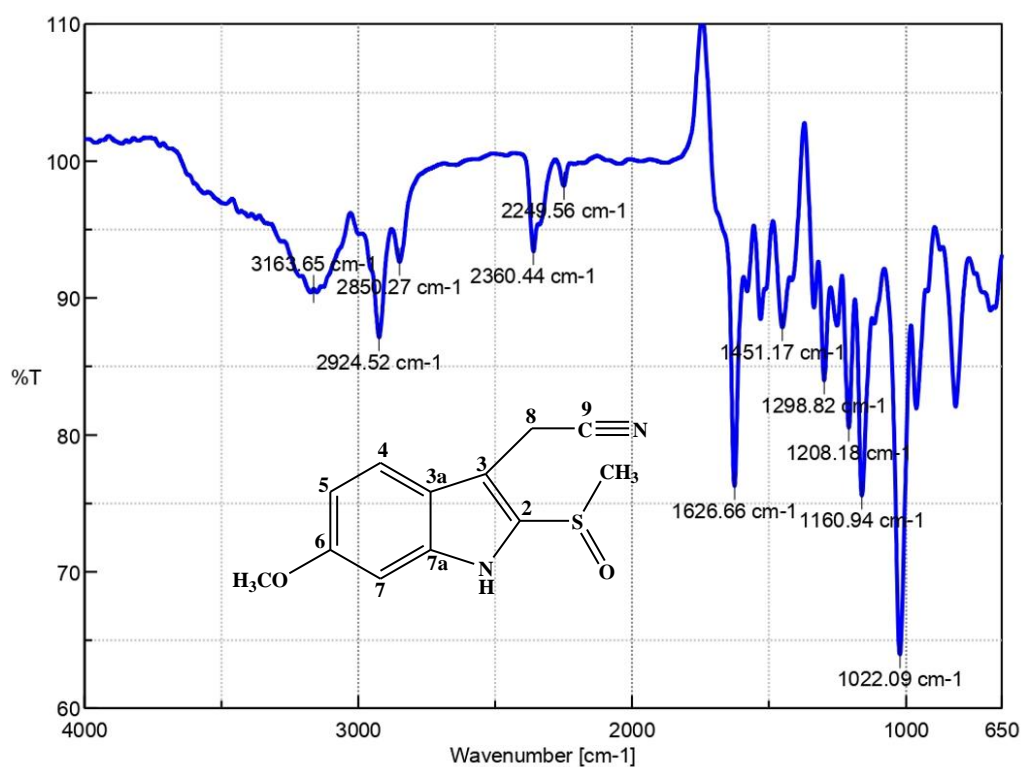
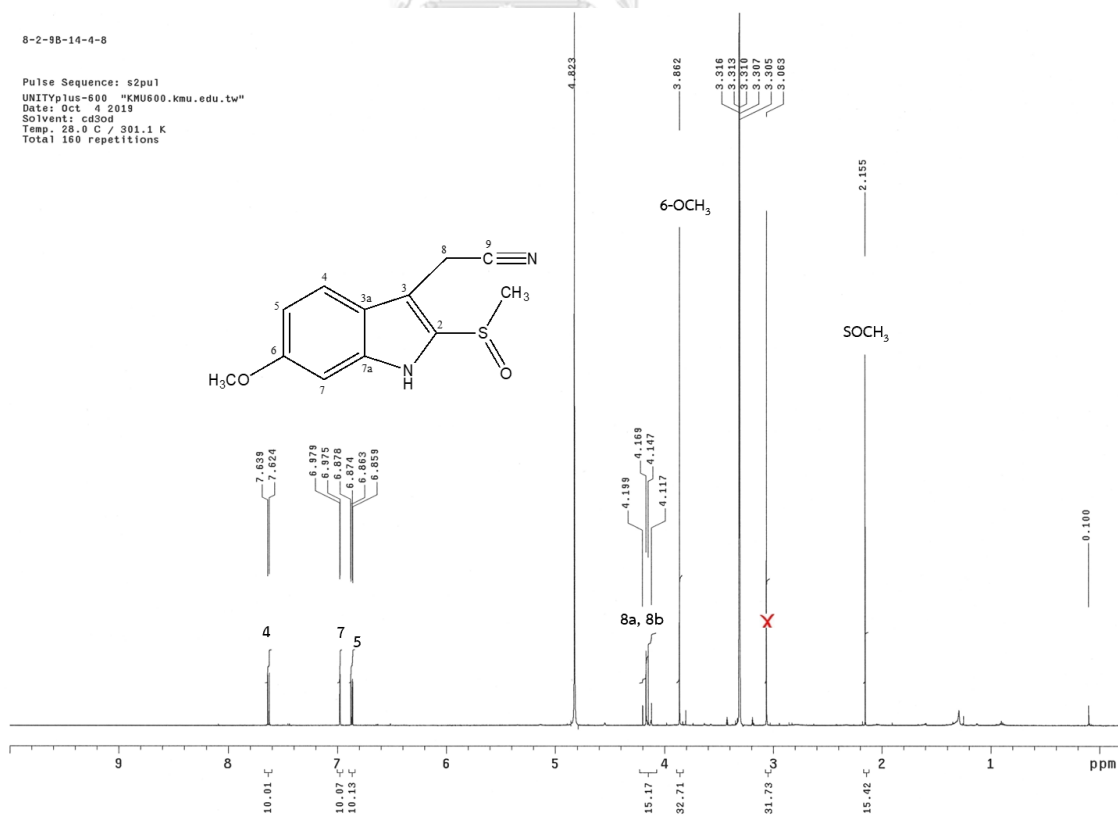
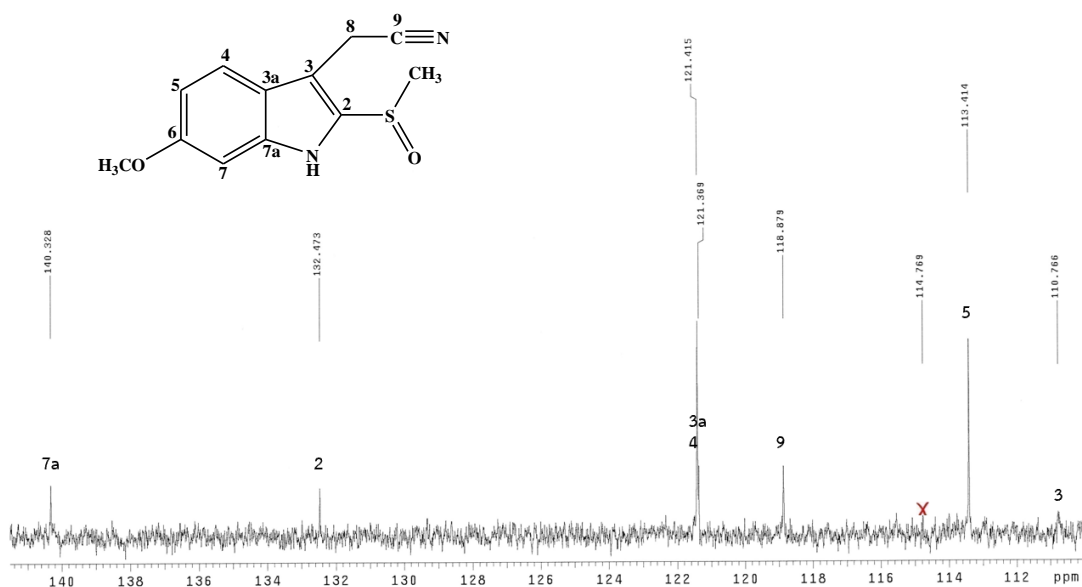
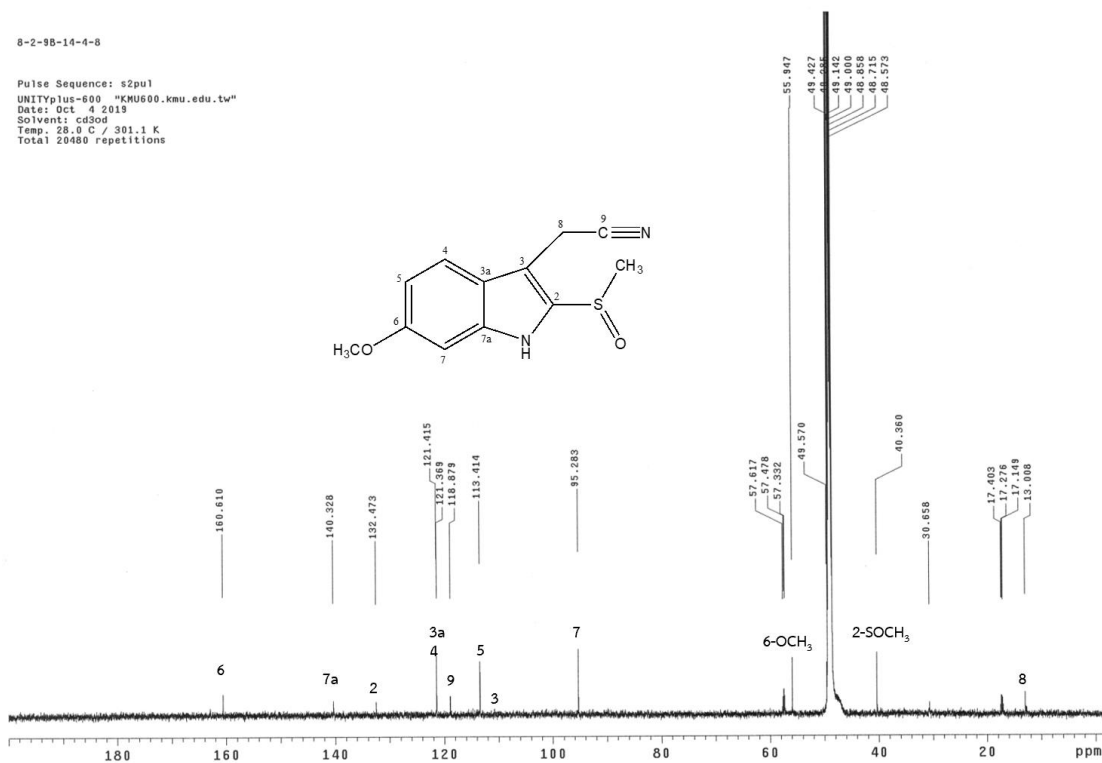


Figure 70. IR spectrum of compound 7

Figure 71. ¹H-NMR spectrum of compound 7 (400 MHz, CD₃OD)



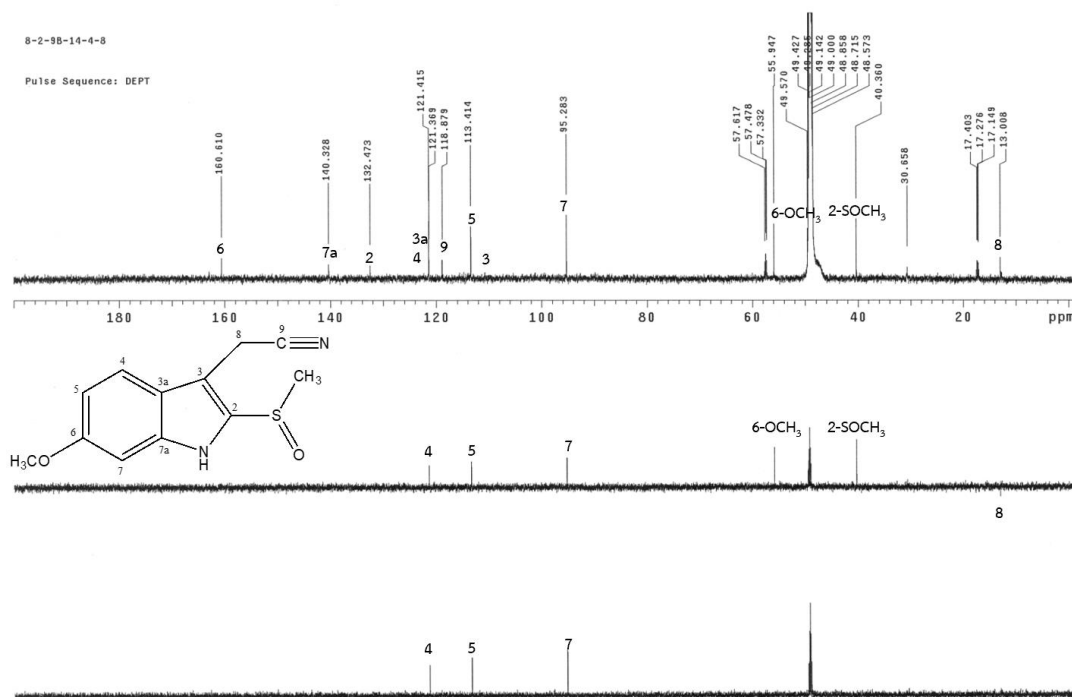


Figure 74. ¹³C-NMR, DEPT 135 and DEPT 90 (150 MHz, CD₃OD) spectra of compound 7

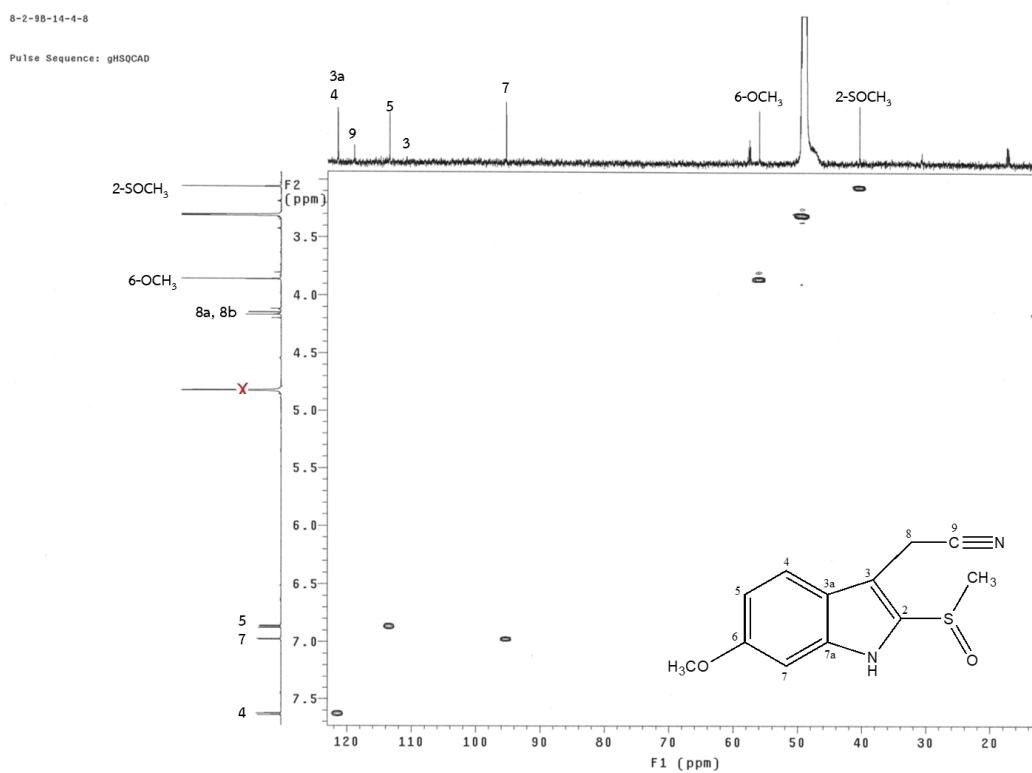
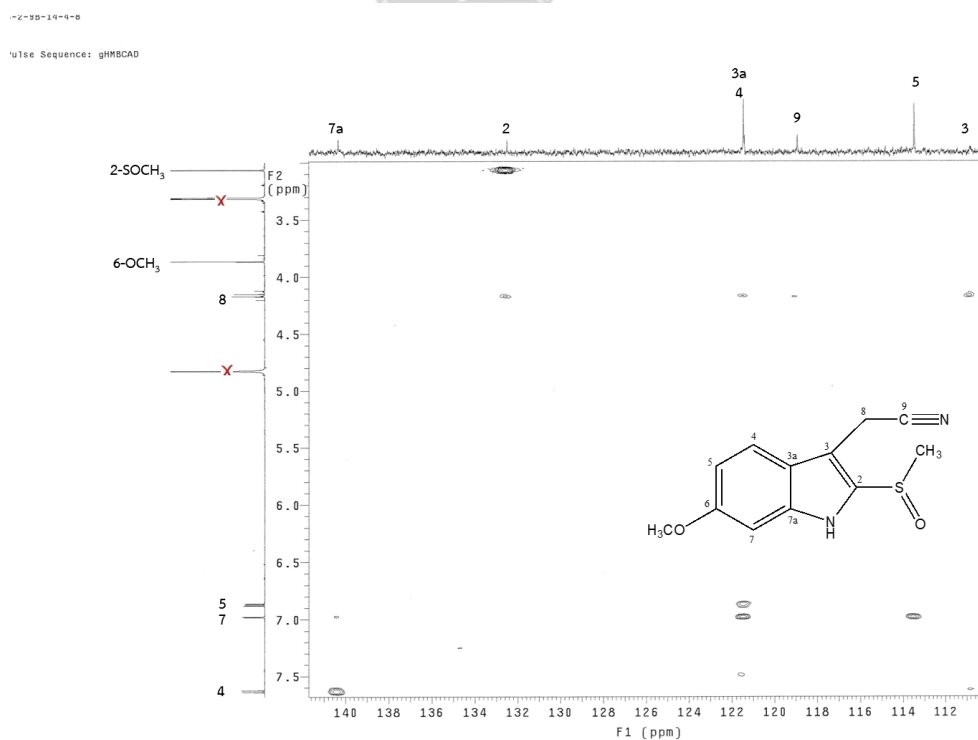
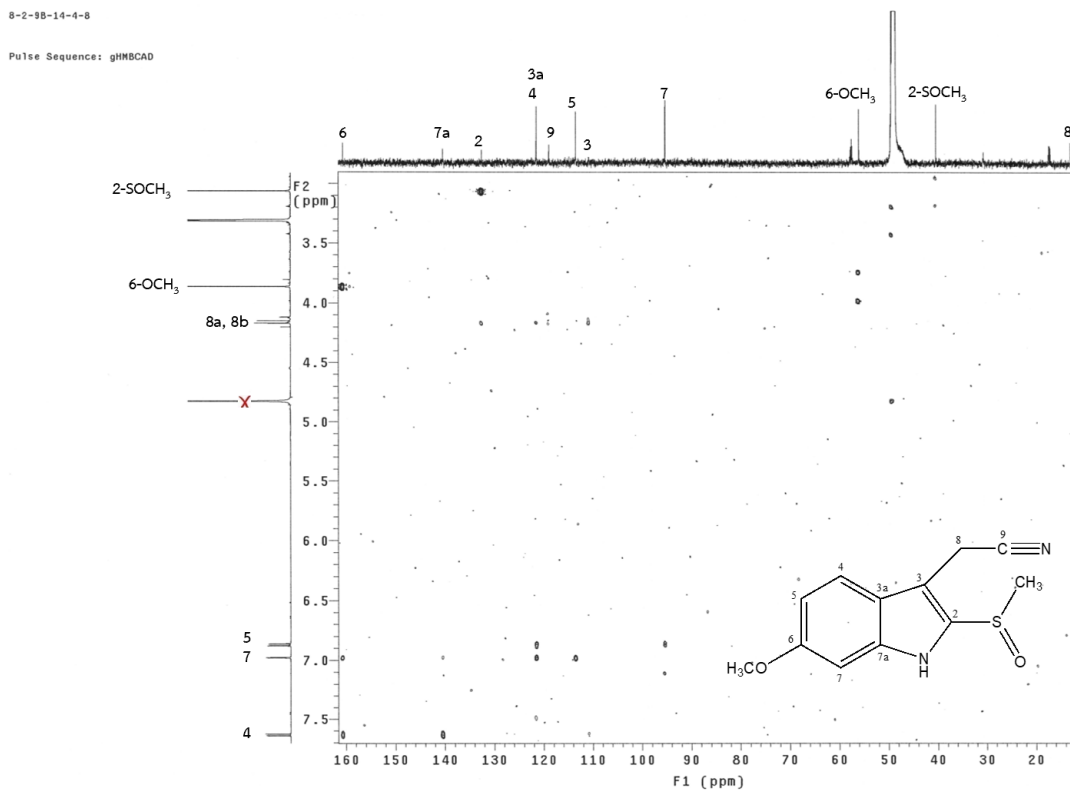
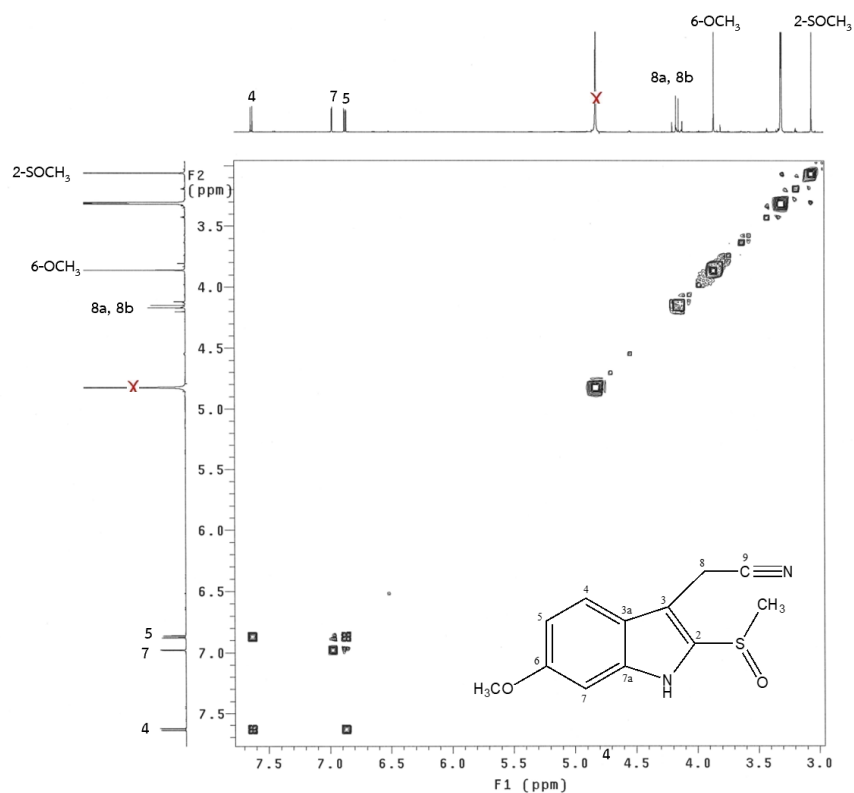


Figure 75. ¹H-¹³C HSQC spectrum of compound 7



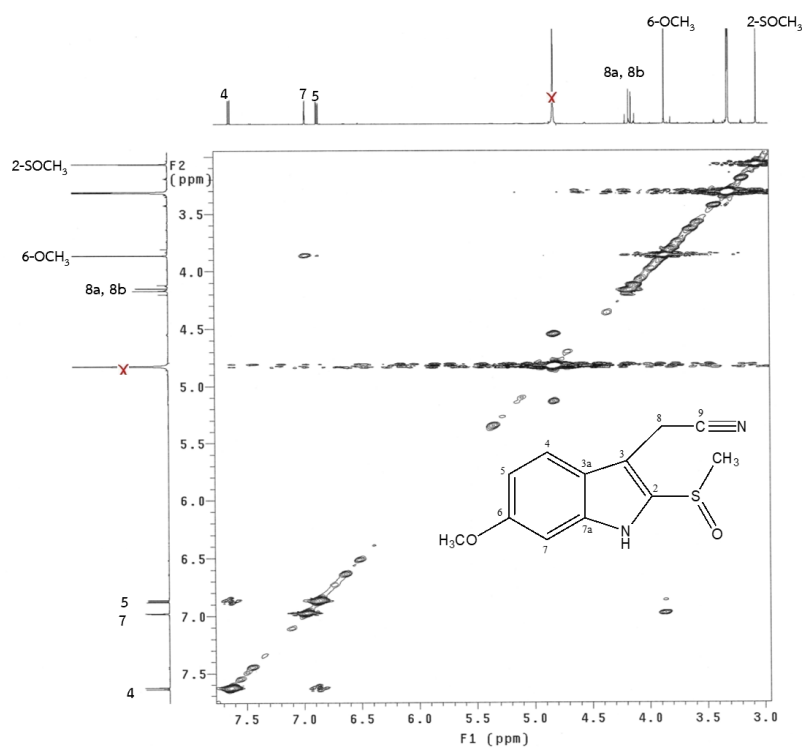
8-2-98-14-4-8

Pulse Sequence: gCOSY

Figure 78. ^1H - ^1H COSY spectrum of compound 7

8-2-98-14-4-8

Pulse Sequence: NOESY

Figure 79. ^1H - ^1H NOESY spectrum of compound 7

4.2.3 Structure elucidation of compound 8 (maeroxime A)

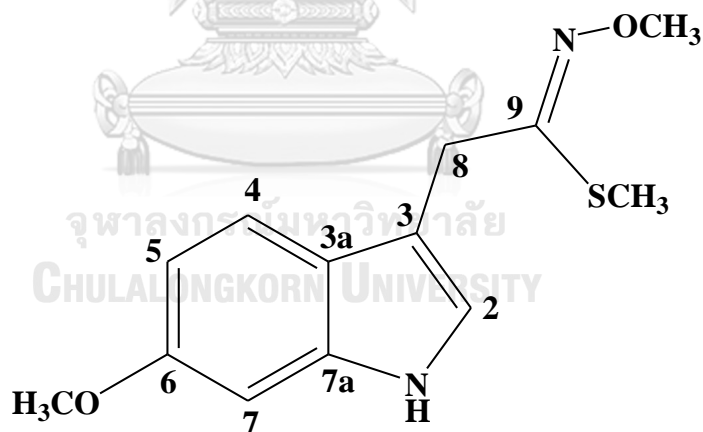
Compound **8** was obtained as a reddish-brown amorphous solid. The molecular formula was determined as $C_{13}H_{16}N_2O_2S$ based on a pseudo-molecular $[M+H]^+$ ion peak observed in its HR-ESI mass spectrum (**Figure 81**) at m/z 265.0999 (calculated for $C_{13}H_{17}N_2O_2S$, 265.1005). This molecular formula suggested a molecule with seven degrees of unsaturation. Its IR spectrum (**Figure 82**) showed absorption bands due to hydroxyl and amine (3370 cm^{-1}), O-methyloxime and aromatic ring (1628 , 1579 and 1457 cm^{-1}). UV absorption maxima of compound **8** were detected at λ_{max} 212, 217, 225 and 269 nm (**Figure 80**).

Its $^1\text{H-NMR}$ data (**Table 11** and **Figure 83-84**) showed an ABX aromatic proton signals, similar to previously discussed indole derivatives at δ_{H} 7.33 (1H, *d*, $J = 8.8$ Hz, H-4), 6.84 (1H, *d*, $J = 2.4$ Hz, H-7) and 6.64 (1H, *dd*, $J = 8.8, 2.4$ Hz, H-5), and also one methoxy proton signal at δ_{H} 3.74 (3H, *s*, 6-OCH₃). In addition, the $^1\text{H NMR}$ spectrum showed resonances of one olefinic methine at δ_{H} 7.03 (1H, *d*, $J = 2.0$ Hz, H-2), one aliphatic methylene at δ_{H} 3.80 (2H, *s*, H-8), another methoxy signal at δ_{H} 3.86 (3H, *s*, N-OCH₃), one methylthio signal at δ_{H} 2.17 (3H, *s*, SCH₃) and one NH broad singlet at δ_{H} 10.72.

In the $^{13}\text{C-NMR}$ spectrum of compound **8** (**Table 11** and **Figure 85**), thirteen carbon signals were observed. They were those of four aromatic and olefinic methines at δ_{C} 123.1 (C-2), 118.9 (C-4), 108.8 (C-5) and 94.5 (C-7), five quaternary carbons at δ_{C} 107.8 (C-3), 121.5 (C-3a), 155.6 (C-6), 136.8 (C-7a) and 157.8 (C-9), one aliphatic methylene at δ_{C} 25.9 (C-8), two methoxy carbons at δ_{C} 61.5 (6-OCH₃) and 55.2 (N-OCH₃), and one methylthio carbon at δ_{C} 12.5.

These NMR data suggested compound **8** could be a 3,6-disubstituted 1*H*-indole derivative, based on a $^1\text{H-}^1\text{H}$ COSY cross peak (**Figure 90**) between signals of NH-1 proton (δ_{H} 10.72) and H-2 (δ_{H} 7.03), as well as $^1\text{H-}^1\text{H}$ NOESY correlations (**Figure 91-92**) between 6-OCH₃ signal with both H-5 (δ_{H} 6.64) and H-7 (δ_{H} 6.84). The indole nucleus is equal to six degrees of unsaturation, hence there should be one double bond in the side chain. A methylene carbon could be connected to position 3, based on $^1\text{H-}^{13}\text{C}$

HMBC cross peaks from proton signal at δ_{H} 3.80 to C-2 (δ_{C} 123.1), C-3 (δ_{C} 107.8) and C-3a (δ_{C} 121.5). The methylene group in the side chain also connected to a quaternary C-9, as evidenced by HMBC correlation from H₂-8 signal to C-9 (δ_{C} 157.8). The methylthio group could also be located at this olefinic carbon of an imine bond, based on three-bond HMBC correlation observed from its proton signal (δ_{H} 2.17) to C-9. Finally, the N-OCH₃ group was placed at the other end of this side chain, completing a methyl-*N*-methoxyethanimidothioate-2-yl substitution at C-3 of the indole nucleus. The NOESY cross peaks were observed between H-8 signal to both H-2 and H-4. The *cis* orientation between the N-OCH₃ and SCH₃ groups was suggested by the most stable conformer due to the lowest relative energy (0.00 kcal/mol) based on a DFT calculation at a B3LYP/6-31g (d,p) level (Figure 93). Thus, the structure of compound **8** was elucidated as methyl (*Z*)-*N*-methoxy-2-(6-methoxy-1*H*-indol-3-yl)ethanimidothioate and trivially named as maeroxime A.



Maeroxime A

Table 11. ^1H -, ^{13}C -NMR and HMBC data of compound **8** (400 MHz, $\text{DMSO-}d_6$)

Position	δ_{H} (mult., J in Hz)	δ_{C}	HMBC correlation with
NH-1	10.72 (<i>br s</i>)	-	C-2, C-3, C-3a, C-7a
2	7.03 (<i>d</i> , 2.0)	123.1	C-3, C-3a, C-7a, C-8
3	-	107.8	-
3a	-	121.5	-
4	7.33 (<i>d</i> , 8.8)	118.9	C-3, C-3a, C-6, C-7a
5	6.64 (<i>dd</i> , 8.8, 2.4)	108.8	C-3a, C-6, C-7
6	-	155.6	-
7	6.84 (<i>d</i> , 2.4)	94.5	C-3a, C-5, C-6, C-7a
7a	-	136.8	-
8	3.80 (<i>s</i>)	25.9	C-2, C-3, C-3a, C-9
9	-	157.8	-
6-OCH ₃	3.74 (<i>s</i>)	55.2	C-6
SCH ₃	2.17 (<i>s</i>)	12.5	C-9
N-OCH ₃	3.85 (<i>s</i>)	61.5	-



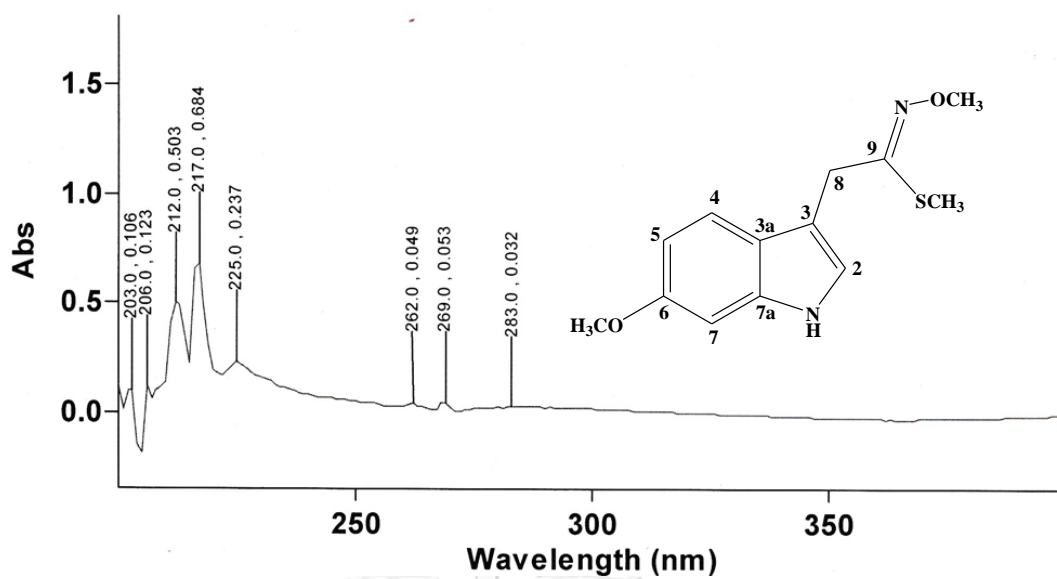


Figure 80. UV spectrum of compound 8

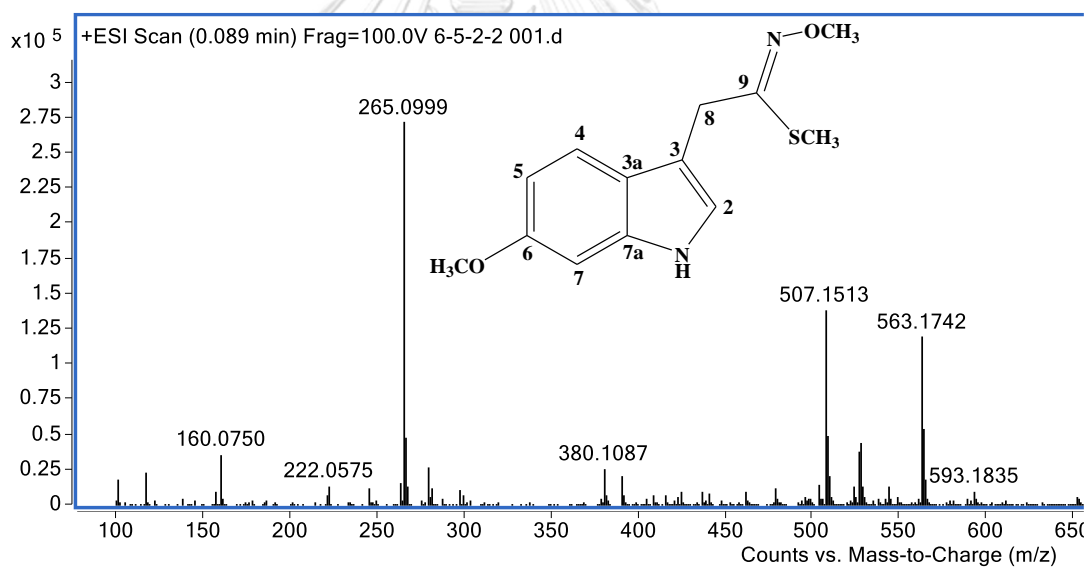
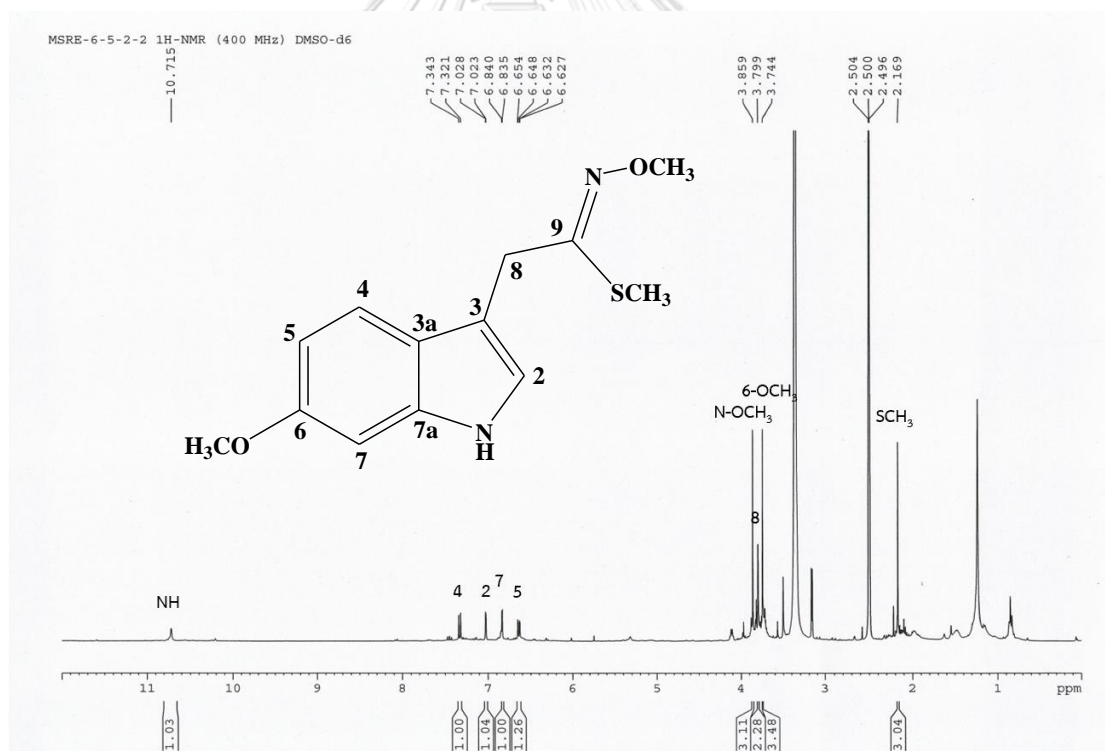
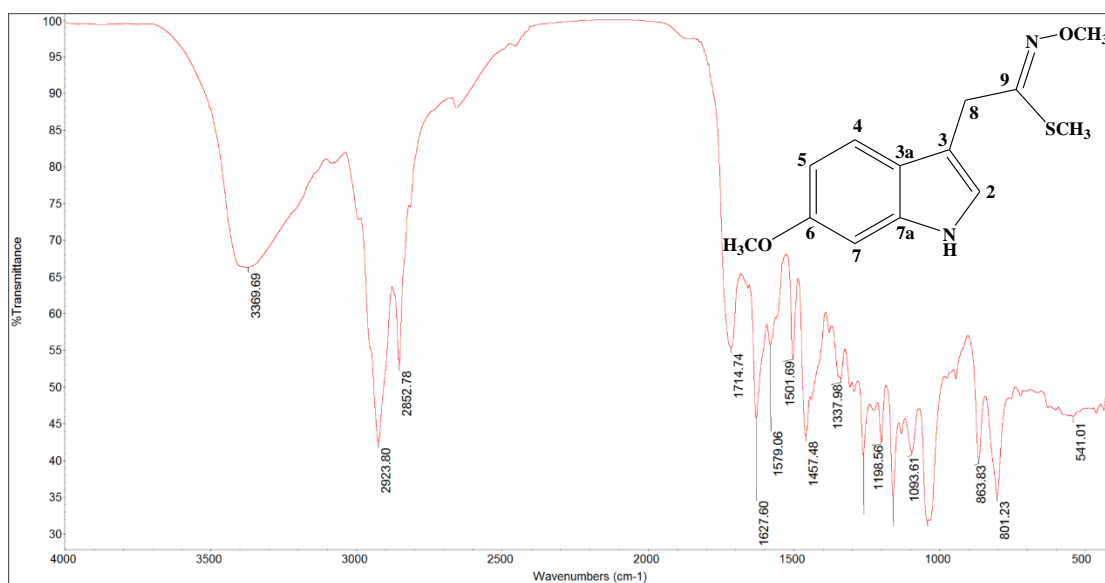


Figure 81. HR-ESI mass spectrum of compound 8



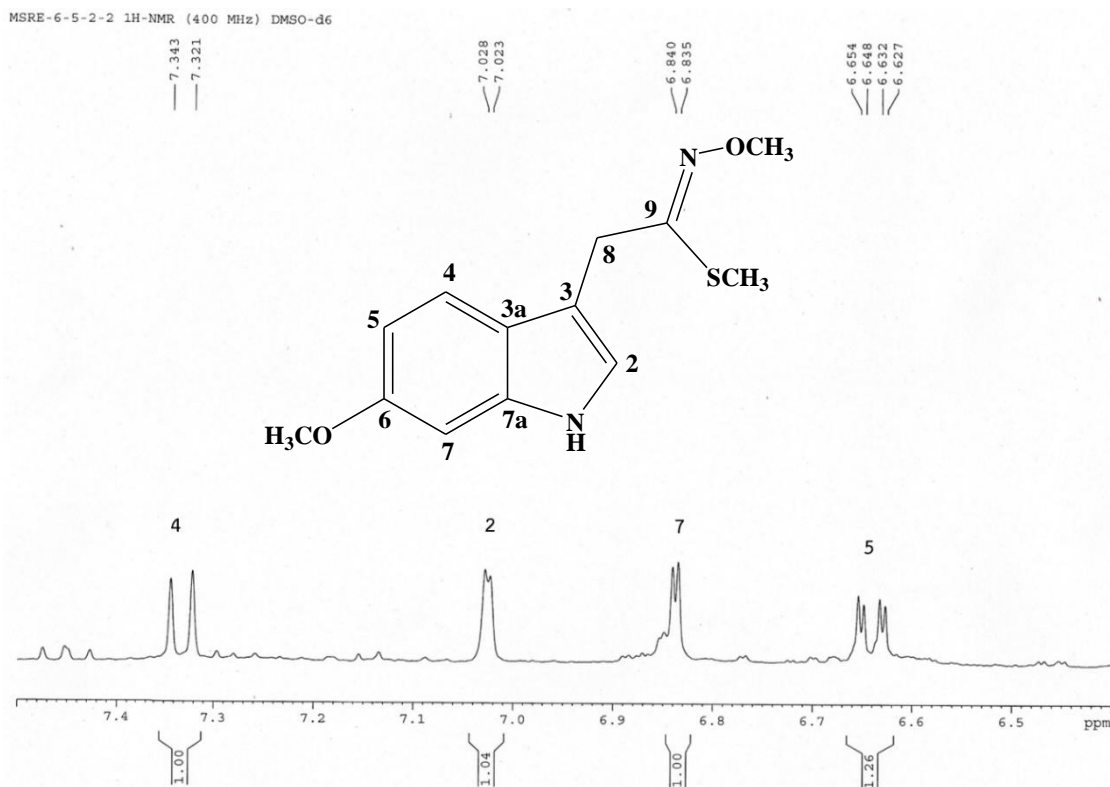


Figure 84. $^1\text{H-NMR}$ spectrum of compound **8** (expansion between δ_{H} 6.4-7.5 ppm)

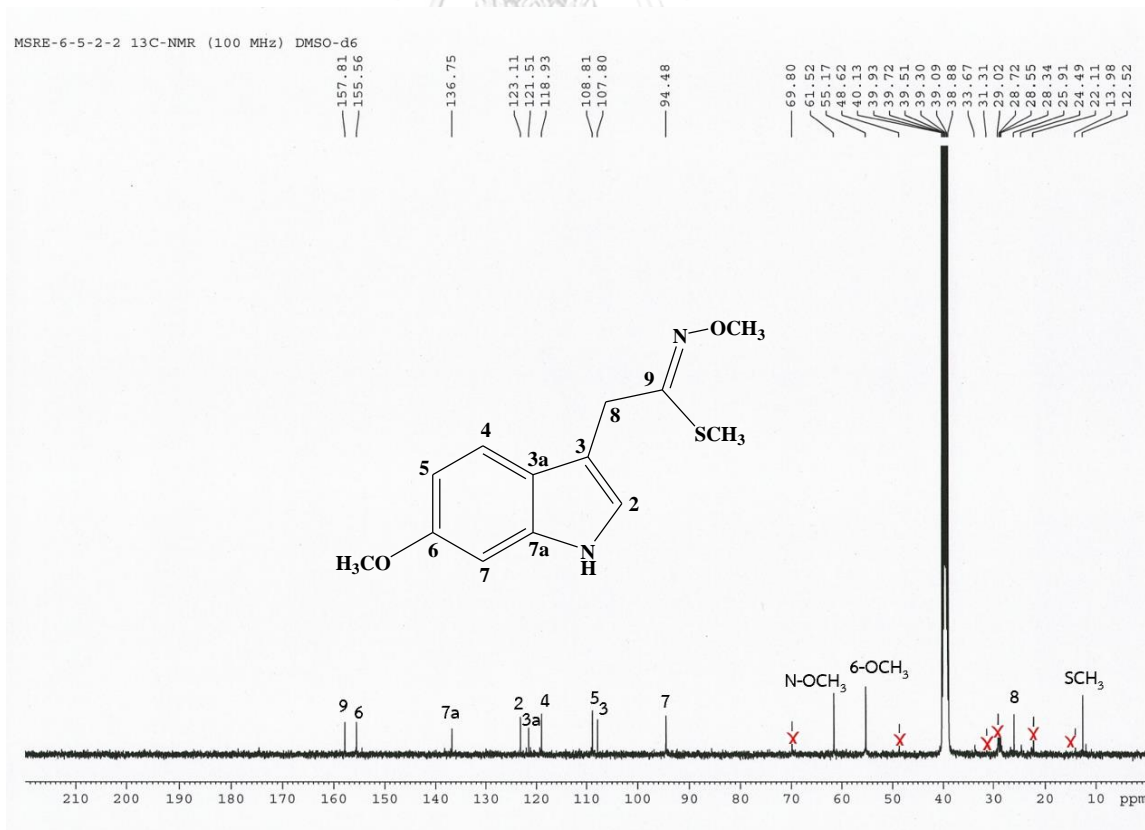
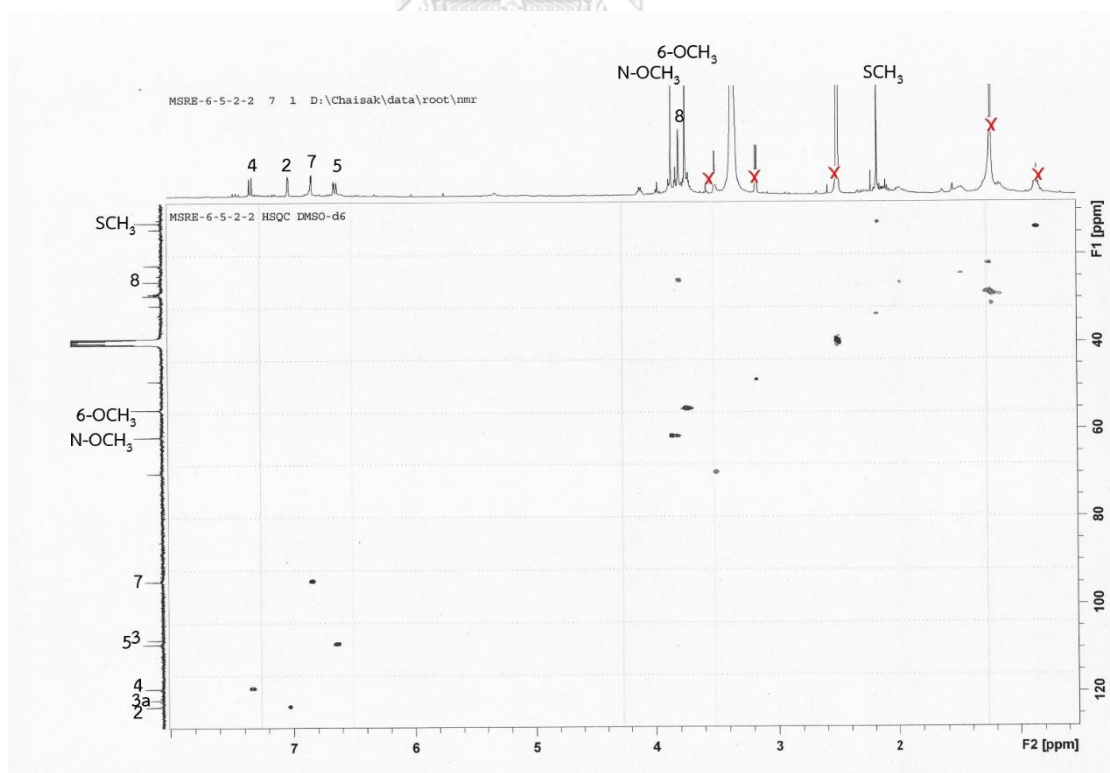
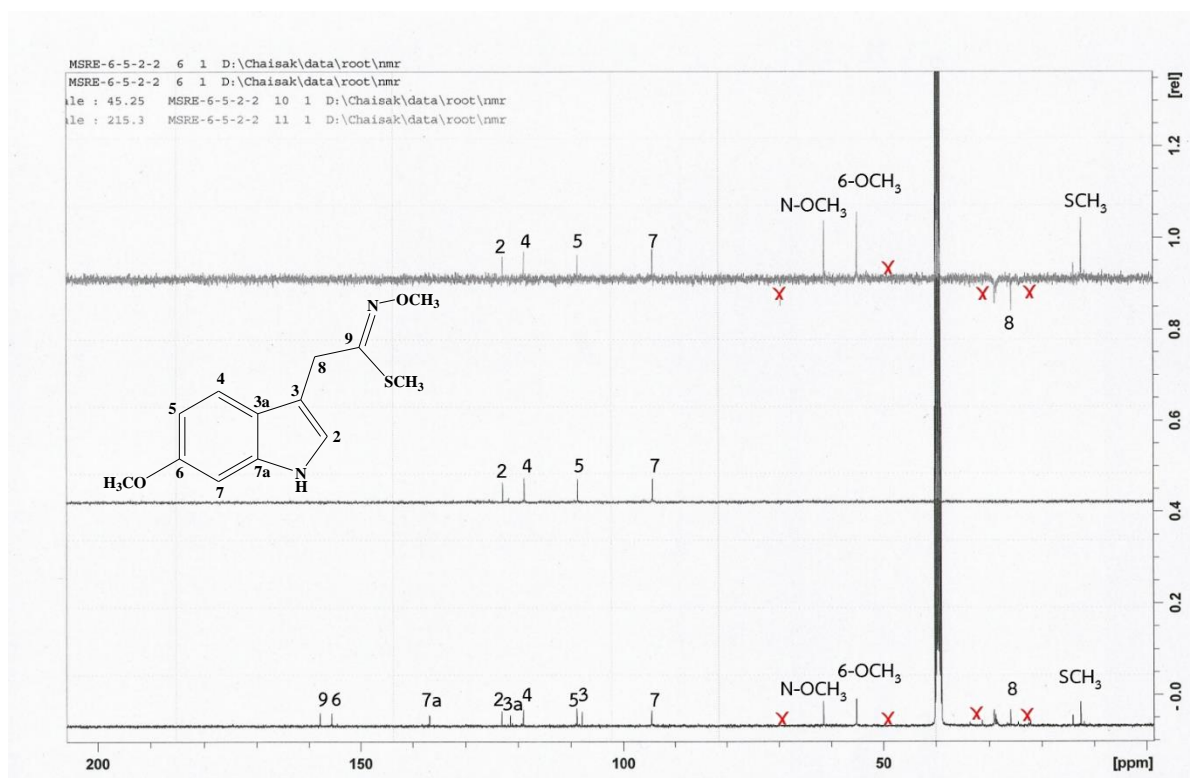


Figure 85. $^{13}\text{C-NMR}$ spectrum of compound **8** (400 MHz, DMSO- d_6)



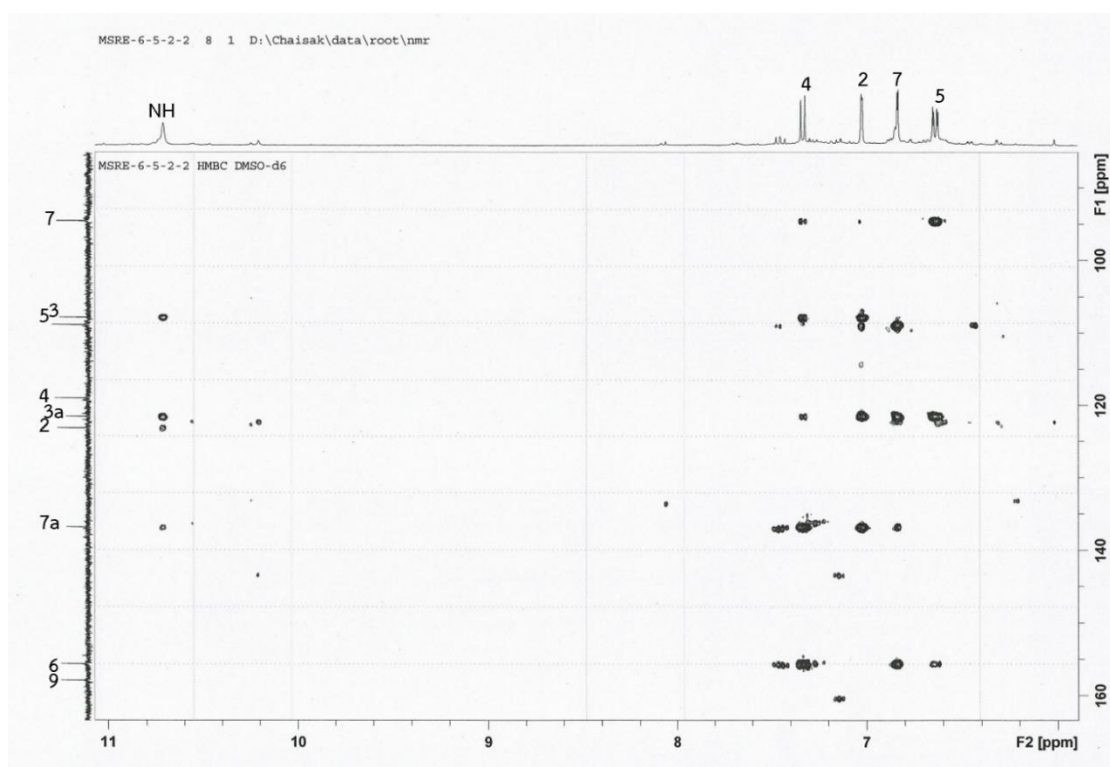


Figure 88. ^1H - ^{13}C HMBC spectrum of compound 8

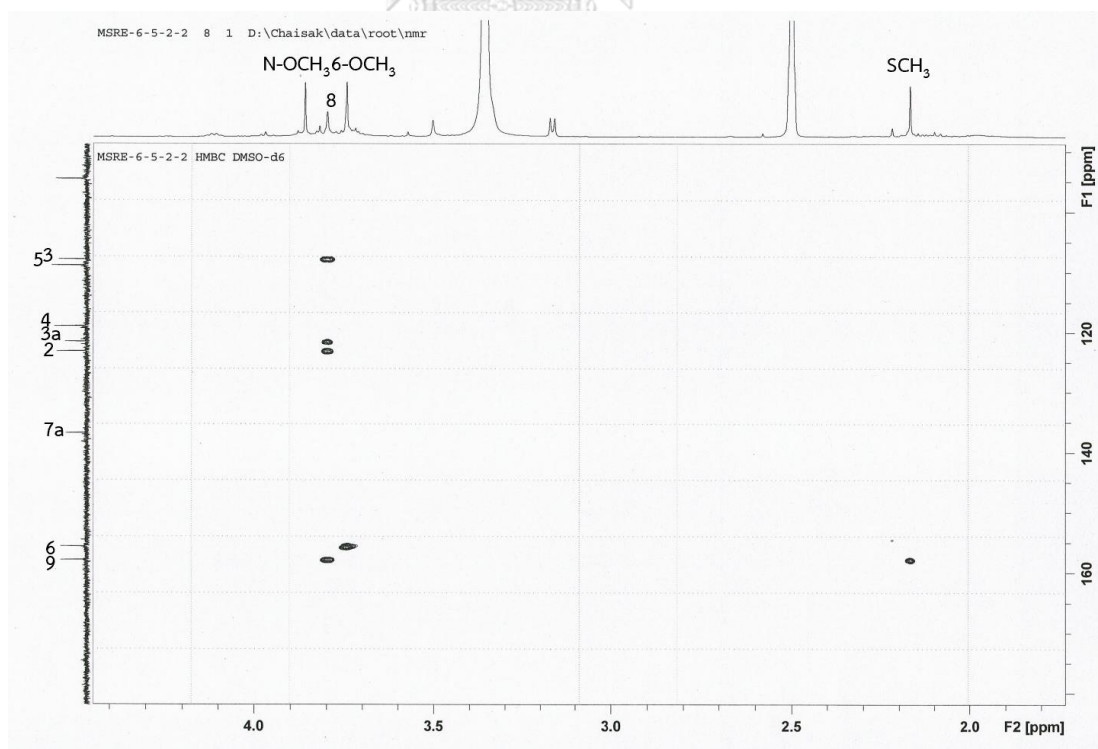
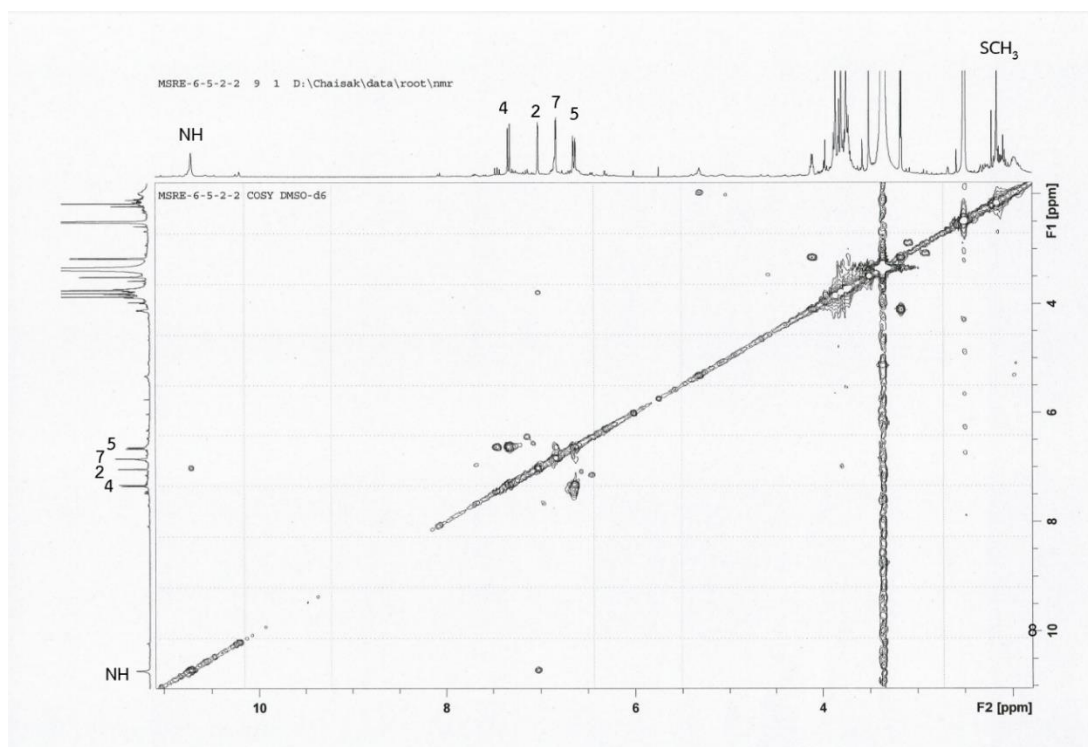
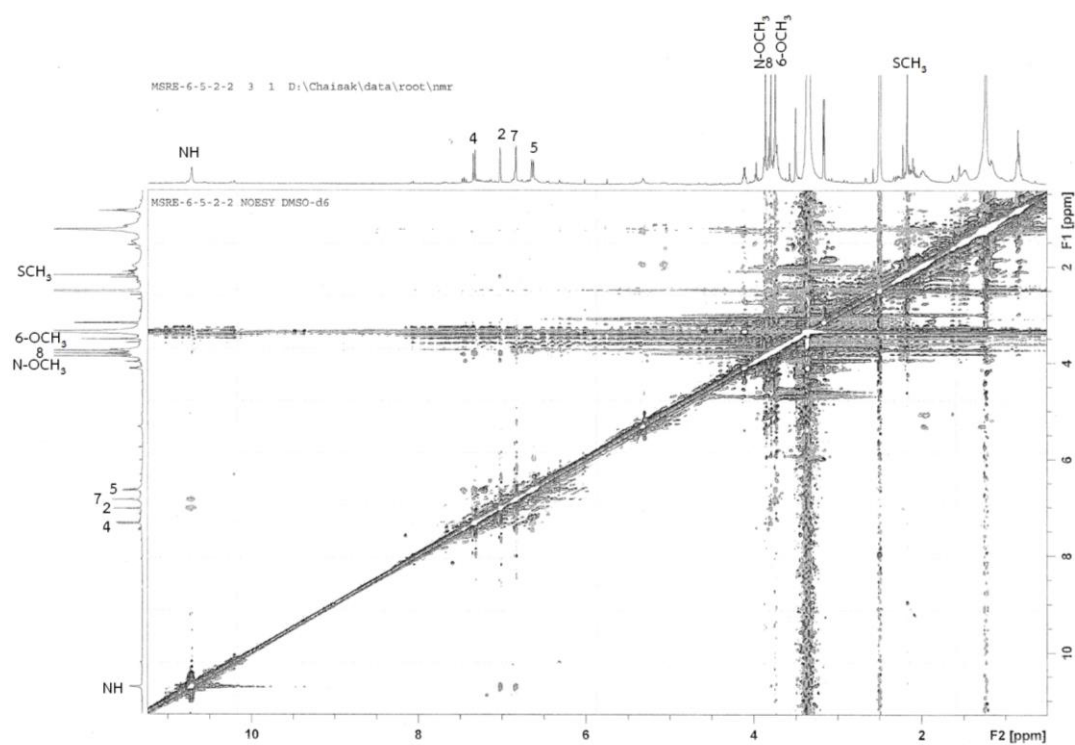


Figure 89. ^1H - ^{13}C HMBC spectrum of compound 8
(expansion between δ_{H} 1.8-4.4 ppm, δ_{C} 90-180 ppm)

Figure 90. ¹H-¹H COSY spectrum of compound 8Figure 91. ¹H-¹H NOESY spectrum of compound 8

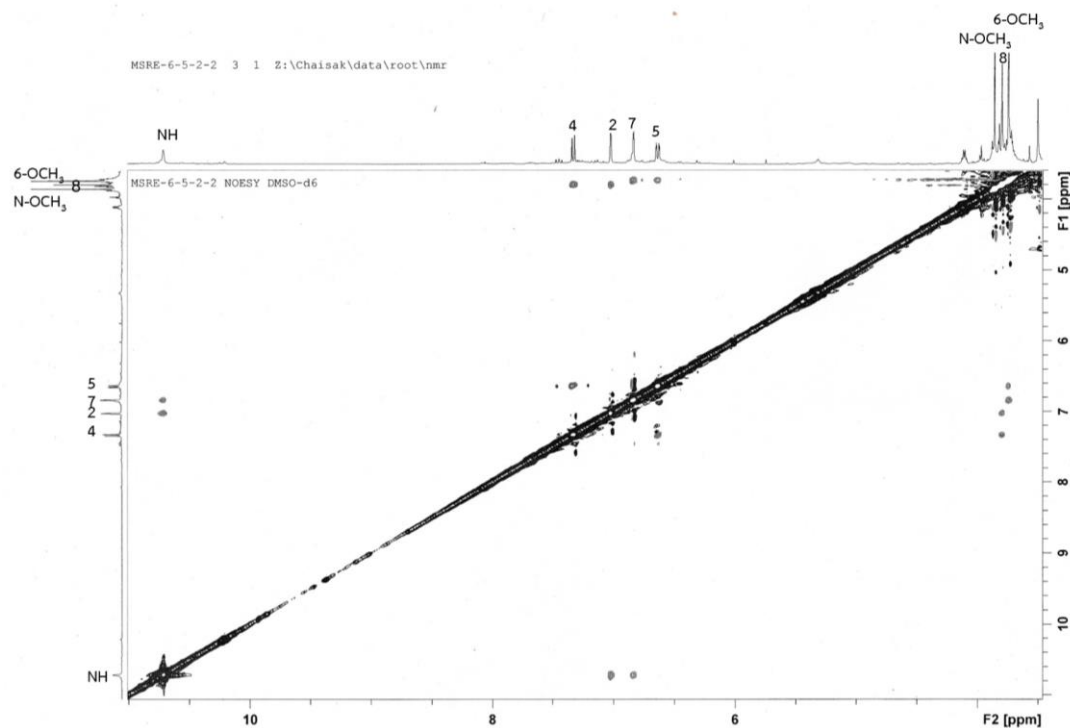


Figure 92. ^1H - ^1H NOESY spectrum of compound **8**
(expansion between δ_{H} 3.5-10.5 ppm)

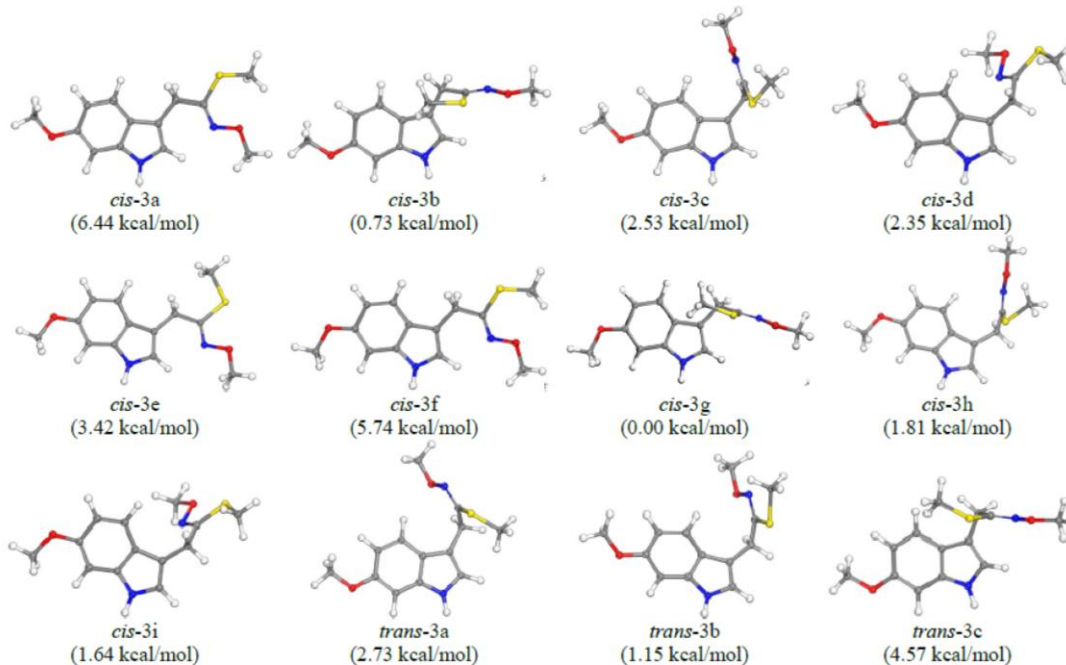


Figure 93. Possible conformations of compound **8**, based on the DFT calculation at B3LYP/6-31g (d, p) level

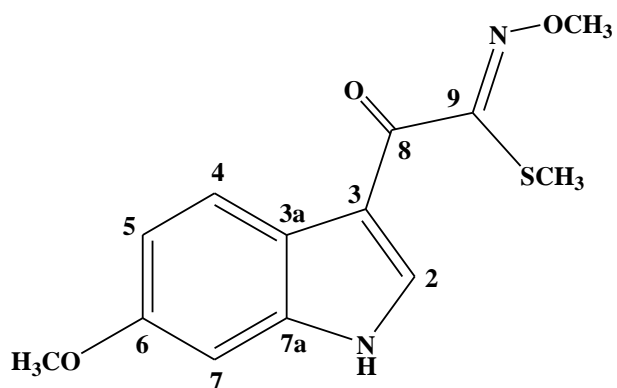
4.2.4 Structure elucidation of compound 9 (maeroxime B)

Compound **9** was obtained as an orange-brown amorphous solid. Its molecular formula was established as $C_{13}H_{14}N_2O_3S$, according to the $[M+H]^+$ ion at m/z 279.0782 (Calculated for $C_{13}H_{15}N_2O_3S$, 279.0803) (Figure 96), revealing more than 14 mass units compared to that of compound **7**. Its IR absorption peaks IR (Figure 95) were similar to those of compounds **8** except a carbonyl peak at 1617 cm^{-1} . UV absorption were detected at λ_{max} 212, 280 and 314 nm (Figure 94).

The $^1\text{H-NMR}$ data (Table 12, Figure 97) showed ABX coupled protons at δ_{H} 7.92 (1H, *d*, $J=8.4\text{ Hz}$, H-4), 7.00 (1H, *s*, H-7) and 6.89 (1H, *d*, $J=8.4\text{ Hz}$, H-5), one methine proton at δ_{H} 7.97 (1H, *s*, H-2), two methoxy groups at δ_{H} 3.79 (3H, *s*, 6-OCH₃) and 3.73 (3H, *s*, N-OCH₃), one methylthio signal at δ_{H} 2.43 (3H, *s*, SCH₃) and one NH proton at δ_{H} 12.10 (1H, *br s*, NH-1).

In $^{13}\text{C-NMR}$ spectrum (Figure 98), thirteen signals represented four methines [δ_{C} 136.7 (C-2), 121.4 (C-4), 112.3 (C-5) and 95.8 (C-7)], six quaternary carbons [δ_{C} 113.6 (C-3), 118.5 (C-3a), 156.9 (C-6), 138.0 (C-7a), 182.5 (C-8), 155.9 (C-9)] and three methyl carbons [δ_{C} 55.3 (6-OCH₃), 61.9 (N-OCH₃) and 12.7 (SCH₃)]. Together with $^1\text{H-}^1\text{H}$ NOESY cross peaks of NH-1 with H-2 and H-7, the $^1\text{H-}$ and $^{13}\text{C-NMR}$ data indicated the structure of compound **9** could be 3,6-disubstituted 1*H*-indole ring as similar with compound **8**, except the presence of carbonyl carbon at δ_{C} 182.5 (C-8). In addition, $^1\text{H-}^{13}\text{C}$ HMBC cross peaks of H-2 to C-3 and C-8, and of SCH₃ to C-9 supported the substitution of 2-oxoethanimidothioate at C-3.

The computational studies suggested that N-methoxy was connected with imine bond as *cis* direction regarding to SCH₃ due to its lowest energy conformation of compound **9** (Figure 104). Thus, the compound **9** was established as methyl (*Z*)-*N*-methoxy-2-(6-methoxy-1*H*-indol-3-yl)-2-oxoethanimidothioate and was named as maeroxime B.



Maeroxime B

Table 12. ^1H -, ^{13}C -NMR and HMBC data of compound **9** (400 MHz, $\text{DMSO-}d_6$)

Position	Compound 9		
	δ_{H} (mult., J in Hz)	δ_{C}	HMBC correlation with
NH-1	12.10, (<i>br s</i>)		-
2	7.97, (<i>s</i>)	136.7	C-3, C-3a, C-7a, C-8
3	-	113.6	-
3a	-	118.5	-
4	7.92 (<i>d</i> , 8.4)	121.4	C-3, C-6, C-7a
5	6.89 (<i>d</i> , 8.4)	112.3	C-3a, C-6, C-7
6		156.9	-
7	7.00, (<i>s</i>)	95.8	C-3a, C-5, C-6, C-7a
7a	-	138.0	-
8	-	182.5	-
9	-	155.9	-
6-OCH ₃	3.79, (<i>s</i>)	55.3	C-6
SCH ₃	2.43, (<i>s</i>)	12.7	C-9
N-OCH ₃	3.73, (<i>s</i>)	61.9	-

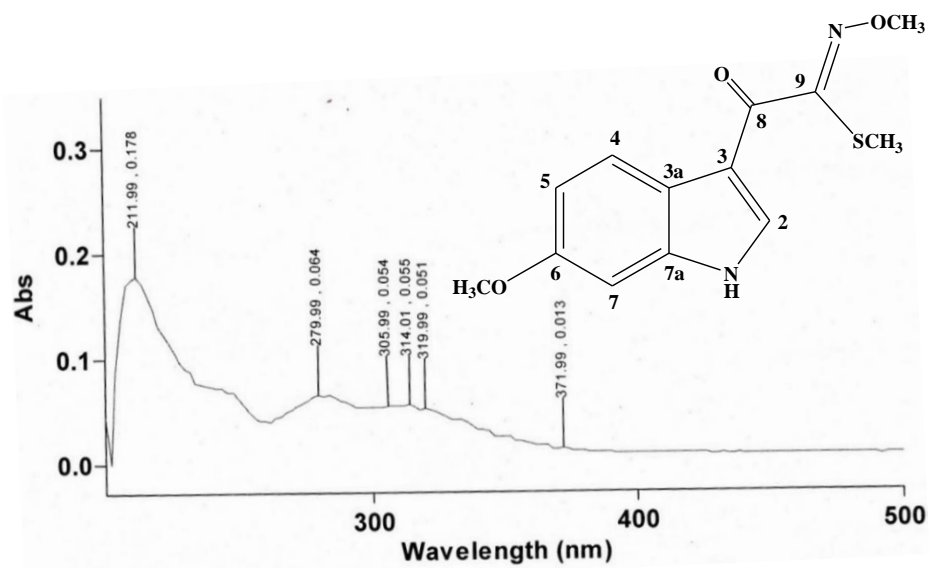


Figure 94. UV spectrum of compound 9

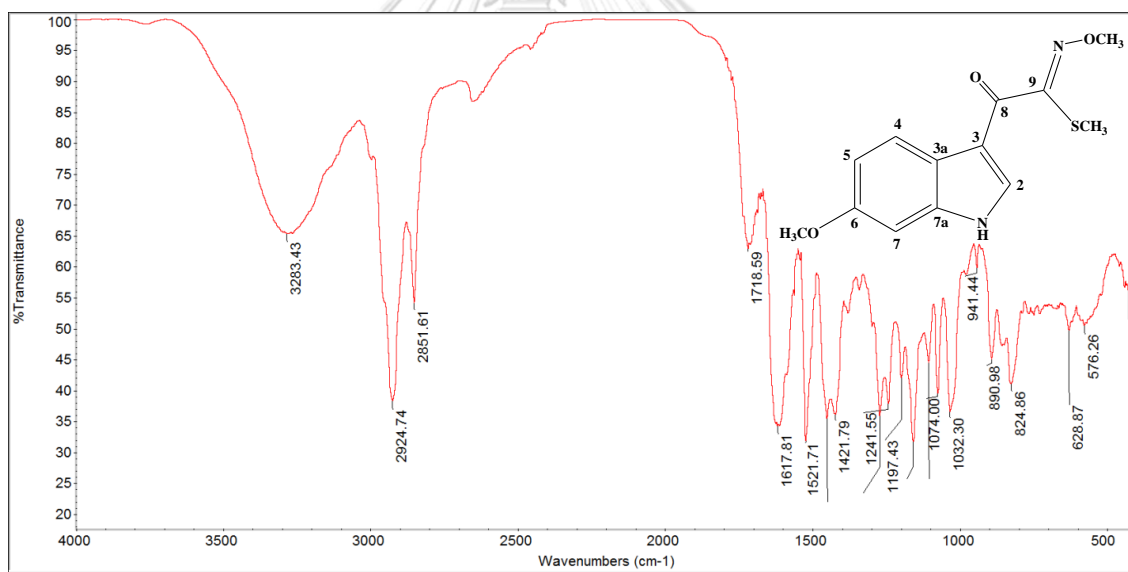


Figure 95. IR spectrum of compound 9

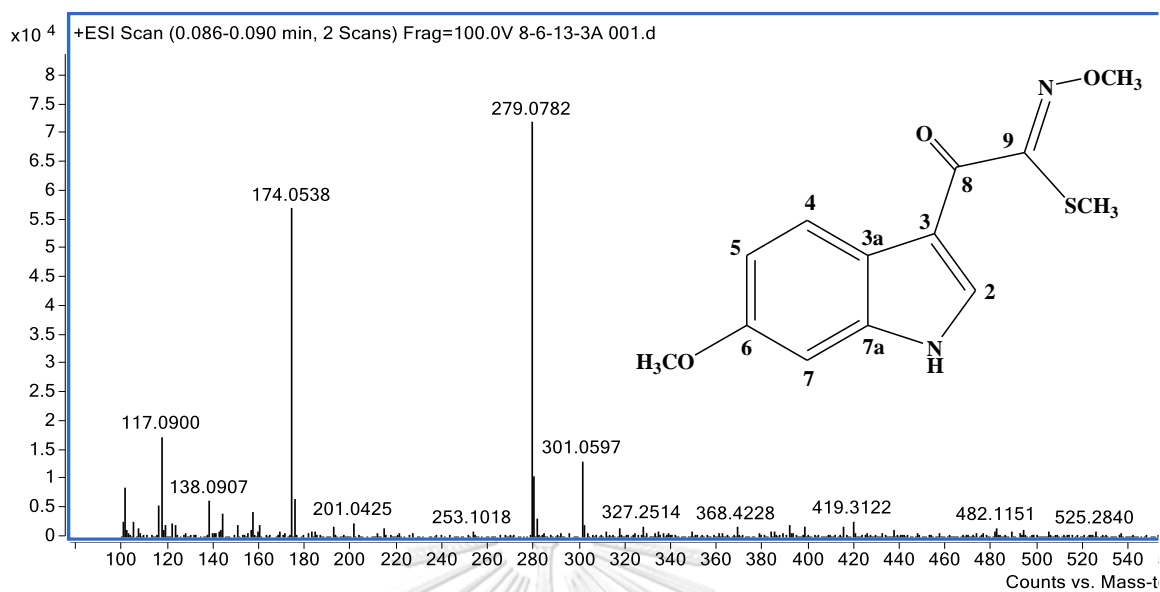
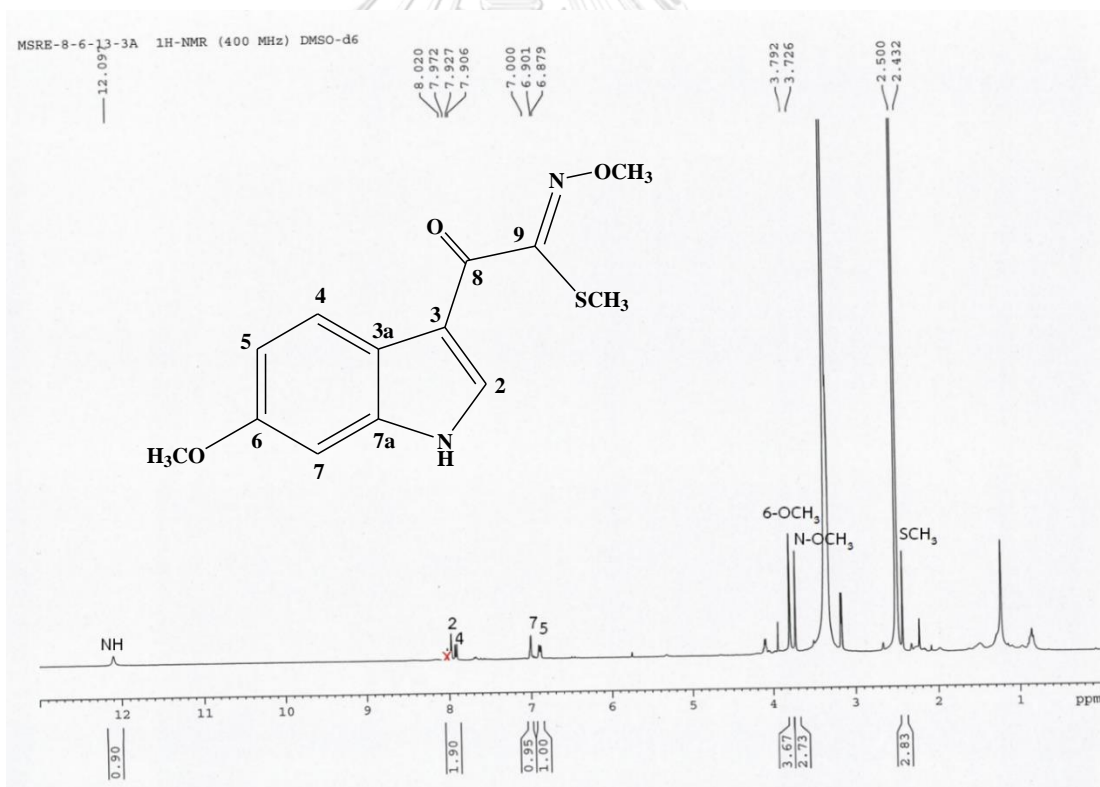


Figure 96. HR-ESI mass spectrum of compound 9

Figure 97. ¹H-NMR spectrum of compound 9 (100 MHz, DMSO-d₆)

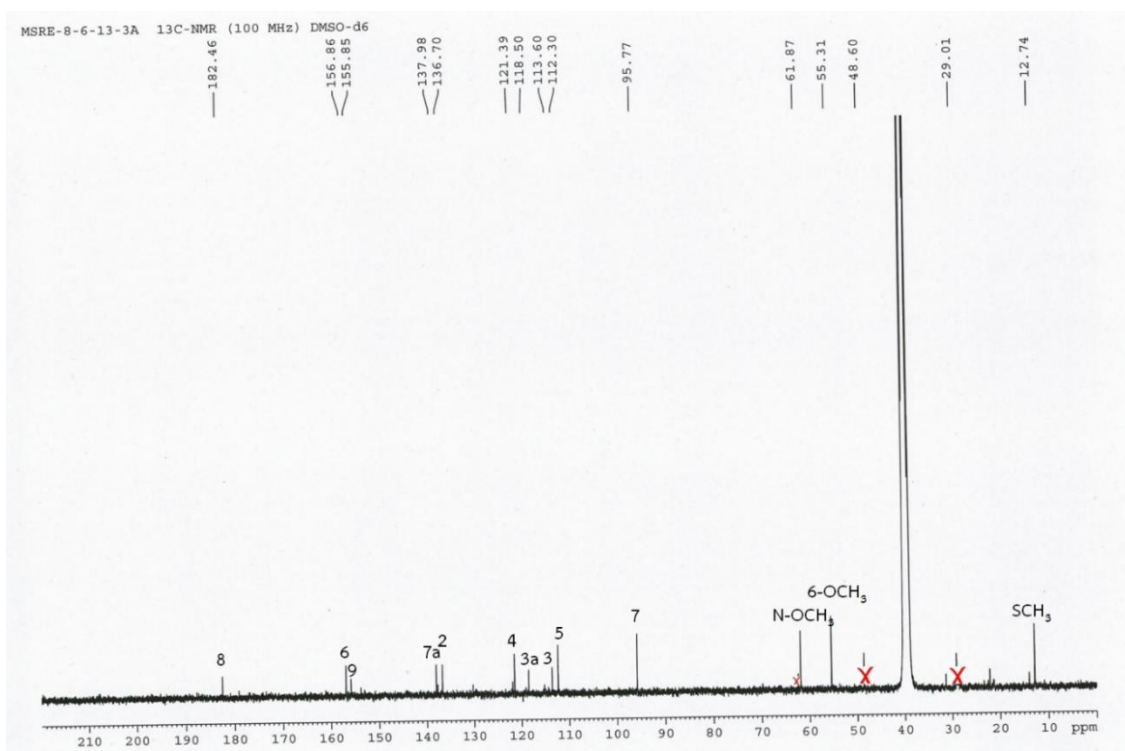


Figure 98. ^{13}C -NMR spectrum of compound **9** (100 MHz, $\text{DMSO-}d_6$)

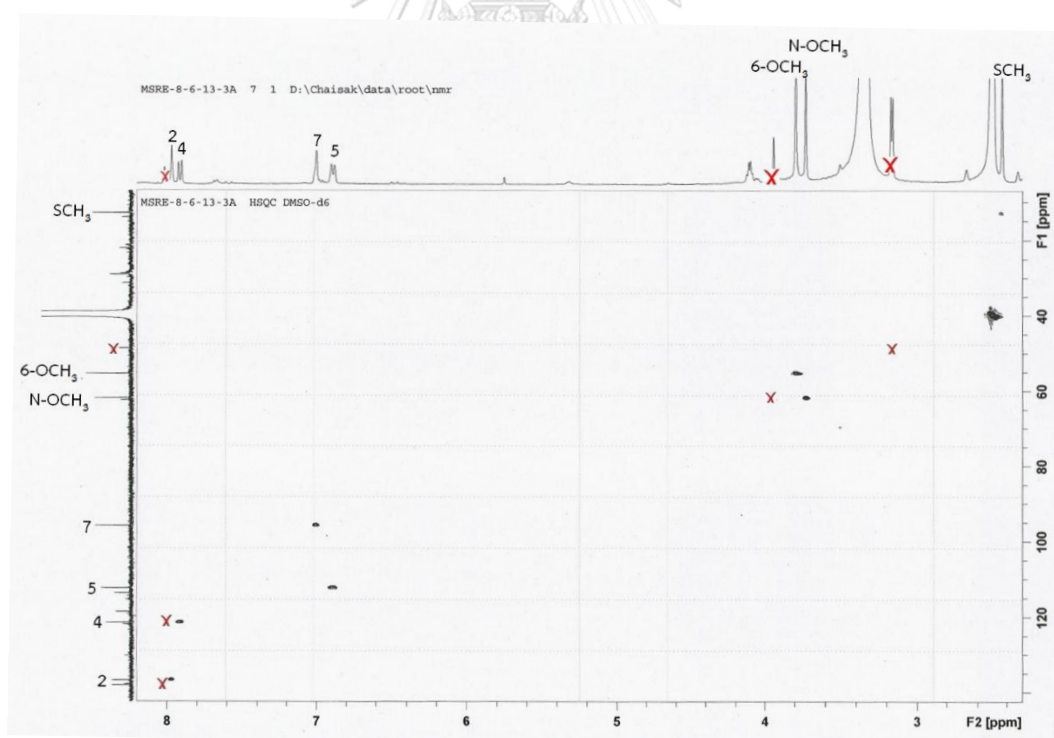


Figure 99. ^1H - ^{13}C HSQC spectrum of compound **9**

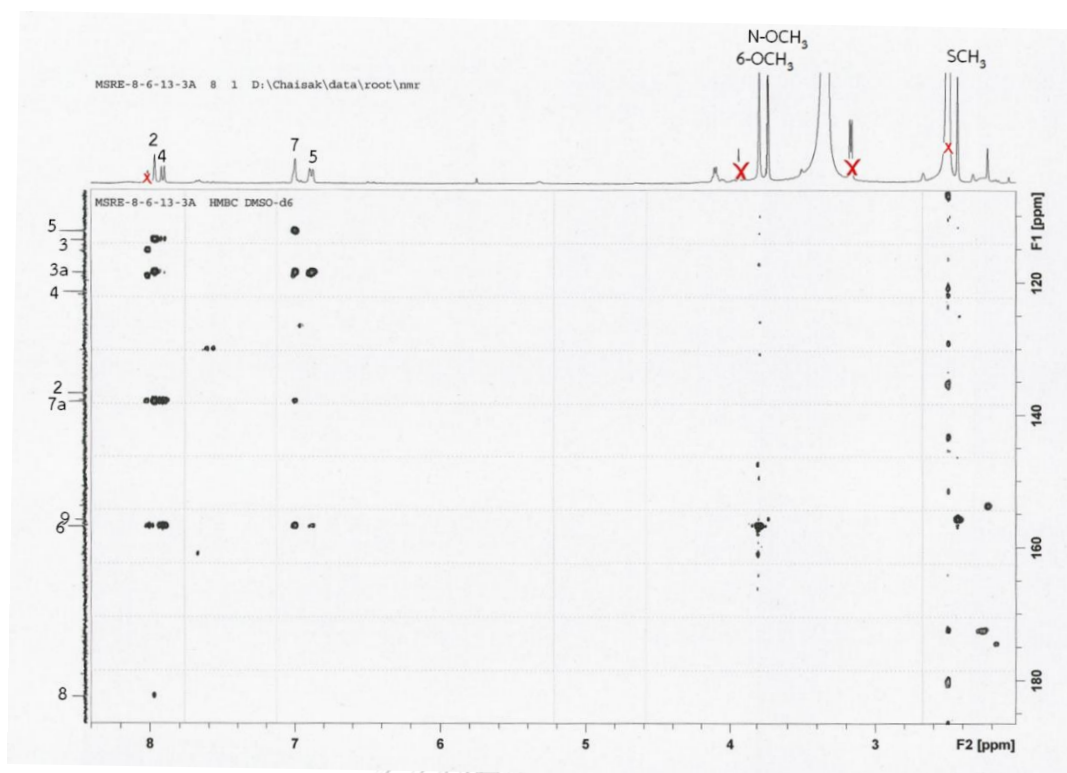


Figure 100. ^1H - ^{13}C HMBC spectrum of compound 9
(expansion between δ_{H} 2.0-8.4 ppm, δ_{C} 100-180 ppm)

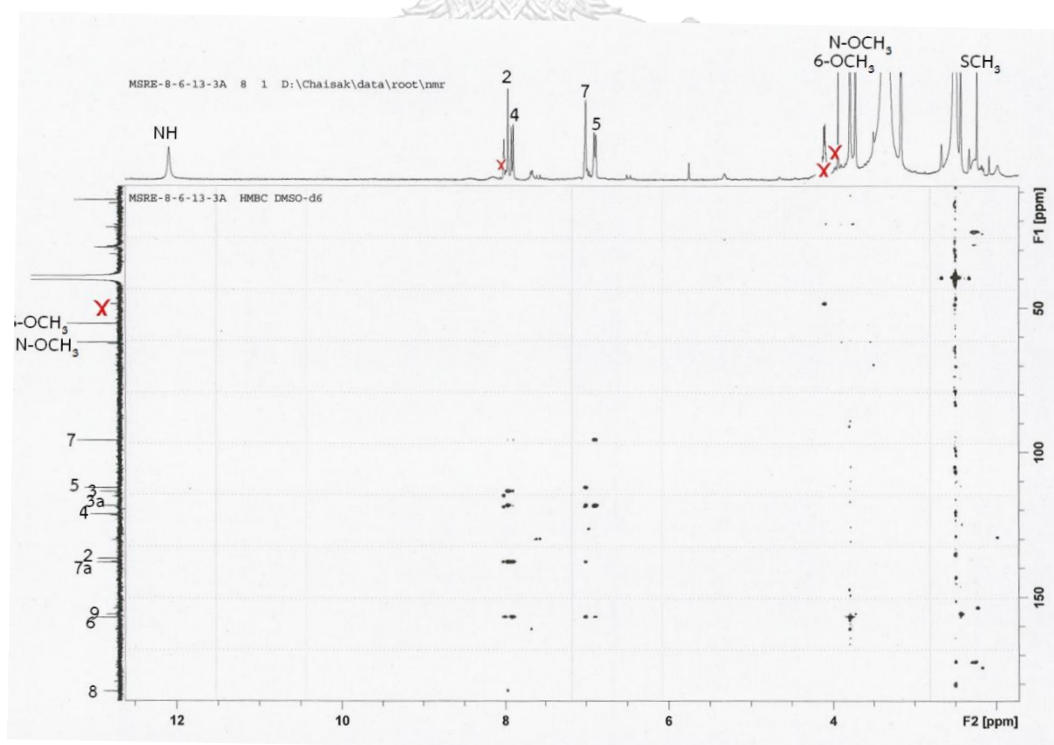


Figure 101. ^1H - ^{13}C HMBC spectrum of compound 9

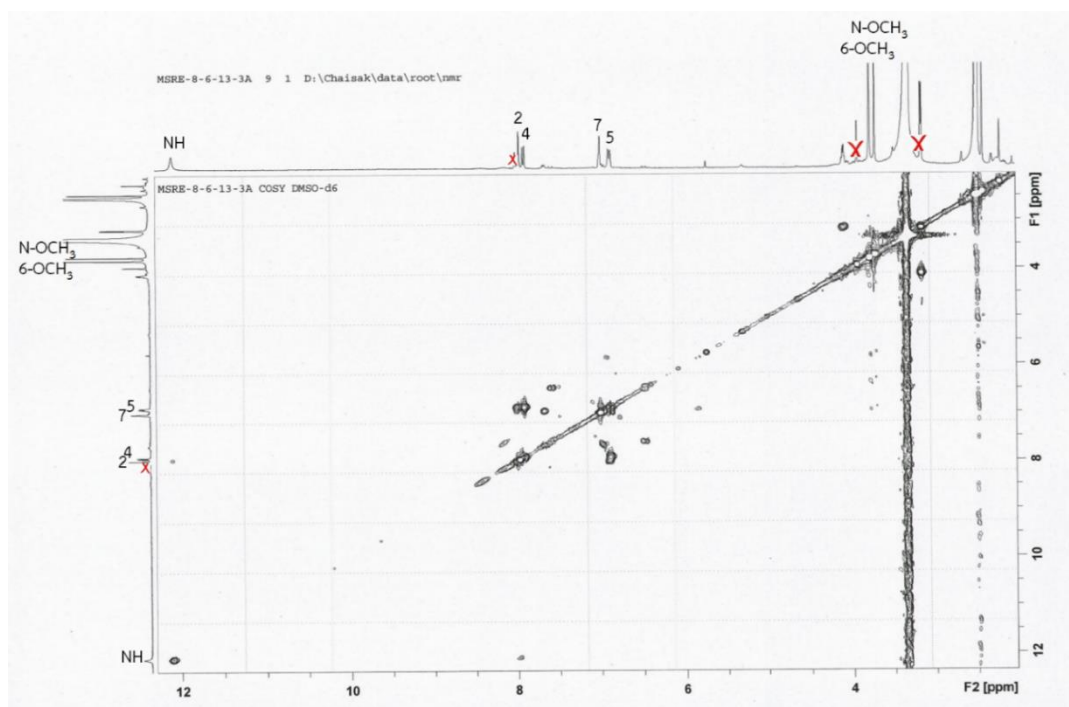


Figure 102. ^1H - ^1H COSY spectrum of compound 9

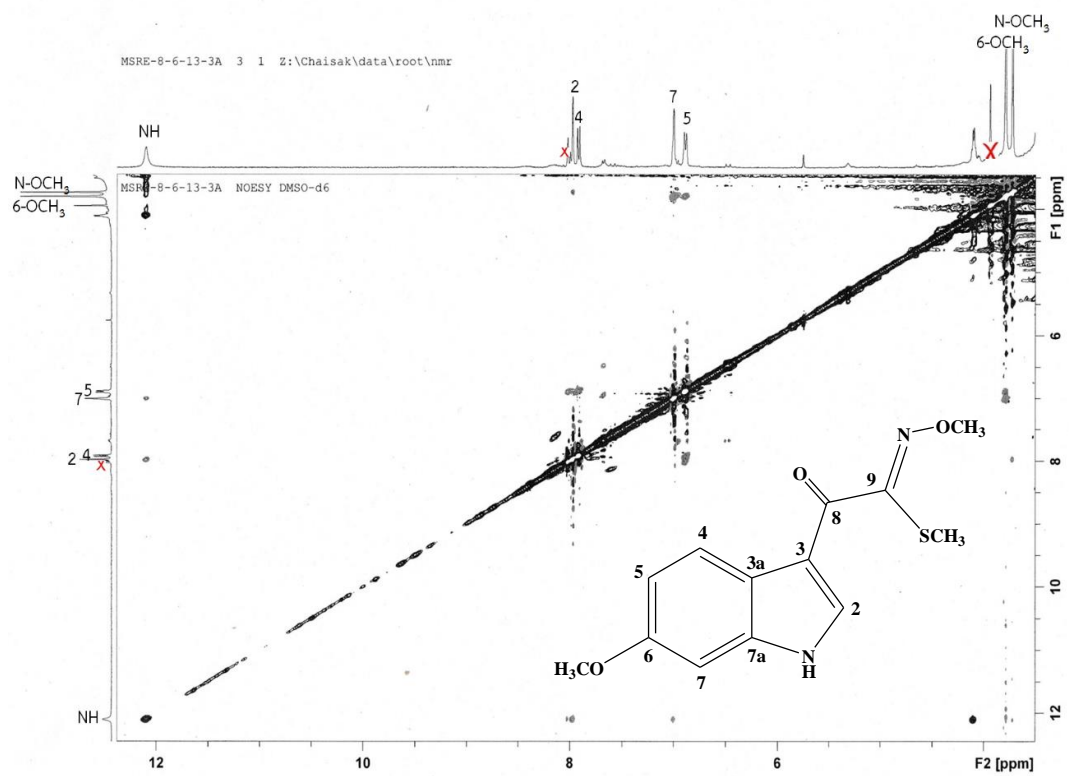


Figure 103. ^1H - ^1H NOESY spectrum of compound 9

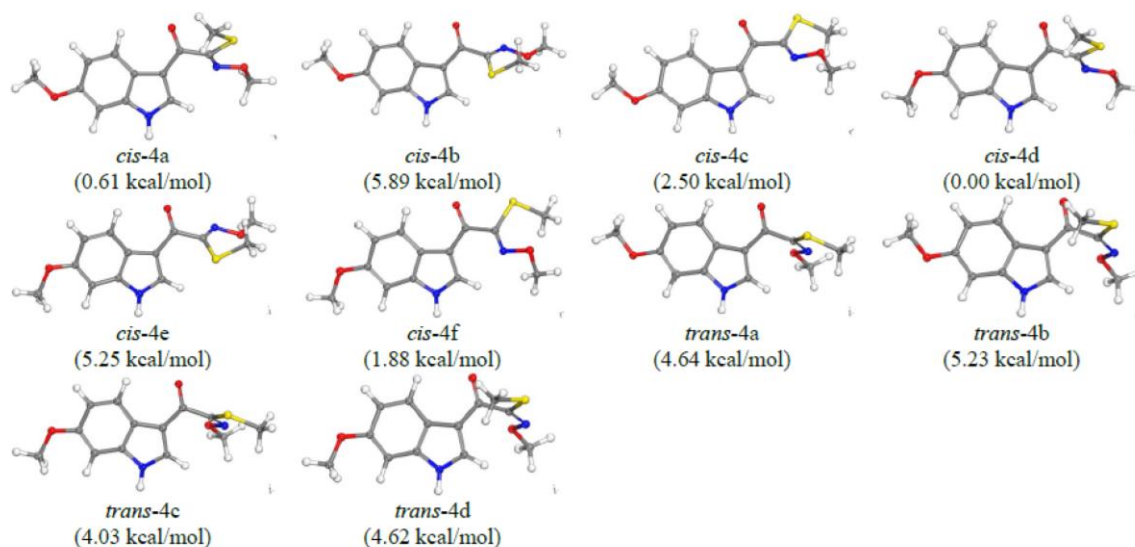


Figure 104. Possible conformations of compound **9**, based on the DFT calculation at B3LYP/6-31g (d, p) level

4.2.5 Structure elucidation of compound **10** (maeroxime **C**)

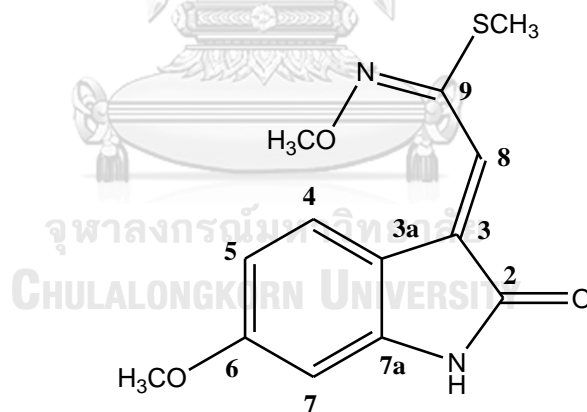
Compound **10** was obtained as a yellow amorphous solid. Its molecular formula was deduced as $C_{13}H_{14}N_2O_3S$ (eight degrees of unsaturation), based on a pseudo-molecular $[M+H]^+$ ion peak observed at m/z 279.0780 (calculated for $C_{13}H_{15}N_2O_3S$, 279.0803) in the HR-ESI mass spectrum (**Figure 106**). Therefore, this compound was a structural isomer of compound **9**. Its major IR absorption bands (**Figure 107**) were observed at 3307 and 1729 cm^{-1} and UV absorption maxima (**Figure 105**) were detected at λ_{max} 208, 272 and 316 nm. These data are characteristic of oxindole moiety, similar to compound **6**.

The 1H -NMR data of compound **10** (**Table 13** and **Figure 108**) showed ABX proton system at δ_H 7.87 (1H, *d*, $J = 8.4$ Hz, H-4), 6.41 (1H, *d*, $J = 2.4$ Hz, H-7) and 6.52 (1H, *dd*, $J = 8.4, 2.4$ Hz, H-5), one olefinic methine proton at δ_H 6.80 (1H, *s*, H-8), two methoxy protons at δ_H 3.78 (3H, *s*, 6-OCH₃) and 4.00 (3H, *s*, N-OCH₃), one methylthio signal at δ_H 2.35 (3H, *s*, SCH₃) and one NH broad singlet at δ_H 10.63.

Its ^{13}C -NMR spectrum (**Table 13** and **Figure 109**) displayed thirteen carbon resonances representing an amide carbonyl at δ_C 168.6 (C-2), four aromatic and olefinic

methines at δ_C 126.5 (C-4), 106.8 (C-5), 96.6 (C-7) and 119.9 (C-8), five quaternary carbons at δ_C 131.1 (C-3), 113.3 (C-3a), 162.2 (C-6), 145.6 (C-7a) and 150.8 (C-9), two methoxy carbons at δ_C 55.5 (6-OCH₃) and 62.5 (N-OCH₃), and one methylthio carbon at δ_C 12.6 (SCH₃).

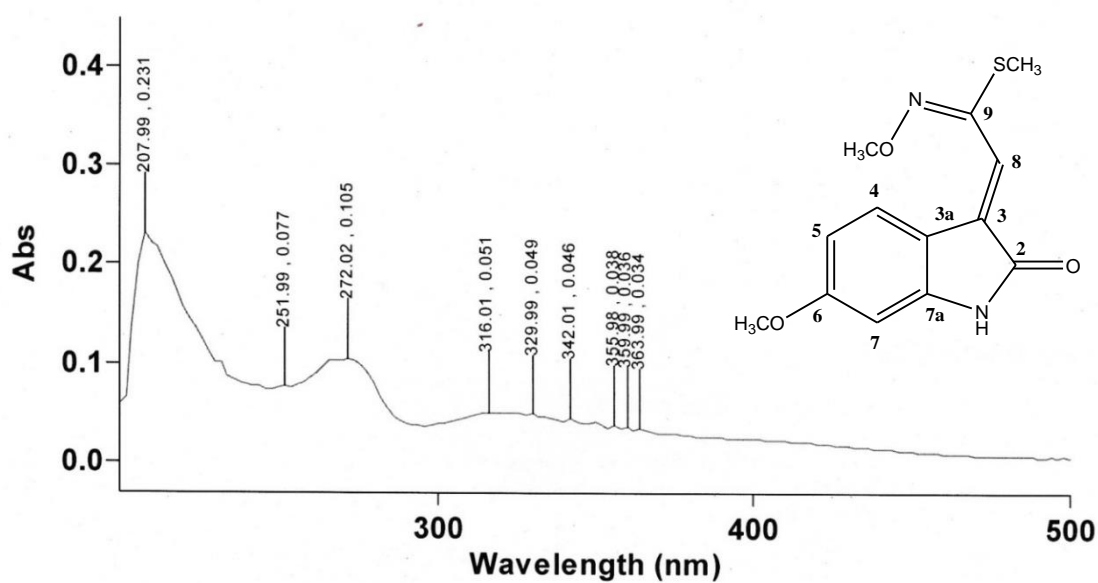
Its oxindole characteristic indicated that position 2 of this 3,6-disubstituted 1*H*-oxindole nucleus should be the amide carbonyl function, hence a double bond was placed to between positions 3 and 8. This was confirmed by ¹H-¹³C HMBC correlations (**Figure 111**) observed from H-8 to C-2, C-3, C-3a and C-9. Other substituents were located the same positions as compound **9**. The *trans, trans* geometric isomer was introduced by the ¹H-¹H NOESY cross peaks of H-4 and N-OCH₃, and of H-8 and SCH₃, together with the lowest energy data from computational analysis (**Figure 113** and **114**). Therefore, the chemical structure of compound **10** was determined as (*E*)-*N*-methoxy-2-((*E*)-6-methoxy-2-oxindolin-3-ylidene) ethanimidothiolate and trivially named maeroxime C.

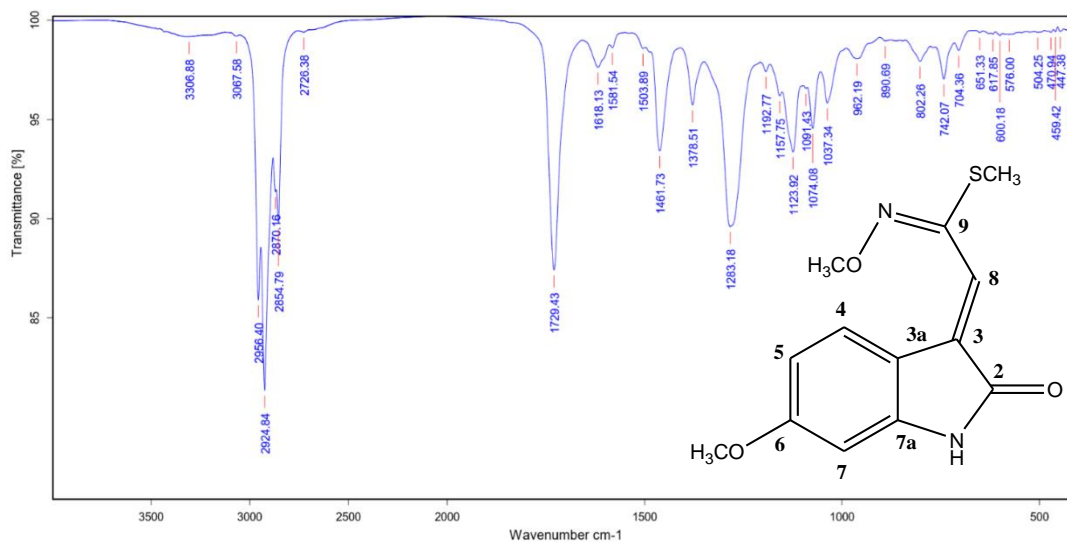
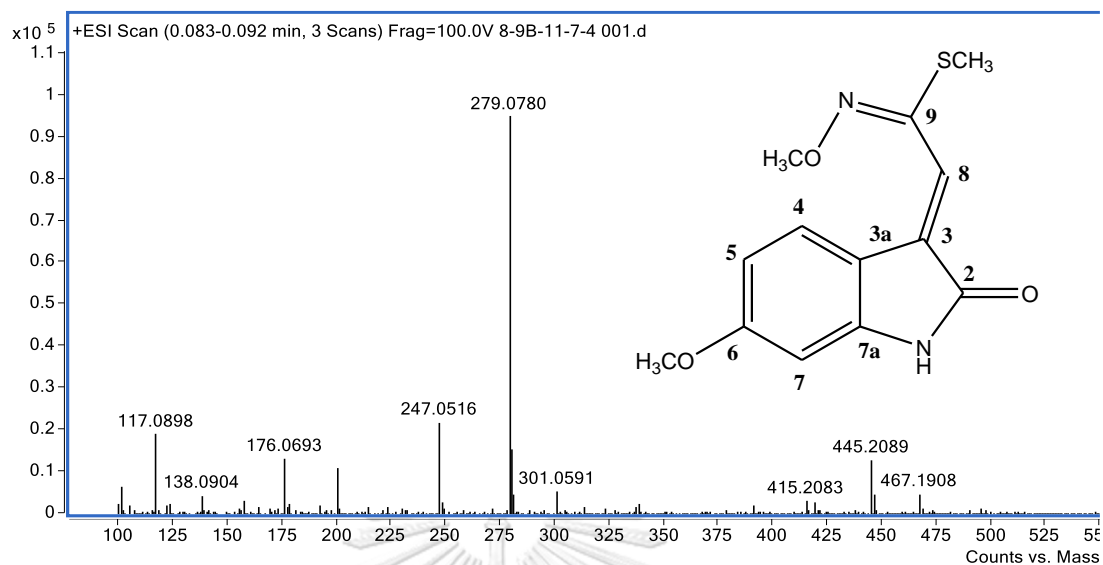


Maeroxime C

Table 13. ^1H -, ^{13}C -NMR and HMBC data of compound **10** (400 MHz, $\text{DMSO-}d_6$)

Position	δ_{H} (mult., J in Hz)	δ_{C}	HMBC correlation with
NH-1	10.63 (<i>br s</i>)	-	C-2, C-3, C-3a, C-7a
2	-	168.6	-
3	-	131.1	-
3a	-	113.3	-
4	7.87 (<i>d</i> , 8.4)	126.5	C-3, C-5, C-6, C-7a
5	6.52 (<i>dd</i> , 8.4, 2.4)	106.8	C-3a, C-6, C-7
6	-	162.2	-
7	6.41 (<i>d</i> , 2.4)	96.6	C-3a, C-5, C-6, C-7a
7a	-	145.6	-
8	6.80 (<i>s</i>)	119.9	C-2, C-3, C-3a, C-9
9	-	150.8	-
6-OCH ₃	3.78 (<i>s</i>)	55.5	C-6
SCH ₃	2.35 (<i>s</i>)	12.6	C-9
N-OCH ₃	4.00 (<i>s</i>)	62.5	-

Figure 105. UV spectrum of compound **10**



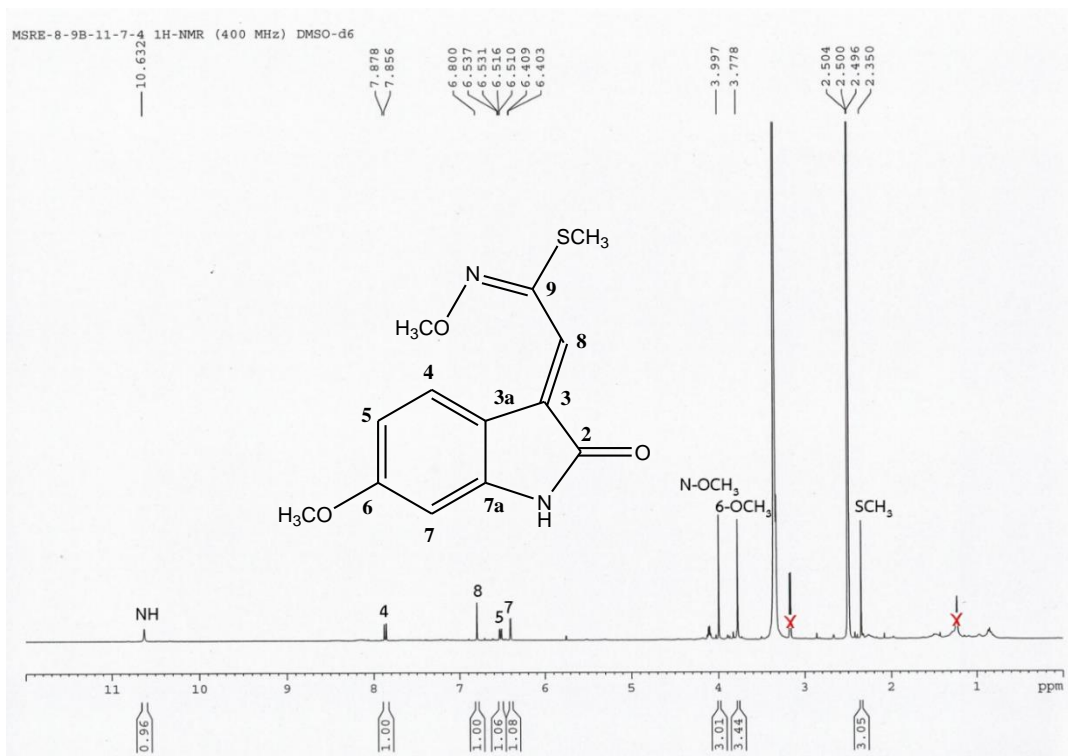


Figure 108. ¹H-NMR spectrum of compound 10 (400 MHz, DMSO-d₆)

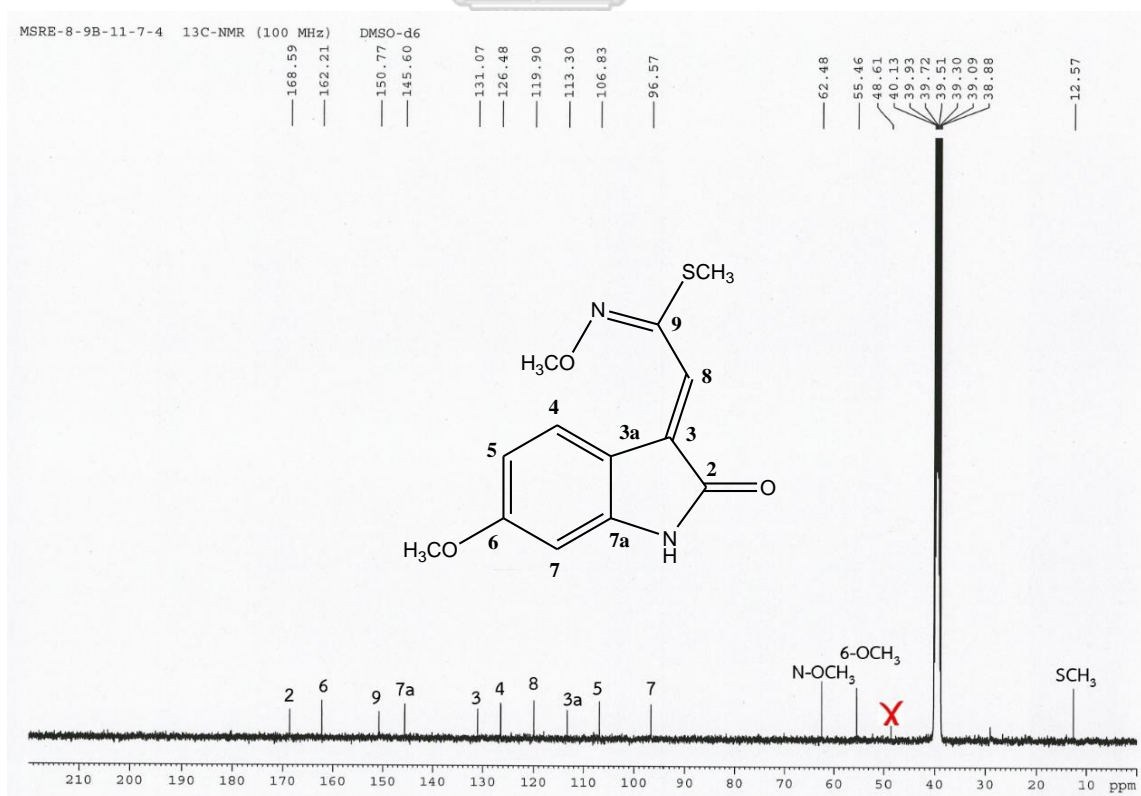


Figure 109. ¹³C-NMR spectrum of compound 10 (100 MHz, DMSO-d₆)

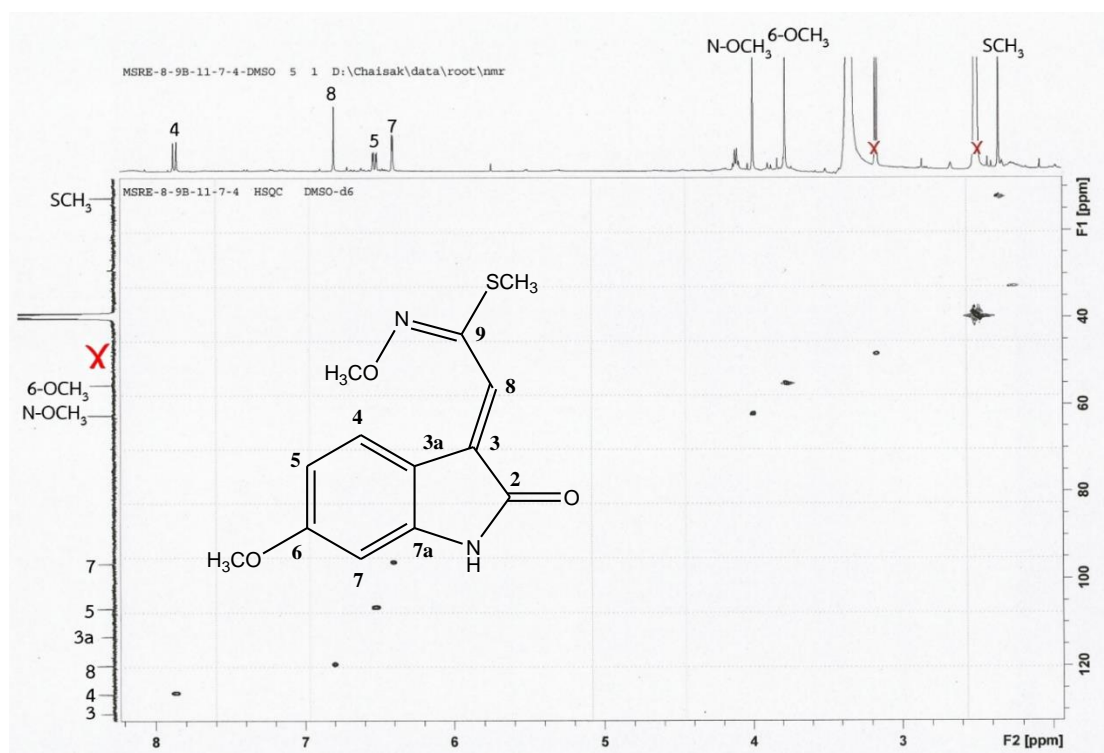


Figure 110. ^1H - ^{13}C HSQC spectrum of compound 10

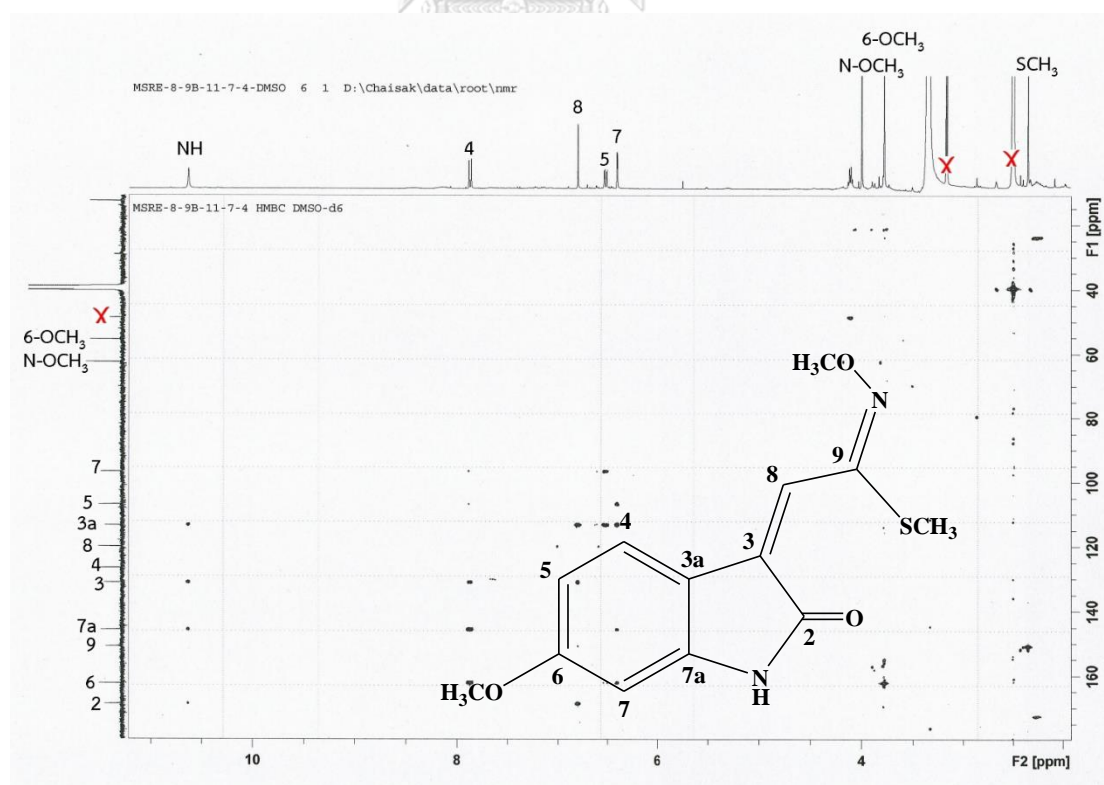
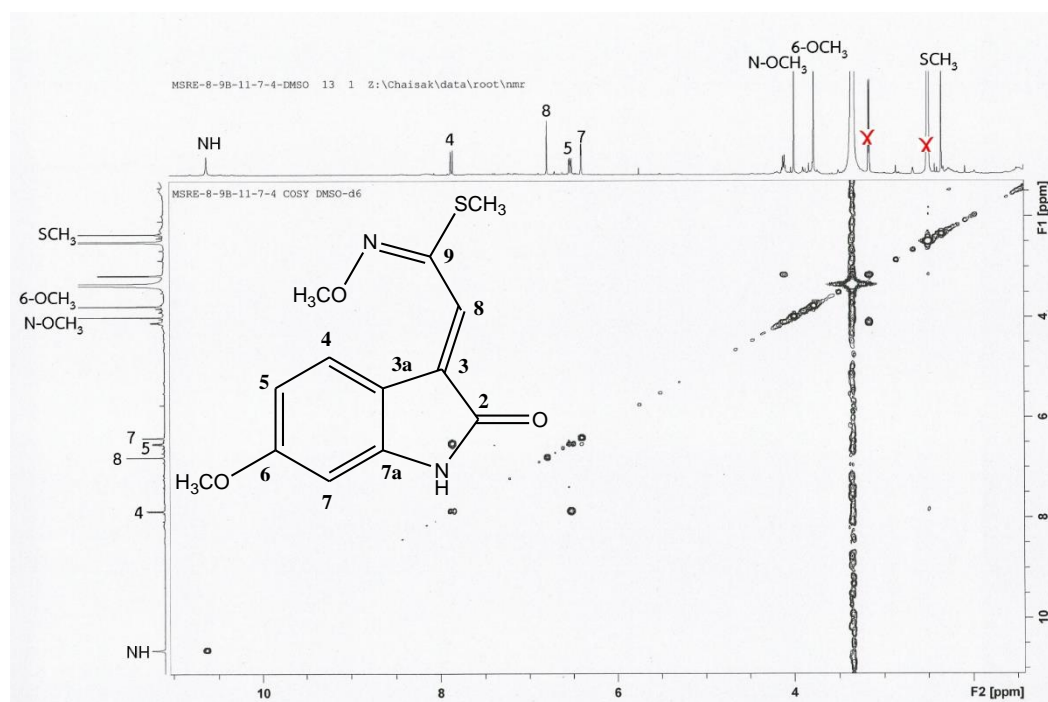
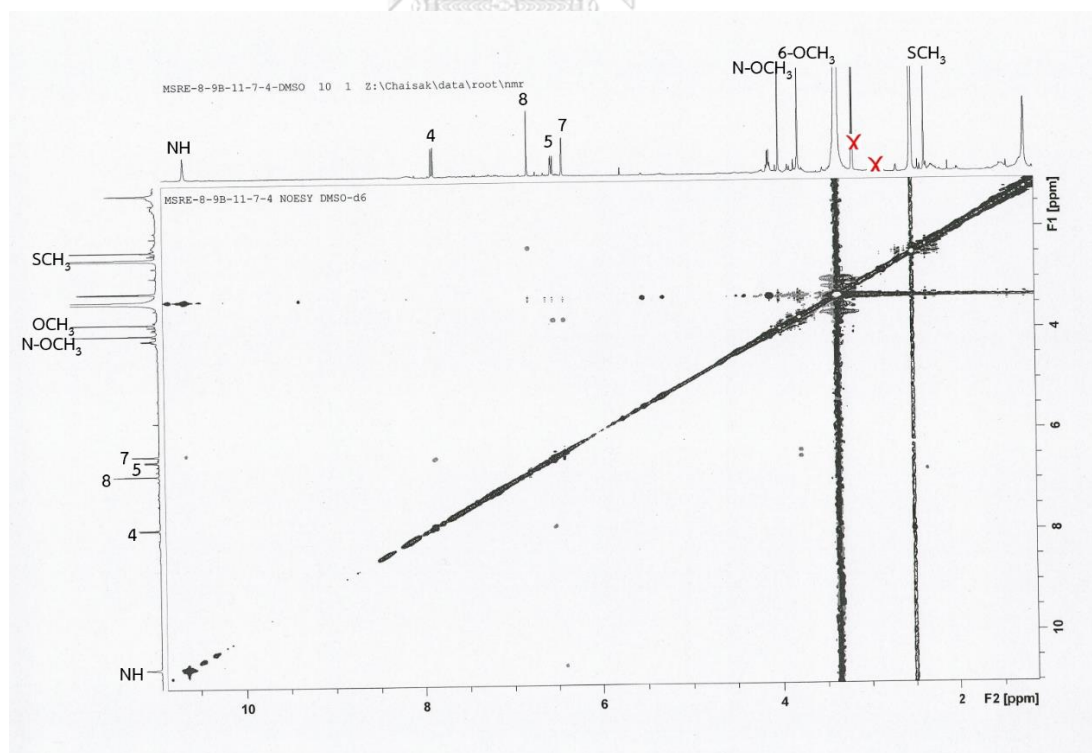


Figure 111. ^1H - ^{13}C HMBC spectrum of compound 10

Figure 112. ^1H - ^1H COSY spectrum of compound 10Figure 113. ^1H - ^1H NOESY spectrum of compound 10

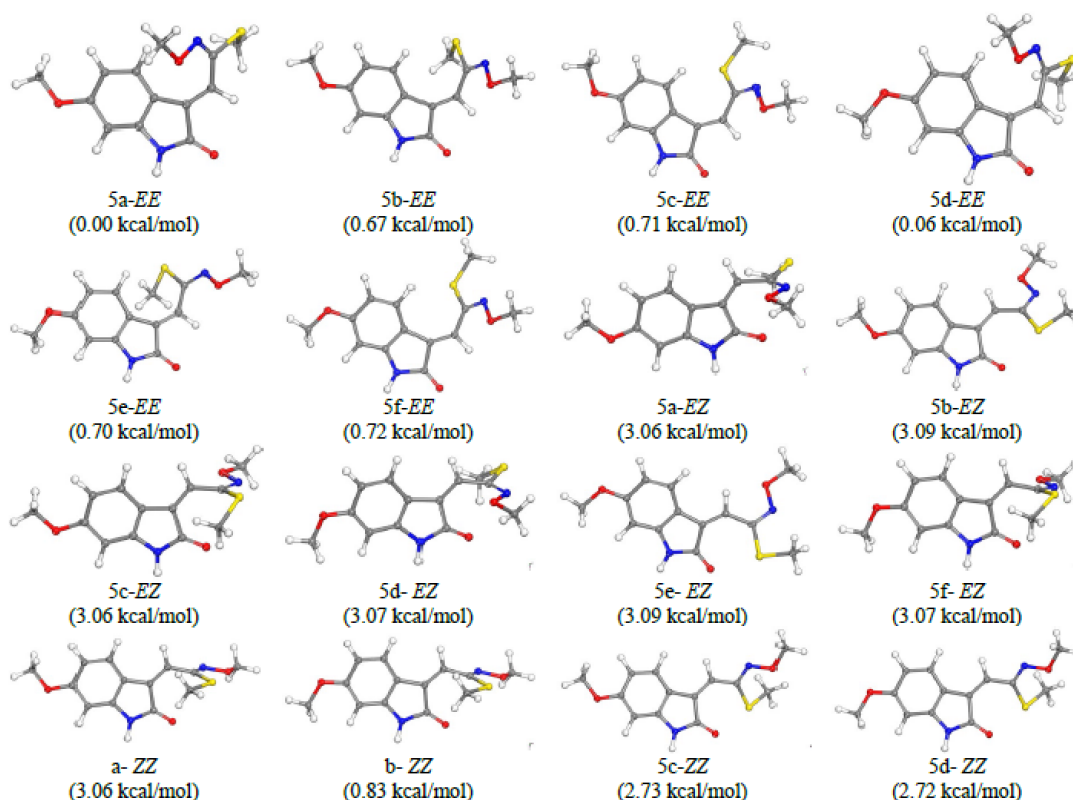


Figure 114. Possible conformations of compound **10**, based on the DFT calculation at B3LYP/6-31g (d, p) level

4.2.6 Structure elucidation of compound **11** (maeruabisindole A)

Compound **11** was isolated as a pale green amorphous solid, showing UV absorption maxima at λ_{max} 210, 270, 315, 355 and 365 nm (**Figure 115**). The HR-ESI mass spectrum (**Figure 116**) exhibited a pseudo-molecular $[M+H]^+$ ion peak at m/z 390.1298, corresponding to a molecular formula of $C_{22}H_{19}N_3O_2S$ (calculated for $C_{22}H_{20}N_3O_2S$, 390.1271), indicating fifteen degrees of unsaturation. Its IR spectrum (**Figure 117**) showed absorption bands of amine and imine at 3384 and 1625 cm^{-1} , respectively.

The $^1\text{H-NMR}$ (400 MHz, $\text{DMSO-}d_6$) data of compound **11** (**Table 14** and **Figure 118-119**) displayed resonances of two set of disubstituted-1*H*-indole moieties at δ_{H} 10.71 (1H, *br s*, NH-1'), 8.05 (1H, *d*, $J = 8.4$ Hz, H-4'), 7.79 (1H, *br s*, H-3'), 6.99 (1H, *d*, $J = 2.4$ Hz, H-7') and 6.78 (1H, *dd*, $J = 8.4, 2.0$ Hz, H-5') and at δ_{H} 11.52 (1H, *br s*, NH-1''),

7.51 (1H, *d*, $J = 2.0$ Hz, H-2''), 7.12 (1H, overlapped, H-7''), 7.10 (1H, overlapped, H-6'') and 6.56 (1H, *dd*, $J = 6.0, 2.4$ Hz, H-5''). Two methoxy signals were observed at δ_{H} 3.81 (3H, *s*, 6'-OCH₃) and 3.52 (3H, *s*, 4''-OCH₃), while a methylthio signal could be seen at δ_{H} 2.59 (3H, *s*, 2-SCH₃). Two indole nuclei, representing sixteen carbon atoms and twelve degrees of unsaturation, indicated that compound **11** was a bisindole alkaloid. Disregarding two methoxy and one methylthio groups, the last part of this molecule should involve one nitrogen atom and three carbon atoms in an imine formation with three degrees of unsaturation.

Its ¹³C-NMR (400 MHz, DMSO-*d*₆) data (Table 14 and Figure 120-121) exhibited 22 signals representing two methoxy groups at δ_{C} 55.2 (6'-OCH₃) and 54.9 (4''-OCH₃), one methylthio group at δ_{C} 14.0 (2-SCH₃), methine and quaternary carbons of two indole moieties at δ_{C} 160.0 (C, C-6'), 153.9 (C, C-4''), 142.9 (C, C-7'a), 137.9 (C, C-7''a), 129.3 (C, C-2'), 125.0 (CH, C-2''), 122.6 (CH, C-4'), 122.5 (CH, C-6''), 116.4 (C, C-3''a), 114.1 (C, C-3'a), 113.0 (C, C-3''), 108.7 (CH, C-5'), 108.5 (CH, C-3'), 105.0 (CH, C-7''), 100.4 (CH, C-5'') and 94.8 (CH, C-7'), and three *sp*² carbons of a 2,3,4-trisubstituted azete moiety (Csaszar *et al.*, 2015) at δ_{C} 144.8 (C-2), 139.5 (C-4) and 133.4 (C-3).

A methoxy group could be located at position 6' of an indole moiety. This was confirmed by ¹H-¹³C HMBC correlations (Figure 123-126) observed from its proton signal (6'-OCH₃) to C-6', from NH-1' to C-2', C-3'a and C-7'a and from H-4' to C-6' and C-7'a, together with ¹H-¹H NOESY cross peaks (Figure 128) between proton signals of NH-1' and H-7'; of H-3' and H-4' and of 6'-OCH₃ with H-5' and H-7'. Another methoxy group was assigned at position 4'' of the second indole moiety based on HMBC correlations observed from the signal of 4''-OCH₃ to C-4''; from NH-1'' to C-3''a and C-7''a and from H-6'' to C-4'' and C-7''a, together with NOESY cross peaks between NH-1'' and H-7'' and between 4''-OCH₃ and H-5''.

Both indole nuclei were connected through an azete ring. The 6'-methoxy indole moiety could be connected via C-2' to this four-membered ring at position 3, based on a HMBC cross peaks from NH-1' and H-3' to C-3, whereas the 4''-methoxy indole moiety was connected via C-3'' to position 4 of the azete ring, as supported by a ¹H-¹H COSY cross peak (Figure 127) between NH-1'' and H-2', and a

HMBC cross peak from H-2'' to C-4 signal. Finally, the methylthio group was located at position 2 of the azete ring based on a HMBC correlation from its proton signal (δ_{H} 2.59) to C-2. Therefore, the structure of compound **11** was elucidated as 4-methoxy-3-(3-(6-methoxy-1*H*-indol-2-yl)-4-(methylthio)azet-2-yl)-1*H*-indole and was trivially named maeruabisindole A. Bisindole alkaloids bearing an azete ring have previously been found in the roots of *Isatis tinctoria* (family Brassicaceae). Two of these indole derivatives, namely isatindigosides G and F, exhibited nitric oxide inhibitory effect (Zhang *et al.*, 2020).

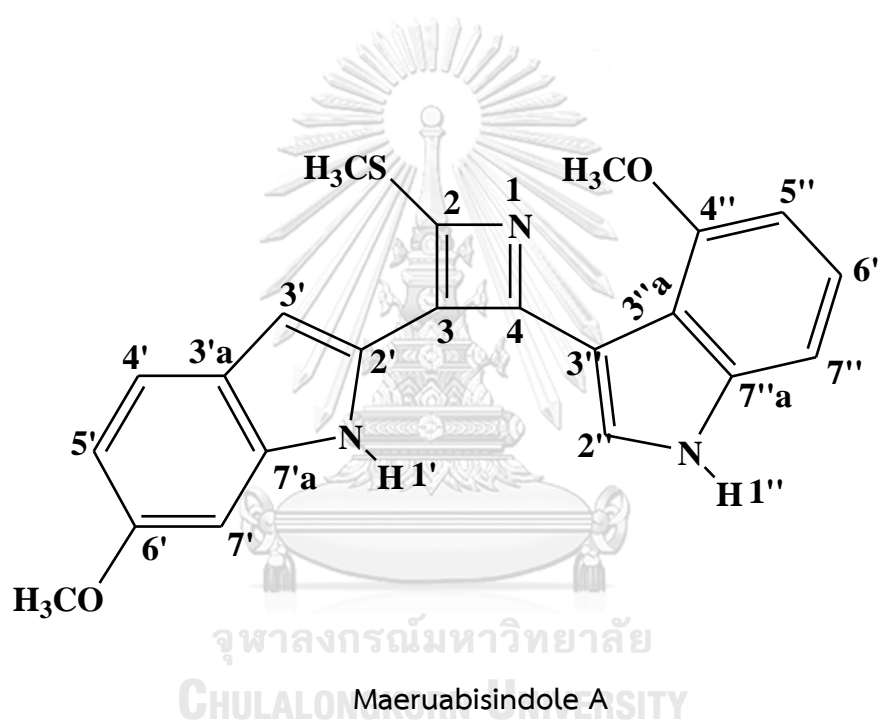


Table 14. ^1H -, ^{13}C -NMR and HMBC data of compound **11** (400 MHz, in $\text{DMSO-}d_6$)

Position	δ_{H} (mult., J in Hz)	δ_{C}	HMBC correlation with
2	-	144.8	
3	-	133.4	-
4	-	139.5	-
NH-1'	10.71 (<i>br s</i>)	-	C-2', C-3'a, C-7'a, C-3
2'	-	129.3	-
3'	7.79 (<i>br s</i>)	108.5	C-3, C-3'a
3'a	-	114.1	-
4'	8.05 (<i>d</i> , 8.4)	122.6	C-6', C-7'a
5'	6.78 (<i>dd</i> , 8.4, 2.0)	108.7	C-3'a, C-7'
6'	-	160.0	-
7'	6.99 (<i>d</i> , 2.4)	94.8	C-3'a, C-5', C-6', C-7a'
7'a	-	142.9	-
NH-1''	11.52 (<i>br s</i>)	-	C-2'', C-3'', C-3''a, C-7''a
2''	7.51 (<i>d</i> , 2.0)	125.0	C-3''
3''	-	113.0	-
3''a	-	116.4	-
4''	-	153.9	-
5''	6.56 (<i>dd</i> , 6.0, 2.4)	100.4	C-3''a, C-4'', C-7''
6''	7.10, overlapped	122.5	C-4'', C-7''a
7''	7.12, overlapped	105.0	C-3''a, C-5''
7''a	-	137.9	-
2-SCH ₃	2.59 (<i>s</i>)	14.0	C-2
6'-OCH ₃	3.81 (<i>s</i>)	55.2	-
4''-OCH ₃	3.52 (<i>s</i>)	54.9	-

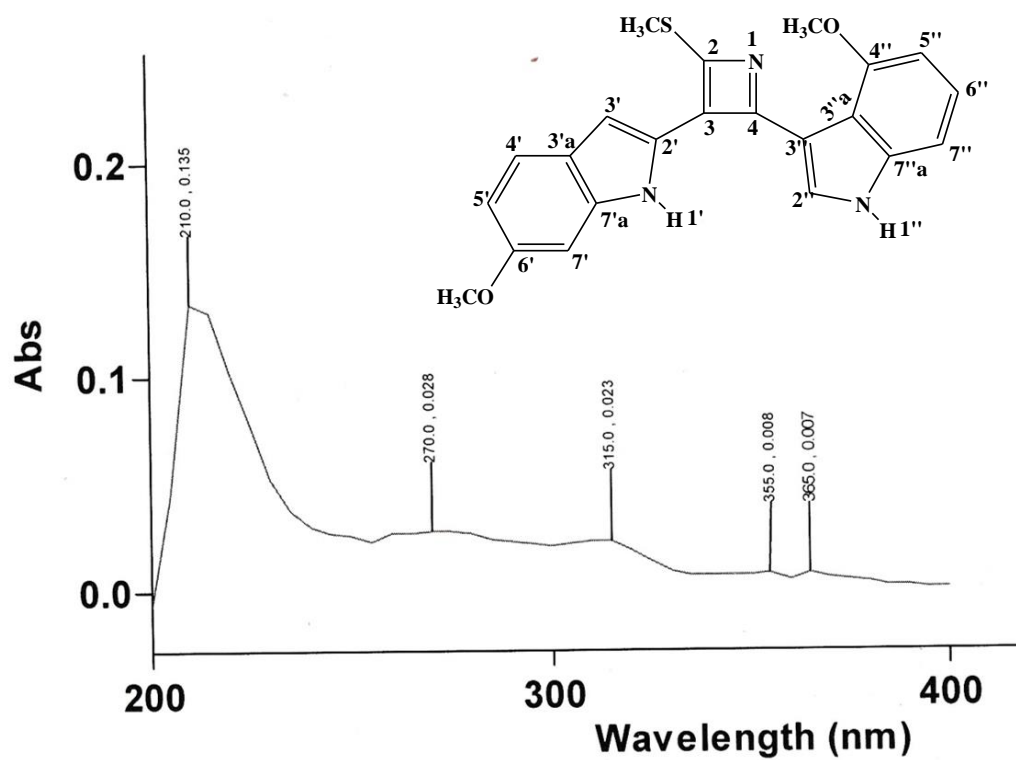


Figure 115. UV spectrum of compound 11

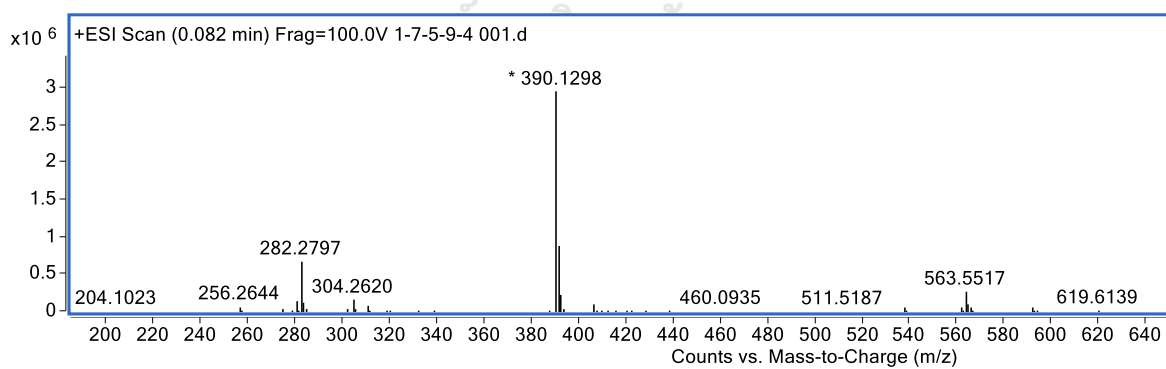


Figure 116. HR-ESI mass spectrum of compound 11

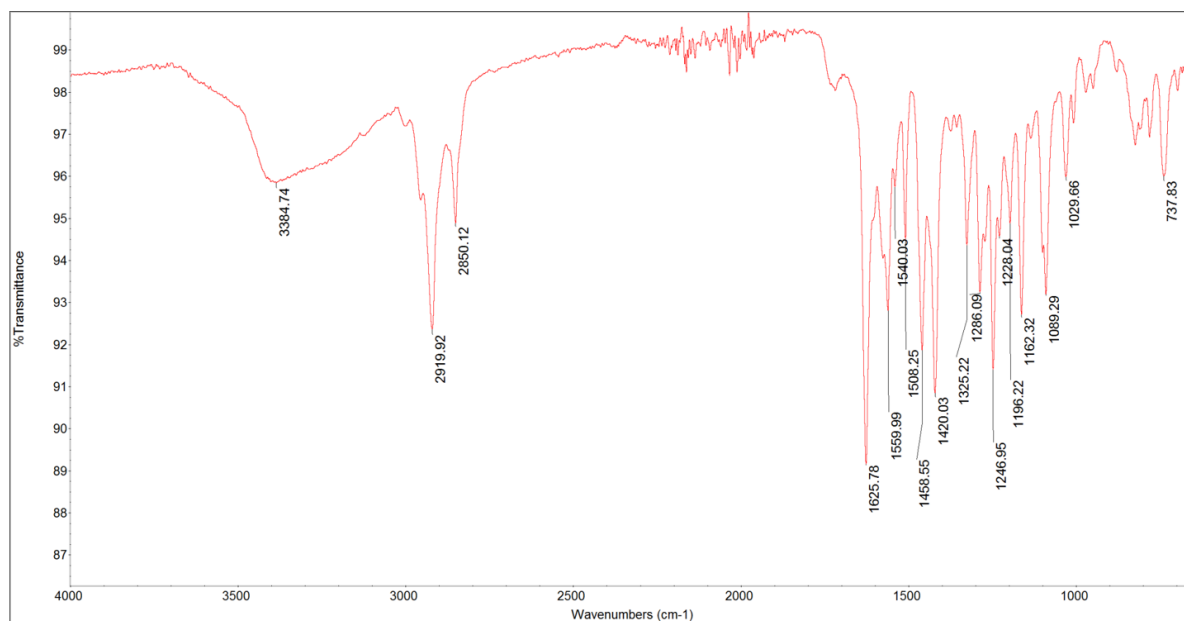


Figure 117. IR spectrum of compound 11

MSRB-1-7-5-9-4 ^1H NMR (400 MHz) in DMSO-d_6

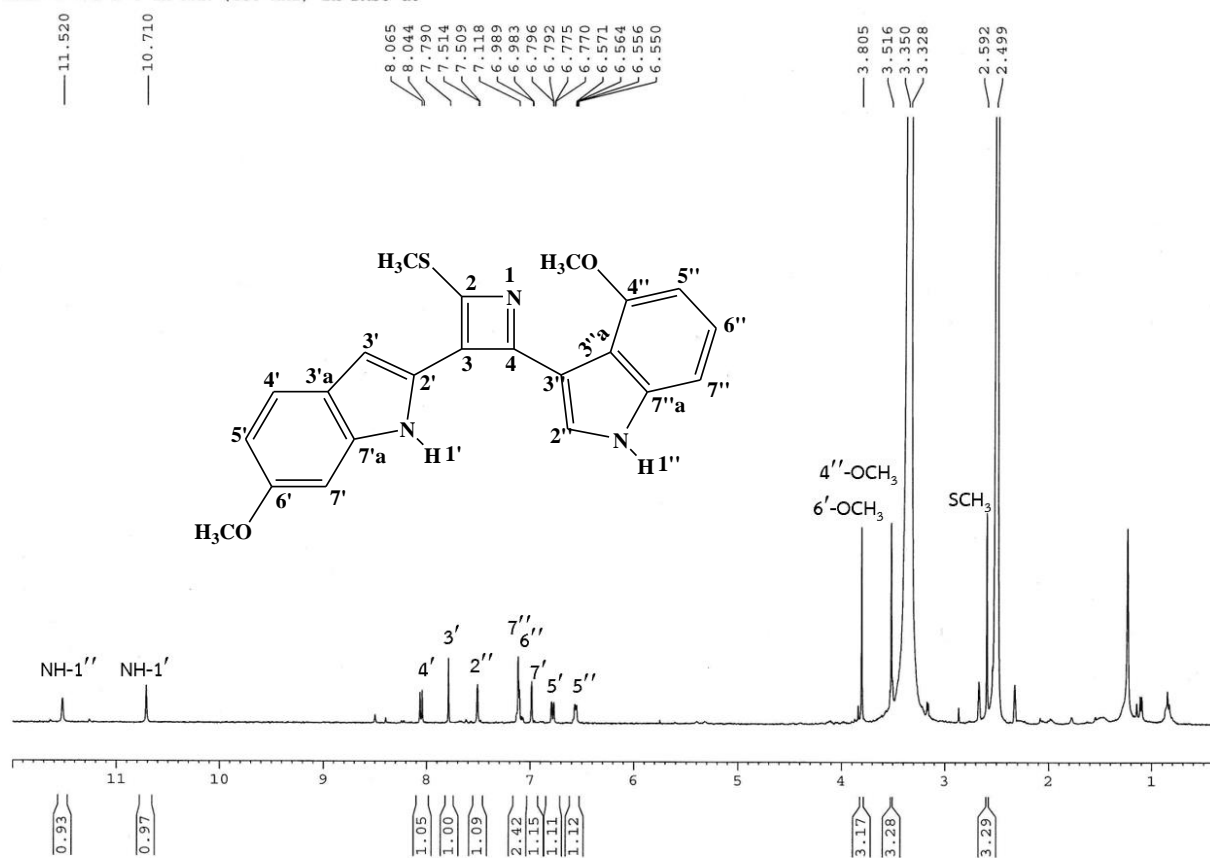
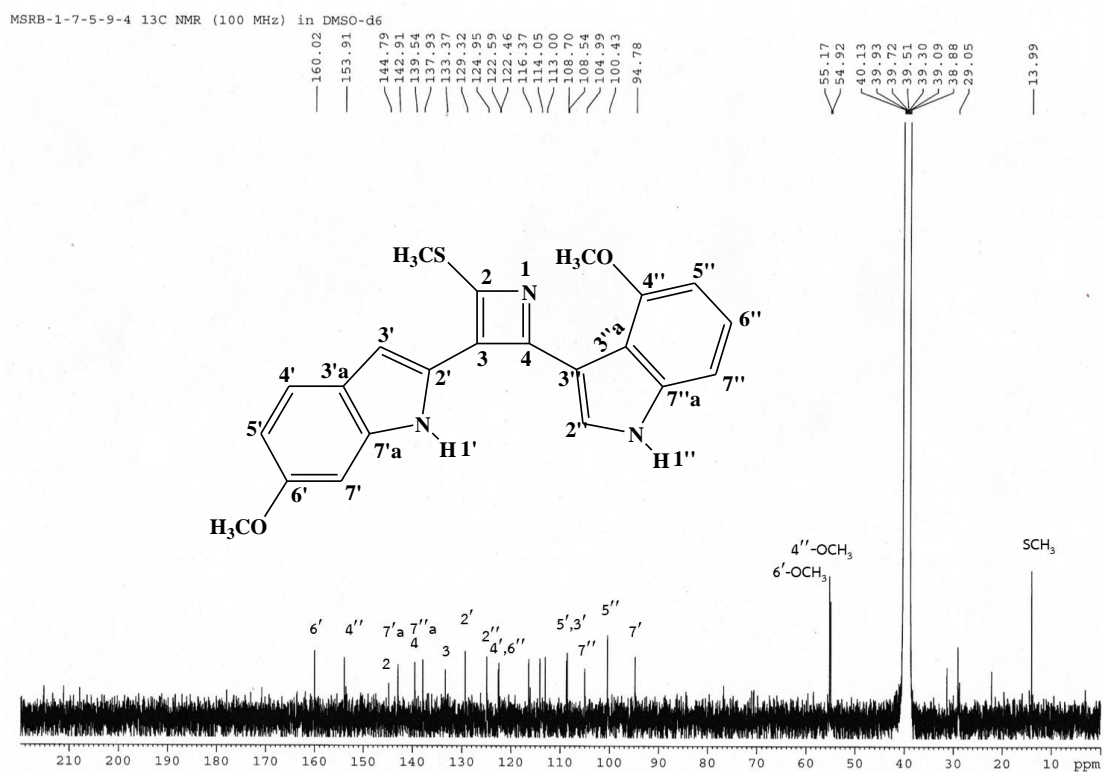
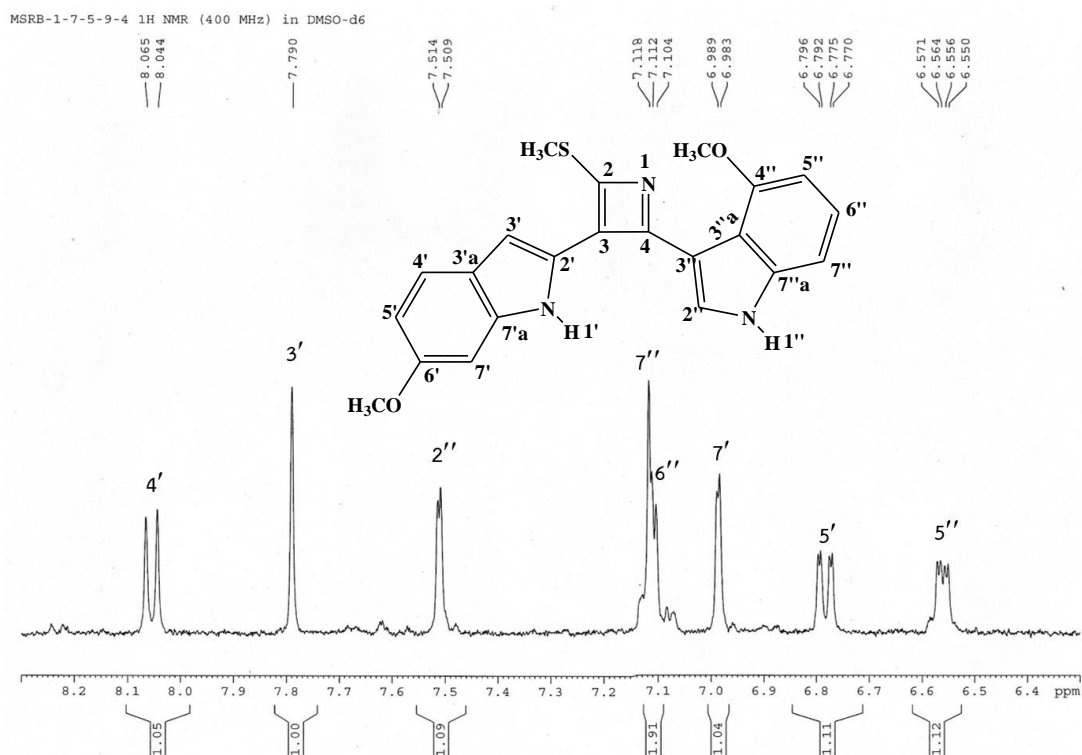


Figure 118. ^1H -NMR spectrum of compound 11 (400 MHz, DMSO-d_6)



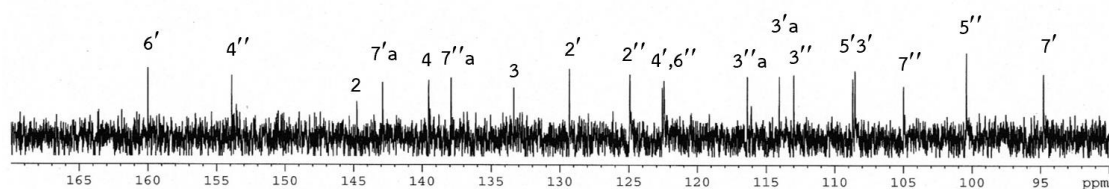
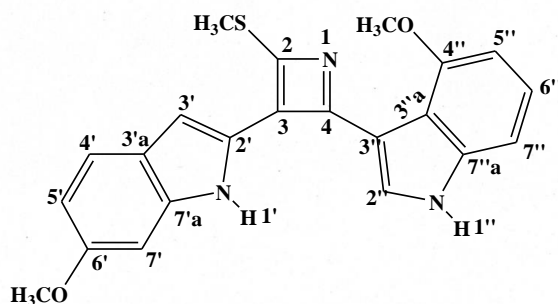
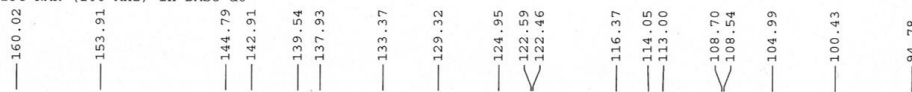
MSRB-1-7-5-9-4 ^{13}C NMR (100 MHz) in DMSO- d_6 

Figure 121. ^{13}C -NMR spectrum of compound **11** (100 MHz, DMSO- d_6)
(expansion between δ_{C} 90-170 ppm)

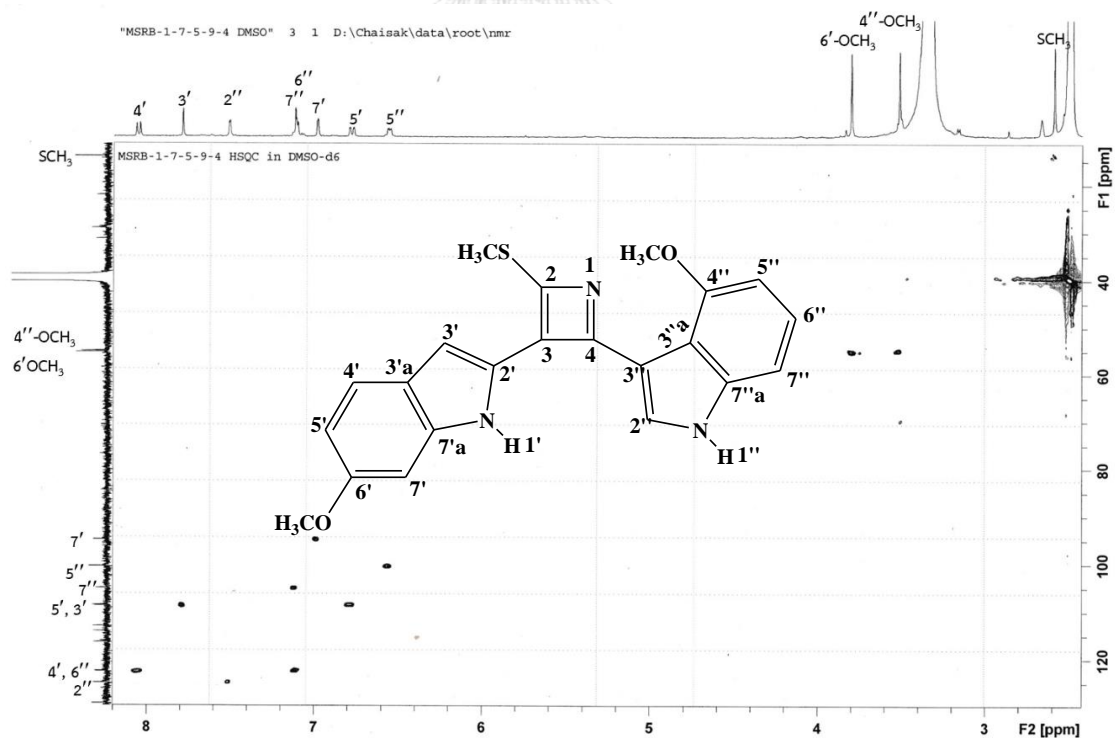


Figure 122. ^1H - ^{13}C HSQC spectrum of compound **11**

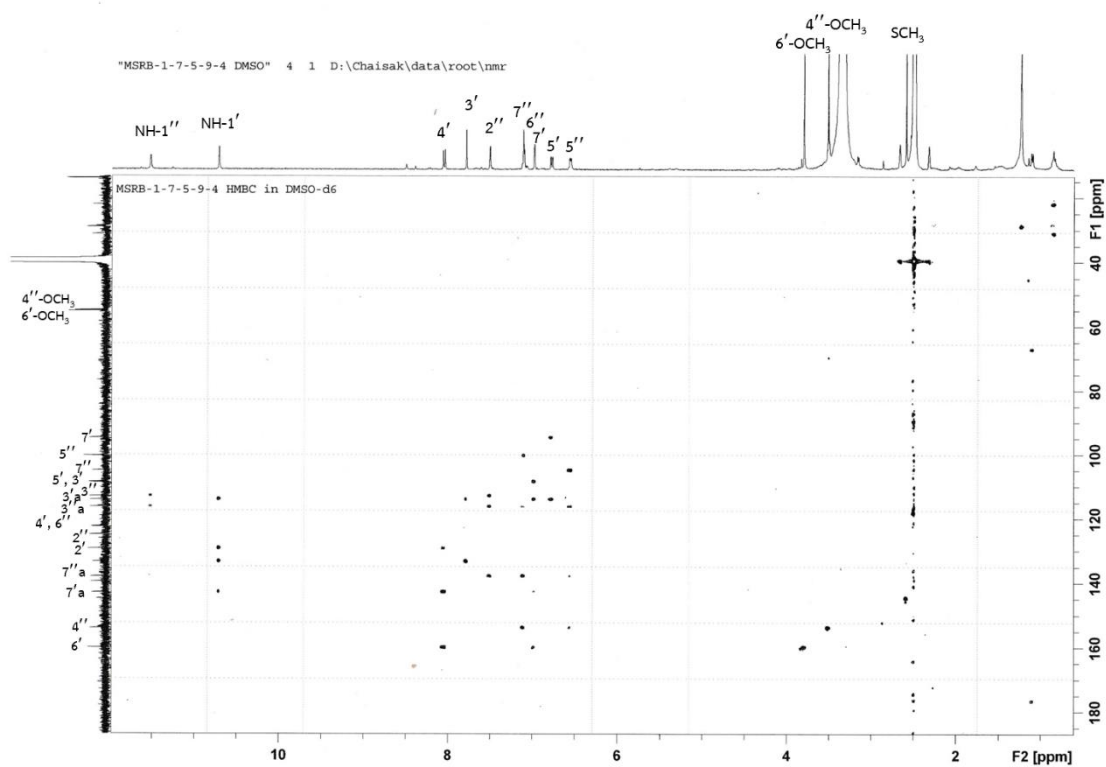


Figure 123. ^1H - ^{13}C HMBC spectrum of compound **11**
(expansion between δ_{H} 0.5-12.0 ppm, δ_{C} 20-180 ppm)

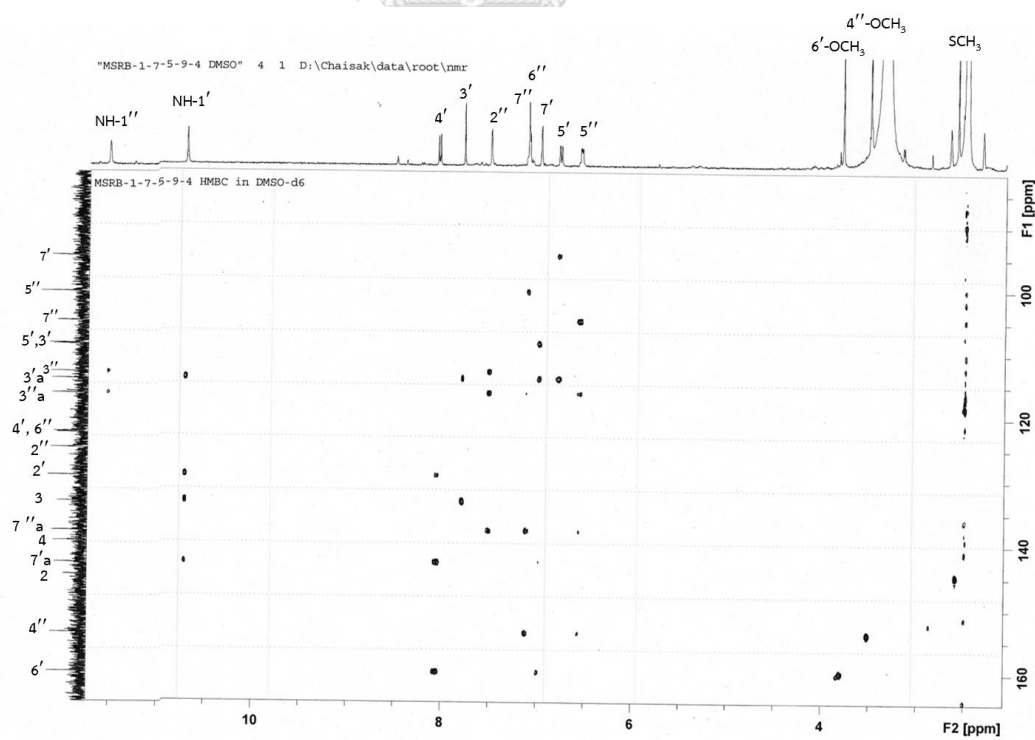


Figure 124. ^1H - ^{13}C HMBC spectrum of compound **11**
(expansion between δ_{H} 2.0-12.0 ppm, δ_{C} 85-160 ppm)

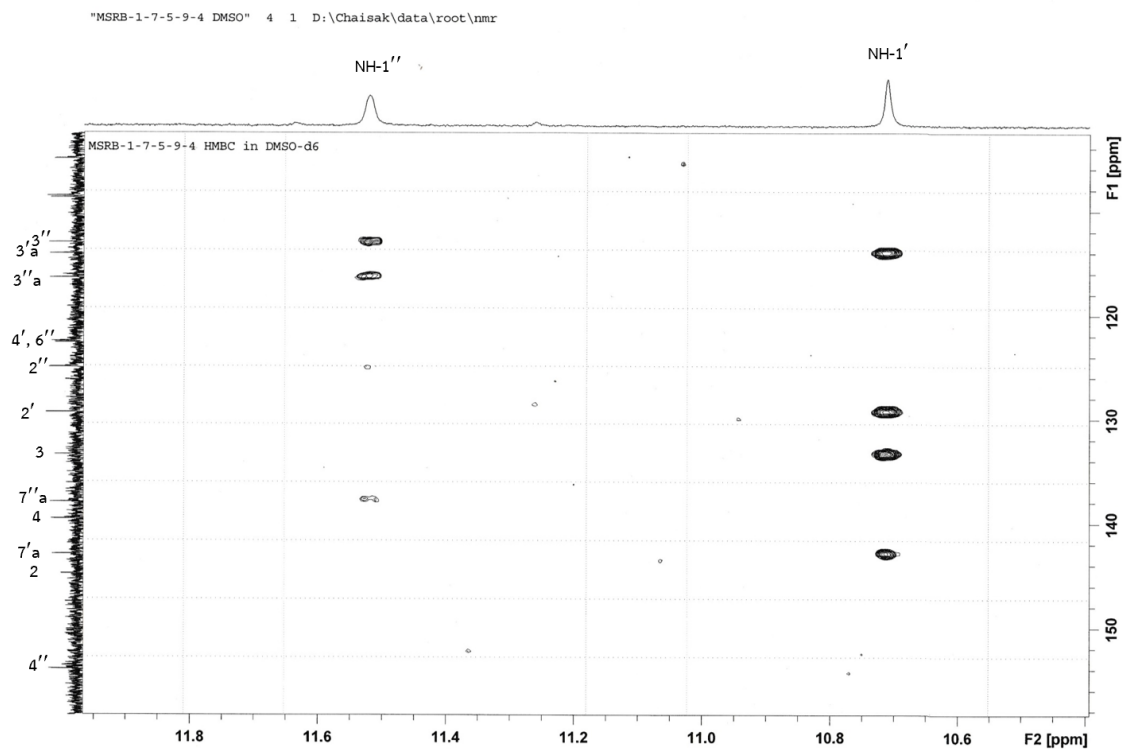


Figure 125. ^1H - ^{13}C HMBC spectrum of compound 11
(expansion between δ_{H} 10.4-12.0 ppm, δ_{C} 104-158 ppm)

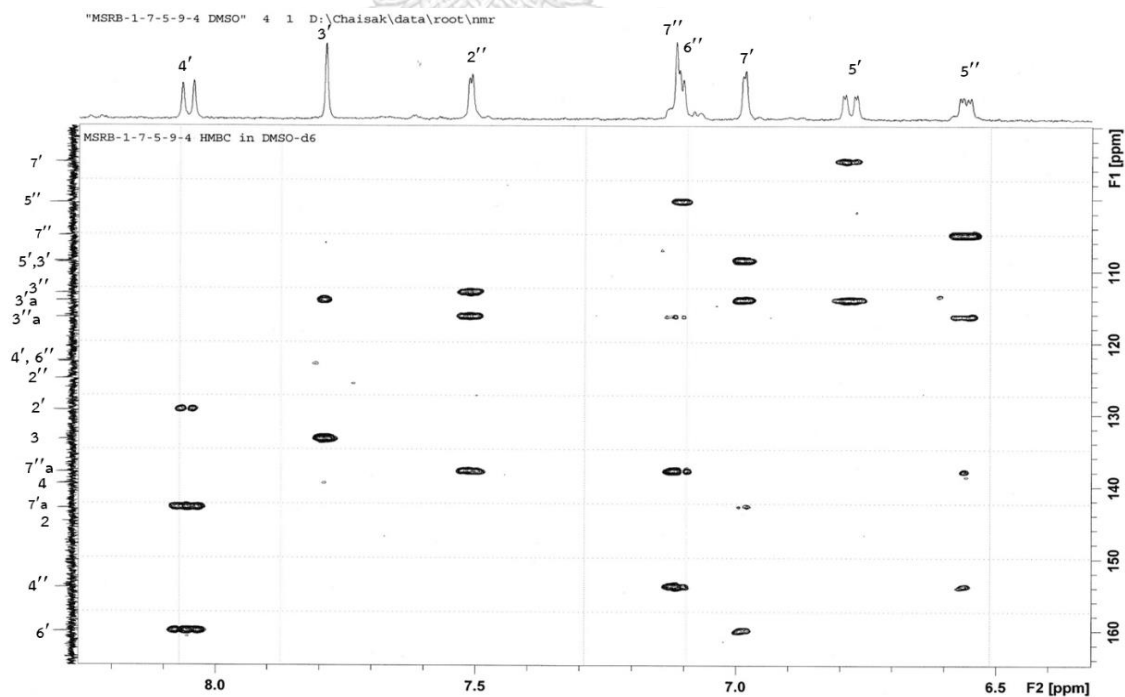
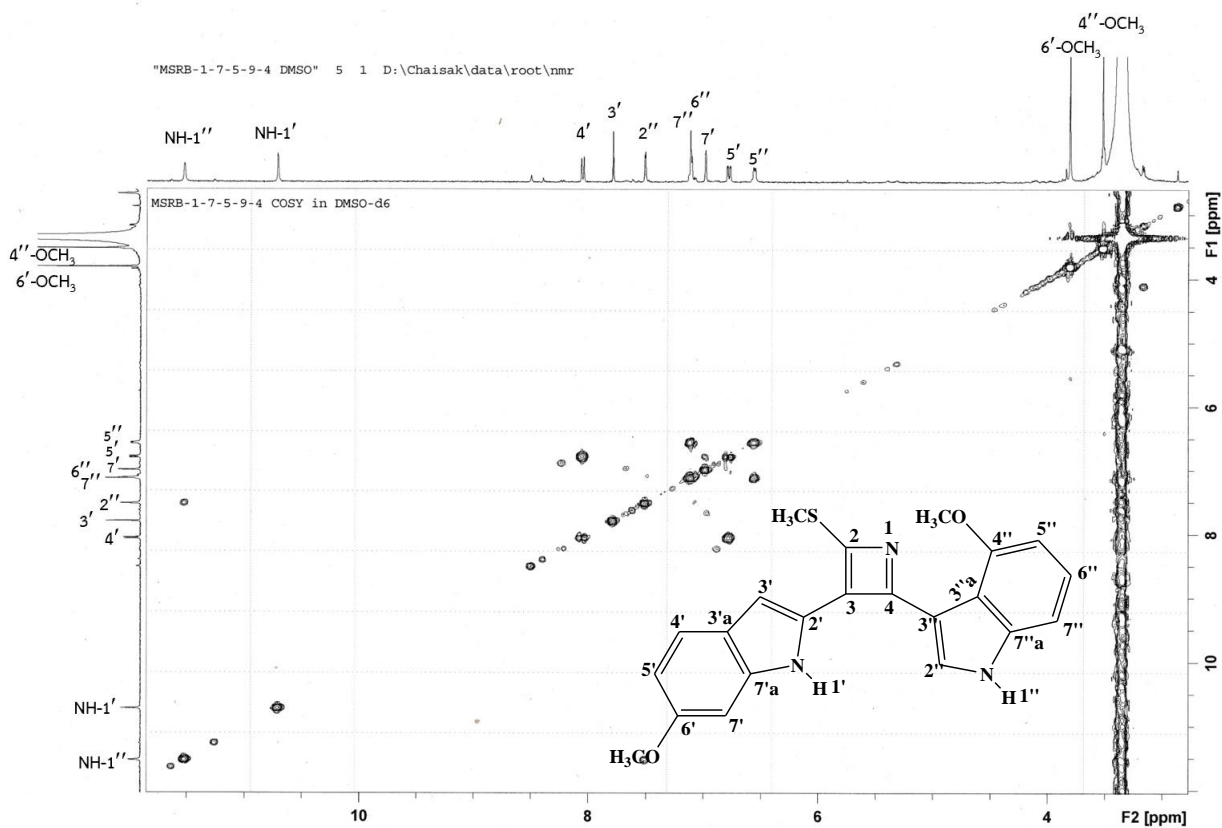
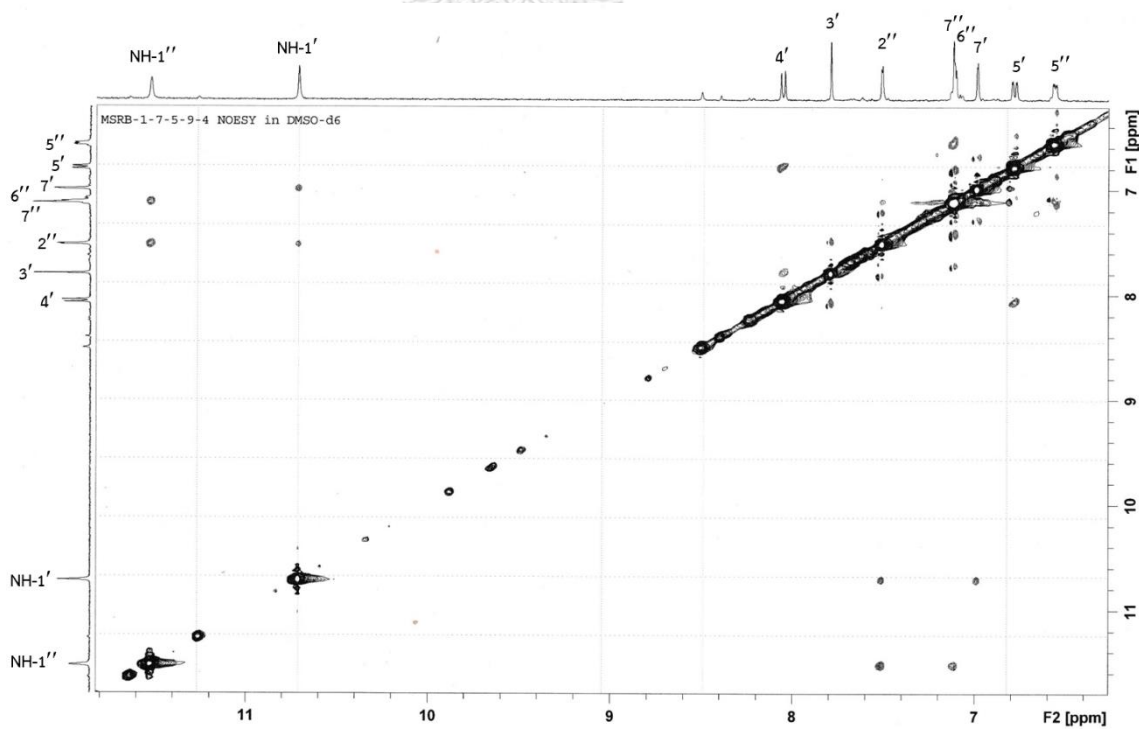


Figure 126. ^1H - ^{13}C HMBC spectrum of compound 11
(expansion between δ_{H} 6.4-8.4 ppm, δ_{C} 90-164 ppm)

Figure 127. ^1H - ^1H COSY spectrum of compound 11Figure 128. ^1H - ^1H NOESY spectrum of compound 11

4.2.7 Structure elucidation of compound 12 (maeruabisindole B)

Compound **12** was obtained as a pale green amorphous solid, showing UV absorption maxima at λ_{\max} 210, 230, 310, 340 and 355 nm (**Figure 129**). The IR spectrum (**Figure 131**) showed absorption bands of amine at 3396 cm^{-1} , imine and aromatic ring at 1602 and 1465 cm^{-1} and sulfoxide group 1025 cm^{-1} . Its molecular formula of $\text{C}_{22}\text{H}_{19}\text{N}_3\text{O}_3\text{S}$ was deduced from a pseudo-molecular $[\text{M}+\text{H}]^+$ ion peak at m/z 406.1224 (calculated for $\text{C}_{22}\text{H}_{20}\text{N}_3\text{O}_3\text{S}$, 406.1220) in the HR-ESI mass spectrum (**Figure 130**).

Its ^1H and ^{13}C -NMR data are mostly similar to those of compound **11**. The ^1H -NMR spectrum of compound **12** (400 MHz, CD_3OD) (**Table 15** and **Figure 132-133**) showed peaks of the 2',6'-disubstituted-1*H*-indole moiety at δ_{H} 8.12 (1H, *d*, $J = 8.4$ Hz, H-4'), 8.43 (1H, *s*, H-3'), 7.05 (1H, *d*, $J = 2.0$ Hz, H-7'), 6.93 (1H, *dd*, $J = 8.4, 2.0$ Hz, H-5') and 3.89 (3H, *s*, 6'-OCH₃) and the 3'',4''-disubstituted-1*H*-indole moiety at δ_{H} 7.54 (1H, *s*, H-2''), 7.14 (1H, *d*, $J = 6.8$ Hz, H-7''), 7.16 (1H, *dd*, $J = 7.6, 6.8$ Hz, H-6''), 6.60 (1H, *d*, $J = 6.8$ Hz, H-5'') and 3.55 (3H, *s*, 4''-OCH₃). A methylthio signal, as seen in compound **11**, was replaced by a methylsulfoxide singlet at δ_{H} 2.98 (3H, *s*, 2-SOCH₃). The H-3' signal appeared at more downfield chemical shift due to the anisotropic effect of S=O bond of the methylsulfoxide group on the nearby azete ring to this proton on the indole nucleus.

The ^{13}C -NMR data of this compound (400 MHz, CD_3OD) (**Table 15** and **Figure 134**) showed 22 carbon peaks representing two methoxy carbons at δ_{C} 56.1 (6'-OCH₃) and 55.7 (4''-OCH₃), one methylsulfoxide carbon at δ_{C} 42.1 (2-SOCH₃), methine carbons at δ_{C} 126.1 (C-2''), 124.4 (C-6''), 123.7 (C-4'), 111.8 (C-5'), 109.3 (C-3'), 106.3 (C-7''), 101.7 (C-5'') and 95.8 (C-7') and quaternary carbons at δ_{C} 163.0 (C-6'), 155.6 (C-4''), 144.9 (C-7'a), 140.0 (C-7''a), 130.8 (C-2'), 118.2 (C-3''a), 116.3 (C-3'a) and 113.2 (C-3''). Three sp^2 carbons of the 2,3,4-trisubstituted azete ring resonated at δ_{C} 151.7 (C-2), 142.7 (C-4) and 137.8 (C-3).

These spectroscopic data indicated that the difference of this compound to compound **11** was the presence of a methylsulfoxide group, instead of a methylthio group, at position 2 of the azete ring. This was confirmed by ^1H - ^{13}C HMBC correlation

between the methylsulfoxide proton signal (δ_{H} 2.98) to C-2 of the azete ring. Linkage of the 2',6'-disubstituted indole unit to the azete ring was confirmed by HMBC cross peaks from H-3' to C-3 and C-3'a. Therefore, the structure of compound **12** was established as 4-methoxy-3-(3-(6-methoxy-1*H*-indol-2-yl)-4-(methylsulfinyl)azet-2-yl)-1*H*-indole and named maeruabisindole B.

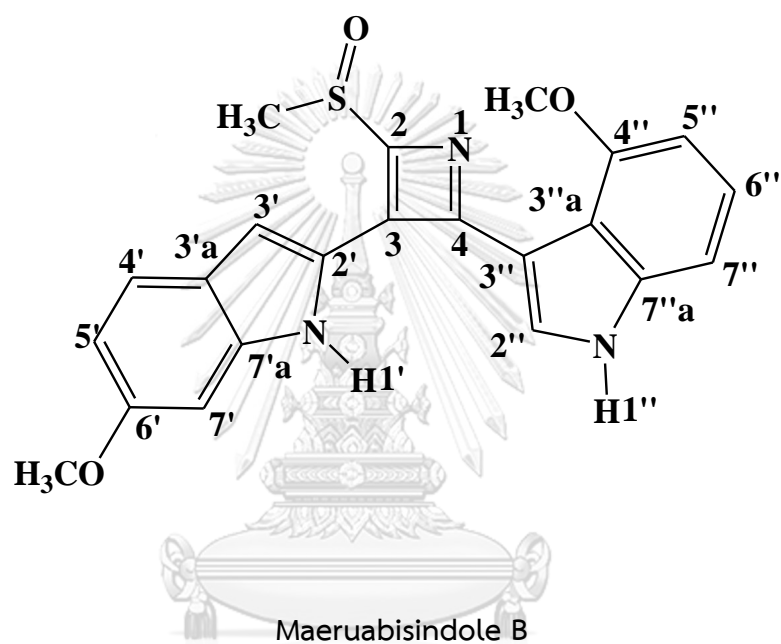


Table 15. ^1H -, ^{13}C NMR and HMBC data of compound **12** (400 MHz, in CD_3OD)

Position	δ_{H} (mult., J in Hz)	δ_{C}	HMBC correlation with
2	-	151.7	
3	-	137.8	-
4	-	142.7	-
2'	-	130.8	-
3'	8.43 (s)	109.3	C-3, C-3'a
3'a	-	116.3	-
4'	8.12 (d, 8.4)	123.7	C-2', C-6', C-7'a
5'	6.93 (dd, 8.4, 2.0)	111.8	C-3'a, C-7'
6'	-	163.0	-
7'	7.05 (d, 2.0)	95.8	C-3'a, C-5', C-6'
7'a	-	144.9	-
2''	7.54 (s)	126.1	C-3'', C-3''a, C-7''a
3''	-	113.2	-
3''a	-	118.2	-
4''	-	155.6	-
5''	6.60 (d, 6.8)	101.7	C-3''a, C-4'', C-7''
6''	7.16 (dd, 7.6, 6.8)	124.4	C-5''
7''	7.14 (d, 6.8)	106.3	C-4'', C-5'', C-7''a
7''a	-	140.0	-
2-SOCH ₃	2.98 (s)	42.1	C-2
6'-OCH ₃	3.89 (s)	56.1	-
4''-OCH ₃	3.55 (s)	55.7	-

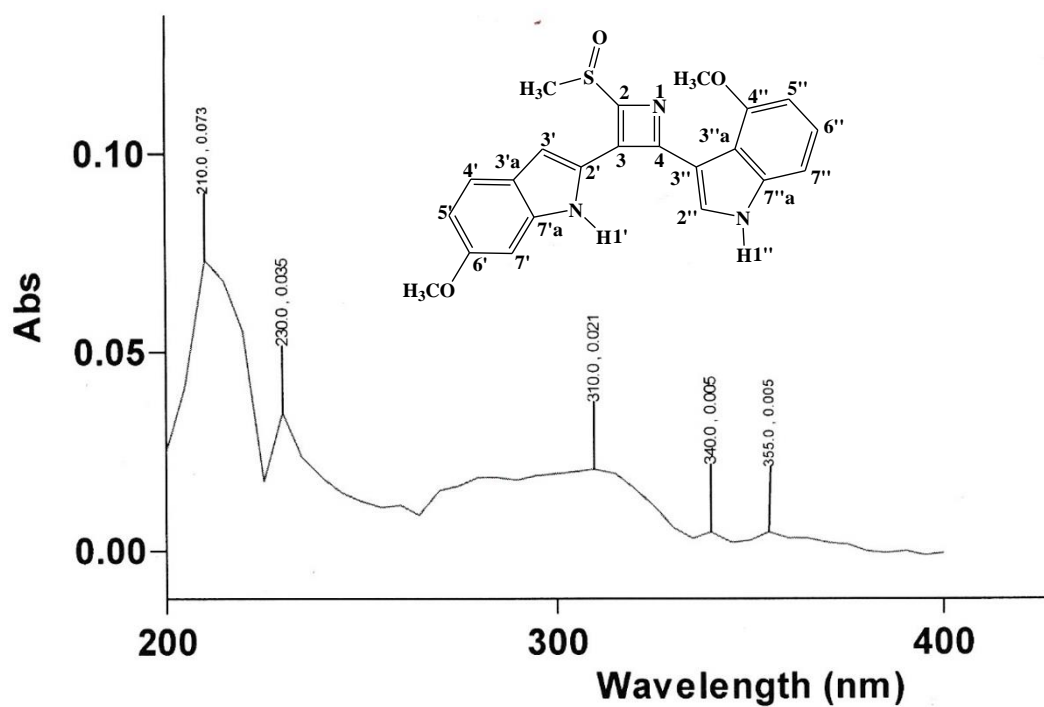


Figure 129. UV spectrum of compound 12

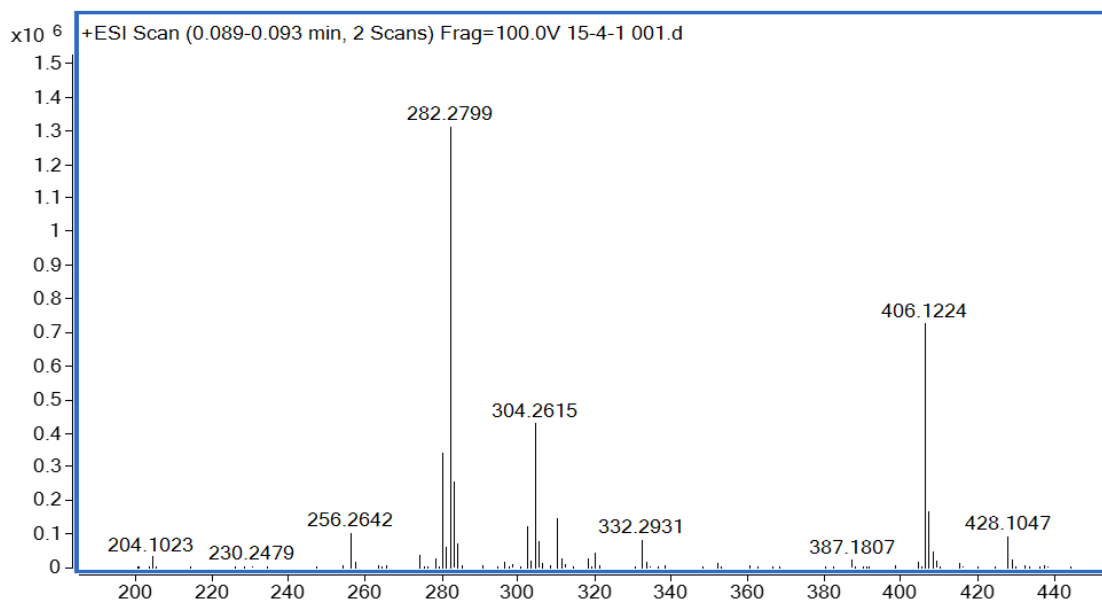
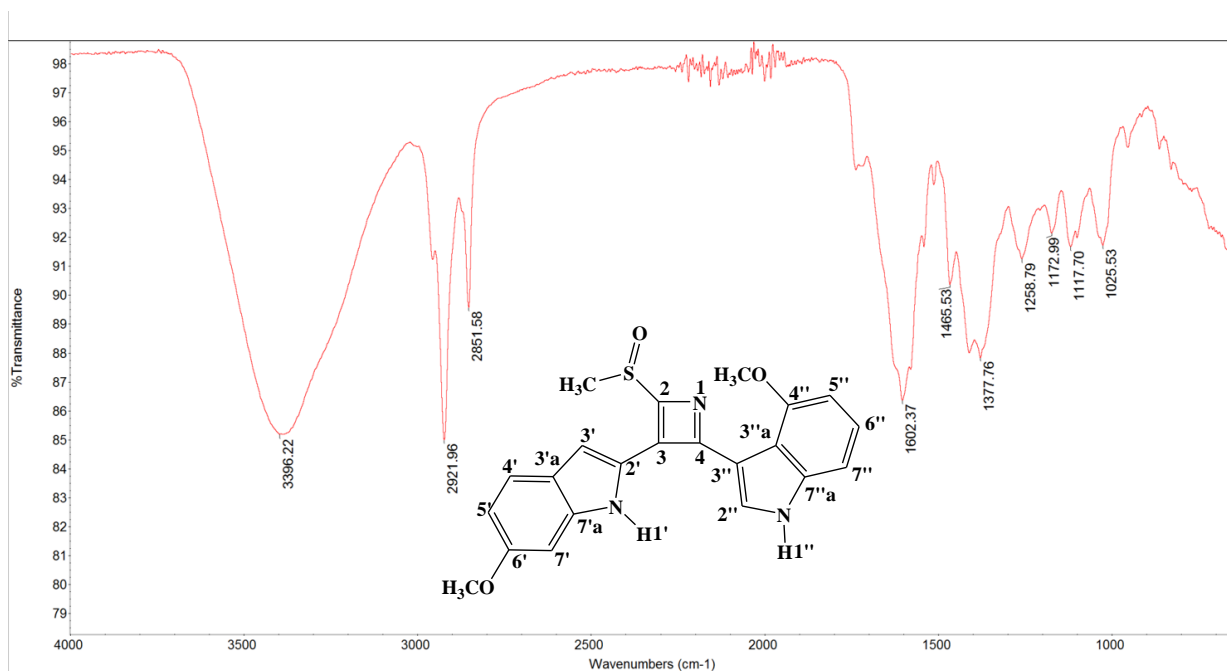
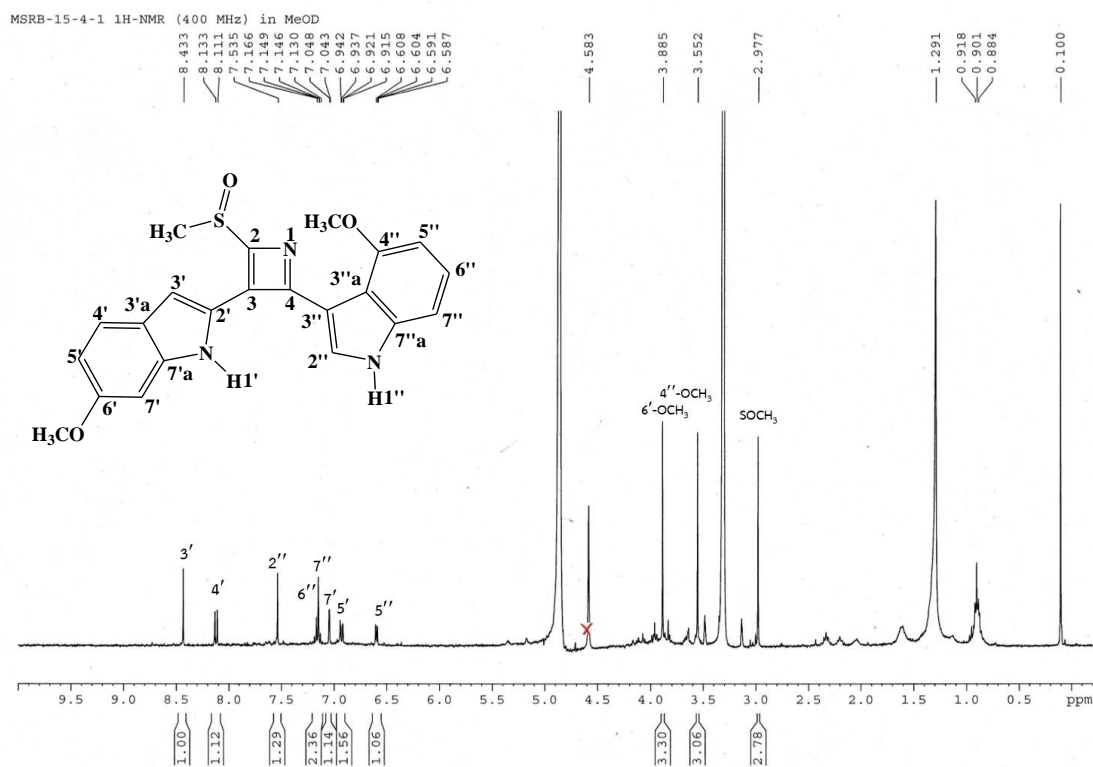


Figure 130. HR-ESI mass of compound 12

Figure 131. IR spectrum of compound **12**Figure 132. ¹H-NMR spectrum of compound **12** (400 MHz, CD₃OD)

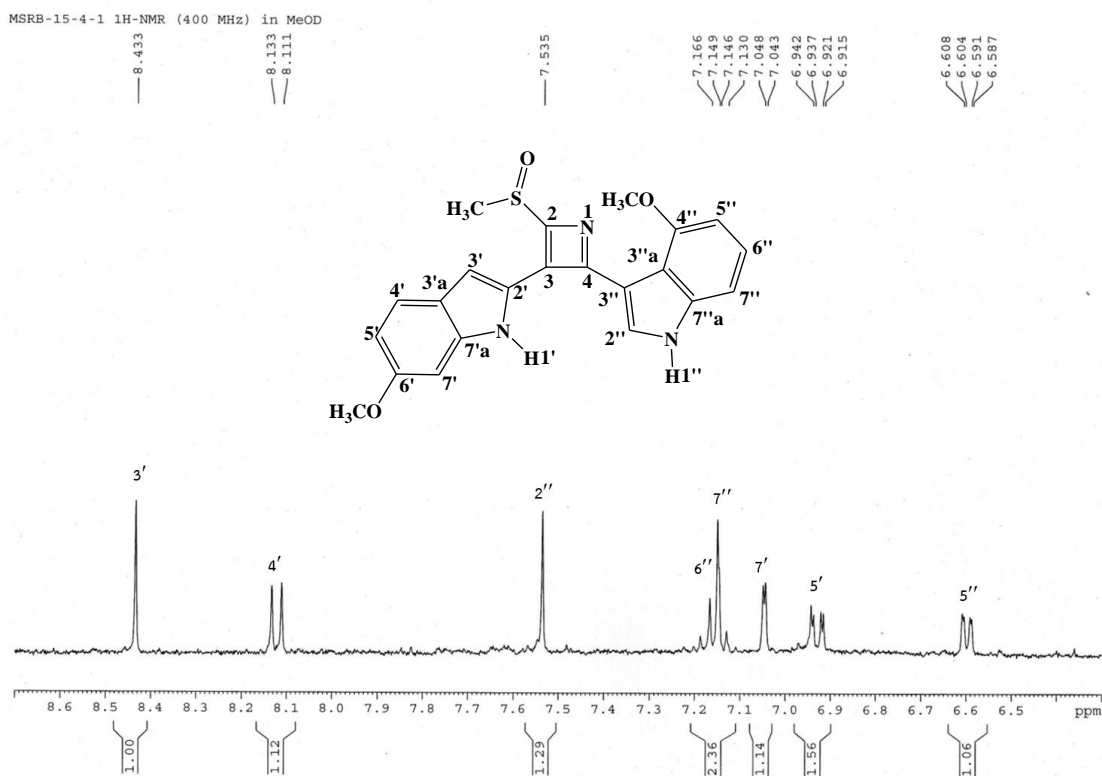


Figure 133. $^1\text{H-NMR}$ spectrum of compound **12** (expansion between δ_{H} 6.3-8.7 ppm)

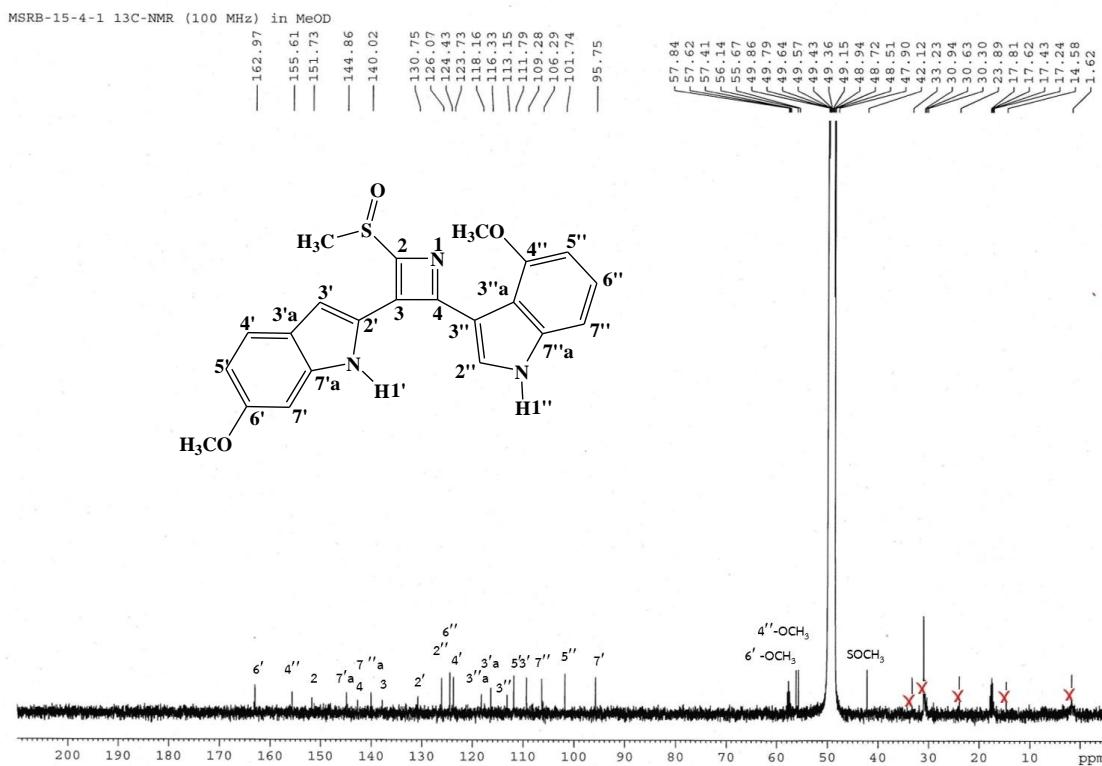
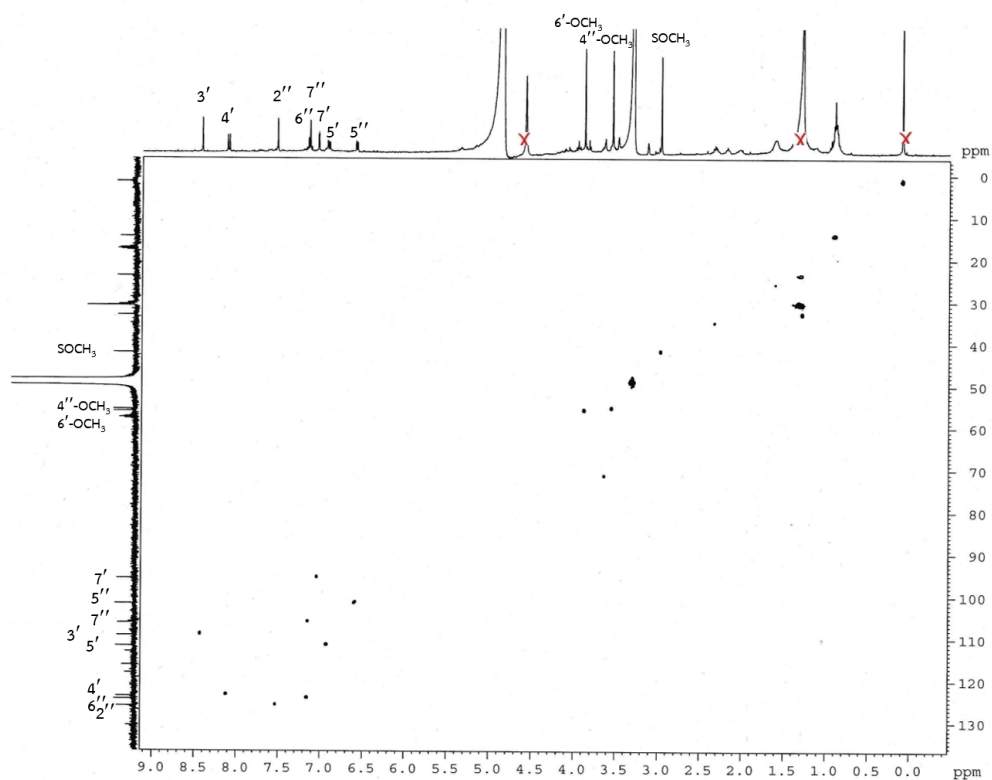
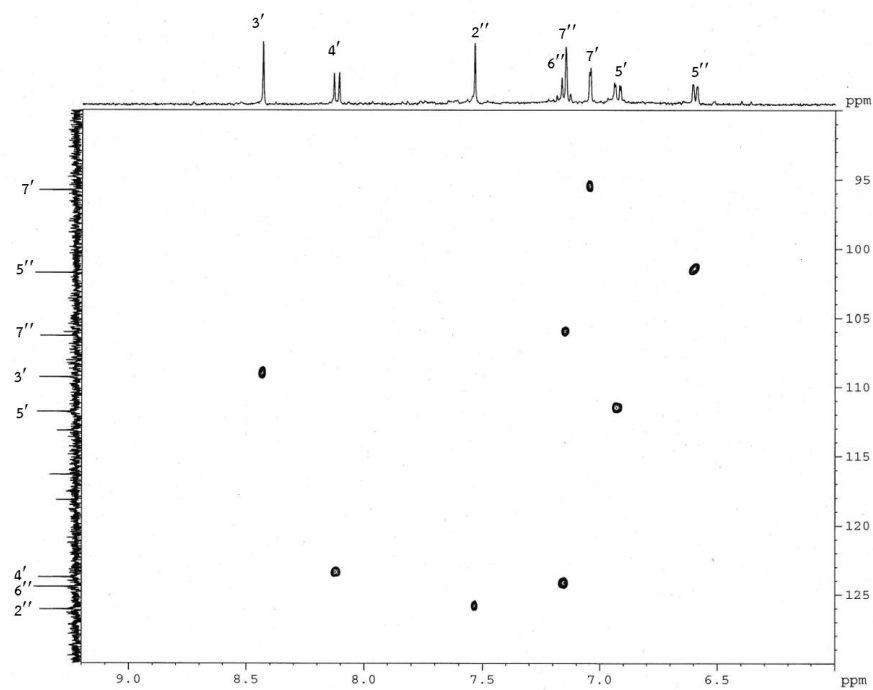


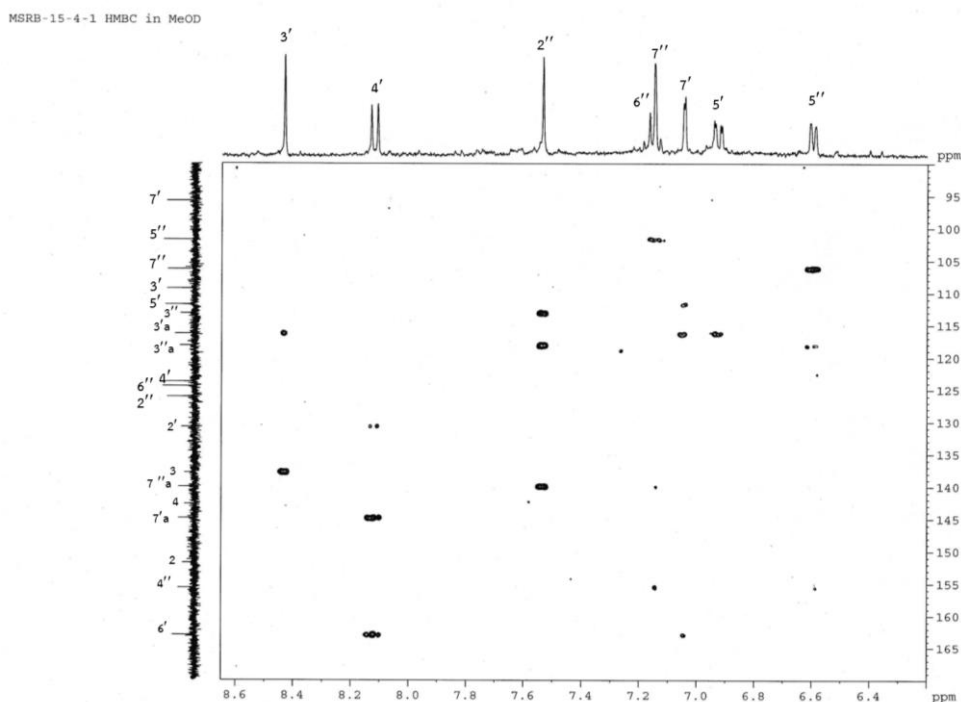
Figure 134. $^{13}\text{C-NMR}$ spectrum of compound **12** (100 MHz, CD_3OD)

MSRB-15-4-1 HSQC in MeOD

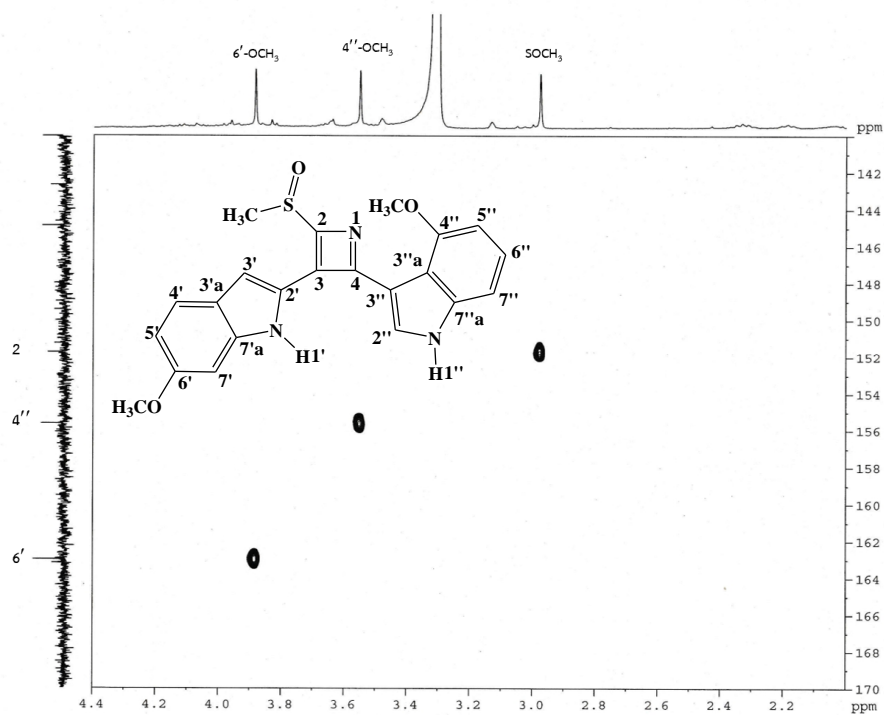
Figure 135. ^1H - ^{13}C HSQC spectrum of compound 12

MSRB-15-4-1 HSQC in MeOD

Figure 136. ^1H - ^{13}C HSQC spectrum of compound 12
(expansion between δ_{H} 6.0-9.1 ppm, δ_{C} 90-130 ppm)



MSRB-15-4-1 HMBC in MeOD



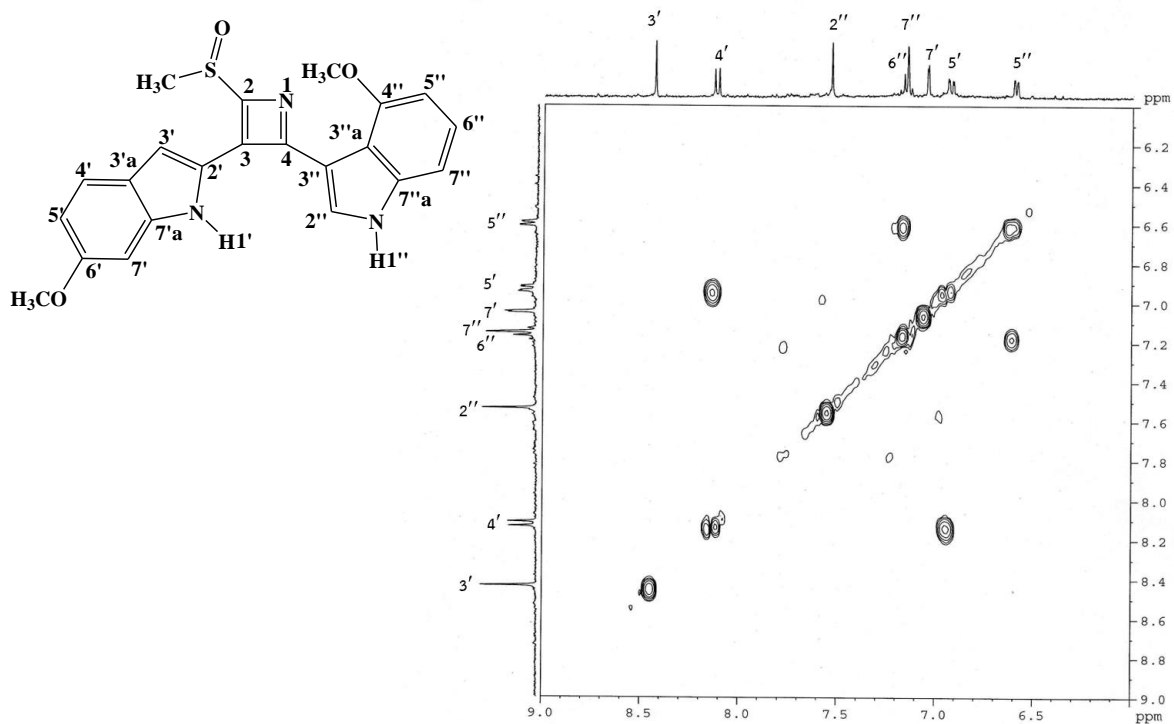


Figure 139. ^1H - ^1H COSY spectrum of compound 12
(expansion between δ_{H} 6.0-9.0 ppm)

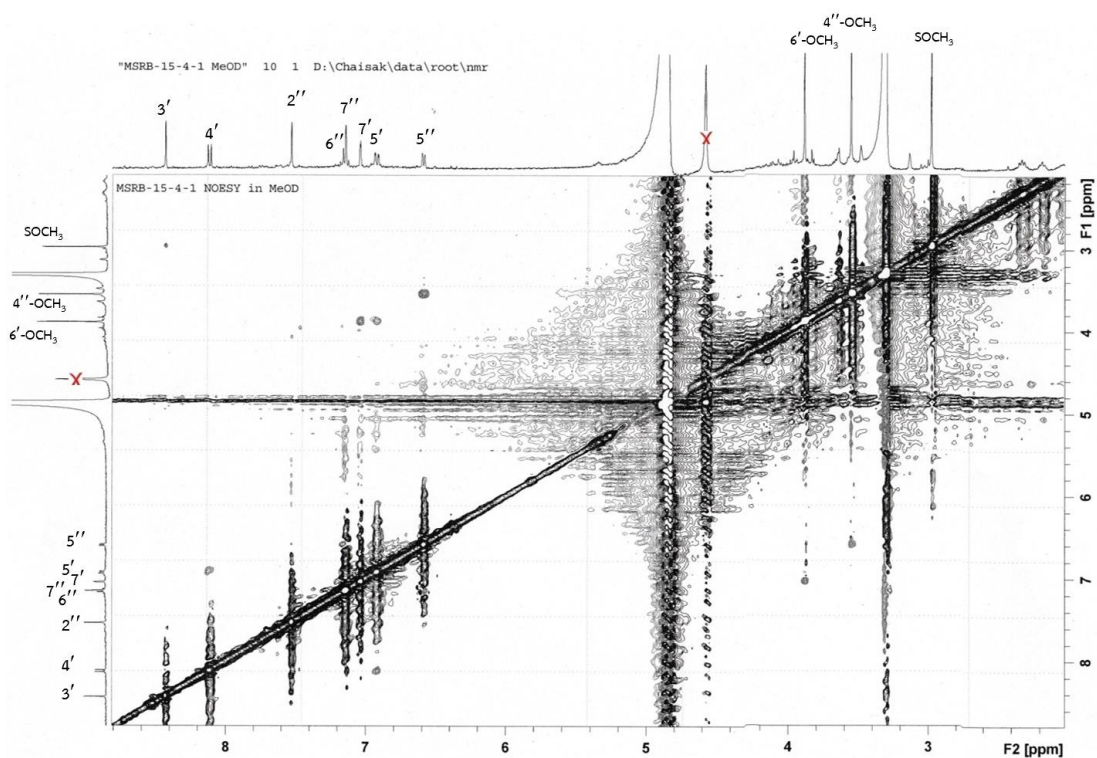


Figure 140. ^1H - ^1H NOESY spectrum of compound 12
(expansion between δ_{H} 2.0-9.0 ppm)

4.2.8 Structure elucidation of compound **13** (maeruabisindole C)

Compound **13** was isolated as a dark green amorphous solid, having a molecular formula of $C_{20}H_{13}N_3O_2$ based on its pseudo molecular $[M-H]^-$ ion peak in the HR-ESI mass spectrum (**Figure 141**) at m/z 326.0968 (calculated for $C_{20}H_{12}N_3O_2$, 326.0935), requiring sixteen degrees of unsaturation. Its IR spectrum (**Figure 143**) showed absorption bands due to hydroxyl and amine groups (3359 cm^{-1}), nitrile (2212 cm^{-1}) and aromatic ring (1632 and 1468 cm^{-1}). Its UV absorption maxima were measured at λ_{max} 210, 285, 355 and 365 nm (**Figure 142**).

The ^1H NMR spectra of compound **13** (**Table 16** and **Figure 144-145**) showed signals of one 1,2,3-trisubstituted benzene ring at δ_{H} 6.80 (1H, *d*, $J = 8.0$ Hz, H-2), 7.40 (1H, *t*, $J = 8.0$ Hz, H-3) and 7.24 (1H, *d*, $J = 8.0$ Hz, H-4), one 1,2,4-trisubstituted benzene ring at δ_{H} 8.33 (1H, *d*, $J = 8.8$ Hz, H-7), 6.86 (1H, *dd*, $J = 8.8, 2.4$ Hz, H-8) and 7.02 (1H, *d*, $J = 2.4$ Hz, H-10), an aromatic proton at δ_{H} 8.53 (1H, *s*, H-12), two NH protons at δ_{H} 10.86 (1H, *br s*, NH-5) and 10.39 (1H, *br s*, NH-11), a methoxy group at δ_{H} 4.12 (3H, *s*, 1-OCH₃) and a hydroxyl group at δ_{H} 8.70 (1H, *br s*, 9-OH).

Its ^{13}C NMR spectra (**Table 16** and **Figure 146-147**) showed signals of eleven quaternary carbons at δ_{C} 113.0 (C-12b), 115.4 (C-6b), 82.5 (C-6), 122.0 (C-12a), 123.0 (C-6a), 138.0 (C-5a), 135.8 (C-11a), 143.4 (C-4a), 144.6 (C-10a), 157.1 (C-1) and 158.8 (C-9), seven methine carbons at δ_{C} 97.5 (C-10), 101.5 (C-2), 105.1 (C-4), 110.0 (C-8), 110.2 (C-12), 122.6 (C-7) and 128.2 (C-3), a methoxy carbon at δ_{C} 56.0 (1-OCH₃), and a nitrile carbon at δ_{C} 118.3 (6-CN).

These spectroscopic data indicated that the structure of compound **13** comprised of two indole rings connected into the core structure of indolo[3,2-*b*]carbazole (Wahlström *et al.*, 2007). The ^1H - ^{13}C HMBC cross peaks from NH-5 to C-5a, C-6, C-12a and C-12b, from NH-11 signal to C-6a, C-6b, and C-10a and from H-12 to C-5a, C-6a, C-12a and C-12b confirmed this skeleton. A methoxy group could be located at C-1 based on a HMBC correlation observed from its proton signal (δ_{H} 4.12) to C-1 and a ^1H - ^1H NOESY cross peak between its signal and that of H-2. The hydroxyl substitution at C-9 was proven by the HMBC correlations of its proton signal (δ_{H} 8.70)

to C-8, C-9 and C-10, as well as its ^1H - ^1H NOESY correlations with both H-8 and H-10. In addition, a NOESY cross peak was also observed between H-12 and NH-11. Finally, the nitrile group could be placed at position 6 of the indolo[3,2-*b*]carbazole nucleus. The downfield chemical shifts of H-7 and NH-5 signals might be due to the anisotropic effect of this nitrile group. Thus, the chemical structure of compound **13** was elucidated as 9-hydroxy-1-methoxy-5,11-dihydroindolo[3,2-*b*]carbazole-6-carbonitrile. It was given the name maeruabisindole C.

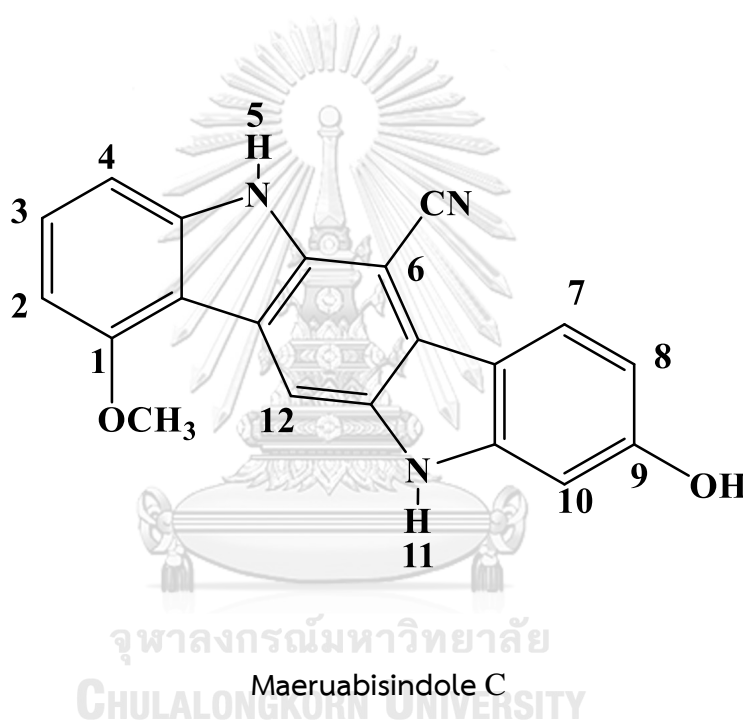


Table 16. ^1H -, ^{13}C NMR and HMBC data of compound **13** (400 MHz, in acetone- d_6)

Position	Compound 13		
	δ_{H} , (mult., J in Hz)	δ_{C}	HMBC correlation with
1		157.1	
2	6.80 (<i>d</i> , 8.0)	101.5	C-1, C-1a, C-4
3	7.40 (<i>t</i> , 8.0)	128.2	C-1, C-1a, C-2, C-4a
4	7.24 (<i>d</i> , 8.0)	105.1	C-1, C-1a, C-2
4a		143.4	-
NH-5	10.86, <i>br s</i>		C-1a, C-5a, C-12a
5a		138.0	-
6		82.5	-
6a		123.0	-
6b		115.4	
7	8.33 (<i>d</i> , 8.8)	122.6	C-6a, C-9, C-10, C-10a
8	6.86 (<i>dd</i> , 8.8, 2.4)	110.0	C-7a, C-9, C-10
9		158.8	-
10	7.02 (<i>d</i> , 2.4)	97.5	C-7a, C-8, C-9
10a		144.6	-
NH-11	10.39, <i>br s</i>		C-6a, C-7a, C-10a
11a		135.8	-
12	8.53, <i>s</i>	110.2	C-1a, C-5a, C-6a
12a		122.0	-
12b		113.0	
1-OCH ₃	4.12, <i>s</i>	56.0	C-1
6-CN		118.3	-
9-OH	8.70, <i>br s</i>		-

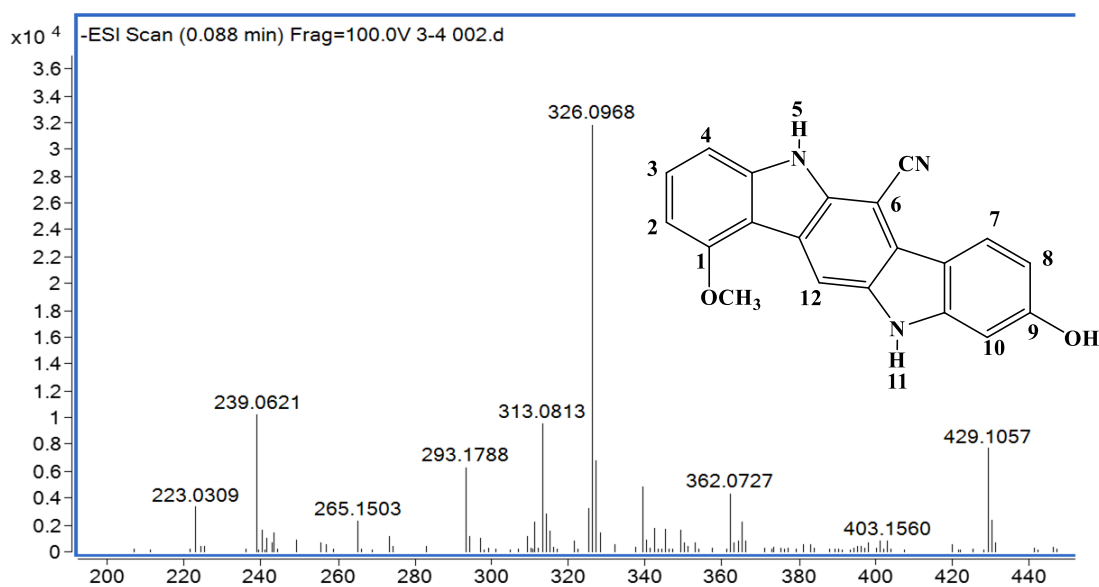


Figure 141. HR-ESI mass spectrum of compound 13

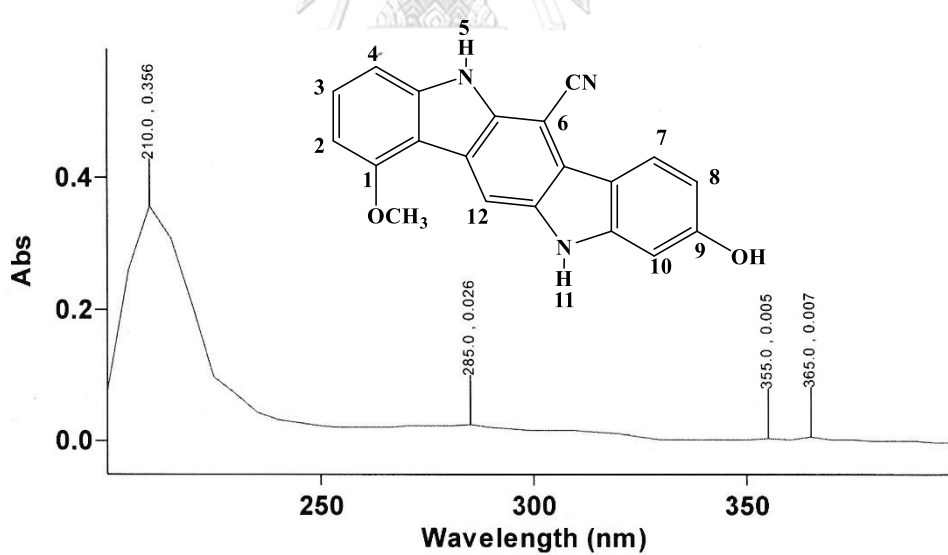


Figure 142. UV spectrum of compound 13

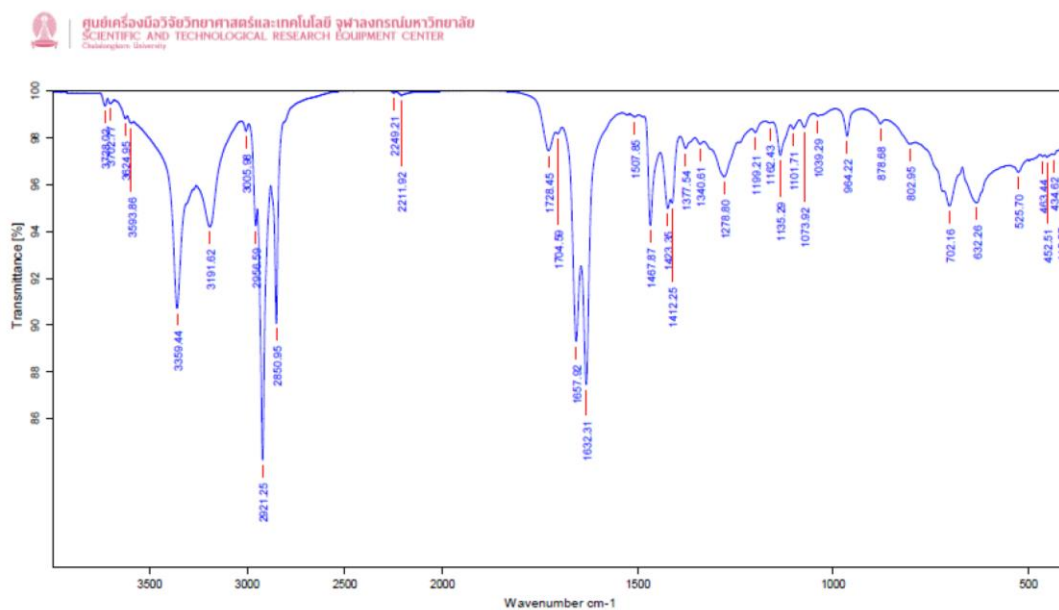
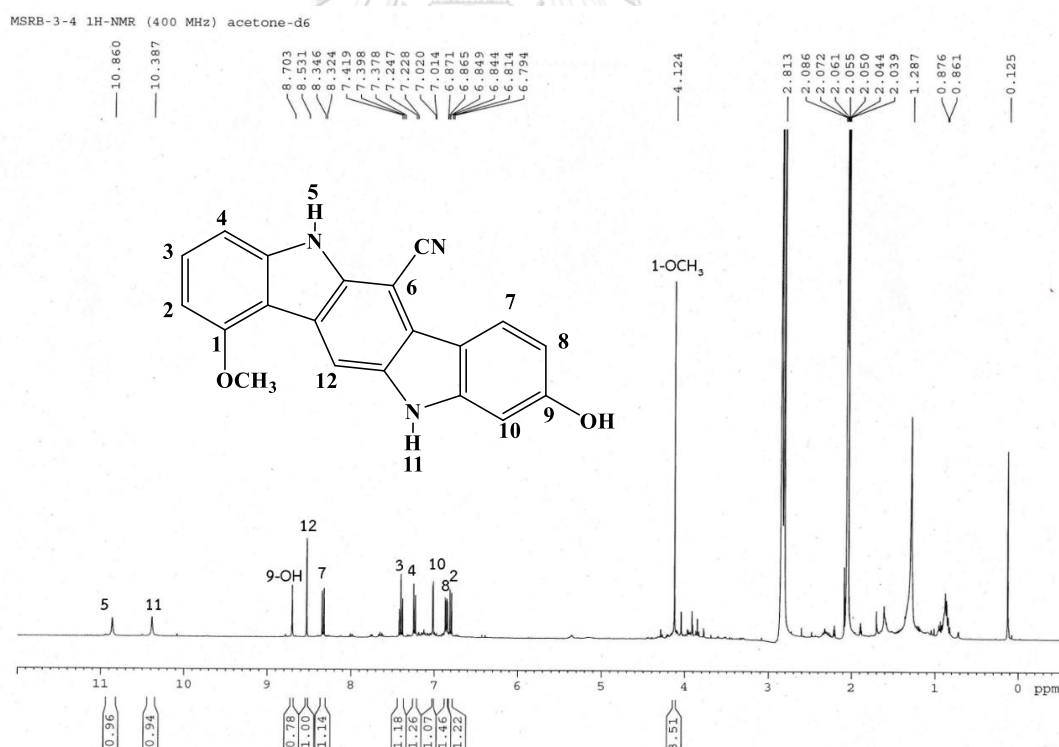
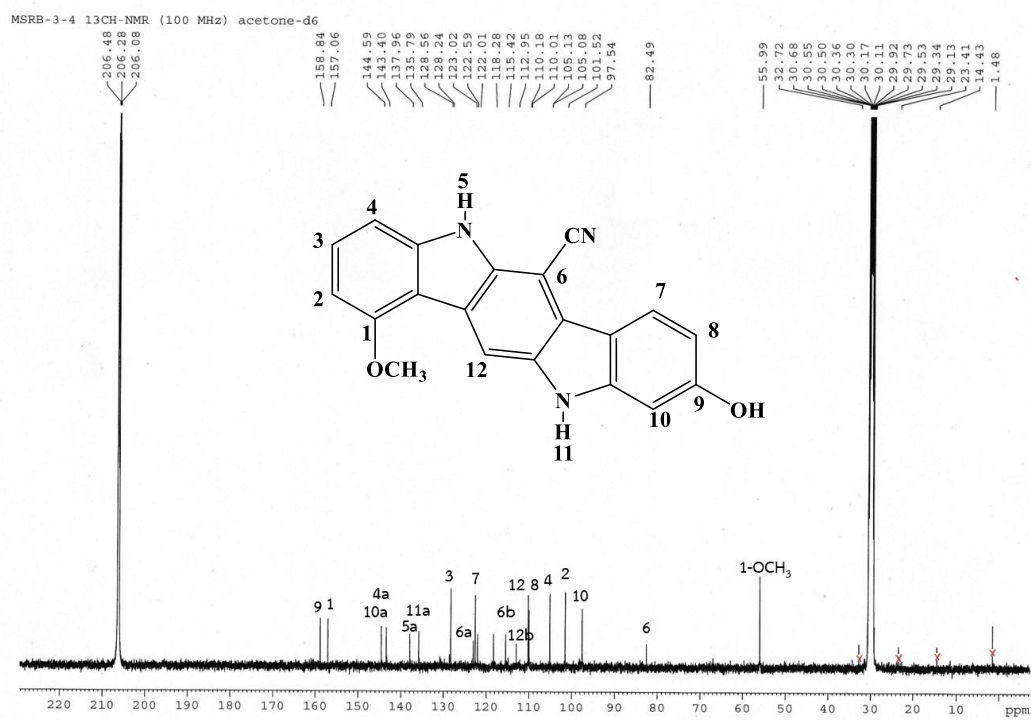
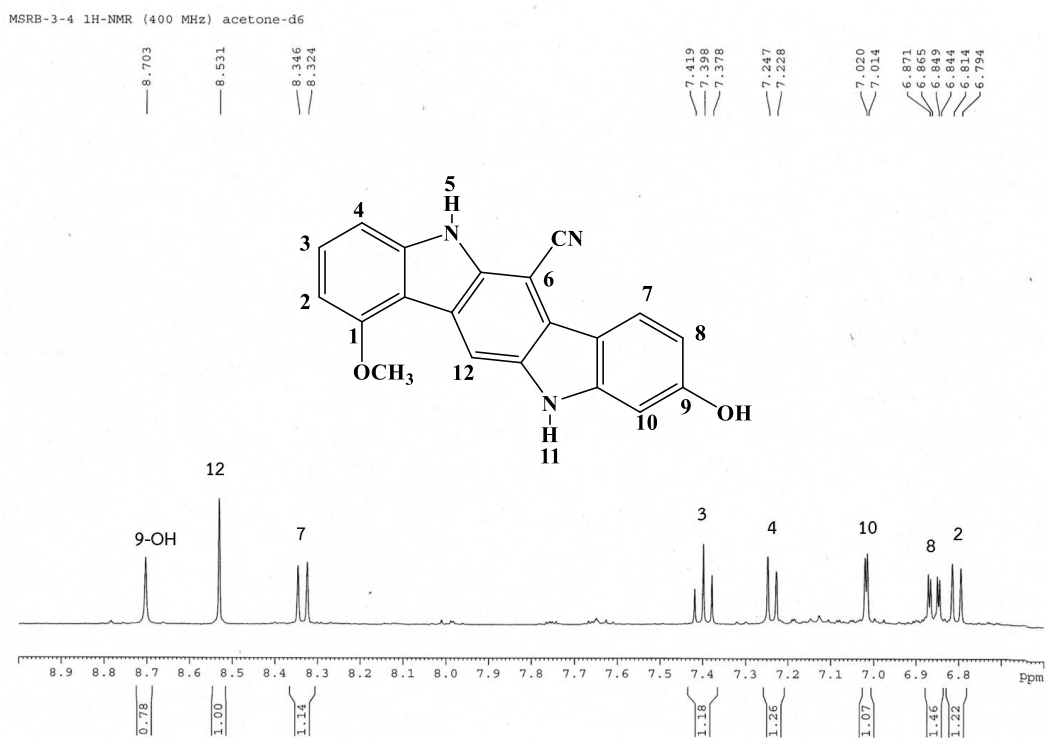


Figure 143. IR spectrum of compound 13

Figure 144. ¹H-NMR spectrum of compound 13 (400 MHz, acetone-d₆)



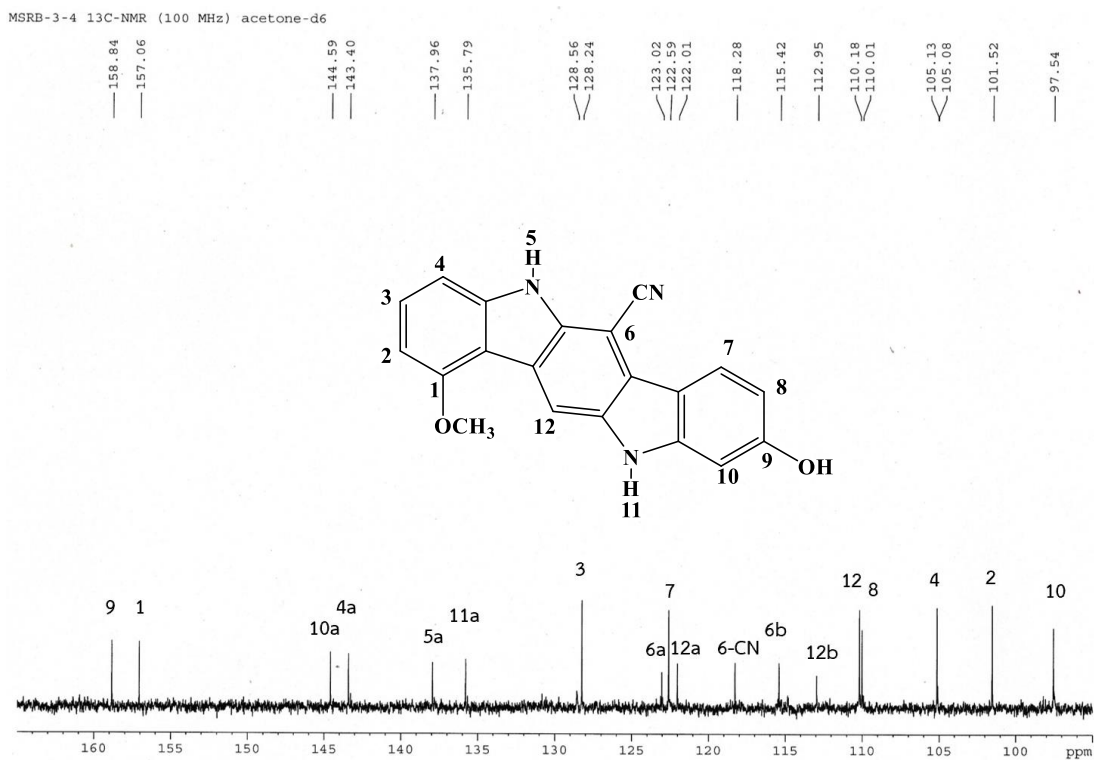


Figure 147. ¹³C-NMR spectrum of compound 13
(expansion between δ_c 95-165 ppm)

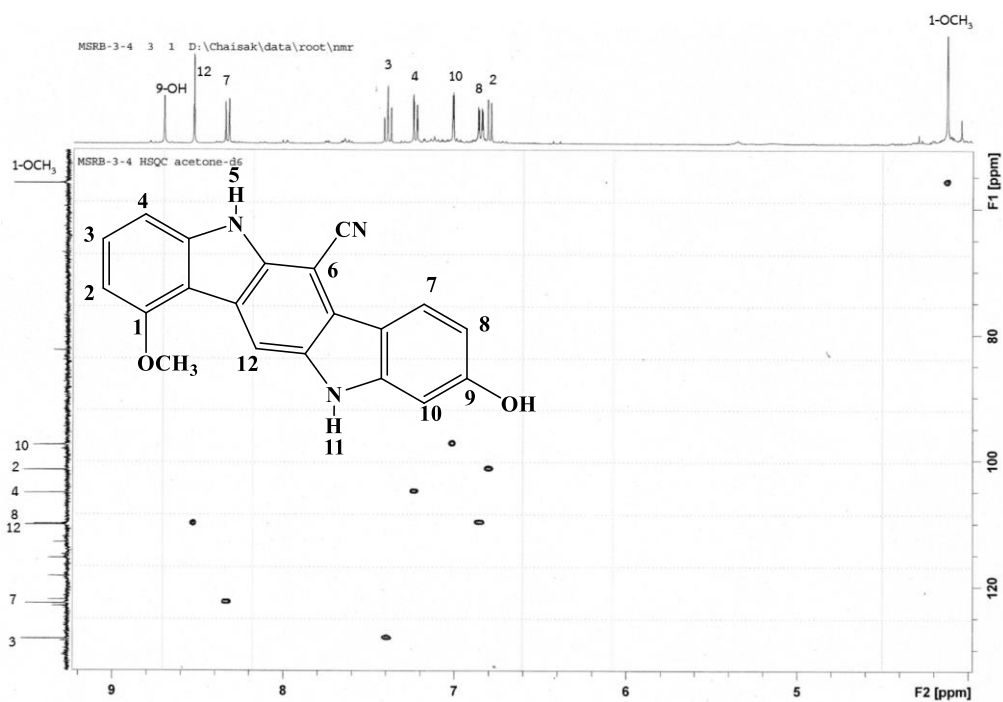


Figure 148. ¹H-¹³C HSQC spectrum of compound 13

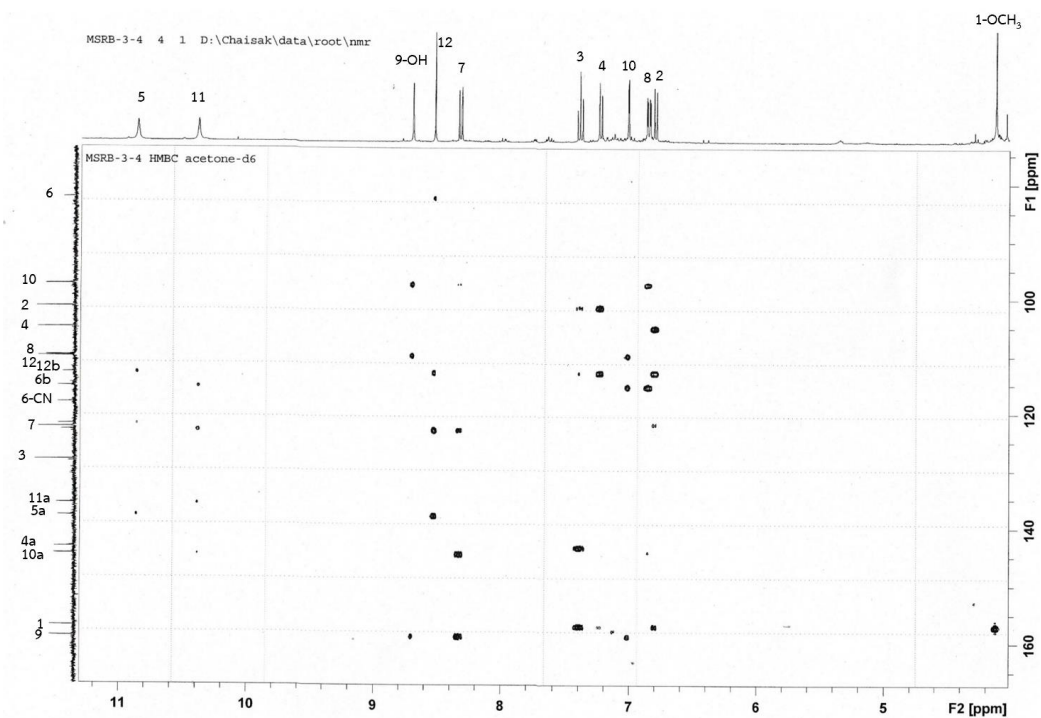


Figure 149. ^1H - ^{13}C HMBC spectrum of compound 13

MSRB-3-4 HMBC acetone-d6

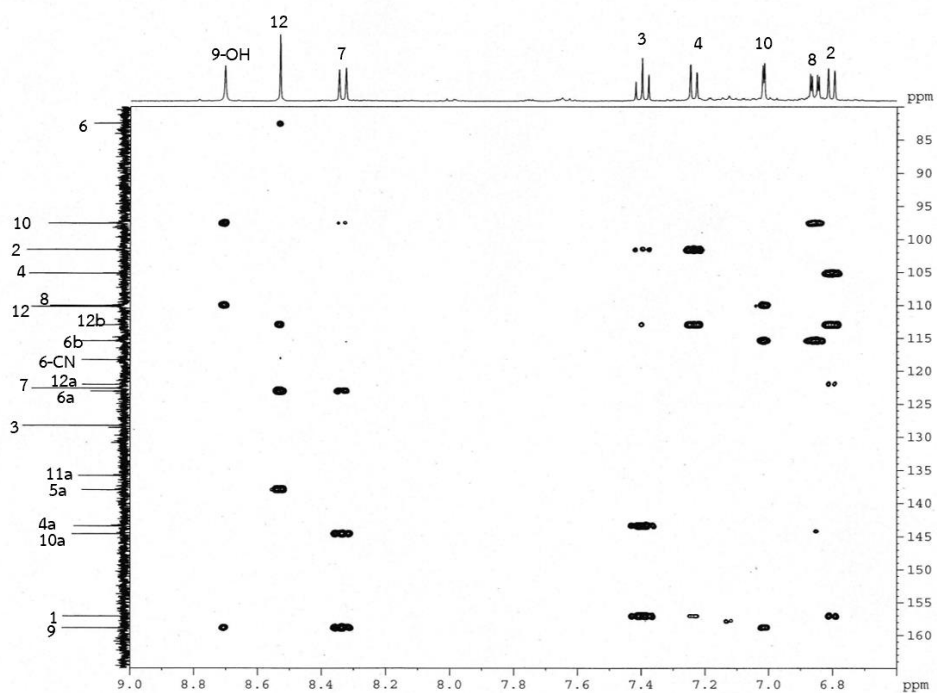


Figure 150. ^1H - ^{13}C HMBC spectrum of compound 13

(expansion between δ_{H} 6.7-9.0 ppm, δ_{C} 80-165 ppm)

MSRB-3-4 HMBC acetone-d6

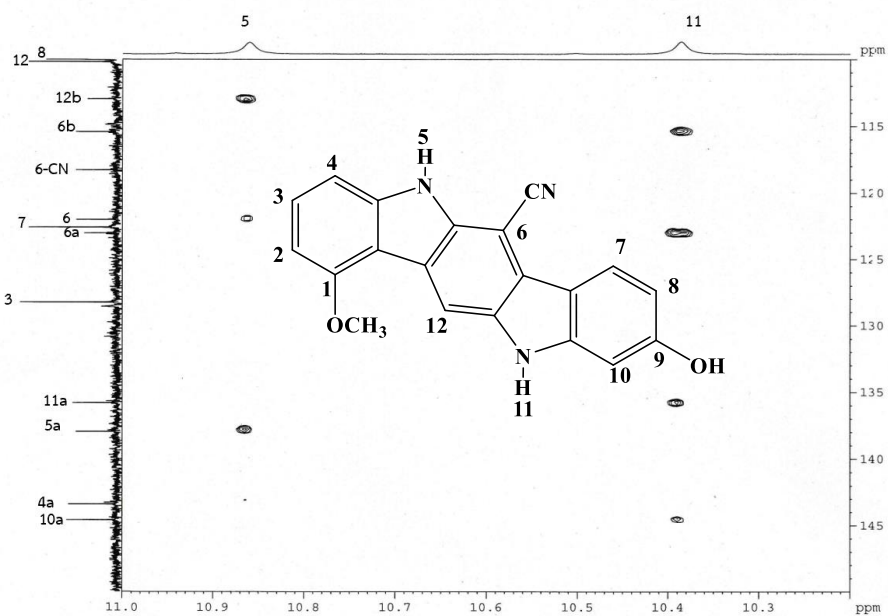


Figure 151. ^1H - ^{13}C HMBC spectrum of compound 13
(expansion between δ_{H} 10.2- 11.0 ppm, δ_{C} 110-150 ppm)

MSRB-3-4 COSY acetone-d6

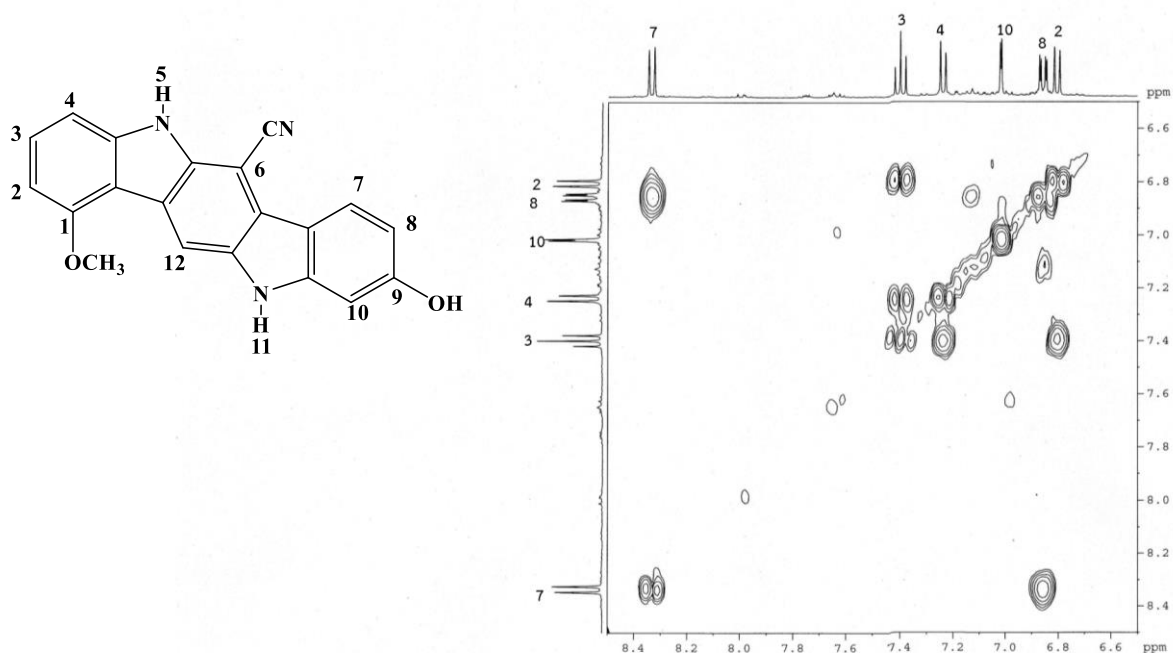
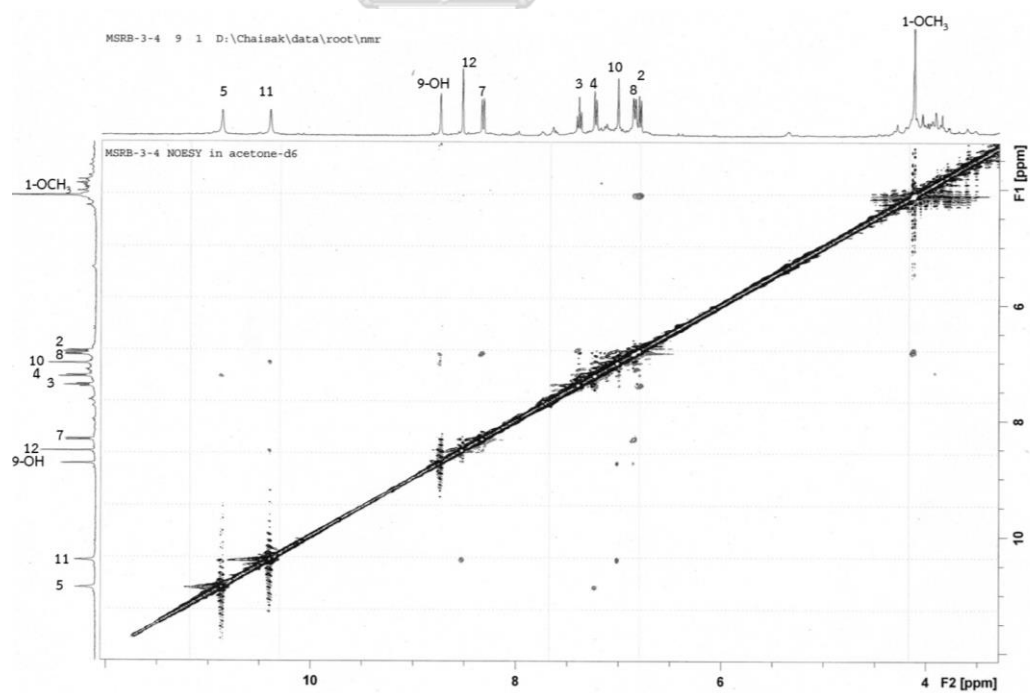
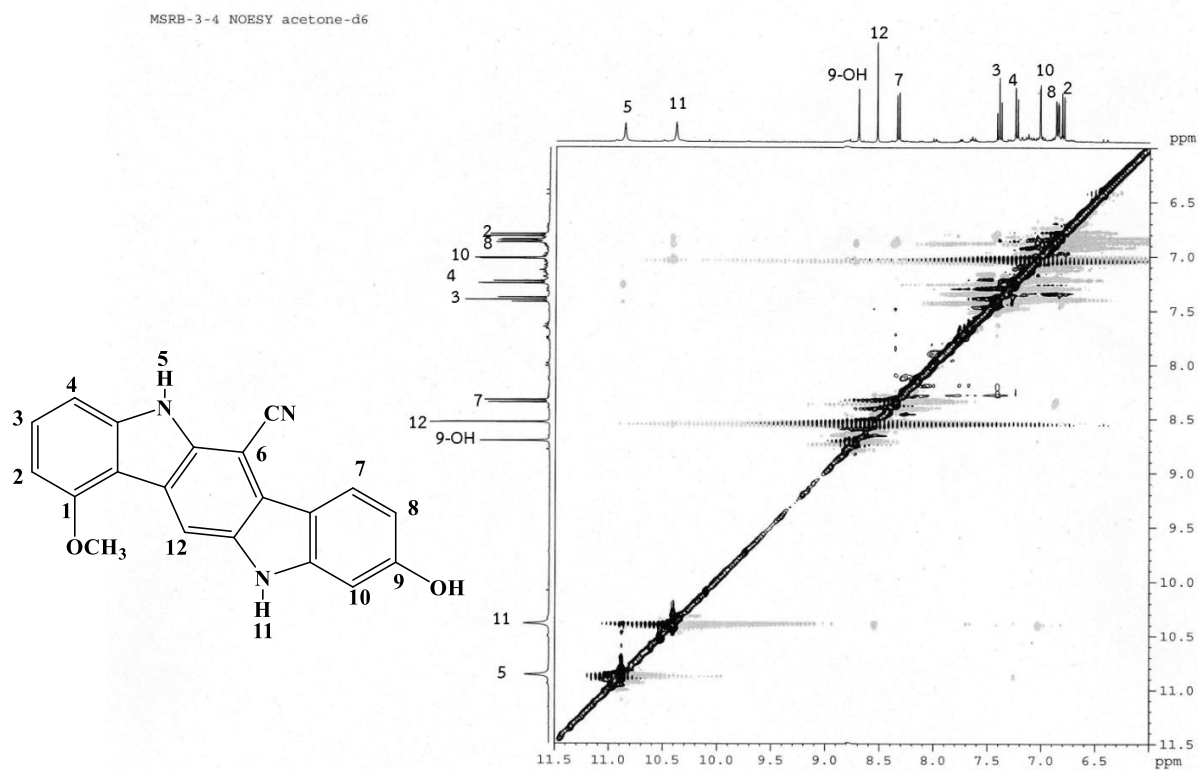


Figure 152. ^1H - ^1H COSY spectrum of compound 13



4.3 Inhibition of nitric oxide production in LPS-induced macrophages RAW 264.7 by isolated compounds

All compounds from *C. micracantha* stems and *M. siamensis* roots were tested for inhibition of nitric oxide production in LPS-induced macrophage RAW 264.7 cells. Among 5 compounds isolated from *C. micracantha*, (–)-pauciflorol E exhibited strong inhibitory activity with an IC₅₀ of 123.40 ± 4.51 μM, whereas methyl 6-methoxy-3-indolecarbonate inhibited NO production with an IC₅₀ of 198.00 ± 5.57 μM (Table 17). Interestingly, the stilbene dimer [(–)-pauciflorol E], having a keto carbonyl at position 8a, possessed NO inhibition activity, whereas the 8a-hydroxy substituted stilbene dimer ((+)-ampelopsin A) was inactive. The NO inhibitory activity of (–)-pauciflorol E, methyl 6-methoxy-3-indolecarbonate, and (–)-syringaresinol was first revealed in this study.

Table 17. Inhibitory concentrations of isolated compounds from *C. micracantha* stems on nitric oxide (NO) production and cell viability in LPS-induced RAW 264.7 cells

Compound	IC ₅₀ of NO inhibition (μM) ^a	Cytotoxicity (μM) ^b
methyl 6-methoxy-3-indolecarbonate (compound 1)	198.00 ± 5.57**	>200
vanillic acid (compound 2)	no activity at 50	no toxicity at 50
(–)-syringaresinol (compound 3)	284.80 ± 7.16**	>200
(+)-ampelopsin A (compound 4)	no activity at 50	no toxicity at 50
(–)-pauciflorol E (compound 5)	123.40 ± 4.51**	>200
Indomethacin	166.30 ± 6.24	>200

** $p < 0.001$ versus indomethacin (positive control)

^a The IC₅₀ of NO inhibition was expressed as Mean ± SEM (standard error of the mean) from three independent experiments.

^b The maximum concentration of test compounds was 200 μM.

As for *M. siamensis*, maerubisindole B showed the strongest NO inhibition (IC_{50} $31.1 \pm 1.0 \mu\text{M}$) among the isolates from *M. siamensis* roots, followed by maerubisindole B (IC_{50} $56.7 \pm 2.2 \mu\text{M}$), maeroxide C (IC_{50} $92.2 \pm 5.1 \mu\text{M}$), (+)-maeruanitrile A (IC_{50} $186.4 \pm 13.0 \mu\text{M}$) and maeruanitrile B (IC_{50} $186.8 \pm 13.3 \mu\text{M}$), compared to indomethacin (IC_{50} $150.0 \pm 16.0 \mu\text{M}$, a positive control) (**Table 18**). Most notably bisindole alkaloids exhibited anti-inflammatory activity; for example, isatindigosides F and G from *Isatis tinctoria* roots (Brassicaceae) showed NO inhibitory activity at IC_{50} of 70.3 ± 6.9 , and $67.3 \pm 5.5 \mu\text{M}$, respectively (Dongdong Zhang *et al.*, 2020). In addition, indole-3-acetonitrile compounds isolated from *Isatis indigotica* roots such as indole-3-acetonitrile, arvelexin, 1-methoxy-indole-3-acetonitrile also demonstrated the NO inhibitory activity (Yang *et al.*, 2014).



Table 18. Inhibition concentrations of isolated compounds from *M. siamensis* roots on nitric oxide (NO) production and cell viability in LPS-induced RAW 264.7 cells

Compound	IC ₅₀ of NO inhibition (μM) ^a	Cytotoxicity (μM) ^c
(+)-maeruanitrile A (compound 6)	186.4 ± 13.0	>200
maeruanitrile B (compound 7)	186.8 ± 13.3	>200
maeroxime A (compound 8)	n.d. ^b	toxicity at 100
maeroxime B (compound 9)	>200 (231.2 ± 11.6 ***)	>200
maeroxime C (compound 10)	92.2 ± 5.1**	>200
maeruabisindole A (compound 11)	n.d. ^b	toxicity at 100
maeruabisindole B (compound 12)	31.1 ± 1.04****	toxicity at 100
maeruabisindole C (compound 13)	56.7 ± 2.2****	>200
indomethacin	150.0 ± 16.0	>200

p* < 0.005 *p* < 0.001 and *****p* < 0.0001 versus indomethacin (positive control)

^a The IC₅₀ of NO inhibition was expressed as Mean ± SEM from three independent experiments.

^b n.d. refers to 'not determined'. The compound could not be determined for IC₅₀ value due to its cytotoxicity

^c The maximum concentration of test compounds was 200 μM. Cytotoxic was indicated by the concentration given that cell viability was lower than 80 %. The tested concentration that exhibited cell viability below 80% was noted as "toxicity at that concentration".

CHAPTER V

CONCLUSION

Phytochemical investigation of *Capparis micracantha* stems and *Maerua siamensis* roots led to the isolation of five known compounds [methyl 6-methoxy-3-indolecarbonate, vanillic acid, (-)-syringaresinol, (+)-ampelopsin A, and (-)-pauciflorol E] from *C. micracantha* and eight new compounds named (+)-maeruanitrile A, maeruanitrile B, maeroximes A – C, and maeruabisindoles A – C from *M. siamensis*. For nitric oxide inhibition assay in LPS-induced macrophages RAW 264.7, (-)-pauciflorol E, methyl 6-methoxy-3-indolecarbonate, (-)-syringaresinol from *C. micracantha* exhibited the activity at IC₅₀ of 123.40 ± 4.51, 198.00 ± 5.57 and 284.80 ± 7.16 µM, respectively. In addition, maeruabisindole B, maeruabisindole C, maeroxime C, maeruanitrile A, and maeruanitrile B displayed nitric oxide inhibition at IC₅₀ of 31.1 ± 1.04, 56.7 ± 2.2, 92.2 ± 5.1, 186.4 ± 13.0, 186.8 ± 13.3, respectively, while an IC₅₀ of indomethacin (a drug for anti-inflammation) is in the range of 150.0 – 166.3 µM.

These findings reveal the anti-inflammatory compounds in *C. micracantha* stems and *M. siamensis* roots which are herbal drugs used for treatment of inflammation according to Thai traditional medicines and supports the use of this herbal drugs. Moreover, the promising nitric oxide inhibitory compounds (maeruabisindoles B and C) could be developed for the potent anti-inflammatory agents in the future.

Furthermore, this study expands knowledge in chemotaxonomy regarding plants in Capparaceae; for example, stilbene oligomers and lignans in *Capparis* species and glucosinolate-derived indole alkaloids and bisindole alkaloids in *Maerua* plants. Lastly, indole alkaloids which is similarly found in plants in the family Brassicaceae, it could be used as chemotaxonomic marker between Capparaceae and Brassicaceae, which are closely related family.

REFERENCES

- Abdel-Mogib, M. (1999). A lupane triterpenoid from *Maerua oblongifolia*. *Phytochemistry*, 51(3), 445-448. [https://doi.org/10.1016/s0031-9422\(98\)00771-7](https://doi.org/10.1016/s0031-9422(98)00771-7)
- Ahmad, I., Fatima, I., Afza, N., Malik, A., Lodhi, M. A. and Choudhary, M. I. (2008). Urease and serine protease inhibitory alkaloids from *Isatis tinctoria*. *Journal of Enzyme Inhibition and Medicinal Chemistry*, 23(6), 918-921. <https://doi.org/10.1080/14756360701743580>
- Ahmad, V. U., Arif, S., Amber, A. R., Nasir, M. A. and Ghani, K. U. (1986). A New alkaloid from root bark of *Capparis decidua*. *Zeitschrift fur Naturforschung B*, 41(8), 1033-1035. <https://doi.org/10.1515/znb-1986-0818>
- Ahmed, Z. F., Rizk, A. M., Hammouda, F. M. and Seif El-Nasr, M. M. (1972). Glucosinolates of egyptian *Capparis* species. *Phytochemistry*, 11(1), 251-256. [https://doi.org/https://doi.org/10.1016/S0031-9422\(00\)89999-9](https://doi.org/https://doi.org/10.1016/S0031-9422(00)89999-9)
- Akoto, O., Oppong, I. V., Mensah-Addae, I., Waibel, R. and Achenbach, H. (2008). Isolation and characterization of dipeptide derivative and phytosterol from *Capparis tomentosa* Lam. *Scientific Research and Essay* 3(8), 355-358.
- Al-Gendy, A. A., El-gindi, O. D., Hafez, A. S. and Ateya, A. M. (2010). Glucosinolates, volatile constituents and biological activities of *Erysimum corinthium* Boiss. (Brassicaceae). *Food Chemistry*, 118(3), 519-524. <https://doi.org/10.1016/j.foodchem.2009.05.009>
- Al-Mahweety, J. A. N. and Alyahawi, A. (2020). Phytochemistry study of plants belonging to *Capparis*. *Universal Journal of Pharmaceutical Research*, 5(2), 38-41. <https://doi.org/10.22270/ujpr.v5i2.387>
- Al-Shehbaz, I. A., Beilstein, M. A. and Kellogg, E. A. (2006). Systematics and phylogeny of the Brassicaceae (Cruciferae): an overview. *Plant Systematics and Evolution*, 259(2-4), 89-120. <https://doi.org/10.1007/s00606-006-0415-z>
- Aliyazicioglu, R., Eyupoglu, O. E., Sahin, H., Yildiz, O. and Baltas, N. (2013). Phenolic components, antioxidant activity, and mineral analysis of *Capparis spinosa* L. *African Journal of Biotechnology*, 12(47), 6643-6649.

- Antoine, F., Fabre, N., Pean, C., Montaut, S., Fauvel, M. T., Rollin, P. and Fouraste, I. (2001). Novel indole-type glucosinolates from woad (*Isatis tinctoria* L.). *Tetrahedron Letters*, 42(51), 9015-9017. [https://doi.org/https://doi.org/10.1016/S0040-4039\(01\)02015-9](https://doi.org/https://doi.org/10.1016/S0040-4039(01)02015-9)
- Bailey, C. D., Koch, M. A., Mayer, M., Mummenhoff, K., O'Kane, S. L., Warwick, S. I., Windham, M. D. and Al-Shehbaz, I. A. (2006). Toward a global phylogeny of the Brassicaceae. *Molecular Biology and Evolution*, 23(11), 2142-2160. <https://doi.org/10.1093/molbev/msl087>
- Beilstein, M. A., Al-Shehbaz, I. A., Mathews, S. and Kellogg, E. A. (2008). Brassicaceae phylogeny inferred from phytochrome A and ndhF sequence data: tribes and trichomes revisited [<https://doi.org/10.3732/ajb.0800065>]. *American Journal of Botany*, 95(10), 1307-1327. <https://doi.org/https://doi.org/10.3732/ajb.0800065>
- Bektas, N., Arslan, R., Goger, F., Kirimer, N. and Ozturk, Y. (2012). Investigation for anti-inflammatory and anti-thrombotic activities of methanol extract of *Capparis ovata* buds and fruits. *Journal of Ethnopharmacology*, 142(1), 48-52. <https://doi.org/10.1016/j.jep.2012.04.011>
- Bishay, D. W., Abdel-Baky, A. M., Ramadan, M. A., Ibraheim, Z. Z., Itokawa, H. and Takeya, K. (1990). Phytochemical study of *Maerua crassifolia* Forssk. growing in Egypt. *Bulletin of Pharmaceutical Sciences*, 13(1), 39-49.
- Browne, L. M., Conn, K. L., Ayert, W. A. and Tewari, J. P. (1991). The camalexins: New phytoalexins produced in the leaves of *Camelina sativa* (cruciferae). *Tetrahedron*, 47(24), 3909-3914. [https://doi.org/https://doi.org/10.1016/S0040-4020\(01\)86431-0](https://doi.org/https://doi.org/10.1016/S0040-4020(01)86431-0)
- Calis, I., Kuruizum, A. and Ruedi, P. (1999). 1H-Indole-3 acetonitrile glycosides from *Capparis spinosa* fruits. *Phytochemistry*, 50(7), 1205-1208. [https://doi.org/https://doi.org/10.1016/S0031-9422\(98\)00669-4](https://doi.org/https://doi.org/10.1016/S0031-9422(98)00669-4)
- Chang, S. W., Kim, K. H., Lee, I. K., Choi, S. U., Ryu, S. Y. and Lee, K. R. (2009). Phytochemical constituents of *Bistorta manshuriensis*. *Natural Product Sciences*, 15(4), 234-240.
- Chayamarit, K. (1991). capparaceae. In T. k. and Smittinand (Ed.), *Flora of Thailand* (Vol. 5 No. 3). Chutima Press Bangkok.
- Chen, J. J., Kuo, W. L., Liao, H. R., Kuo, Y. H., Chen, I. S., Shu, C. W., Sung, P. J., Lim, Y. P., Wang, T. C., Cheng, M. J. and Xu, R. (2017). A new benzenoid and anti-

- inflammatory constituent of *Capparis acutifolia*. *Chemistry of Natural Compounds*, 53(1), 21-23. <https://doi.org/10.1007/s10600-017-1901-y>
- Chen, M., Gan, L., Lin, S., Wang, X., Li, L., Li, Y., Zhu, C., Wang, Y., Jiang, B., Jiang, J., Yang, Y. and Shi, J. (2012). Alkaloids from the root of *Isatis indigotica*. *Journal of Natural Products*, 75(6), 1167-1176. <https://doi.org/10.1021/np3002833>
- Chen, C. Y., Wu, T. Y., Chang, F. R. and Wu, Y. C. (1998). Lignans and kauranes from the stems of *Annona cherimola*. *Journal of the Chinese Chemical Society*, 45, 629-634. <https://doi.org/10.1002/jccs.199800095>
- Chripkova, M., Drutovic, D., Pilatova, M., Mikes, J., Budovska, M., Vaskova, J., Broggin, M., Mirossay, L. and Mojzis, J. (2014). Brassinin and its derivatives as potential anticancer agents. *Toxicology in Vitro*, 28(5), 909-915. <https://doi.org/https://doi.org/10.1016/j.tiv.2014.04.002>
- Cristina, I., Diego, R., Ma Concepcion, O., Francisco, A. and Jose-Antonio, B. (2006). A systematic revision of *Capparis* section (CAPPARACEAE). *Annals of the Missouri Botanical Garden*, 93(1), 122-149. [https://doi.org/10.3417/0026-6493\(2006\)93\[122:ASROCS\]2.0.CO;2](https://doi.org/10.3417/0026-6493(2006)93[122:ASROCS]2.0.CO;2)
- Cronquist, A. (1981). *A Integrated System of Classification of Flowering Plants*. Columbia University Press, New York, 248-250.
- Csaszar, A. G., Demaison, J. and Rudolph, H. D. (2015). Equilibrium structures of three-, four-, five-, six-, and seven-membered unsaturated N-containing heterocycles. *J Phys Chem A*, 119(9), 1731-1746. <https://doi.org/10.1021/jp5084168>
- Danz, H., Stoyanova, S., Thomet, O. A., Simon, H. U., Dannhardt, G., Ulbrich, H. and Hamburger, M. (2002). Inhibitory activity of tryptanthrin on prostaglandin and leukotriene synthesis. *Planta Medica*, 68(10), 875-880. <https://doi.org/10.1055/s-2002-34922>
- Danz, H., Stoyanova, S., Wippich, P., Brattstrom, A. and Hamburger, M. (2001). Identification and isolation of the cyclooxygenase2 inhibitory principle in *Isatis tinctoria*. *Planta Medica* 67, 411-416. <https://doi.org/10.1055/s-2001-15805>
- Devys, M., Barbier, M., Kollmann, A., Rouxel, T. and Bousquet, J. F. (1990). Cyclobraassinin sulphoxide, a sulphur-containing phytoalexin from *Brassica juncea*.

- Phytochemistry*, 29(4), 1087-1088. [https://doi.org/https://doi.org/10.1016/0031-9422\(90\)85408-8](https://doi.org/https://doi.org/10.1016/0031-9422(90)85408-8)
- Forster, Y., Ghaffar, A. and Bienz, S. (2016). A new view on the codonocarpine type alkaloids of *Capparis decidua*. *Phytochemistry*, 128, 50-59. <https://doi.org/https://doi.org/10.1016/j.phytochem.2016.03.019>
- Frechard, A., Fabre, N., Pean, C., Montaut, S., Fauvel, M. T., Rollin, P. and Fouraste, I. (2001). Novel indole-type glucosinolates from woad (*Isatis tinctoria* L.). *Tetrahedron Letters*, 42(51), 9015-9017. [https://doi.org/https://doi.org/10.1016/S0040-4039\(01\)02015-9](https://doi.org/https://doi.org/10.1016/S0040-4039(01)02015-9)
- Fu, X. P., Wu, T., Abdurahim, M., Su, Z., Hou, X. L., Aisa, H. A. and Wu, H. (2008). New spermidine alkaloids from *Capparis spinosa* roots. *Phytochemistry Letters*, 1(1), 59-62. <https://doi.org/https://doi.org/10.1016/j.phytol.2008.01.001>
- Gazioglu, I., Semen, S., Acar, O. O., Kolak, U., Sen, A. and Topcu, G. (2020). Triterpenoids and steroids isolated from Anatolian *Capparis ovata* and their activity on the expression of inflammatory cytokines. *Pharm Biol*, 58(1), 925-931. <https://doi.org/10.1080/13880209.2020.1814356>
- Gmelin, R., Saarivirta, M. and Virtanen, A. I. (1960). Glucobrassicin, der precursor von thiocyanat-ion and ascorbigen in *Brassica oleracea* species. *Suomen Kemist(B33)*, 172.
- Gramosa, N. V., Lemos, T. L. G. and Braz-Filho, R. (1997). Volatile constituents isolated from *Capparis flexuosa* of Brazil. *Journal of Essential Oil Research*, 9(6), 709-712. <https://doi.org/10.1080/10412905.1997.9700819>
- Gross, D., Porzel, A. and Schmidt, J. (1994). Phytoalexine mit Indolstruktur aus Kohlrabi (*Brassica oleracea* var. gongylodes)+/Indole Phytoalexins from the Kohlrabi (*Brassica oleracea* var. gongylodes)⁺. *Zeitschrift fur Naturforschung C*, 49(5-6), 281-286.
- Guo, Q., Li, D., Xu, C., Zhu, C., Guo, Y., Yu, H., Wang, X. and Shi, J. (2020). Indole alkaloid glycosides with a 1'-(phenyl)ethyl unit from *Isatis indigotica* leaves. *Acta Pharmaceutica Sinica B*, 10(5), 895-902. <https://doi.org/https://doi.org/10.1016/j.apsb.2019.09.001>

- Hall, J. C., Sytsma, K. J. and Iltis, H. H. (2002). Phylogeny of Capparaceae and Brassicaceae based on chloroplast sequence data [<https://doi.org/10.3732/ajb.89.11.1826>]. *American Journal of Botany*, 89(11), 1826-1842. <https://doi.org/https://doi.org/10.3732/ajb.89.11.1826>
- Heywood, V. H. (1993). *Flowering Plants of the World*. Oxford University Press.
- Hong, W., Xi, Y., Zhou W., Huang X. and S., S. (2019). Research review on the main chemical constituents and pharmacological properties of the leaves of *Isatis indigotica* Fortune. *Asian Journal of Traditional Medicines*, 14(5), 227-236.
- Hong, Y., Choi, Y. H., Han, Y. E., Oh, S. J., Lee, A., Lee, B., Magnan, R., Ryu, S. Y., Choi, C. W. and Kim, M. S. (2021). Central administration of ampelopsin A isolated from *Vitis vinifera* ameliorates cognitive and memory function in a scopolamine-induced dementia model. *Antioxidants*, 10(6). <https://doi.org/10.3390/antiox10060835>
- Ibraheim, Z. Z. (1995). A new ionol glucoside from *Maerua crassifolia* forssk grown in egypt. *Bulletin of Pharmaceutical Sciences*, 18(1), 27-31.
- Ibrahim, A. K., Youssef, A. I., Arafa, A. S. and Ahmed, S. A. (2013). Anti-H5N1 virus flavonoids from *Capparis sinaica* Veill. *Natural Product Research*, 27(22), 2149-2153. <https://doi.org/10.1080/14786419.2013.790027>
- Jao, C. W., Lin, W. C., Wu, Y. T., and Wu, P. L. (2008). Isolation, structure elucidation, and synthesis of cytotoxic tryptanthrin analogues from *Phaius mishmensis*. *Journal of Natural Product*, 71, 1275-1279.
- Jimenez, L. D., Ayer, W. A. and Tewari, J. P. (1997). Phytoalexins produced in the leaves of *Capsella bursa-pastoris* (shepherd's purse). *Phytoprotection*, 78(3), 99-103. <https://doi.org/https://doi.org/10.7202/706124ar>
- Kamel, W. M., Abd El-Ghani, M. M. and El-Bous, M. M. (2009). Taxonomic study of Capparaceae from Egypt: Revisited. *African Journal of Plant Science and Biotechnology*(3), 27-35.
- Khanfar, M. A., Sabri, S. S., Zarga, M. H. and Zeller, K. P. (2003). The chemical constituents of *Capparis spinosa* of Jordanian origin. *Natural Product Research*, 17(1), 9-14. <https://doi.org/10.1080/10575630290034302>

- Khang, P. V., Thuong, S. D., Nhung, V. V., Shen, S. and Ma, L. (2021). Two new polycyclic compounds and cytotoxic activities of ethanol and ethyl acetate extract of leaves of *Capparis dongvanensis* (Sy.) and their chemotaxonomic significance. *Polycyclic Aromatic Compounds*, 1-7. <https://doi.org/10.1080/10406638.2020.1871383>
- Kim, H. S., Lee, J. H., Moon, S. H., Ahn, D. U. and Paik, H. D. (2020). Ovalbumin hydrolysates inhibit nitric oxide production in LPS-induced RAW 264.7 macrophages. *Food Science of Animal Resources*, 40(2), 274-285. <https://doi.org/10.5851/kosfa.2020.e12>
- Kim, J. S., Choi, Y. H., Seo, J. H., Lee, J. W., Kim, Y. S., Ryu, S. Y., Kang, J. S., Kim, Y. K. and Kim, S. H. (2004). Chemical constituents from the root of *Brassica campestris* ssp. *rapa*. *Korean Journal of Pharmacognosy*, 35(3), 259-263.
- Kim, S. M., Oh, E. Y., Lee, J. H., Nam, D., Lee, S. G., Lee, J., Kim, S. H., Shim, B. S. and Ahn, K. S. (2015). Brassinin combined with capsaicin enhances apoptotic and anti-metastatic effects in PC-3 human prostate cancer cells [<https://doi.org/10.1002/ptr.5478>]. *Phytotherapy Research*, 29(11), 1828-1836. <https://doi.org/https://doi.org/10.1002/ptr.5478>
- Kinashi, H., Suzuki, Y., Takeuchi, S. and Kawarada, A. (1976). Possible metabolic intermediates from IAA to β -acid in rice bran. *Agricultural and Biological Chemistry*, 40(12), 2465-2470. <https://doi.org/10.1080/00021369.1976.10862405>
- Li, B., Chen, W. S., Zhang, H. M., Zhang, W. D., Yang, G. J. and Qiao, C. Z. (2003). A new alkaloids isolated from *tetraploidy banlangen*. *Acta Pharmaceutica Sinica*, 38(6), 430-432.
- Li, Y. Q., Yang, S. L., Li, H. R. and Xu, L. Z. (2008). Two new alkaloids from *Capparis himalayensis*. *Chemical and Pharmaceutical Bulletin*, 56(2), 189-191.
- Li, Z., Zhao, J., Zhou, H., Li, L., Ding, Y., Li, J., Zhou, B., Jiang, H., Zhong, N., Hu, W. and Yang, Z. (2018). Cappariloside A shows antiviral and better anti-inflammatory effects against influenza virus via regulating host IFN signaling, *in vitro* and *vivo*. *Life Sciences*, 200, 115-125. <https://doi.org/10.1016/j.lfs.2018.03.033>
- Lincy, M. P., Mohan, V. R. and Jeeva, S. (2014). Antiinflammatory activity of aerial part of *Maerua apetala* Roth (Jacobs) against carrageenan induced paw edema. *Current Pharmaceutical Review and Research*, 5(4), 131-137.

- Lingjie, M., Guo, Q., Chen, M., Jiang, J., Li, Y. and Shi, J. (2018). Isatindolignanose A, a glucosidic indole-lignan conjugate from an aqueous extract of the *Isatis indigotica* roots. *Chinese Chemical Letters*, 29(8), 1257-1260. <https://doi.org/https://doi.org/10.1016/j.ccllet.2017.12.001>
- Liu, J. F., Jiang, Z. Y., Wang, R. R., Zheng, Y. T., Chen, J. J., Zhang, X. M. and Ma, Y. B. (2007). Isatisine A, a novel alkaloid with an unprecedented skeleton from leaves of *Isatis indigotica*. *Organic Letters*, 9(21), 4127-4129. <https://doi.org/10.1021/ol701540y>
- Liu, Y., Wang, X., Chen, M., Lin, S., Li, L. and Shi, J. (2016). Three pairs of alkaloid enantiomers from the root of *Isatis indigotica*. *Acta Pharmaceutica Sinica B*, 6(2), 141-147. <https://doi.org/https://doi.org/10.1016/j.apsb.2016.01.003>
- Liu, Y. F., Chen, M. H., Guo, Q. L., Lin, S., Xu, C. B., Jiang, Y. P., Li, Y. H., Jiang, J. D. and Shi, J. G. (2015). Antiviral glycosidic bisindole alkaloids from the roots of *Isatis indigotica*. *Journal of Asian Natural Products Research*, 17(7), 689-704. <https://doi.org/10.1080/10286020.2015.1055729>
- Lu, H. T., Liu, J., Deng, R. and Song, J. Y. (2012). Preparative isolation and purification of indigo and indirubin from *Folium isatidis* by high-speed counter-current chromatography. *Phytochemical Analysis*, 23(6), 637-641. <https://doi.org/https://doi.org/10.1002/pca.2366>
- Mabberley, D. J. (1997). *The plant book: A Portable Dictionary of the Higher Plants*. Cambridge University Press.
- Matthaus, B. and Ozcan, M. (2002). Glucosinolate composition of young shoots and flower buds of capers (*Capparis* Species) growing wild in Turkey. *Journal of Agricultural and Food Chemistry*, 50(25), 7323-7325. <https://doi.org/10.1021/jf020530+>
- Mehta, R. G., Liu, J., Constantinou, A., Thomas, C. F., Hawthorne, M., You, M., Gerhauser, C., Pezzuto, J. M., Moon, R. C. and Moriarty, R. M. (1995). Cancer chemopreventive activity of brassinin, a phytoalexin from cabbage. *Carcinogenesis*, 16(2), 399-404. <https://doi.org/10.1093/carcin/16.2.399>
- Meng, L., Guo, Q., Liu, Y., Chen, M., Li, Y., Jiang, J. and Shi, J. (2017). Indole alkaloid sulfonic acids from an aqueous extract of *Isatis indigotica* roots and their antiviral activity. *Acta Pharm Sin B*, 7(3), 334-341. <https://doi.org/10.1016/j.apsb.2017.04.003>

- Meng, L. J., Guo, Q. L., Zhu, C. G., Xu, C. B. and Shi, J. G. (2018). Isatindigodiphindoside, an alkaloid glycoside with a new diphenylpropylindole skeleton from the root of *Isatis indigotica*. *Chinese Chemical Letters*, 29(1), 119-122. <https://doi.org/10.1016/j.ccllet.2017.05.019>
- Mithen, R., Bennett, R. and Marquez, J. (2010). Glucosinolate biochemical diversity and innovation in the Brassicales. *Phytochemistry*, 71(17), 2074-2086. <https://doi.org/https://doi.org/10.1016/j.phytochem.2010.09.017>
- Monde, K., Sasaki, K., Shirata, A. and Takasugi, M. (1990). 4-Methoxybrassinin, a sulphur-containing phytoalexin from *Brassica oleracea*. *Phytochemistry*, 29(5), 1499-1500. [https://doi.org/https://doi.org/10.1016/0031-9422\(90\)80108-5](https://doi.org/https://doi.org/10.1016/0031-9422(90)80108-5)
- Monde, K., Sasaki, K., Shirata, A. and Takasugi, M. (1991a). Brassicanal C and two dioxindoles from cabbage. *Phytochemistry*, 30(9), 2915-2917. [https://doi.org/https://doi.org/10.1016/S0031-9422\(00\)98224-4](https://doi.org/https://doi.org/10.1016/S0031-9422(00)98224-4)
- Monde, K., Sasaki, K., Shirata, A. and Takasugi, M. (1991b). Methoxybrassenins A and B, sulphur-containing stress metabolites from *Brassica oleracea* var. *Capitata*. *Phytochemistry*, 30(12), 3921-3922. [https://doi.org/https://doi.org/10.1016/0031-9422\(91\)83435-N](https://doi.org/https://doi.org/10.1016/0031-9422(91)83435-N)
- Monde, K., Takasugi, M. and Shirata, A. (1995). Three sulphur-containing stress metabolites from Japanese radish. *Phytochemistry*, 39(3), 581-586. [https://doi.org/https://doi.org/10.1016/0031-9422\(95\)00011-U](https://doi.org/https://doi.org/10.1016/0031-9422(95)00011-U)
- Nabavi, S. F., Maggi, F., Daglia, M., Habtemariam, S., Rastrelli, L. and Nabavi, S. M. (2016). Pharmacological Effects of *Capparis spinosa* L. *Phytotherapy Research*, 30(11), 1733-1744. <https://doi.org/10.1002/ptr.5684>
- Nobsathian, S., Bullangpoti, V., Kumrungsee, N., Wongs, N. and Ruttanakum, D. (2018). Larvicidal effect of compounds isolated from *Maerua siamensis* (Capparidaceae) against *Aedes aegypti* (Diptera: Culicidae) larvae. *Chemical and Biological Technologies in Agriculture*, 5(1). <https://doi.org/10.1186/s40538-018-0120-5>
- Oberthur, C., Schneider, B., Graf, H. and Hamburger, M. (2004). The Elusive Indigo Precursors in Woad (*Isatis tinctoria* L.) – Identification of the Major Indigo Precursor, Isatan A, and a Structure Revision of Isatan B

- [<https://doi.org/10.1002/cbdv.200490009>]. *Chemistry & Biodiversity*, 1(1), 174-182.
<https://doi.org/https://doi.org/10.1002/cbdv.200490009>
- Oshima, Y., Ueno, Y., Hikino, H., Ling-Ling, Y. and Kun-Ying, Y. (1990). Ampelopsins A, B and C, new oligostilbenes of ampelopsis Brevipedunculata VAR. Hancei. *Tetrahedron*, 46(15), 5121-5126. [https://doi.org/https://doi.org/10.1016/S0040-4020\(01\)87819-4](https://doi.org/https://doi.org/10.1016/S0040-4020(01)87819-4)
- Palo, T., Thaworn, A., Charoenkij, P., Thamsermsang, O., Chotewuttakorn, S., Tripatara, P., Laohapand, T. and Akarasereenont, P. (2017). The Effects of Thai Herbal Ha-Rak Formula on COX Isoform Expression in Human Umbilical Vein Endothelial Cells Induced by IL-1 β . *Evidence-Based Complementary and Alternative Medicine*, 2017, 9383272. <https://doi.org/10.1155/2017/9383272>
- Pedras, M., Soledade C., Montaut, S. and Suchy, M. (2004). Phytoalexins from the Crucifer Rutabaga: Structures, Syntheses, Biosyntheses, and Antifungal Activity. *The Journal of Organic Chemistry*, 69(13), 4471-4476. <https://doi.org/10.1021/jo049648a>
- Pedras, M., Soledade C. and Sorensen, J. L. (1998). Phytoalexin accumulation and antifungal compounds from the crucifer wasabi. *Phytochemistry*, 49(7), 1959-1965. [https://doi.org/https://doi.org/10.1016/S0031-9422\(98\)00424-5](https://doi.org/https://doi.org/10.1016/S0031-9422(98)00424-5)
- Pedras, M., Soledade C., Sorensen, J. L., Okanga, F. I. and Zaharia, I. L. (1999). Wasalexins A and B, new phytoalexins from wasabi: Isolation, synthesis, and antifungal activity. *Bioorganic & Medicinal Chemistry Letters*, 9(20), 3015-3020. [https://doi.org/https://doi.org/10.1016/S0960-894X\(99\)00523-5](https://doi.org/https://doi.org/10.1016/S0960-894X(99)00523-5)
- Pedras, M., Soledade C. and Yaya, E. E. (2010). Phytoalexins from Brassicaceae: News from the front. *Phytochemistry*, 71(11), 1191-1197. <https://doi.org/https://doi.org/10.1016/j.phytochem.2010.03.020>
- Pedras, M., Soledade C. and Zaharia, I. L. (2000). Sinalbins A and B, phytoalexins from *Sinapis alba*: Elicitation, isolation, and synthesis. *Phytochemistry*, 55(3), 213-216. [https://doi.org/https://doi.org/10.1016/S0031-9422\(00\)00277-6](https://doi.org/https://doi.org/10.1016/S0031-9422(00)00277-6)
- Pedras, M., Soledade C., Sarwar, Mohammed G., Suchy, M. a. and Adio, A. M. (2006). The phytoalexins from cauliflower, caulilexins A, B and C: Isolation, structure

- determination, syntheses and antifungal activity. *Phytochemistry*, 67(14), 1503-1509. <https://doi.org/https://doi.org/10.1016/j.phytochem.2006.05.020>
- Pedras, M. S. (2008a). The chemical ecology of crucifers and their fungal pathogens: boosting plant defenses and inhibiting pathogen invasion. *The Chemical Record*, 8(2), 109-115. <https://doi.org/10.1002/tcr.20140>
- Pedras, M. S. (2008b). The chemical ecology of crucifers and their fungal pathogens: Boosting plant defenses and inhibiting pathogen invasion. *The Chemical Record*, 8(2), 109-115. <https://doi.org/10.1002/tcr.20140>
- Pedras, M. S., Zheng, Q. A. and Gadagi, R. S. (2007). The first naturally occurring aromatic isothiocyanates, rapalexins A and B, are cruciferous phytoalexins. *Chemical Communications journal*(4), 368-370. <https://doi.org/10.1039/b615424g>
- Pedras, M. S. C., Chumala, P. B. and Suchy, M. (2003). Phytoalexins from *Thlaspi arvense*, a wild crucifer resistant to virulent *Leptosphaeria maculans*: Structures, syntheses and antifungal activity. *Phytochemistry*, 64(5), 949-956. [https://doi.org/https://doi.org/10.1016/S0031-9422\(03\)00441-2](https://doi.org/https://doi.org/10.1016/S0031-9422(03)00441-2)
- Pedras, M. S. C., Zheng, Q. A., Schatte, G. and Adio, A. M. (2009). Photochemical dimerization of wasalexins in UV-irradiated *Thellungiella halophila* and *in vitro* generates unique cruciferous phytoalexins. *Phytochemistry*, 70(17), 2010-2016. <https://doi.org/https://doi.org/10.1016/j.phytochem.2009.09.008>
- Pilatova, M., Sarissky, M., Kutschy, P., Mirossay, A., Mezencev, R., Curillova, Z., Suchy, M., Monde, K., Mirossay, L. and Mojzic, J. (2005). Cruciferous phytoalexins: Antiproliferative effects in T-Jurkat leukemic cells. *Leukemia Research*, 29(4), 415-421. <https://doi.org/https://doi.org/10.1016/j.leukres.2004.09.003>
- Ramadan, M. A., Lbraheim, Z. Z., Abdel-Baky, A. M., Bishay, D. W. and Itokawa, H. (1999). Minor constituents from *Maerua crassifolia* Forssk growing in Egypt. *Bulletin of Pharmaceutical Sciences*, 21(1), 109-115.
- Rathee, P., Rathee, D., Rathee, D. and Rathee, S. (2012). *In-vitro* cytotoxic activity of β -sitosterol triacontenate isolated from *Capparis decidua* (Forsk.) Edgew. *Asian Pacific Journal of Tropical Medicine*, 5(3), 225-230. [https://doi.org/https://doi.org/10.1016/S1995-7645\(12\)60029-7](https://doi.org/https://doi.org/10.1016/S1995-7645(12)60029-7)

- Robert, L. J. and Morrow, J. D. (2006). *Analgesic-antipyretic and antiinflammatory agents and drugs employed in the treatment of gout*. McGraw-Hill. New York
- Sharma, J. N., Al-Omran, A. and Parvathy, S. S. (2007). Role of nitric oxide in inflammatory diseases. *Inflammopharmacology*, 15(6), 252-259. <https://doi.org/10.1007/s10787-007-0013-x>
- Shi, S. P., Tu, P. F., Dong, C. X. and Jiang, D. (2006). Alkaloids from *Clematis manshurica* Rupr. *Journal of Asian Natural Products Research*, 8(1-2), 73-78. <https://doi.org/10.1080/10286020500480324>
- Simpson, M. G. (2019). 8 - Diversity and classification of flowering plants: Eudicots. In M. G. Simpson (Ed.), *Plant Systematics (Third Edition)* (pp. 285-466). Academic Press. <https://doi.org/https://doi.org/10.1016/B978-0-12-812628-8.50008-0>
- Soledade, M., Pedras, C. and Smith, K. C. (1997). Sinalexin, a phytoalexin from white mustard elicited by destruxin B and *Alternaria brassicae*. *Phytochemistry*, 46(5), 833-837. [https://doi.org/https://doi.org/10.1016/S0031-9422\(97\)00362-2](https://doi.org/https://doi.org/10.1016/S0031-9422(97)00362-2)
- Somei, M., Tanimoto, A., Orita, H., Yamada, F. and Ohta, T. (2001). Syntheses of wasabi phytoalexin (methyl 1-methoxyindole-3-carboxylate) and its 5-iodo derivative, and their nucleophilic substitution reactions. *Heterocycles (Sendai)*, 54(1), 425-432.
- Speranza, J., Miceli, N., Taviano, M. F., Ragusa, S., Kwiecien, I., Szopa, A. and Ekiert, H. (2020). *Isatis tinctoria* L. (Woad): A review of its botany, ethnobotanical uses, phytochemistry, biological activities, and biotechnological studies. *Plants*, 9(3). <https://doi.org/10.3390/plants9030298>
- Sritularak, B., Duangrak, N. and Likhitwitayawuid, K. (2011). A new bibenzyl from *Dendrobium secundum*. 66(5-6), 205-208. <https://doi.org/doi:10.1515/znc-2011-5-602>
- Stevenson, P. C., Green, P. W. C., Farrell, I. W., Brankin, A., Mvumi, B. M. and Belmain, S. R. (2018). Novel agmatine derivatives in *Maerua edulis* with bioactivity against *Callosobruchus maculatus*, A cosmopolitan storage insect pest. *Frontiers in Plant Science*, 9, 1506. <https://doi.org/10.3389/fpls.2018.01506>

- Takasugi, M., Monde, K., Kaisui, N. and Shirata, A. (1987). Spirobrassinin, a novel sulfur-containing phytoalexin from the daikon *Rhaphanus sativus* L. var. *hortensis* (Cruciferae). *Chemistry letters*, 16(8), 1631-1632.
- Theanphong, O. and Somwong, P. (2022). Combination of selected Thai traditional pain relief medicinal plants with anti-inflammatory abilities in a protein denaturation assay. *Pharmacia*, 69, 745-753. <https://doi.org/10.3897/pharmacia.69.e86904>
- Tlili, N., Elfalleh, W., Saadaoui, E., Khaldi, A., Triki, S. and Nasri, N. (2011). The caper (*Capparis* L.): Ethnopharmacology, phytochemical and pharmacological properties. *Fitoterapia*, 82(2), 93-101. <https://doi.org/https://doi.org/10.1016/j.fitote.2010.09.006>
- Truscott, R. J. W., Minchinton, I. and Sang, J. (1983). The isolation and purification of indole glucosinolates from *brassica* species [<https://doi.org/10.1002/jsfa.2740340308>]. *Journal of the Science of Food and Agriculture*, 34(3), 247-254. <https://doi.org/https://doi.org/10.1002/jsfa.2740340308>
- Tsai, D. H., Riediker, M., Berchet, A., Paccaud, F., Waeber, G., Vollenweider, P. and Bochud, M. (2019). Effects of short-and long-term exposures to particulate matter on inflammatory marker levels in the general population. *Environmental Science and Pollution Research*, 26(19), 19697-19704.
- Tsai, Y. C., Lee, C. L., Yen, H. R., Chang, Y. S., Lin, Y. P., Huang, S. H. and Lin, C. W. (2020). Antiviral action of tryptanthrin isolated from *Strobilanthes cusia* leaf against human coronavirus NL63. *Biomolecules*, 10(3). <https://doi.org/10.3390/biom10030366>
- Turner, M. D., Nedjai, B., Hurst, T. and Pennington, D. J. (2014). Cytokines and chemokines: At the crossroads of cell signalling and inflammatory disease. *Biochimica et Biophysica Acta (BBA) - Molecular Cell Research*, 1843(11), 2563-2582. <https://doi.org/https://doi.org/10.1016/j.bbamcr.2014.05.014>
- Vane, J. R. and Botting, R. M. (1998). Anti-inflammatory drugs and their mechanism of action. *Inflammation Research*, 47(2), 78-87.
- Verma, P. D., Dangar, R. D. and Suhagia, B. N. (2013). Evaluation of anti-inflammatory activity of *Capparis decidua* Edgew. *Stem. International Journal* 3(1), 16-19.

- Vig, A. P., Rampal, G., Thind, T. S. and Arora, S. (2009). Bio-protective effects of glucosinolates – A review. *LWT - Food Science and Technology*, 42(10), 1561-1572. <https://doi.org/https://doi.org/10.1016/j.lwt.2009.05.023>
- Wahlström, N., Slätt, J., Stensland, B., Ertan, A., Bergman, J. and Janosik, T. (2007). Synthetic applications of cyanoacetylated bisindoles: Synthesis of novel cycloheptadiindoles, indolocarbazoles, and related aza analogues. *The Journal of Organic Chemistry*, 72(15), 5886-5889. <https://doi.org/10.1021/jo0706729>
- Wang, K. T., Chen, L. G., Tseng, S. H., Huang, J. S., Hsieh, M. S. and Wang, C. C. (2011). Anti-inflammatory effects of resveratrol and oligostilbenes from *Vitis thunbergii* var. *taiwaniana* against lipopolysaccharide-induced arthritis. *Journal of Agricultural and Food Chemistry*, 59(8), 3649-3656. <https://doi.org/10.1021/jf104718g>
- Warinhomhoun, S., Khine, H. E., Sritularak, B., Likhitwitayawuid, K., Miyamoto, T., Tanaka, C., Punsawad, C., Punpreuk, Y., Sungthong, R. and Chaotham, C. (2022). Secondary metabolites in the *Dendrobium heterocarpum* methanolic extract and their Impacts on viability and lipid storage of 3T3-L1 pre-adipocytes. *Nutrients*, 14(14).
- Wei, H., Yufei, X., Weiyu, Z., Xiaoxiao, H. and Shaojiang, S. (2019). Research review on the main chemical constituents and pharmacological properties of the leaves of *Isatis indigotica* Fortune. *Asian Journal of Traditional Medicines*, 14(5), 227-236. <https://chula.idm.oclc.org/login?url=https://search.ebscohost.com/login.aspx?direct=true&db=asn&AN=139879758&site=eds-live>
- Weller, L. E., Wittwer, S. and Sell, H. M. (1953). The detection of 3-indoleacetic acid in caxdiflowerheads. Chromatographic behavior of some indole compounds1, 2. *Journal of the American Chemical Society*, 76(2), 629-630.
- Wiese, S., Wubshet, S. G., Nielsen, J. and Staerk, D. (2013). Coupling HPLC-SPE-NMR with a microplate-based high-resolution antioxidant assay for efficient analysis of antioxidants in food – Validation and proof-of-concept study with caper buds. *Food Chemistry*, 141(4), 4010-4018. <https://doi.org/https://doi.org/10.1016/j.foodchem.2013.06.115>
- Yahia, Y., Benabderrahim, M. A., Tlili, N., Hannachi, H., Ayadi, L. and Elfalleh, W. (2020). Comparison of three extraction protocols for the characterization of caper

- (*Capparis spinosa* L.) leaf extracts: Evaluation of phenolic acids and flavonoids by liquid chromatography – electrospray ionization – tandem mass spectrometry (LC–ESI–MS) and the antioxidant activity. *Analytical Letters*, 53(9), 1366-1377. <https://doi.org/10.1080/00032719.2019.1706546>
- Yang, L., He, C., Sudunabuqi, Bao, X., Wang, X. and Ao, W. (2020). Alkaloids from the leaves of *Isatis indigotica* fortune and their chemotaxonomic significance. *Biochemical Systematics and Ecology*, 93, 104163. <https://doi.org/10.1016/j.bse.2020.104163>
- Yang, L., Wang, G., Wang, M., Jiang, H., Chen, L., Zhao, F. and Qiu, F. (2014). Indole alkaloids from the roots of *Isatis indigotica* and their inhibitory effects on nitric oxide production. *Fitoterapia*, 95, 175-181. <https://doi.org/https://doi.org/10.1016/j.fitote.2014.03.019>
- Yang, T., Wang, C. H., Chou, G. X., Wu, T., Cheng, X. M. and Wang, Z. T. (2010). New alkaloids from *Capparis spinosa*: Structure and X-ray crystallographic analysis. *Food Chemistry*, 123(3), 705-710. <https://doi.org/10.1016/j.foodchem.2010.05.039>
- Zhang, D., Ruan, D., Li, J., Chen, Z., Zhu, W., Guo, F., Chen, K., Li, Y. and Wang, R. (2020). Four undescribed sulfur-containing indole alkaloids with nitric oxide inhibitory activities from *Isatis tinctoria* L. roots. *Phytochemistry*, 174, 112337. <https://doi.org/https://doi.org/10.1016/j.phytochem.2020.112337>
- Zhang, D., Shi, Y., Li, J., Ruan, D., Jia, Q., Zhu, W., Chen, K., Li, Y. and Wang, R. (2019). Alkaloids with nitric oxide inhibitory activities from the roots of *Isatis tinctoria*. *Molecules*, 24(22). <https://doi.org/10.3390/molecules24224033>
- Zhang, D., Sun, Y., Chen, Z., Jia, Q., Zhu, W., Chen, K., Li, Y. and Wang, R. (2020). Bisindole alkaloids with nitric oxide inhibitory activities from an alcohol extract of the *Isatis indigotica* roots. *Fitoterapia*, 146, 104654. <https://doi.org/10.1016/j.fitote.2020.104654>
- Zhang, D., Sun, Y., Shi, Y., Wu, X., Jia, Q., Chen, K., Li, Y. and Wang, R. (2022). Four new indole alkaloids from the roots of *Isatis tinctoria*. *Natural Product Research*. <https://doi.org/https://doi.org/10.1080/14786419.2020.1779716>

- Zhang, H. and Ma, Z. F. (2018). Phytochemical and pharmacological properties of *Capparis spinosa* as a medicinal plant. *Nutrients*, 10(2). <https://doi.org/10.3390/nu10020116>
- Zhang, L., Jiang, X., Zhang, J., Gao, H., Yang, L., Li, D., Zhang, Q., Wang, B., Cui, L. and Wang, X. (2021). (-)-Syringaresinol suppressed LPS-induced microglia activation via downregulation of NF- κ B p65 signaling and interaction with ER β . *International Immunopharmacology*, 99, 107986. <https://doi.org/https://doi.org/10.1016/j.intimp.2021.107986>
- Zhang, S., Hu, D. B., He, J. B., Guan, K. Y. and Zhu, H. J. (2014). A novel tetrahydroquinoline acid and a new racemic benzofuranone from *Capparis spinosa* L., a case study of absolute configuration determination using quantum methods. *Tetrahedron*, 70(4), 869-873. <https://doi.org/https://doi.org/10.1016/j.tet.2013.12.024>
- Zhou, H. F., Xie, C., Jian, R., Kang, J., Li, Y., Zhuang, C. L., Yang, F., Zhang, L. L., Lai, L., Wu, T., and Wu, X. (2011). Biflavonoids from caper (*Capparis spinosa* L.) fruits and their effects in inhibiting NF-kappa B activation. *Journal of Agricultural and Food Chemistry*, 59(7), 3060-3065. <https://doi.org/10.1021/jf105017j>
- Zhou, H., Jian, R., Kang, J., Huang, X., Li, Y., Zhuang, C., Yang, F., Zhang, L., Fan, X., Wu, T. and Wu, X. (2010). Anti-inflammatory effects of caper (*Capparis spinosa* L.) fruit aqueous extract and the isolation of main phytochemicals. *Journal of Agricultural and Food Chemistry*, 58(24), 12717-12721. <https://doi.org/10.1021/jf1034114>
- Zhou, H. F., Xie, C., Jian, R., Kang, J., Li, Y., Zhuang, C. L., Yang, F., Zhang, L. L., Lai, L., Wu, T. and Wu, X. (2011). Biflavonoids from caper (*Capparis spinosa* L.) fruits and their effects in inhibiting NF-kappa B activation. *J Agric Food Chem*, 59(7), 3060-3065. <https://doi.org/10.1021/jf105017j>
- Zou, P. and Koh, H. L. (2007). Determination of indican, isatin, indirubin and indigotin in *Isatis indigotica* by liquid chromatography/electrospray ionization tandem mass spectrometry [<https://doi.org/10.1002/rcm.2954>]. *Rapid Communications in Mass Spectrometry*, 21(7), 1239-1246. <https://doi.org/https://doi.org/10.1002/rcm.2954>



จุฬาลงกรณ์มหาวิทยาลัย
CHULALONGKORN UNIVERSITY

VITA

NAME Sasiwimon Nukulkit

DATE OF BIRTH July 1994

PLACE OF BIRTH Bangkok

INSTITUTIONS ATTENDED B.Sc. in Thai Traditional Medicine (Second Class Honors),
2017, Prince of Songkhla University, Thailand

HOME ADDRESS Bangkok

PUBLICATION Nukulkit, S., Jantimaporn, A., Poldorn, P., Khongkow, M.,
Rungrotmongkol, T., Chang, H. S., Suttisri, R., and
Chansriniyom, C. (2022). Eight Indole Alkaloids from the
Roots of *Maerua siamensis* and Their Nitric Oxide Inhibitory
Effects. *Molecules*, 27(21).